

---

Theses and Dissertations

---

Fall 2011

# Bifunctional cyclooctynes in copper-free click chemistry for applications in radionuclide chemistry and 4-Alkylpyridine derivatives in intramolecular dearomatization and heterocycle synthesis

Sharavathi Guddehalli Parameswarappa  
*University of Iowa*

Copyright 2011 Sharavathi Guddehalli Parameswarappa

This dissertation is available at Iowa Research Online: <http://ir.uiowa.edu/etd/2710>

---

## Recommended Citation

Guddehalli Parameswarappa, Sharavathi. "Bifunctional cyclooctynes in copper-free click chemistry for applications in radionuclide chemistry and 4-Alkylpyridine derivatives in intramolecular dearomatization and heterocycle synthesis." PhD (Doctor of Philosophy) thesis, University of Iowa, 2011.  
<http://ir.uiowa.edu/etd/2710>.

---

Follow this and additional works at: <http://ir.uiowa.edu/etd>

 Part of the [Chemistry Commons](#)

BIFUNCTIONAL CYCLOOCTYNES IN COPPER-FREE CLICK CHEMISTRY  
FOR APPLICATIONS IN RADIONUCLIDE CHEMISTRY AND  
4-ALKYLPYRIDINE DERIVATIVES IN INTRAMOLECULAR  
DEAROMATIZATION AND HETEROCYCLE SYNTHESIS

by

Sharavathi Guddehalli Parameswarappa

An Abstract

Of a thesis submitted in partial fulfillment  
of the requirements for the Doctor of  
Philosophy degree in Chemistry  
in the Graduate College of  
The University of Iowa

December 2011

Thesis Supervisor: Associate Professor F. Christopher Pigge

## ABSTRACT

Part A. Bifunctional cyclooctynes in copper-free click chemistry for applications in radionuclide chemistry: A new monofluorinated cyclooctyne (MFCO) with a reasonable kinetic profile was synthesized in three steps. We have demonstrated that MFCO can be used as a lynchpin to conjugate biomolecules to radionuclide chelators using copper-free 1,3-dipolar cycloaddition reactions with azides. Many bifunctional biomolecule-chelators were synthesized, and then radiolabelled with very high radiochemical purity and specific activity. MFCO-amine analogues were also synthesized and used in construction of chelator-biomolecule conjugates (particularly, NDP- $\alpha$ -MSH analogues) for applications in radioimaging. Bis-MFCO based bivalent ligands with various linker lengths were also synthesized as precursors to multivalent ligands for use in cancer diagnosis and therapy.

Part B. 4-Alkylpyridine derivatives in intramolecular dearomatization and heterocycle synthesis: 4-Alkylpyridine derivatives substituted with different carbon nucleophiles were synthesized and subjected to intramolecular spirocyclization under various conditions to afford synthetically useful diazaspiro[4.5]decanes as well as diazaspiro[5.5]undecanes in good yields. The same 4-alkyl substrates were used to synthesize anhydrobase intermediates which, then participated in aldol-like condensation in the presence of Lewis acid to yield highly conjugated dihydropyridines. Acid hydrolysis produced substituted pyridines tethered with functionalized butyro- and valero lactams. The synthesis of related azaspiro[4.5]decanes and azaspiro[5.5]undecanes from reaction of hypervalent iodine reagents with 4-methoxy-substituted benzyl and phenethyl substrates linked to  $\beta$ -keto amide nucleophiles was also briefly investigated.

Abstract Approved: \_\_\_\_\_  
Thesis Supervisor

\_\_\_\_\_  
Title and Department

\_\_\_\_\_  
Date

BIFUNCTIONAL CYCLOOCTYNES IN COPPER-FREE CLICK CHEMISTRY  
FOR APPLICATIONS IN RADIONUCLIDE CHEMISTRY AND  
4-ALKYLPYRIDINE DERIVATIVES IN INTRAMOLECULAR  
DEAROMATIZATION AND HETEROCYCLE SYNTHESIS

by

Sharavathi Guddehalli Parameswarappa

A thesis submitted in partial fulfillment  
of the requirements for the Doctor of  
Philosophy degree in Chemistry  
in the Graduate College of  
The University of Iowa

December 2011

Thesis Supervisor: Associate Professor F. Christopher Pigge

Copyright by  
SHARAVATHI GUDDEHALLI PARAMESWARAPPA  
2011  
All Rights Reserved

Graduate College  
The University of Iowa  
Iowa City, Iowa

CERTIFICATE OF APPROVAL

---

PH.D. THESIS

---

This is to certify that the Ph.D. thesis of

Sharavathi Guddehalli Parameswarappa

has been approved by the Examining Committee  
for the thesis requirement for the Doctor of Philosophy  
degree in Chemistry at the December 2011 graduation.

Thesis Committee:

\_\_\_\_\_  
F. Christopher Pigge, Thesis Supervisor

\_\_\_\_\_  
Michael K. Schultz

\_\_\_\_\_  
James B. Gloer

\_\_\_\_\_  
Leonard R. MacGillivray

\_\_\_\_\_  
Christopher M. Cheatum

To my parents, and to my brother and sister



There is way to do it better-find it.

-Thomas Alva Edison

..... I shall be telling this with a sigh  
Somewhere ages and ages hence:  
Two roads diverged in a wood, and I-  
I took the one less travelled by,  
And that has made all the difference.

-Robert Frost

## ACKNOWLEDGMENTS

It is my pleasure to thank people who influenced my graduate life in many aspects. First and foremost, I would like to express my deepest gratitude to my advisor, Dr. F. Christopher Pigge, who has been a great mentor and made it all possible. His encouragement, enthusiasm and passion for chemistry has kept me going during ups and downs of my graduate school life. I am grateful to him for giving me the freedom and opportunity to think and work creatively in the laboratory for the past five years and for making this a fantastic experience.

I would like to also thank my committee members for their timely guidance and support, especially, Dr. Michael Schultz for giving me the opportunity to work on a fruitful collaborative project which helped me to diversify my area for the graduate studies. I also want to sincerely acknowledge all the faculty and staff members of Department of Chemistry, University of Iowa for their support.

I would like to extend my gratitude to Dr. Nicholas Baumhover and Kyle Kloepping from Schultz group and Dr. Molly Martin for their help and support with required studies for the collaborative project. I deeply acknowledge the immense help from Dr. Santana Vellupillai (NMR facility), and Lynn Teesch and Vick Parcell from Mass spectrometry facility during my graduation studies. My sincere thanks to Janet Kugley and Sharon Robertson who's crucial, behind the scene work made my life in this department very peaceful. I also want to thank Peter Hatch (glass shop), Frank Turner (machine shop), Brian Morrison (Laboratory specialist), Tim Koon and Andrew Lynch (chemistry stores) for their help during these days.

Life in Iowa City has been a memorable one because of many friends. I would like to thank my senior lab mates Mayuri and Rashmi, undergraduates (John Widen, Cristie Donaghy and Thomas Speake) and my all lab mates and Iowa City friends for their support. I would like to express my deepest gratitude to

Dr. Dhanya Panicker, a post-doc from our group and a good friend of mine for helping me in crucial times of first year in the United States.

My sincere thanks to my lab-mate and friend Pradeep Kapadia who never gets tired of telling PJ's and who also has been my designated driver in Iowa City, and to Ashish Datt who has been a great source of entertainment for couple of years. I also want to express my deepest gratitude to both of my friends Lokesh Pawar who has been my lab-mate for past four good years and to my friend and roommate Amninder Kaur who always listened to my blabbermouth of success as well as frustration about the research, people (!! ) and the world.

I would like to express deepest gratitude to Dr. Sathya Shanker (Syngene) for his support and faith in me. I would also like to thank my best friends back home (India): Safia, Shekar, Subramanya Tantry, Umesh and many more for their everlasting support and friendship. My family has always been a constant source of love, care and encouragement for me. I always enjoyed spending time with my niece Prarthana, My nephew Manoj, Sister-in-law Suma, and brother-in-law Prabhakar. My best friend and companion for life, Claney Lebev Pereira has been a constant source of encouragement, his love, trust and comfort during past five years of my graduate life made this journey wonderful and his brutal criticism about my weaknesses kept me always on my toes.

This thesis is dedicated to my parents, my brother, Nagaraj and my sister, Nethravathi whose unselfishness and belief in me always mesmerized me. Their love and encouragement boost my confidence at every step of my life.

## ABSTRACT

Part A. Bifunctional cyclooctynes in copper-free click chemistry for applications in radionuclide chemistry: A new monofluorinated cyclooctyne (MFCO) with a reasonable kinetic profile was synthesized in three steps. We have demonstrated that MFCO can be used as a lynchpin to conjugate biomolecules to radionuclide chelators using copper-free 1,3-dipolar cycloaddition reactions with azides. Many bifunctional biomolecule-chelators were synthesized, and then radiolabelled with very high radiochemical purity and specific activity. MFCO-amine analogues were also synthesized and used in construction of chelator-biomolecule conjugates (particularly, NDP- $\alpha$ -MSH analogues) for applications in radioimaging. Bis-MFCO based bivalent ligands with various linker lengths were also synthesized as precursors to multivalent ligands for use in cancer diagnosis and therapy

Part B. 4-Alkylpyridine derivatives in intramolecular dearomatization and heterocycle synthesis: 4-Alkylpyridine derivatives substituted with different carbon nucleophiles were synthesized and subjected to intramolecular spirocyclization under various conditions to afford synthetically useful diazaspiro[4.5]decanes as well as diazaspiro[5.5]undecanes in good yields. The same 4-alkyl substrates were used to synthesize anhydrobase intermediates which, then participated in aldol-like condensation in the presence of Lewis acid to yield highly conjugated dihydropyridines. Acid hydrolysis produced substituted pyridines tethered with functionalized butyro- and valero lactams. The synthesis of related azaspiro[4.5]decanes and azaspiro[5.5]undecanes from reaction of hypervalent iodine reagents with 4-methoxy-substituted benzyl and phenethyl substrates linked to  $\beta$ -keto amide nucleophiles was also briefly investigated.

## TABLE OF CONTENTS

LIST OF TABLES .....	x
LIST OF FIGURES .....	xi
LIST OF TRIALS .....	xiii
LIST OF SCHEMES.....	xiv
PART A. BIFUNCTIONAL CYCLOOCTYNES IN COPPER-FREE CLICK CHEMISTRY FOR APPLICATIONS IN RADIONUCLIDE CHEMISTRY .....	1
CHAPTER	
ONE. BIFUNCTIONAL TARGET-SPECIFIC RADIOPHARMACEUTICALS FOR CANCER DIAGNOSIS AND THERAPY .....	2
1.1 Introduction.....	2
1.2 Chelators, radionuclides, and biomolecules .....	4
1.3 Bioconjugation challenges associated with bifunctional chelators (BFCs).....	8
1.4 Click chemistry strategies for BFC synthesis.....	11
1.5 Copper-catalyzed click reaction.....	13
1.6 Copper-free click reaction.....	15
1.7 Cyclooctynes for copper-free click chemistry .....	17
1.8 Multivalent ligand approach.....	19
1.9 Conclusion.....	21
TWO. BIFUNCTIONAL CYCLOOCTYNES AND THEIR APPLICATION IN RADIONUCLIDE CHEMISTRY .....	22
2.1 Introduction.....	22
2.2 Background .....	23
2.3 Results and discussion.....	26
2.4 Conclusion.....	41
2.5 Experimental section .....	42
THREE. PART A: SUMMARY AND FUTURE DIRECTIONS.....	65
3.1 Summary .....	65
3.2 Future directions.....	66
PART B. 4-ALKYLPYRIDINE DERIVATIVES IN INTRAMOLECULAR DEAROMATIZATION AND HETEROCYCLE SYNTHESIS.....	70

## CHAPTER

FOUR. DEAROMATIZATION STRATEGIES IN ORGANIC SYNTHESIS .....	71
4.1 Introduction.....	71
4.2 General methods for heterocyclic synthesis via dearomatization .....	72
4.3 Transition metal-mediated dearomatization.....	77
4.4 Oxidative dearomatization .....	80
4.5 Pyridine based dearomatization .....	83
4.6 Intramolecular dearomatization of pyridine derivatives.....	91
4.7 Conclusion.....	93
FIVE. DIAZASPIRO[4.5]DECANES FROM 4-ALKYLPYRIDYL-BETA-AMIDO ESTER SPIROCYCLIZATION .....	94
5.1 Introduction.....	94
5.2 Background .....	97
5.3 Results and discussion.....	100
5.4 Conclusion.....	117
5.5 Experimental section .....	118
SIX. EXTENDED STUDY OF 4-ALKYLPYRIDINE SPIROCYCLIZATION.....	150
6.1 Introduction.....	150
6.2 Results and discussion.....	151
6.3 Conclusion.....	166
6.4 Experimental section .....	166
SEVEN. BENZYLIC CYCLIZATION REACTIONS OF ACTIVATED 4-ALKYLPYRIDINES.....	204
7.1 Introduction.....	204
7.2 Results and discussion.....	208
7.3 Conclusion.....	222
7.4 Experimental section .....	223
EIGHT. SYNTHESIS OF AZASPIROCYCLES VIA OXIDATIVE DEAROMATIZATION USING HYPERVALENT IODINE REAGENTS.....	250
8.1 Introduction.....	250
8.2 Background .....	250
8.3 Results and discussion.....	253
8.4 Conclusion.....	261
8.5 Experimental section .....	262

NINE. PART B: SUMMARY AND FUTURE DIRECTIONS .....	276
9.1 Summary .....	276
9.2 Future directions.....	277
9.3 Experimental Section.....	283
APPENDIX A. X-RAY CRYSTALLOGRAPHIC DATA FOR SPIROCYCLE <b>6.23 (5.48)</b> .....	288
APPENDIX B. X-RAY CRYSTALLOGRAPHIC DATA FOR CONJUGATED PRODUCT <b>7.62</b> .....	291
APPENDIX C. NMR SPECTROSCOPIC DATA FOR <b>9.16</b> .....	294
BIBLIOGRAPHY.....	301

## LIST OF TABLES

Table 5.1. Initial screening of the reaction conditions. ....	106
Table 5.2. Electrophiles examined for the spirocyclization .....	107
Table 6.1. Reaction conditions screened for spirocyclization of <b>6.22 (5.45)</b> .....	157
Table 6.2. Spirocyclization reaction conditions screened for substrate <b>6.24</b> . ...	162
Table 6.3. Generality of spirocyclization of 4-alkylpyridine with $\beta$ -keto amides side chains.....	163
Table 7.1. Optimization studies for the synthesis of <b>7.35</b> .....	212
Table 7.2. Synthesis of functionalized lactams via benzylic condensation .....	214
Table 8.1. Reaction conditions screened for cyclization of <b>8.14</b> .....	258
Table A.1. Crystal structure data for <b>6.23 (5.48)</b> .....	289
Table B.1. Crystal structure data for <b>7.62</b> .....	292



## LIST OF FIGURES

Figure 1.1. Schematic representation of PET imaging <sup>4</sup> .....	3
Figure 1.2. Some examples of popular chelating agents.....	5
Figure 1.3. Schematic representation of BFCs .....	8
Figure 1.4. Schematic representation of target specific bifunctional approach to tumor imaging .....	9
Figure 1.5. Examples of activated cyclooctynes used in Cu-free click chemistry. Percentages refer to overall yield of synthesis. Second order rate constants reflect rate of reaction of indicated cyclooctyne with benzyl azide.....	17
Figure 1.6. Schematic representation of application of cyclooctynes in biological systems.....	19
Figure 2.1. Radio-HPLC chromatogram for <sup>68</sup> Ga and <sup>64</sup> Cu labeled DOTA-click-hex-NDP- $\alpha$ -MSH (A and C) and NOTA-click-hex-NDP- $\alpha$ -MSH (B and D) .....	36
Figure 2.2. <i>In vitro</i> competitive binding studies of NDP- $\alpha$ -MSH derivatives. A = NDP- $\alpha$ -MSH; B = <b>2.42</b> ; C = DOTA-amide-NDP- $\alpha$ -MSH; D = <b>2.43</b> ; E = <b>2.44</b> . .....	37
Figure 2.3. Bio distribution studies of <sup>68</sup> Ga-DOTA-click-Hex-NDP- $\alpha$ -MSH (A) and <sup>68</sup> Ga-DOTA-amide-Hex-NDP- $\alpha$ -MSH (B).....	38
Figure 2.4. RP-HPLC chromatogram of <b>2.27</b> indicating the presence of two regioisomers .....	49
Figure 2.5. Radio-HPLC chromatogram of <sup>68</sup> Ga labeled <b>2.27</b> in 5 $\mu$ mol (top) and 5 nmol (bottom).....	50
Figure 2.6. HPLC and Mass spectra of <b>2.43</b> (top) and <b>2.44</b> (bottom) .....	58
Figure 4.1. Representation of reactivity of transition metal-arene complexes ....	78
Figure 5.1. Azaspirocycles and fused ring systems in natural products and pharmacologically active compounds .....	94
Figure 5.2. General approach for pyridine based spirocyclization .....	98
Figure 5.3. Examination of the scope of 4-alkylpyridine spirocyclization .....	109
Figure 5.4. Substrates that failed to undergo spirocyclization .....	111
Figure 5.5. Examples from arene-ruthenium approach to spirocyclization .....	112
Figure 6.1. Few examples of diazaspiro[5.5]decanes in medicinal chemistry ..	150

Figure 6.2. Examples of diazaspiro[5.5]undecane framework synthesis .....	154
Figure 6.3. Carbamate analogues of the spirocycle <b>6.23</b> .....	158
Figure 7.1. Anhydrobases of alkyl pyridines .....	204
Figure 7.2. Examples of marine alkaloids bearing a bis(piperidine) core structure.....	207
Figure 8.1. Azaspirocycles and fused ring systems in medicinal chemistry.....	250
Figure 8.2. Mechanism of hypervalent iodine reagent-mediated oxidative dearomatization .....	258
Figure 9.1. NOESY correlations of 1,4-dihydropyridine <b>9.16</b> .....	281
Figure 9.2. Molecular modeling of <b>9.16</b> .....	282
Figure A.1. Crystal structure of spirocycle <b>6.23 (5.48)</b> .....	288
Figure B.1. Crystal structure of conjugated product <b>7.62</b> .....	291

## LIST OF TRIALS

Trial 2.1. Initial concentrations: <b>2.21</b> (20 mM): benzyl azide (18.4 mM).....	63
Trial 2.2. Initial concentrations: <b>2.21</b> (20 mM): benzyl azide (18.4 mM).....	64
Trial 2.3. Initial concentrations: <b>2.21</b> (20.1 mM): benzyl azide (18.9 mM).....	64

## LIST OF SCHEMES

Scheme 1.1. Synthesis of functionalized chelators.....	6
Scheme 1.2. Synthesis of CB-TE2A-(propionamide linker)-c[RGDfK(S)] ( <b>1.18</b> ).....	10
Scheme 1.3. Synthesis of NOTA-based [Tyr <sup>3</sup> ] octreotide derivative (NODAGATOC) ( <b>1.21</b> ) .....	11
Scheme 1.4. Synthesis of photosensitive DNA probe ( <b>1.24</b> ) via Cu- catalyzed click reaction .....	13
Scheme 1.5. Synthesis of DOTA- $\alpha_v\beta_3$ integrin-cyclo[Arg-Gly-Asp-D-Phe- Lys] (RGD) peptide dendrimers ( <b>1.28</b> ) .....	14
Scheme 1.6. Synthesis of c(RGD)-CF <sub>3</sub> -triazole-DTPA conjugate <b>1.31</b> via tandem crDA .....	16
Scheme 2.1. Synthesis of chelator-biomolecule using copper(I) catalyzed click chemistry.....	23
Scheme 2.2. Synthesis of DIFO ( <b>2.11</b> ) using Bertozzi's approach .....	24
Scheme 2.3. Synthesis of 1,3-diketone ( <b>2.4</b> ) using Pirrung's method .....	25
Scheme 2.4. Synthesis of MFCO ( <b>2.21</b> ) .....	27
Scheme 2.5. Click reaction of MFCO ( <b>2.21</b> ) with benzyl azide .....	28
Scheme 2.6. Synthesis of Biotin-MFCO ( <b>2.25</b> ) .....	29
Scheme 2.7. Synthesis of bifunctional DOTA-MFCO-Biotin derivative ( <b>2.27</b> ) ....	31
Scheme 2.8. Synthesis of DOTA-MFCO-Neuropeptide Y conjugate ( <b>2.31</b> ) .....	32
Scheme 2.9. Synthesis of MFCO-amine ( <b>2.35</b> ) .....	33
Scheme 2.10. Synthesis of Chelator-MFCO-amine conjugates.....	34
Scheme 2.11. Synthesis of DOTA-click-hex-NDP- $\alpha$ -MSH derivative ( <b>2.43</b> ) .....	35
Scheme 2.12. Synthesis of NOTA-click-hex-NDP- $\alpha$ -MSH derivative ( <b>2.44</b> ) .....	36
Scheme 2.13. Synthesis of bis-MFCO-PEG-3-amide ( <b>2.46</b> ) .....	39
Scheme 2.14. Synthesis of bis-MFCO linkers <b>2.47</b> and <b>2.49</b> .....	41
Scheme 3.1. Synthesis of MFCO-chelators.....	67
Scheme 3.2. Bis-MFCO for bivalent ligands synthesis .....	67
Scheme 3.3. Synthesis of multivalent-MFCO with varying linker length and spacers .....	69

Scheme 4.1. Diastereoselective Birch reduction in synthesis of (+)-cepharamine ( <b>4.4</b> ) .....	72
Scheme 4.2. Dearomatization using radical addition .....	74
Scheme 4.3. Synthesis of penifulvin A ( <b>4.15</b> ) via radical cyclization.....	75
Scheme 4.4. Synthesis of (+)-fendleridine ( <b>4.20</b> ) using cycloaddition cascade reaction .....	76
Scheme 4.5. Dearomatization via anionic cyclization .....	77
Scheme 4.6. Nucleophilic dearomatization using $\eta^6$ -coordinated chromium metal-arene complex in natural product synthesis .....	79
Scheme 4.7. $\eta^2$ -coordinated osmium metal-arene complex in electrophilic dearomatization.....	79
Scheme 4.8. Functionalized cyclohexenones ( <b>4.34</b> ) from electrophilic dearomatization using $\eta^2$ -coordinated osmium metal-arene complex.....	80
Scheme 4.9. Synthesis of ( $\pm$ )-cleroindicin D ( <b>4.38</b> ) using oxidative dearomatization.....	81
Scheme 4.10. Synthesis of cortistatin A ( <b>4.43</b> ) using hypervalent iodine mediated oxidative dearomatization.....	82
Scheme 4.11. Synthesis of (-)-platensimycin ( <b>4.48</b> ).using oxidative dearomatization.....	83
Scheme 4.12. General representation of nucleophilic additions to activated pyridine ring .....	84
Scheme 4.13. Nucleophilic additions to pyridinium salts and their regioselectivity.....	85
Scheme 4.14. Asymmetric induction in nucleophilic addition to activated pyridine ring .....	87
Scheme 4.15. Intramolecular pyridine dearomatization in natural product synthesis (Comins <i>et al</i> approach) .....	88
Scheme 4.16. Synthesis of (-)-barrenazines by Charette <i>et al</i> using intramolecular pyridine dearomatization.....	89
Scheme 4.17. Examples of intramolecular pyridine dearomatization .....	91
Scheme 4.18. Asymmetric induction in intramolecular pyridine dearomatization.....	92
Scheme 4.19. Examples of intramolecular pyridine dearomatization from the Clayden group.....	93

Scheme 5.1. Azaspirocycles of arene-ruthenium complexes of $\beta$ -amido phosphonates .....	95
Scheme 5.2. Morita-Baylis-Hillman cyclization of arene-ruthenium acrylamides .....	96
Scheme 5.3. Intramolecular cyclization of pyridine derivatives.....	97
Scheme 5.4. Diastereoselective synthesis of azaspirocycles.....	98
Scheme 5.5. Our approach to alkylpyridine dearomatization .....	100
Scheme 5.6. General synthesis of 4-alkyl substituted pyridine with nucleophile $\beta$ -amido ester side chains .....	102
Scheme 5.7. Synthesis of alkylpyridine- $\beta$ -amido ester substrates.....	103
Scheme 5.8. Intramolecular dearomatization of <b>5.19</b> .....	105
Scheme 5.9. Possible mechanism for the Ti(O <sup>i</sup> Pr) <sub>4</sub> catalyzed 4-alkylpyridyl spirocyclization.....	106
Scheme 5.10. Additional examination of 4-alkylpyridine cyclizations .....	110
Scheme 5.11. Functionalization of the spirocycle <b>5.39</b> .....	113
Scheme 5.12. Alkylation of the lactam carbon of the spirocycle <b>5.39</b> .....	114
Scheme 5.13. Gold(III)-catalyzed cycloisomerization .....	115
Scheme 5.14. Mechanism of gold(III)-catalyzed cycloisomerization.....	116
Scheme 5.15. Attempts to manipulate the spirocycle <b>5.39</b> into building blocks .....	117
Scheme 6.1. Synthesis of 4-alkylpyridyl substrates.....	152
Scheme 6.2. Synthesis of diazaspiro[5.5]decane system.....	153
Scheme 6.3. Hydrogenation of 1,4-dihydropyridine <b>6.15</b> .....	155
Scheme 6.4. Elaboration of spirocycle <b>6.15</b> into complex building blocks .....	155
Scheme 6.5. Spirocyclization of substrate <b>6.22 (5.25)</b> .....	157
Scheme 6.6. Synthesis of alkylpyridines with $\beta$ -keto amides.....	159
Scheme 6.7. Spirocyclization of <b>6.24</b> .....	161
Scheme 6.8. Elaboration of the spirocycle <b>6.23</b> .....	165
Scheme 6.9. Alkylation of <b>6.23</b> .....	165
Scheme 7.1. Synthesis of acylated anhydrobases .....	205

Scheme 7.2. Synthesis of heterocycle <b>7.7</b> from anhydrobase <b>7.5</b> .....	205
Scheme 7.3. Anhydrobase utilization in natural product synthesis .....	206
Scheme 7.4. Synthesis of 4-alkylpyridyl substrates.....	209
Scheme 7.5. First evidence of anhydrobase formation.....	210
Scheme 7.6. Synthesis of highly conjugated anhydrobases of <b>7.29</b> and <b>7.31</b> ..	210
Scheme 7.7. Reactivity of <b>7.25</b> under KO <sup>t</sup> Bu condition .....	211
Scheme 7.8. One pot synthesis of <b>7.35</b> .....	212
Scheme 7.9. Possible mechanism for benzylic condensation .....	213
Scheme 7.10. Additional substrates subjected to conditions of benzylic cyclization. Reaction conditions: 1) EtCO <sub>2</sub> Cl (1.5 equiv), DIPEA (1.5 equiv), Ti(O <sup>i</sup> Pr) <sub>4</sub> (0.5 equiv), THF, reflux, 20 min. 2) TFA, H <sub>2</sub> O.....	217
Scheme 7.11. Synthesis of carbon analogues of 4-alkylpyridines.....	219
Scheme 7.12. Substituted pyridines from carbon analogue condensation .....	220
Scheme 7.13. Functionalization of conjugated anhydrobases.....	221
Scheme 8.1. Spiroannulation via hypervalent iodine oxidation.....	252
Scheme 8.2. Initial attempts to perform oxidative dearomatization (R. Dalvi, unpublished results).....	253
Scheme 8.3. Azaspirocyclization via oxidative dearomatization .....	253
Scheme 8.4. Synthesis of precursors for oxidative dearomatization .....	255
Scheme 8.5. Azaspirocyclization of <b>8.14</b> .....	257
Scheme 8.6. Generality of spiroannulation via oxidative dearomatization.....	260
Scheme 8.7. Functionalization studies of azaspirocycles.....	261
Scheme 9.1. Benzylic cyclization of 4-alkylpyridines in potential natural product synthesis .....	278
Scheme 9.2. Bicyclic ring systems from 3-pyridyl dearomatization .....	279
Scheme 9.3. Fused ring systems from 3-alkylpyridine dearomatization.....	280
Scheme 9.4. 3-Alkylpyridyl substrates in natural product synthesis .....	283

PART A

BIFUNCTIONAL CYCLOOCTYNES IN COPPER-FREE CLICK  
CHEMISTRY FOR APPLICATIONS IN RADIONUCLIDE CHEMISTRY



# CHAPTER ONE

## BIFUNCTIONAL TARGET-SPECIFIC RADIOPHARMACEUTICALS FOR CANCER DIAGNOSIS AND THERAPY

### 1.1 Introduction

Humankind has made remarkable advancements in science and technology, many issues pertaining to health and environment are still unanswered. According to WHO reports, cancer was the world's leading cause of death in 2008.<sup>1</sup> Cancer killed 7.6 million people (about 13% of all deaths) in 2008, more than HIV/AIDS, malaria, and tuberculosis combined. Three quarters of cancer deaths were in developing countries. By 2030, the annual death toll from cancer is predicted to increase to 11 million. Up to 30% of cancer deaths could be prevented by proper diagnosis, therapy, and care. A number of drugs are currently available for the treatment of several types of cancer, and more are in clinical trials. Still, cancer is a prevalent disease because of its heterogeneity and its ability to invade organs and tissues distant from primary tumors (via metastasis). Early detection and effective treatment is the only way to decrease cancer-related mortality rates.

Molecular imaging of cancerous tumors is an integral part of cancer research. This tool is widely used for diagnosis of malignancies, and for understanding, monitoring, and measuring response to therapy. Positron Emission Tomography (PET) and Single Photon Emission Computed Tomography (SPECT) have emerged as the most widely used imaging techniques for visualizing and quantifying malignant tumors non-invasively *in vivo*.<sup>2,3</sup> The general schematic representation of PET/SPECT imaging is shown in Figure 1.1.<sup>4</sup> Radionuclides such as  $^{68}\text{Ga}$  or  $^{18}\text{F}$ , which decay by positron emission, are examples of radionuclides used for PET imaging. These positrons

are very unstable, and after travelling a short distance, are annihilated by electrons in the surrounding body tissue and generate two  $\gamma$ -rays which are emitted at  $180^\circ$  and can be detected by an external imaging device (figure 1.1). Positron emitting radionuclides give a resolved image of the radioactivity distribution inside the body without harming the patient. Since bifunctional radiopharmaceuticals are used as radionuclide probes in molecular imaging studies, the development of bifunctional chelators that can be efficiently radiolabelled and are stable *in vivo* is crucial to enhance the value of PET/SPECT in research and development of cancer diagnosis and treatment.

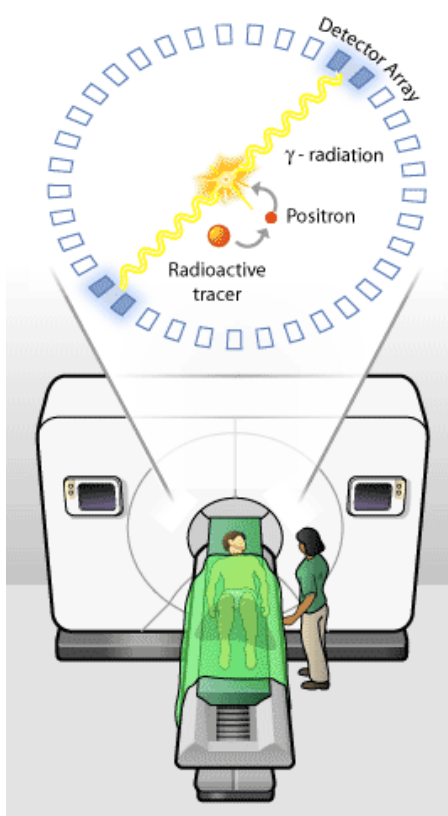


Figure 1.1. Schematic representation of PET imaging<sup>4</sup>

## 1.2 Chelators, radionuclides, and biomolecules

Bifunctional radiopharmaceuticals have some significant characteristics associated with them and they are used extensively in target specific molecular imaging. Generally they are made of three main components: a chelating moiety, a radionuclide ion, and a biomolecule.<sup>5</sup> Bifunctional chelating agents (BFCs) consist of a radionuclide chelator attached to a targeting unit (biomolecule) that specifically binds to specific cell receptors. Many varieties of chelators which can coordinate to radionuclides are known.<sup>6</sup> These chelators are mainly made of polyamino polycarboxylic functionalities and they can form very stable complexes with chosen metal ions. Based on their structures, these polyamino polycarboxylic acid ligands are categorized as cyclic or acyclic. Complexation of metals with acyclic ligands such as DTPA (diethylenetriaminopentaacetic acid) (**1.1**) and EDTA (ethylenediaminetetraacetic acid) (**1.2**) (Figure 1.2) is faster compared to macrocyclic ligands, but the complexes tend to be thermodynamically unstable and are more prone to release the metal ion *in vivo* because of transmetallation.<sup>7</sup> Most of these ligands form negatively charged metal complexes with  $Y^{3+}$ ,  $Ln^{3+}$ ,  $Ga^{3+}$ ,  $^{99m}Tc$  and  $In^{3+}$ .<sup>5,8</sup> Many acyclic ligands are commercially available and feature a variety of donor atoms, coordination capacity and synthetic tunability to achieve desired radionuclide binding. These are a few reasons why acyclic ligands are prominent in molecular imaging.

Widely used macrocyclic ligands are based on DOTA (1,4,7,10-tetraazacyclododecane-1,4,7,10-tetraacetic acid) (**1.3**), NOTA (1,4,7-triazacyclononane-1,4,7-triacetic acid) (**1.4**) and TETA (1,4,8,11-tetraazacyclotetradecane-1,4,8,11-tetraacetic acid) (**1.5**) (Figure 1.2). These ligands are synthesized from the parent azamacrocycles, such as cyclen and cyclam.<sup>9,10</sup> These macrocyclic ligands show selective coordination properties to many radionuclides and form thermodynamically stable complexes with di- and

trivalent metal ions.<sup>6</sup> These complexes are also kinetically inert to transmetallation with endogeneous metal ions such as  $\text{Ca}^{2+}$  and  $\text{Zn}^{2+}$ , making them potential probes for imaging when longer biostability is required.<sup>5</sup> In particular, DOTA derivatives, which are octadentate ligands equipped with four amino and four carboxylic acid groups, are well known for their superior chelating capability to lanthanide ions to form highly thermodynamically and kinetically stable complexes.<sup>6,11</sup> DOTA derivatives can also form stable complexes with trivalent ions such as  $^{68}\text{Ga}$ ,  $^{90}\text{Y}$ ,  $^{111}\text{In}$  and divalent ions such as  $^{64}\text{Cu}$ , and thus find application in diagnostic and therapeutic radionuclide chemistry. Hence, functionalization of DOTA has been a topic of interest for some time and many derivatives (e.g., **1.10a-b**) have been synthesized by manipulating a pendant arm or by introducing substitution on the ring (Scheme 1.1).<sup>12,13</sup>

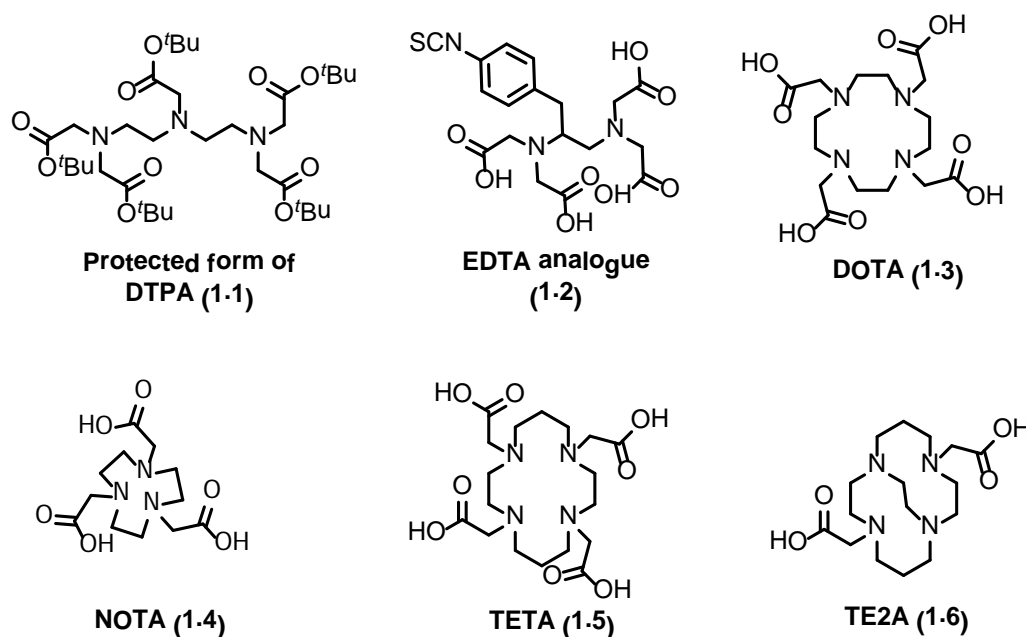
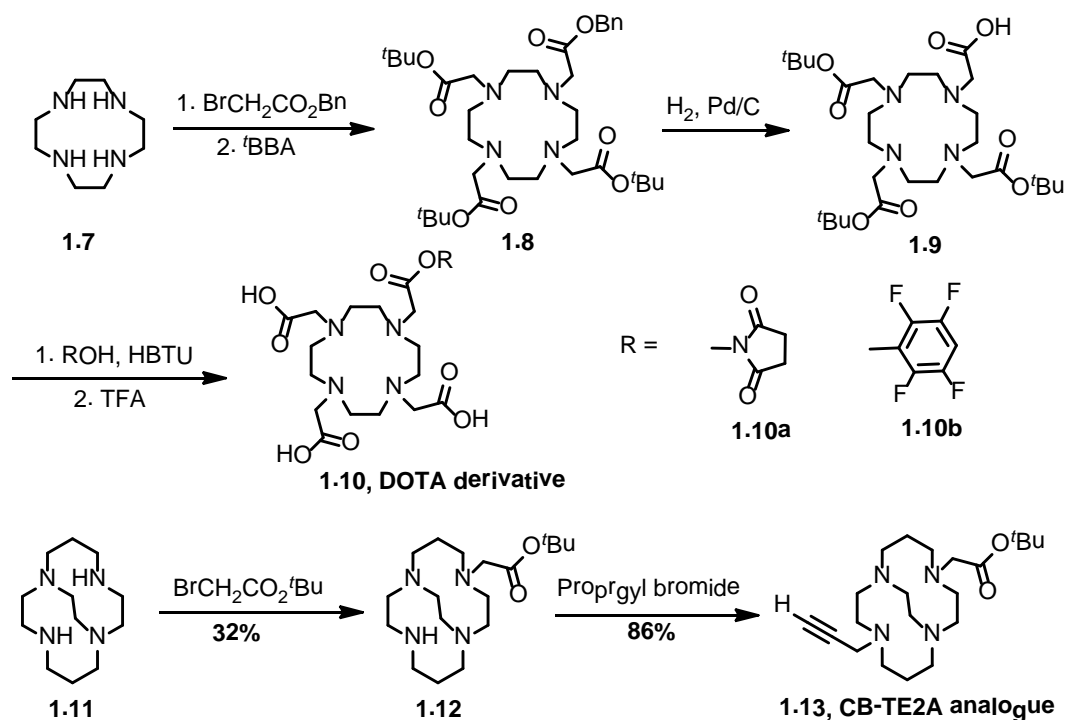


Figure 1.2. Some examples of popular chelating agents

Developing optimal metal chelators is a critical step in designing systems for the *in vivo* delivery of radionuclides. In this context, the cross-bridged (CB) cyclic ligands such as TE2A (1,4,8,11-tetraazacyclobicyclo[6.6.2]hexadecane-4,11-diacetic acid) (**1.6**) (Figure 1.2) containing non-adjacent nitrogens connected by an ethylene bridge have been useful.<sup>14</sup> These CB-TE2A ligands form remarkably stable and kinetically inert complexes with metal ions (e.g.,  $\text{Cu}^{2+}$ ) by adopting low energy conformations having clamshell-like clefts of nitrogen lone pairs.<sup>15,16</sup> Because these complexes have only two pendant carboxymethyl arms, they form six-coordinate neutral complexes with divalent cations. Synthesis of cross-bridged bifunctional chelators such as **1.13** can be achieved from substituting a carboxymethyl arm of TE2A by different functionality as shown in Scheme 1.1.<sup>17</sup>



Scheme 1.1. Synthesis of functionalized chelators

The radionuclide itself is an important variable in obtaining suitable target-specific radiopharmaceuticals for diagnosis and therapy. The choice of radioisotope mainly depends on commercial availability, half-life, decay properties, shelf life, production cost, radiolabelling efficiency, and toxicity and coordination chemistry with an array of chelators.  $^{99m}\text{Tc}$ ,  $^{188}\text{Re}$ ,  $^{68}\text{Ga}$ ,  $^{90}\text{Y}$ ,  $^{111}\text{In}$  and  $^{64}\text{Cu}$  are examples of radionuclides used extensively in target-specific radiopharmaceutical research.<sup>5,8</sup> For PET imaging, radioisotopes that are 511 keV positron emitters are desired because this reduces the burden of radiation for the patient and, due to high  $\beta^+$  energy, also increases spatial resolution for imaging.  $^{68}\text{Ga}$  (half-life of 68 min),  $^{90}\text{Y}$  (half-life of 2.7 days), and  $^{64}\text{Cu}$  (half-life of 12.7 h) are a few positron emitting radioisotopes with considerably high  $\beta^+$  energies. For SPECT, gamma-emitting radioisotopes such as  $^{99m}\text{Tc}$  (half-life of 6 h) and  $^{111}\text{In}$  (half-life of 2.8 days) are considered. Coordination chemistry of the metal ions also plays a significant role in nuclear medicine, and largely depends upon the size and coordination geometry of the metal ion. Introduction of metal ions can also change the pharmacokinetics of radiopharmaceuticals.

Bifunctional radionuclide complexes such as radiolabelled antibodies, peptides and peptidomimetics can be used as imaging markers to target diseased cells. To achieve high target-to-background signals, the radiolabelled BFCs should have short blood residence time, high hydrophilicity (hence rapid renal clearance), and should be able to reach the specific receptor sites at the target (tumor) quickly.<sup>5</sup> Criteria for selection of biomolecule-targeting vectors are governed by whether the target is a surface protein or an intercellular component such as DNA and mRNA. Successful radiolabeling lies in the ability of the imaging marker to preferentially bind to the target at the expense of cognate ligands.

### 1.3 Bioconjugation challenges associated with bifunctional chelators (BFCs)

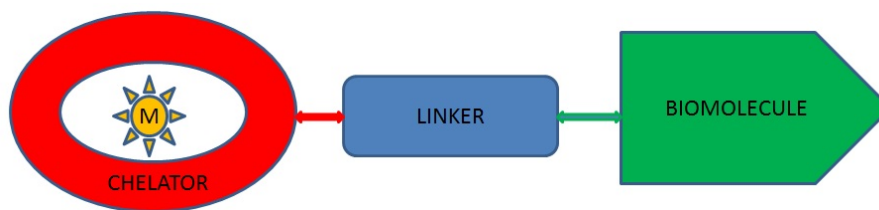


Figure 1.3. Schematic representation of BFCs

Target-specific bifunctional approaches are the most popular among radiopharmaceutical designs to locate and treat widely dispersed disease when the disease sites are unknown. Schematic representation of a typical bifunctional radiopharmaceutical is shown in Figure 1.3 and mainly consists of three units; a target specific biomolecule connected to a radiometal labeled chelator via an appropriate linker. The biomolecule is often a high affinity ligand for targeted receptor known to be expressed (or over expressed) in the cancer being imaged, and the presence of radiometal often does not alter the binding affinity to this receptor.<sup>8</sup> The linker between radiolabelled chelator and the biomolecule assists with keeping the radiometal away from the biomolecule as well as with pharmacokinetic modification. Generally, the biomolecule is the target carrier unit of the BFCs and binds to the specific receptor, thus increasing the probability of finding increased radioactivity near the disease site which, in turn, increases the intensity of PET imaging for diagnosis of malignant cells (Figure 1.4).<sup>18</sup> Because multiple parameters are involved, BFC approach faces issues such as maximizing the retention time of radioactivity at the tumor sites, *in vivo*

metabolism of the BFC's and an efficient method of attachment of the biomolecule to the chelator.

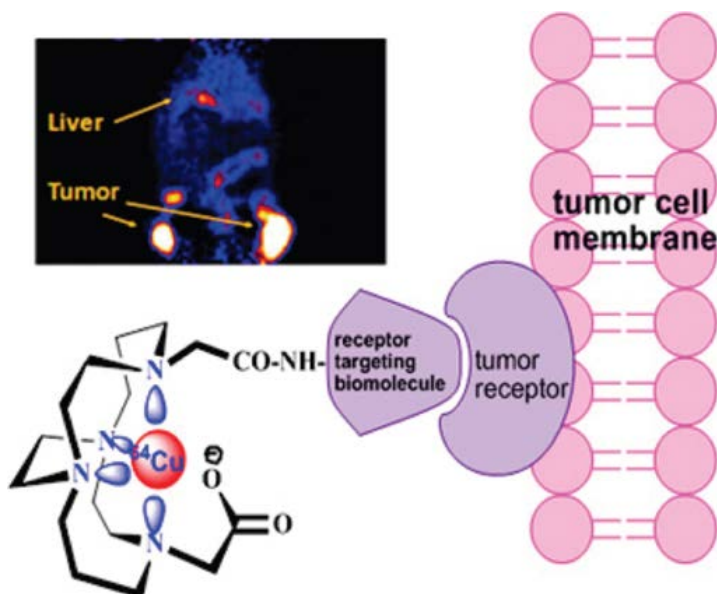
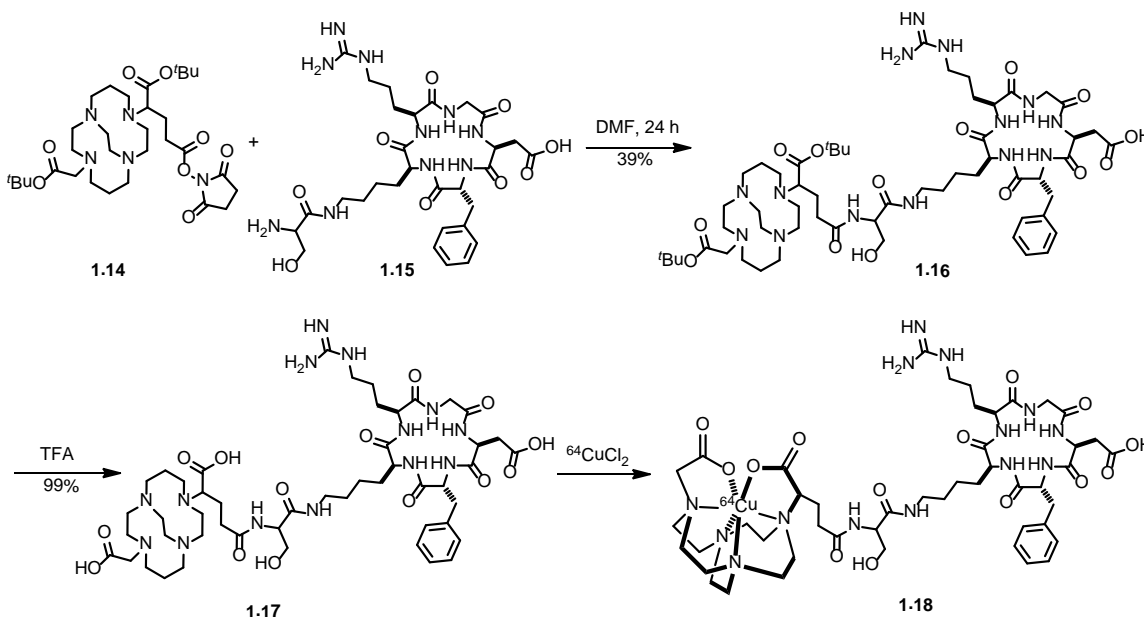


Figure 1.4. Schematic representation of target specific bifunctional approach to tumor imaging

Since most biomolecule targeting ligands have functionalized peptide sequences in their structure, traditional coupling of an amine to a carboxylic acid to form stable amide bond is used widely in chelator conjugation to biomolecules. Because functionalization of peptide chains can be performed by introducing different amines or carboxyl groups at various positions, this permits researchers to synthesize and tune the properties of biomolecules for further studies. Although a few chelator derivatives possessing reactive functional groups to facilitate bioconjugation (such as NHS esters and isothiocyanates) are commercially available, suitable chelators for specific bioconjugations often need to be synthesized. For example, Boswell and coworkers synthesized a CB-TE2A-



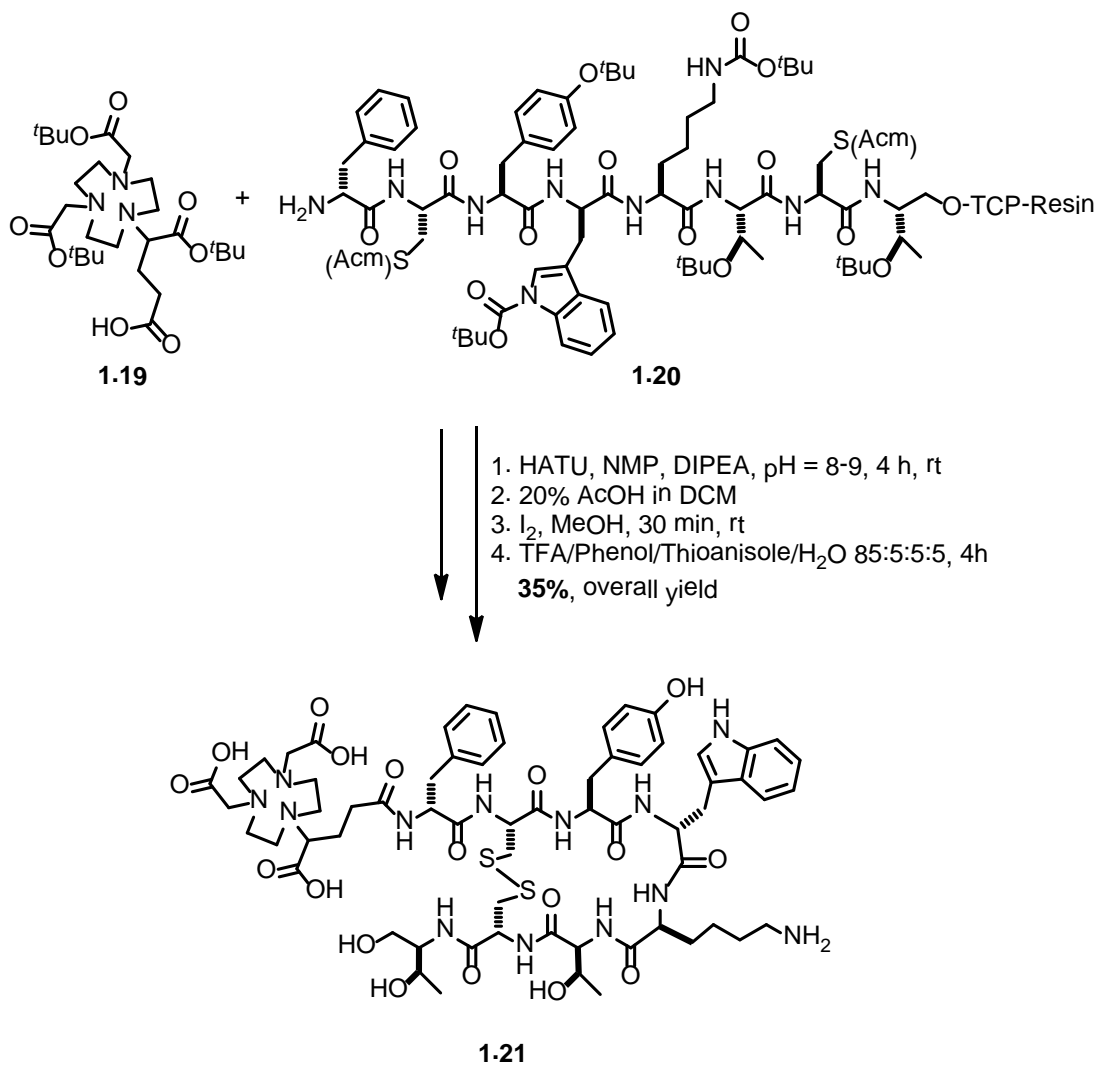
(propionamide linker)-c[RGDfK(S)] (**1.16**) via standard amide formation strategy using CB-TE2A-NHS ester (**1.14**) and corresponding amine functionalized cyclic peptide (**1.15**) in DMF in moderate yield (Scheme 1.2).<sup>19</sup> Compound **1.16** was subsequently deprotected using TFA and radiolabelled with <sup>64</sup>Cu to afford **1.18**.



Scheme 1.2. Synthesis of CB-TE2A-(propionamide linker)-c[RGDfK(S)] (**1.18**)

Eisenwiener and coworkers have synthesized a NOTA-based [Tyr<sup>3</sup>] octreotide derivative (NODAGATOC) (**1.21**) using solid phase synthesis by coupling carboxylic acid group of NOTA based chelator (**1.19**) with N-terminus of peptide (**1.20**). The resulting BFC (**1.21**) was radiolabelled with <sup>67</sup>Ga and <sup>111</sup>In and used to visualize primary tumors and metastases which express somatostatin receptor subtype 2 (Scheme 1.3).<sup>20</sup> Standard amide coupling strategies employed in the examples discussed above often require multiple step synthesis of chelators, functionalization of biomolecules, laborious protection and

deprotection reactions, and tedious, inefficient and time consuming purifications, thus resulting in a less attractive approach for BFCs.<sup>12,21</sup>



Scheme 1.3. Synthesis of NOTA-based [Tyr<sup>3</sup>] octreotide derivative (NODAGATOC) (1.21)

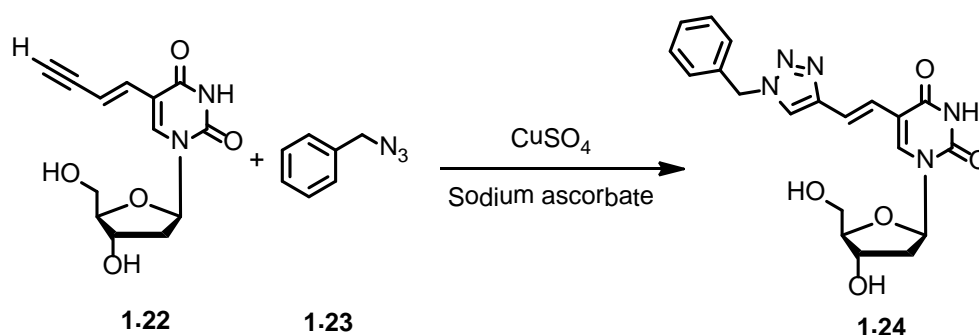
#### 1.4 Click chemistry strategies for BFC synthesis

Click chemistry is defined as a modular reaction which is wide in scope, gives high yield of product under mild physiological conditions, is stereospecific,

produces benign byproducts, and uses simple purification and isolation methods.<sup>22</sup> Generally click reactions are thermodynamically favored and tend to form selectively a single product in short reaction times. Four classes of chemical transformations are considered to be click reactions:<sup>3,22</sup> 1) non-aldol type carbonyl chemistry such as formation of ureas, thioureas, oxime ethers, hydrazones, amides and aromatic heterocycles; 2) nucleophilic substitution reactions involving ring opening of strained heterocyclic electrophiles such as epoxides, aziridines and aziridinium ions; 3) addition reactions to C-C multiple bonds such as Michael addition, epoxidation, aziridation and dihydroxylation; and 4) cycloaddition reactions such as 1,3-dipolar cycloaddition and Diels-Alder reaction. Since click chemistry provides a pathway for rapid synthesis of new molecules, these transformations are prominent in drug discovery and combinatorial research.<sup>23</sup> Particularly, 1,3-dipolar cycloaddition (1,3-Huisgen reaction) of an alkyne and an azide to form five membered triazole is the best example of a click reaction. This reaction has been known for more than a century and in the 1960's Huisgen and his coworkers thoroughly studied this reaction.<sup>24,25</sup> Recently, it has gained popularity in medicinal chemistry and biomedical research. This is because azides and alkynes are stable, inert to other functionalities present in biomolecules (bioorthogonal), and survive reaction conditions of living organisms. These two functional groups can be incorporated into a wide range of substrates, and triazole products arising from click reactions are usually biocompatible.<sup>26</sup> Generally, thermal click reactions between alkynes and azides are very slow, and proceed with extremely low reaction rates for unactivated reactants and requires very high temperature and long reaction times.<sup>25</sup> Even though the cycloaddition reaction is exothermic, unfavorable kinetics results from a high activation barrier for the reaction. Regioisomeric mixtures of 1,4-disubstituted and 1,5-disubstituted 1,2,3-triazole products are usually obtained in

these reactions. Metal-catalyzed azide-alkyne cycloaddition reactions, however, display all the characteristics of click reactions.

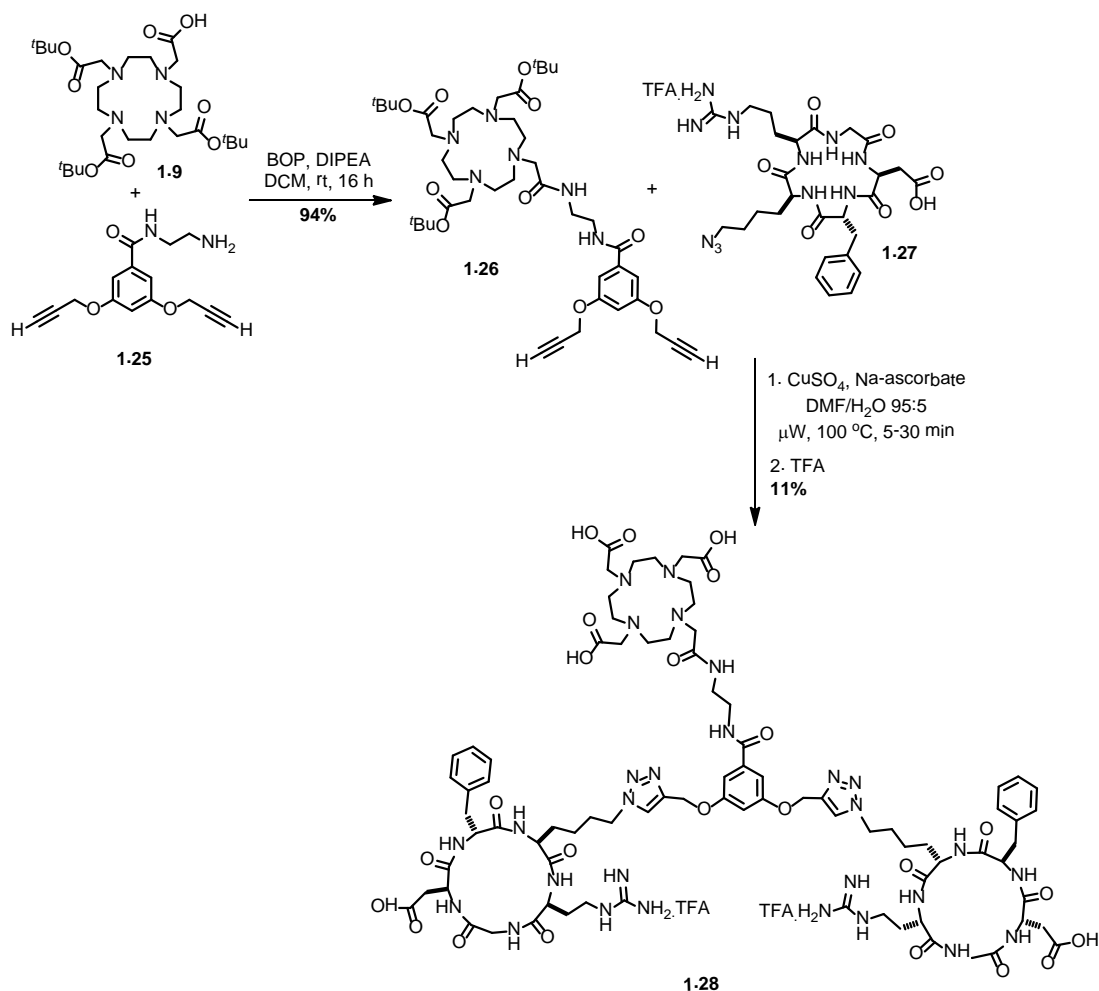
### 1.5 Copper-catalyzed click reaction



Scheme 1.4. Synthesis of photosensitive DNA probe (**1.24**) via Cu-catalyzed click reaction

Copper catalyzed cycloaddition of alkynes with azides was reported independently by the groups of Meldal and Sharpless in 2002.<sup>27,28</sup> It was found that copper(I) catalysts were able to accelerate the rate of 1,3-cycloaddition by a factor of  $10^7$  compared to the thermal reaction. Copper catalyzed reactions are fast, require low temperature, and can be used to covalently attach any fragment containing an azide functionality to terminal alkynes without being affected by the sterics or electronics of the substrates. Copper catalyzed azide-alkyne 1,3-dipolar cycloaddition (CuAAC) is believed to proceed through copper acetylide formation with the terminal alkyne which drastically changes the mechanism and kinetics of triazole formation relative to the uncatalyzed version. Furthermore, only 1,4-disubstituted triazole products are obtained.<sup>29</sup> Hence this reaction has been used extensively in organic synthesis, combinatorial chemistry, polymer chemistry and chemical biology.<sup>30</sup> CuAAC is used in labeling of oligonucleotides,

coupling of oligonucleotides to monolayers, template strand ligation, spin labeling studies of proteins and nucleic acids and in genetic science.<sup>31,32</sup> For example, Ami and coworkers reported the synthesis of photosensitive DNA probes (e.g., **1.24**) with triazole rings using copper(I) catalyzed click reaction for single nucleotide polymorphism (SNP) typing studies (Scheme 1.4).<sup>33</sup> This approach assisted them in the rapid synthesis of several photosensitive DNA probes with different substitutions for photoligation purposes.



Scheme 1.5. Synthesis of DOTA- $\alpha_v\beta_3$  integrin-cyclo[Arg-Gly-Asp-D-Phe-Lys] (RGD) peptide dendrimers (**1.28**)

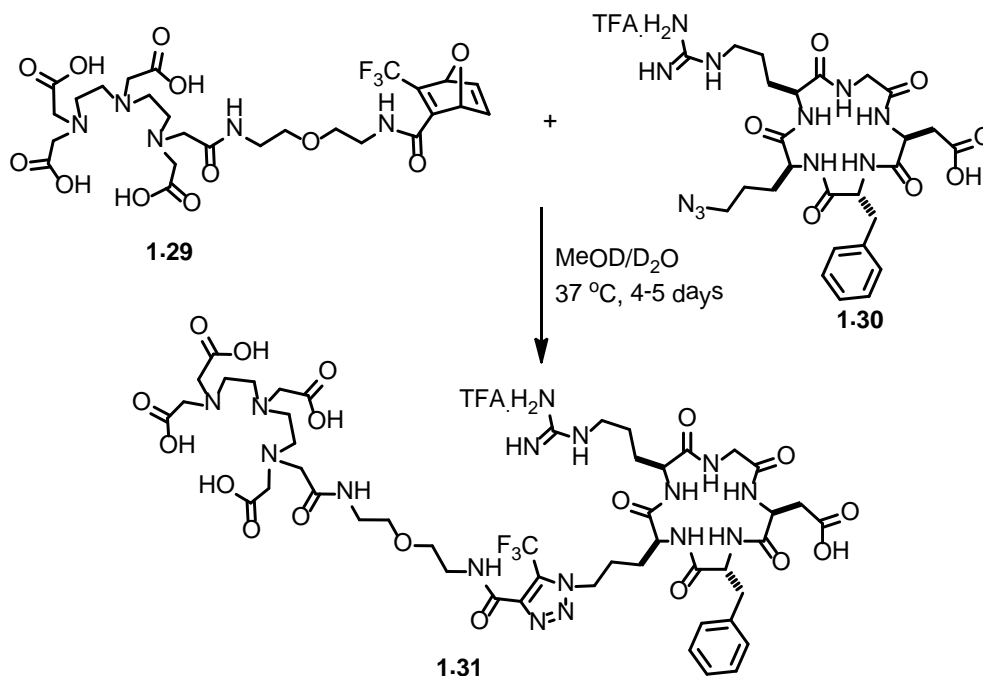
DOTA-conjugated to multivalent integrin  $\alpha_v\beta_3$  directed-cyclo[Arg-Gly-Asp-D-Phe-Lys] (RGD) peptide dendrimers (e.g., **1.28**) were synthesized via microwave assisted CuAAC by Dijkgraaf and coworkers for biological evaluation in mice with subcutaneously grown human SK-RC-52 tumors for tumor imaging purposes (Scheme 1.5).<sup>34</sup> Results obtained showed that *in vivo* uptake in  $\alpha_v\beta_3$  integrin expressing tumors was enhanced with <sup>111</sup>In radiolabelled tetrameric RGD-dendrimers compared to dimeric (**1.28**) and monomeric dendrimers.

Despite the many positive attributes of Cu-catalysed click reactions, very few reports describing CuAAC to couple chelators to biomolecules have appeared. This is mainly because the Cu catalyst used in the reaction has a high affinity for the chelator unit and coordinates to the chelator, thus complicating its removal to obtain metal-free material. The presence of copper in the BFCs interferes with subsequent radiolabelling processes and reduces achievable specific radioactivity which is a significant factor in molecular imaging. Copper is also toxic to bacterial and mammalian cells.<sup>35,36</sup> These issues can be addressed by using protected DOTA-derivatives or by removal of copper traces from triazole adducts via precipitation with Na<sub>2</sub>S, but this increases the number of steps to obtain pure BFCs.<sup>17</sup> Copper-free click reactions provide alternative approaches for the synthesis of these BFCs.

### 1.6 Copper-free click reaction

The combination of ring strain and electron deficiency (such as in oxabridged bicyclic ring systems) can increase the reactivity of molecules toward cycloaddition reactions and these features have been used to promote bioconjugation reactions. For example, a spontaneous tandem [3 + 2] cycloaddition retro-Diels-Alder reaction (tandem crDA) was used to synthesize stable 1,2,3-triazoles from oxanorbornadienes and azides. The reaction affords

products similar to those obtained using CuAAC with alkynes. Berkel and coworkers observed that reaction rates of cycloaddition involving oxanorbornadienes with azides were fivefold higher than that with alkynes and yielded mixtures of triazole regioisomers.<sup>37</sup>



Scheme 1.6. Synthesis of c(RGD)-CF<sub>3</sub>-triazole-DTPA conjugate **1.31** via tandem crDA

The same group utilized trifluoromethyl substituted oxanorbornadienes in tandem-crDA to synthesize PEGylated oligopeptides for bioconjugation to proteins used in subsequent labeling experiments.<sup>38</sup> These researchers also reported conjugation of DTPA-functionalized oxanorbornadiene **1.29** to N- $\delta$ -azido-cyclo(-Arg-Gly-Asp-D-Phe-Orn-) ligand (**1.30**) to obtain c(RGD)-CF<sub>3</sub>-triazole-DTPA conjugate **1.31** (Scheme 1.6) which showed a good IC<sub>50</sub> value and pharmacokinetically favorable hydrophilicity *in vivo* during biological evaluation.

This strategy, however, is limited by issues such as longer reaction times (4-5 days) and undesired formation of substituted furans, a byproduct which is the result of azide cycloaddition to the unsubstituted double bond of the oxanorbornadiene.

### 1.7 Cyclooctynes for copper-free click chemistry

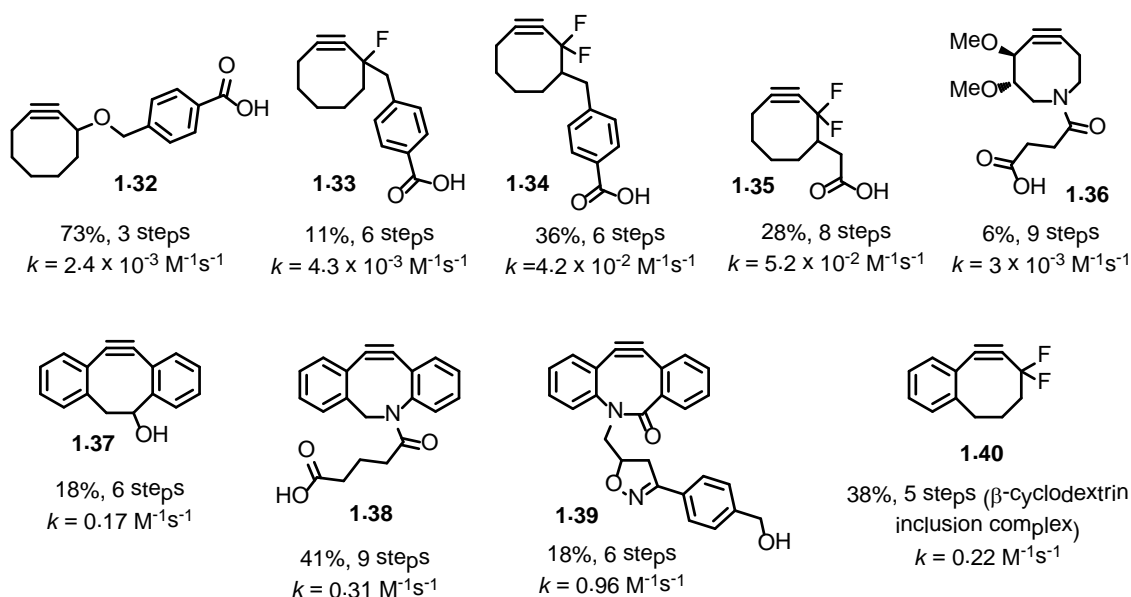


Figure 1.5. Examples of activated cyclooctynes used in Cu-free click chemistry. Percentages refer to overall yield of synthesis. Second order rate constants reflect rate of reaction of indicated cyclooctyne with benzyl azide

In the 1960's, Wittig and Krebs reported that reaction of cyclooctyne, the smallest stable cycloalkyne with phenyl azide proceeded through an explosion to give a single triazole product.<sup>39</sup> Strained cyclooctynes have deformed alkyne bond angle of up to  $163^\circ$ , which results in 18 kcal/mol of ring strain.<sup>40</sup> Much of this energy is released during the reaction transition state relative to the



destabilized ground state in [3+2] cycloaddition with an azide, thus accelerating the rate of reaction compared to unstrained alkynes.<sup>41,42</sup>

Bertozzi and coworkers synthesized many functionalized cyclooctynes for cycloaddition purposes (Figure 1.5).<sup>43-45</sup> It was found that cyclooctyne **1.32** underwent uncatalyzed cycloaddition with an accelerated rate compared to linear alkynes, but the rate was not fast enough for applications in living systems. It was postulated that the lowest unoccupied molecular orbital (LUMO) of the alkyne and the highest occupied molecular orbital (HOMO) of the azide were involved in the transition state leading to triazole product. Consequently, the rate of the reaction may be accelerated by lowering the LUMO of the alkyne through introduction of electron withdrawing groups and thus increasing HOMO-LUMO interactions. Bertozzi and her coworkers pursued this further by synthesizing cyclooctynes substituted with various electron withdrawing groups (Figure 1.5). They found that introduction of single fluorine (MOFO **1.33**) accelerated the cycloaddition reaction by three fold whereas introduction of the second fluorine (DIFO **1.34-1.35**) increased the rate by 60 fold relative to cyclooctyne **1.32**.<sup>36</sup> But these cyclooctynes generally had solubility issues in water. To overcome these solubility issues in aqueous media, Bertozzi's group synthesized cyclooctyne **1.36**, a dimethoxy azacyclooctyne where heteroatoms are incorporated in the ring to improve hydrophilicity.<sup>46</sup> Boons and coworkers synthesized dibenzocyclooctynol **1.37** (DIBO) where the cyclooctyne ring is sandwiched between two aromatic rings. **1.37** showed increased reactivity for the cycloaddition with azides because of increased ring strain imposed by the aromatic rings.<sup>47</sup> Debets and coworkers synthesized an aza-dibenzocyclooctyne **1.38**, suitable for biological applications such as PEGylation of proteins by combining the favorable kinetics of Boons's DIBO (**1.37**) and increased hydrophilicity of Bertozzi's (**1.36**).<sup>48</sup> Bertozzi's group synthesized improved DIBO

**1.39** by incorporating an amide bond in the cyclooctyne ring which showed very high reactivity and hydrophilicity for the cycloaddition with azide.<sup>49</sup> The same group has also synthesized difluorobenzocyclooctyne (DIFBO) **1.40**, a hybrid of DIFO and DIBO to obtain a cyclooctyne which was more reactive than either of its parent molecules and underwent homotrimerization in solution. Consequently, **1.40** was isolated as an inclusion complex with  $\beta$ -cyclodextrin.<sup>50</sup> These functionalized cyclooctynes have been utilized in biological applications as represented in Figure 1.6. They have been used in PEGylation of enzymes, to label cells containing surface glycoproteins, to react with azides incorporated into cell-surface glycans via unnatural sugars, to monitor protein-protein interactions in non-ribosomal peptide biosynthesis, and in synthesizing crosslinking photodegradable star polymers.<sup>30,36,40,44,51</sup>

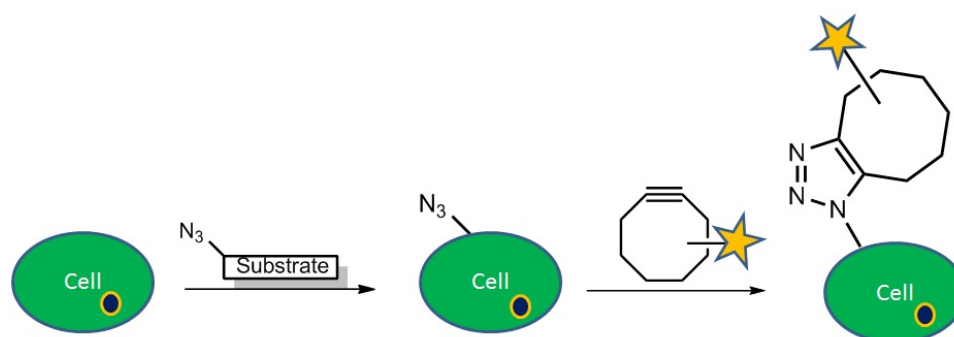


Figure 1.6. Schematic representation of application of cyclooctynes in biological systems

### 1.8 Multivalent ligand approach

The effective treatment of tumor malignancies by killing or inhibiting cancer cells with minimum deleterious effects on normal cells is the major goal of cancer diagnosis and therapy. The majority of available cancer diagnosis and

therapy approaches target specific genes or overexpressed cell receptors in malignant cells.<sup>52</sup> Increasingly, evidence indicates that many cell surface receptors exist as homo- and/or hetero-oligomers. Potential interaction of oligomeric receptors with homo- or heterovalent ligands may result in binding with enhanced affinity (avidity) and specificity compared to monovalent ligands.<sup>53-</sup><sup>55</sup> Homo-multivalent ligands consist of multiple copies of the same ligand connected by an appropriate linker, whereas hetero-multivalent ligands consist of different ligands assembled in the same molecule. Homo-multimeric ligands may display enhanced binding to homo-oligomeric cell surface assemblies, while hetero-multimeric ligands may selectively bind to specific hetero-oligomeric cell surface receptor assemblies. For example, Handl and coworkers found that homo-bivalent NDP- $\alpha$ -MSH(7) peptide ligands exhibited more than tenfold affinity compared to monovalent MSH(7) for binding to the GPCR (G-protein coupled receptor) melanocortin receptor subtype 4.<sup>56</sup> In these studies, it is impossible to differentiate noncovalent crosslinking of receptors from statistical effects in multivalent ligand-receptor interactions.<sup>57,58</sup> Hetero-multivalent ligands target different receptor combinations and thus enable researchers to specifically target cancer cells using unique combinations expressed in malignant cells compared to normal cells. Cell receptor oligomers such as GPCR dimers are located at certain distances from each other and multivalent ligands must have a proper linker length to bind effectively and achieve enhanced binding affinity. It is estimated by Monguchi and coworkers from GPCR dimer modeling studies that the average distance between adjacent receptors is about 25-50 Å, and may increase up to 100 Å.<sup>59</sup> So, linker length is an important factor in designing multivalent ligands, and information about cross linking and statistical binding in cells can be extracted by varying linker length. Linkers are also required to have a balance between flexibility, rigidity and favorable conformation with minimum

entropic penalty. Linker-ligand assemblies must also possess good physiochemical properties such as solubility, low non-specific binding, and low toxicity.<sup>58,60</sup> Multivalent radionuclide targeting may represent the next generation of radioimaging and radiotherapeutic agents. While this area has not been extensively explored, the synthesis of multivalent ligand-DOTA conjugates for investigation of multivalent radioimaging has been reported.<sup>61-67</sup>

### 1.9. Conclusion

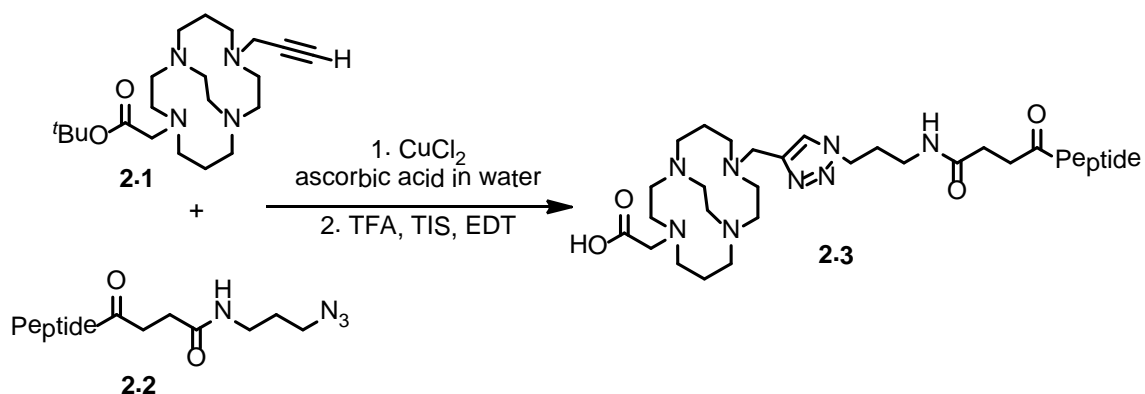
Bifunctional chelators play significant roles in target-specific molecular imaging, diagnosis and therapy of cancer. Even though many methods are available to conjugate chelators, radionuclides and biomolecules, issues with synthetic efficiency, purification, and preparation time persist. As an alternative, copper(I) catalyzed 1,3-dipolar cycloaddition “click reaction” of an alkyne and an azide has been used to obtain BFCs in very high yield and shorter time, but removal of trace amounts of toxic copper catalyst from the BFC's is challenging. Copper-free click reactions involving activated cyclooctynes with azides to yield stable triazoles is a substitute for CuAAC and has found applications in biological systems. The development of novel methods for the synthesis and application of BFCs incorporating monovalent as well as multivalent ligands has significant prospects in target specific molecular imaging.

## CHAPTER TWO

### BIFUNCTIONAL CYCLOOCTYNES AND THEIR APPLICATION IN RADIONUCLIDE CHEMISTRY

#### 2.1 Introduction

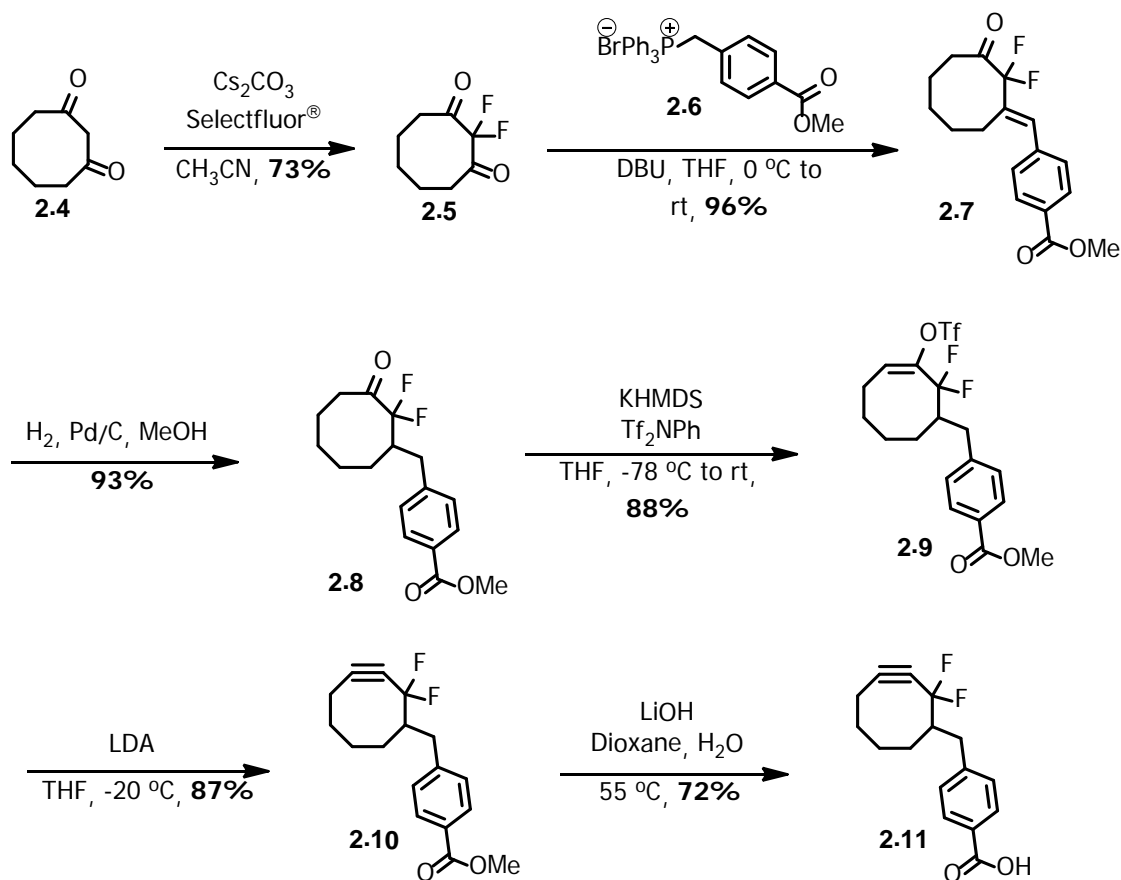
Cancer is one of the world's leading causes of premature human death. Diagnosis and therapy of malignant tumors at early stages would reduce these numbers. Positron Emission Tomography (PET) and Single Photon Emission Computed Tomography (SPECT) imaging techniques are widely used to diagnose malignancies.<sup>2,3</sup> Bifunctional radionuclide chelators such as 1,4,7,10-tetraazacyclododecane-1,4,7,10-tetraacetic acid (DOTA) provide critically needed stable radiometal complexes for targeted diagnostics and therapeutics.<sup>6,61</sup> A challenge in designing new radioimaging and radiotherapy agents concerns developing efficient methods for attaching metal chelators to various biotargeting moieties (such as peptides, RNA, or sugars). Many methods to synthesize bifunctional DOTA derivatives have been reported in the literature, but issues related to synthetic utility and efficiency persist. This is because often the synthesis of chelators and their conjugation to biomolecules consists of lengthy synthetic sequences, extensive protection and deprotection strategies and tedious, inefficient purifications. So called "click" chemistry offers an attractive, efficient method for bioactive molecule syntheses (Scheme 2.1).<sup>17</sup> However, the need for a metal catalyst reduces the enthusiasm for this approach. In this context, "click chemistry" involving activated cyclooctynes and an azide is emerging as the alternative solution for achieving bio-orthogonal biomolecule conjugation.



Scheme 2.1. Synthesis of chelator-biomolecule using copper(I) catalyzed click chemistry

## 2.2 Background

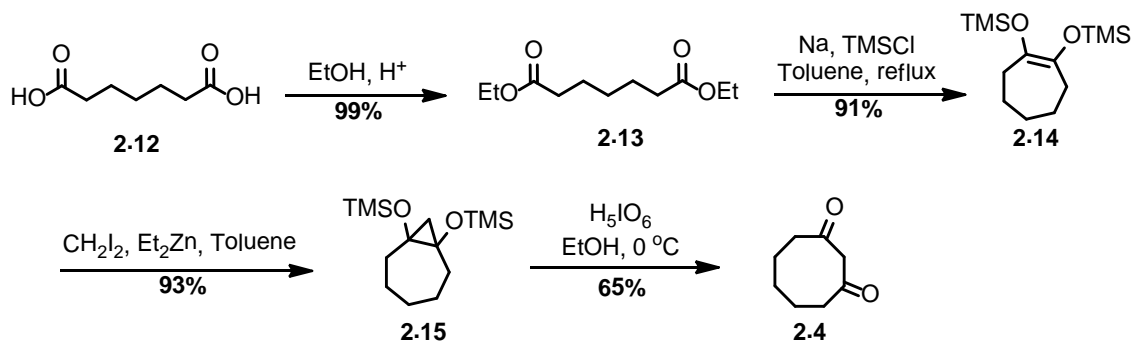
We are interested in synthesizing chelator biomolecules for applications in radioimaging, diagnosis and therapy for a collaborative project. Attempts to prepare various DOTA-biomolecule conjugates using copper(I) catalyzed azide–alkyne chemistry by our collaborators met with limited success. Efforts to remove the copper catalyst from reaction mixtures using sodium sulfide resulted in the destruction of the biomolecule. As an alternative approach, we decided to investigate the use of strain induced click chemistry to achieve chelator bioconjugation under copper-free conditions. Specifically, cyclooctynes have been shown to undergo spontaneous cycloadditions with azides under mild reaction conditions. A particularly reactive cyclooctyne (DIFO, **2.11**) has been reported by Bertozzi and co-workers.<sup>43</sup> In addition to bio-orthogonal reactivity, **2.11** also displays excellent stability. Thus, we initially envisioned utilizing DIFO **2.11** as a lynchpin reagent for conjugation of radiochelators to bio-targeting groups via copper-free click chemistry.



Scheme 2.2. Synthesis of DIFO (**2.11**) using Bertozzi's approach

Bertozzi's DIFO (**2.11**) has a good kinetic profile (second order rate constant is  $k = 4.2 \times 10^{-2} \text{ M}^{-1}\text{s}^{-1}$ ) for the cycloaddition reaction with benzyl azide and it can be prepared in good overall yield from the known diketone **2.4** (Scheme 2). But in reality, starting material diketone (**2.4**) has to be synthesized using a synthetic route published by Pirrung and coworkers from commercially available pimelic acid (Scheme 2.3).<sup>68</sup> The synthesis of the diketone **2.4** began with the esterification of pimelic acid to obtain ethyl pimelate **2.13**. This, on treatment with sodium metal and TMSCl, yielded compound **2.14** through a silyl-acyloin condensation reaction. Substrate **2.14** on Simmons-Smith

cyclopropanation using  $\text{CH}_2\text{I}_2$  and  $\text{Et}_2\text{Zn}$  afforded **2.15** which, on oxidative cleavage using periodic acid, gave the required diketone **2.4**.



Scheme 2.3. Synthesis of 1,3-diketone (**2.4**) using Pirrung's method

Using the protocol reported by Bertozzi's group (Scheme 2.2), the diketone (**2.4**) was difluorinated using Selectfluor<sup>®</sup> to yield compound **2.5** which underwent Wittig reaction with substrate **2.6** to give the mono olefinated product (**2.7**). Hydrogenation of **2.7** produced intermediate **2.8** which, on treatment with KHMDS and  $\text{Tf}_2\text{NPh}$ , yielded the vinyl triflate **2.9**. On base induced elimination using LDA, this vinyl triflate (**2.9**) formed the cyclooctyne (**2.10**) which, on saponification, produced **2.11**. This synthesis of DIFO (~ 12 steps) was time consuming and utilized expensive reagents. We felt we needed a more reliable, reproducible, and fast synthetic route to a bifunctional cyclooctyne in order to adequately explore the feasibility of metal-free click radiochelator bioconjugation. As part of an effort to circumvent some of the shortcomings in Bertozzi's cyclooctyne **2.11**, we undertook the design and synthesis of a simpler bifunctional cyclooctyne derivative with the idea of facilitating chelator-biomolecule conjugation via Cu-free click chemistry.

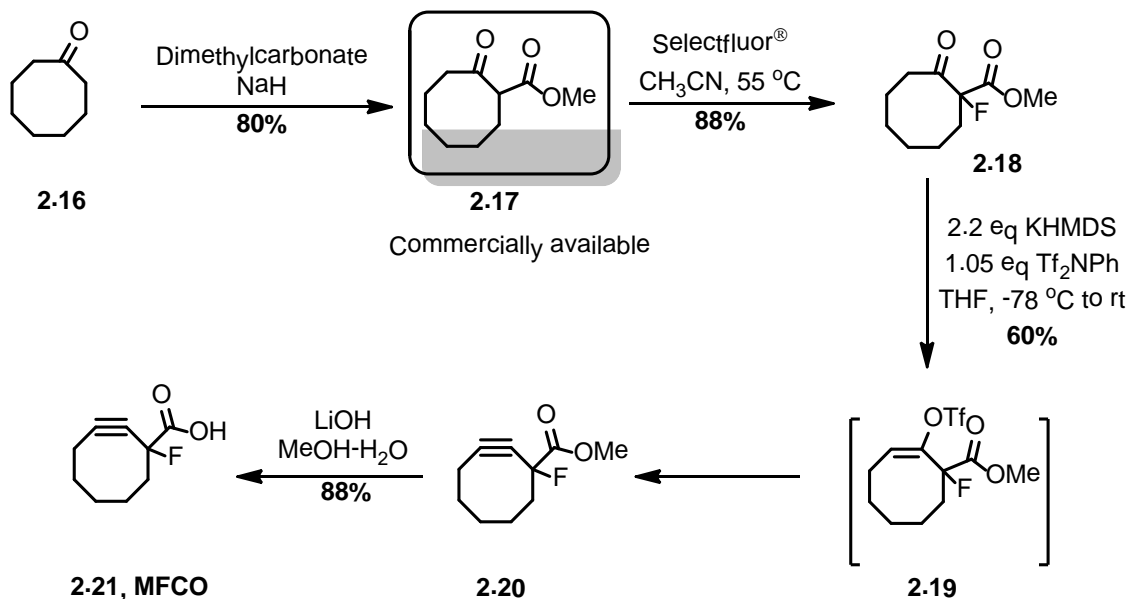


## 2.3 Results and discussion

### **Synthesis of activated cyclooctyne derivative**

We successfully designed and synthesized an activated cyclooctyne as shown in Scheme 2.4.<sup>69</sup> We envisioned that the cyclooctyne should have at least one fluorine group next to the alkyne to activate it for the cycloaddition reaction. An electron withdrawing carboxyl group was used instead of the second fluorine at the  $\alpha$ -position. This carboxyl group could be used to activate the alkyne for the click chemistry as well as a functional group handle for further manipulation. Thus, the bifunctional monofluorinated cyclooctyne (MFCO) should have reasonable kinetic profile for the 1,3-dipolar cycloaddition reaction. Importantly, the projected synthesis of MFCO could proceed from commercially available starting material in a minimal number of steps and so should be able to available in much greater quantities than cyclooctynes requiring more labor-intensive syntheses.

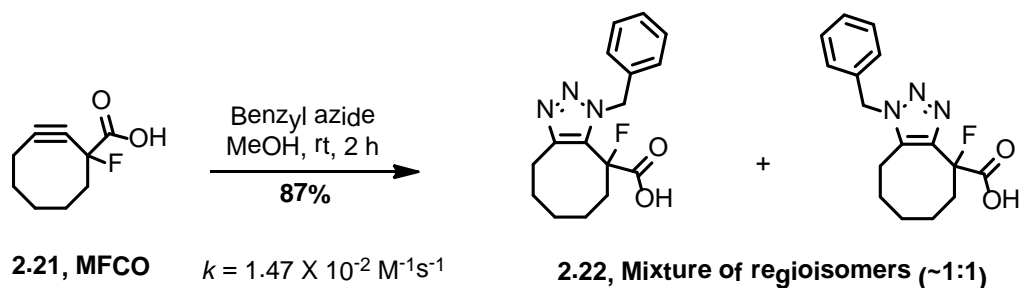
Our synthetic strategy began with the conversion of commercial cyclooctanone **2.16** into the  $\beta$ -keto ester **2.17** (commercially available but expensive) by treating with dimethylcarbonate and sodium hydride (Scheme 2.4).<sup>70</sup> Intermediate **2.17** was then fluorinated using Selectfluor<sup>®</sup> to give the monofluorinated compound **2.18** in excellent yield.<sup>71</sup> Compound **2.18** was then converted into the desired cyclooctyne **2.20** by elimination of the *in situ* generated vinyl triflate **2.19** in good yield. Saponification of methyl ester **2.20** afforded monofluorinated cyclooctyne (MFCO, **2.21**) in good yield. All the intermediates and the MFCO were stable under the reaction conditions and purification using silica gel column chromatography. MFCO was found to be stable at -25 °C for a few days. but decomposition was observed after storing for a few weeks at -25 °C.



Scheme 2.4. Synthesis of MFCO (**2.21**)

Next, the reactivity of MFCO (**2.21**) was probed using a model reaction with benzyl azide in methanol at room temperature. The expected triazole product (**2.22**) was obtained as a mixture of regioisomers in good yield (Scheme 2.5). The next aim was to examine the kinetic profile of the MFCO (**2.21**) in this 1,3-dipolar cycloaddition reaction. Kinetic studies were performed to determine the second order rate constant ( $k$ ) for the click reaction with benzyl azide in CD<sub>3</sub>CN using <sup>1</sup>H NMR. A plot of 1/[azide] vs time was analyzed using linear regression methods and the rate constant was determined to be  $(1.47 \pm 0.21) \times 10^{-2} \text{ M}^{-1}\text{s}^{-1}$  (see experimental section for details). As expected, the rate of cycloaddition is slower than the same reaction using Bertozzi's DIFO (**2.11**,  $k = 4.2 \times 10^{-2} \text{ M}^{-1}\text{s}^{-1}$ ), but one order of magnitude faster than the monofluorinated cyclooctyne (**1.3**) (see figure 1.5, Chapter One).<sup>45</sup> The kinetic profile of MFCO also compares favorably with other cyclooctynes used in Cu-free click reactions,

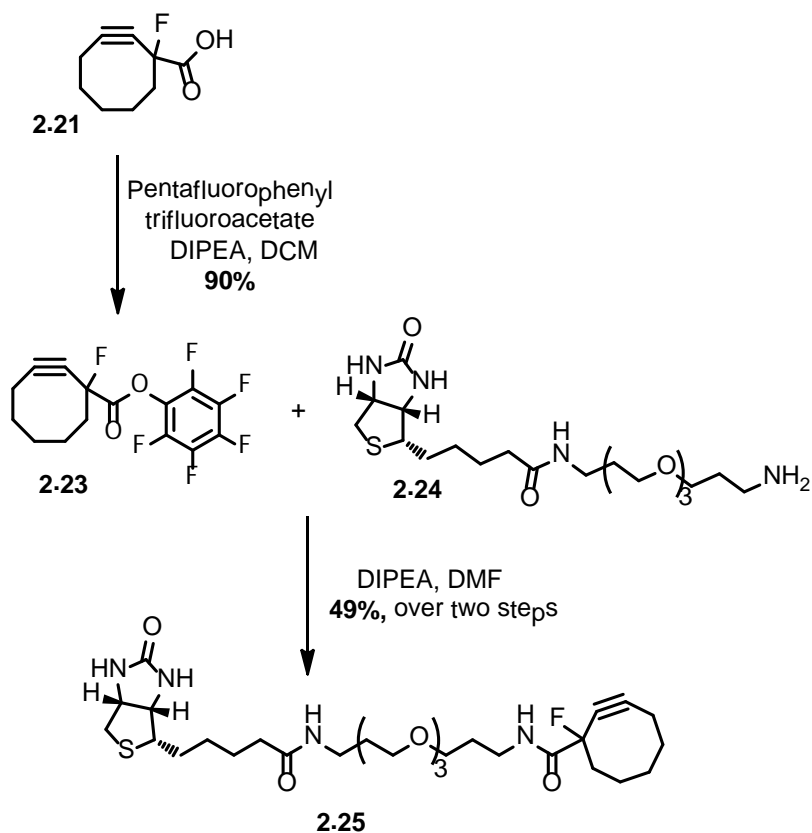
and its synthesis is much simpler than many other cyclooctynes (see Figure 1.5, Chapter One).



Scheme 2.5. Click reaction of MFCO (**2.21**) with benzyl azide

### Bifunctional biomolecule-chelator synthesis using MFCO

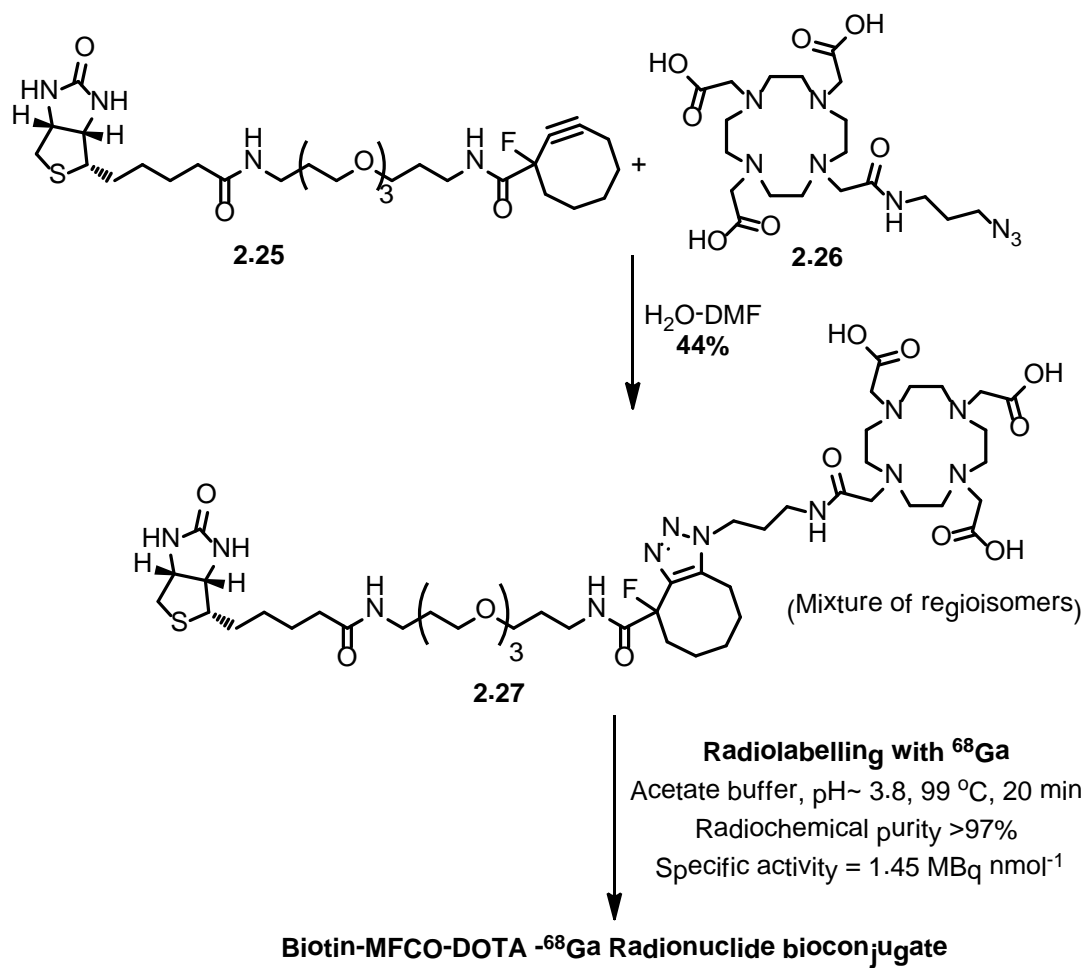
With MFCO (**2.21**) in hand, we sought to demonstrate the feasibility of our coupling strategy by conjugating a prototypical bioligand (biotin) to a DOTA derivative. First, a pentafluorophenyl ester of MFCO (**2.23**) was prepared by treating with pentafluorophenyltrifluoroacetate in the presence of diisopropylethylamine.<sup>43,72</sup> This activated ester was then used without further purification to acylate amine functionalized biotin (**2.24**) in DMF to give biotin-MFCO derivative **2.25** (Scheme 2.6).<sup>72,73</sup>



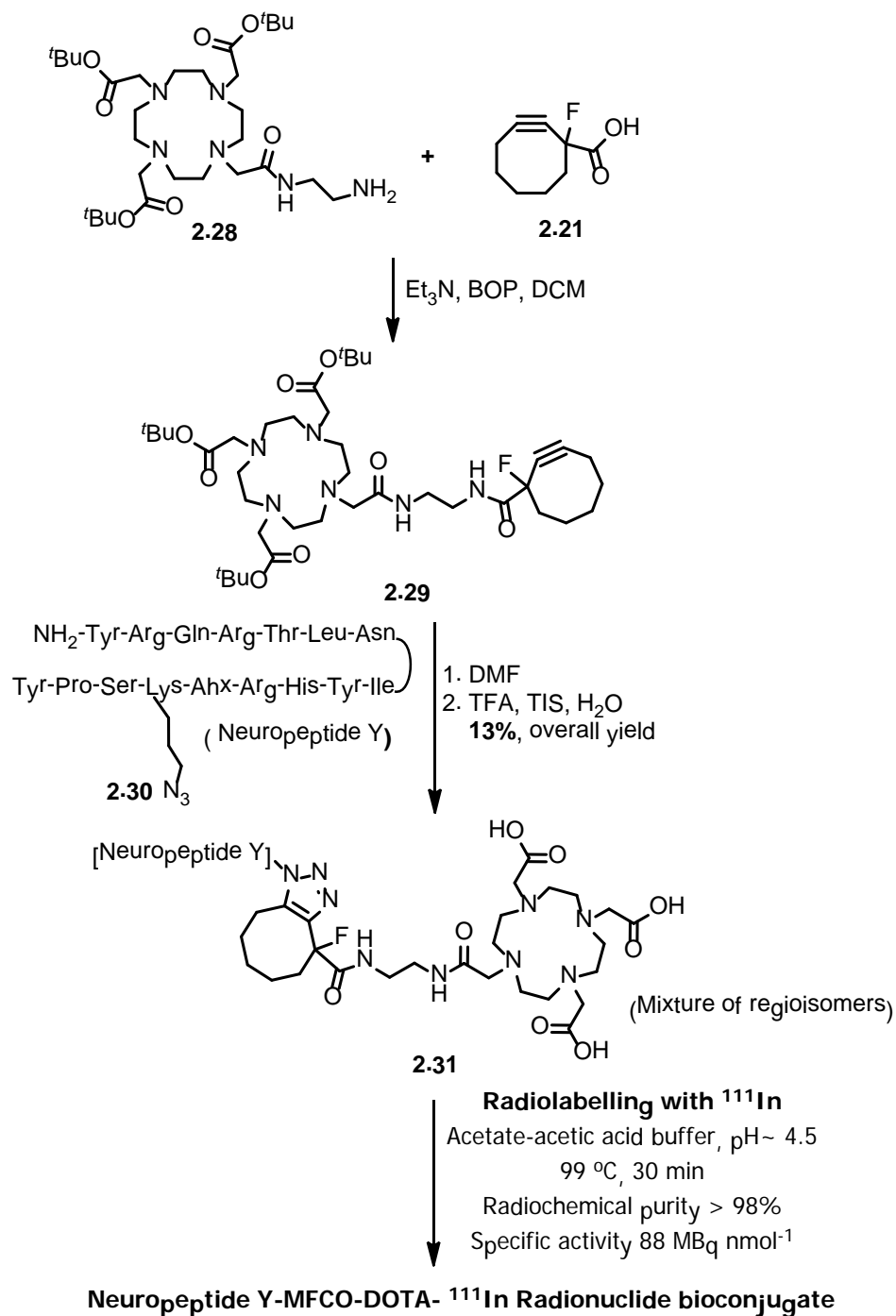
Scheme 2.6. Synthesis of Biotin-MFCO (**2.25**)

MFCO-biotin derivative (**2.25**) was then conjugated to a fully deprotected azide modified DOTA chelator (**2.26**) via ring strain promoted cycloaddition in aq. DMF to obtain DOTA-biotin conjugate (**2.27**) in good isolated yield after HPLC purification (Scheme 2.7). This product was then successfully labeled with  $^{68}\text{Ga}$  to afford a radiolabelled adduct in high specific activity and high radiochemical purity. This radiolabelling study was performed by our collaborators in the Department of Radiology, University of Iowa. This synthesis of DOTA-MFCO-Biotin showed us that MFCO can act as a lynchpin for the conjugation studies and supported our concept of preparing DOTA-biomolecules for radionuclide chemistry.

Inspired by this success, we focused on reversing the conjugation sequence using MFCO. We thought that if we could couple a chelator to MFCO and then use click chemistry to attach the biomolecule that would increase the versatility of MFCO-based chelator-bioconjugation strategies. In a specific study using solid phase synthesis, the cyclooctyne MFCO (**2.21**) was coupled to amine modified DOTA chelator (**2.28**) through an amide linkage to give compound **2.29**.<sup>74</sup> DOTA-MFCO (**2.29**) was then subjected to cycloaddition with azide modified side chain of Lys incorporated into a neuropeptide Y analog (**2.30**) attached to Rink resin (Scheme 2.8).<sup>75</sup> The product **2.31** was then successfully cleaved from the resin and deprotected using TFA/TIS/water, precipitated in ice cold ether and purified by semipreparative HPLC (see experimental details). It was then radiolabelled with <sup>111</sup>In for potential imaging of neuroblastoma. This synthesis of **2.31** and subsequent radiolabelling study was performed by our collaborators in the Department of Radiology, University of Iowa.



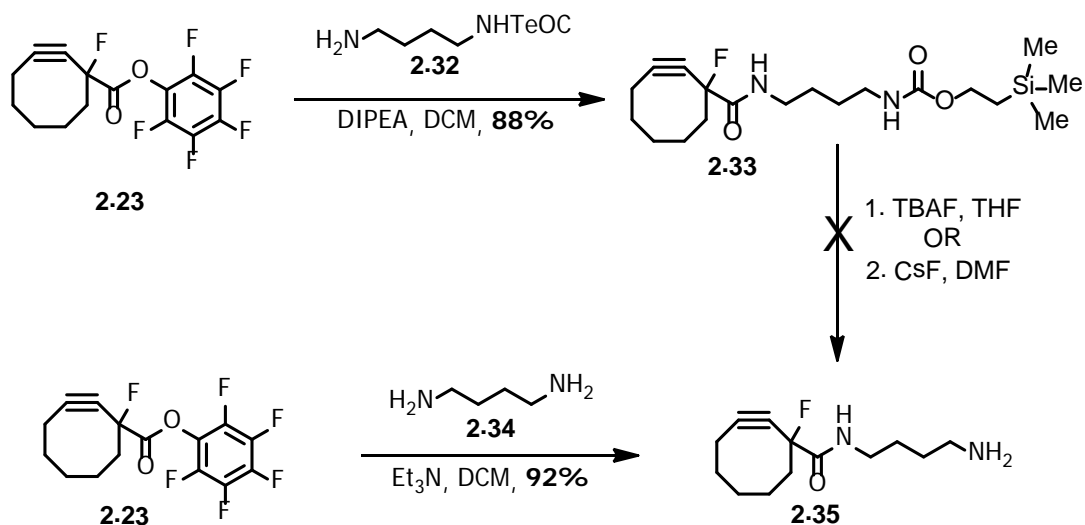
Scheme 2.7. Synthesis of bifunctional DOTA-MFCO-Biotin derivative (2.27)



Scheme 2.8. Synthesis of DOTA-MFCO-Neuropeptide Y conjugate (2.31)

## Synthesis and application of a MFCO-amine derivative

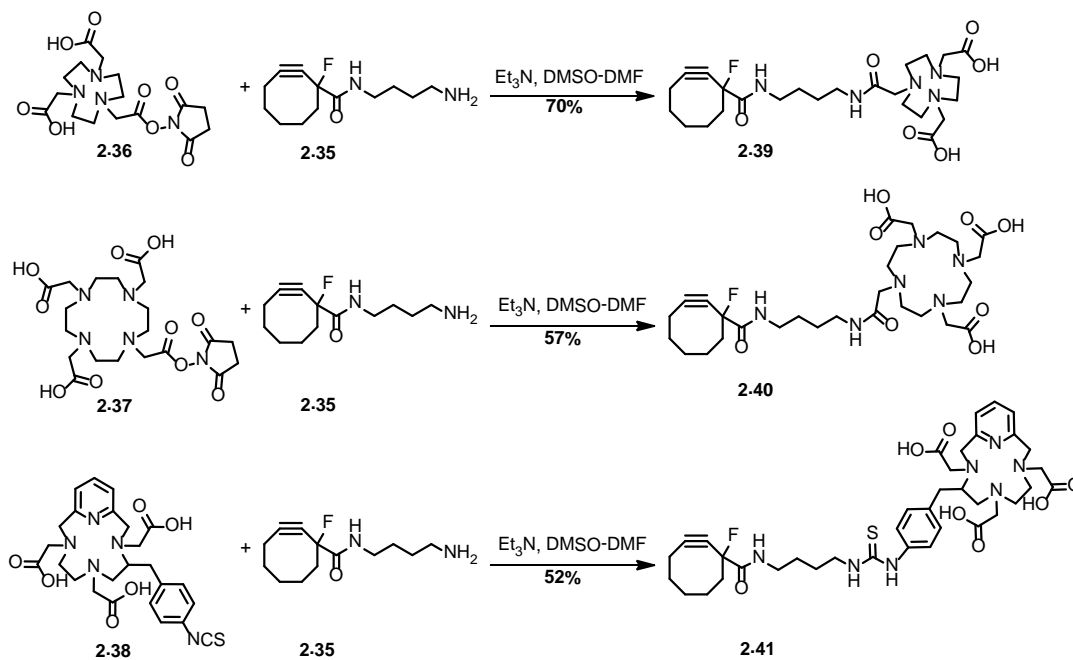
To complement our carboxylic acid functionalized cyclooctyne, we also designed an amine-modified MFCO so that we could easily attach our cyclooctyne reagent to activated esters, thereby expanding its utility in bioconjugation chemistry. Toward this end, amine-modified MFCO **2.35** was targeted (Scheme 2.9). In an initial approach, MFCO-PFP ester (**2.23**) was coupled to the mono N-TeOC protected 1,4-diamino butane (**2.32**) in DCM.<sup>76</sup> Unfortunately, attempts to deprotect the N-TeOC group of **2.33** using TBAF as well as CsF failed to produce the desired MFCO-amine derivative **2.35**.<sup>77,78</sup> Alternatively, MFCO-PFP ester (**2.23**) was treated directly with an excess of 1,4-diamino butane (**2.34**) and triethylamine in dichloromethane at room temperature to afford **2.35** in high yield.<sup>79</sup> MFCO-amine **2.35** was not stable to purification and so subsequent manipulations were performed using crude material isolated directly from reaction mixtures.



Scheme 2.9. Synthesis of MFCO-amine (**2.35**)



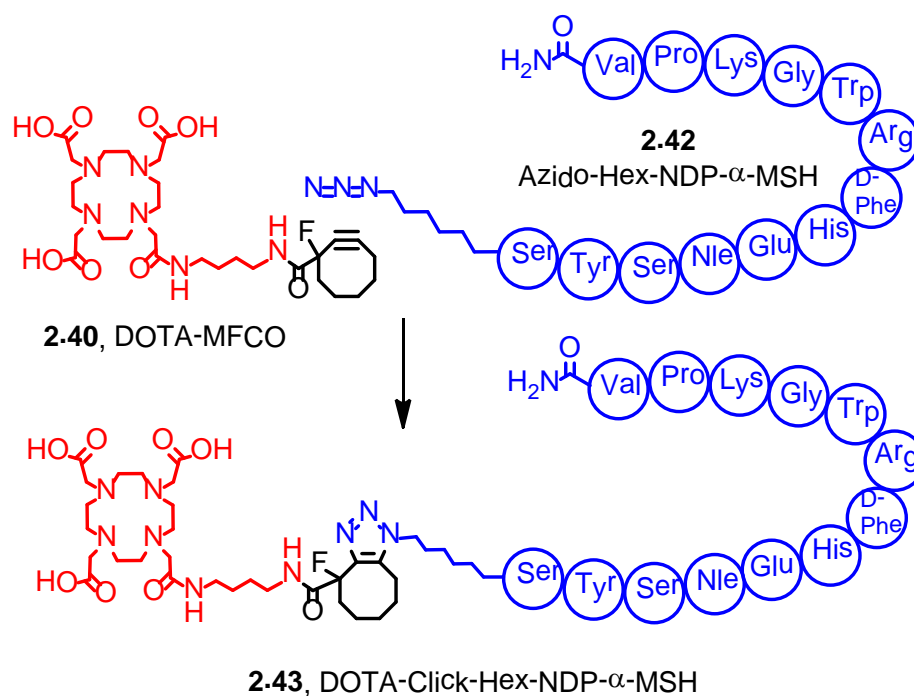
MFCO-amine (**2.35**) was then coupled to commercially available radionuclide chelators such as NOTA-NHS ester (**2.36**), DOTA-NHS ester (**2.37**), and PCTA-isothiocyanate (**2.38**) that possessed an activated acylating moiety (NHS ester or isothiocyanate). In each case the desired MFCO-chelators **2.39**, **2.40** and **2.41** were obtained in very good yield and high purity after HPLC purification (Scheme 2.10). A particularly notable feature of this procedure is that these substrates underwent coupling without any protecting group manipulation to yield desired chelator-cyclooctyne conjugates.



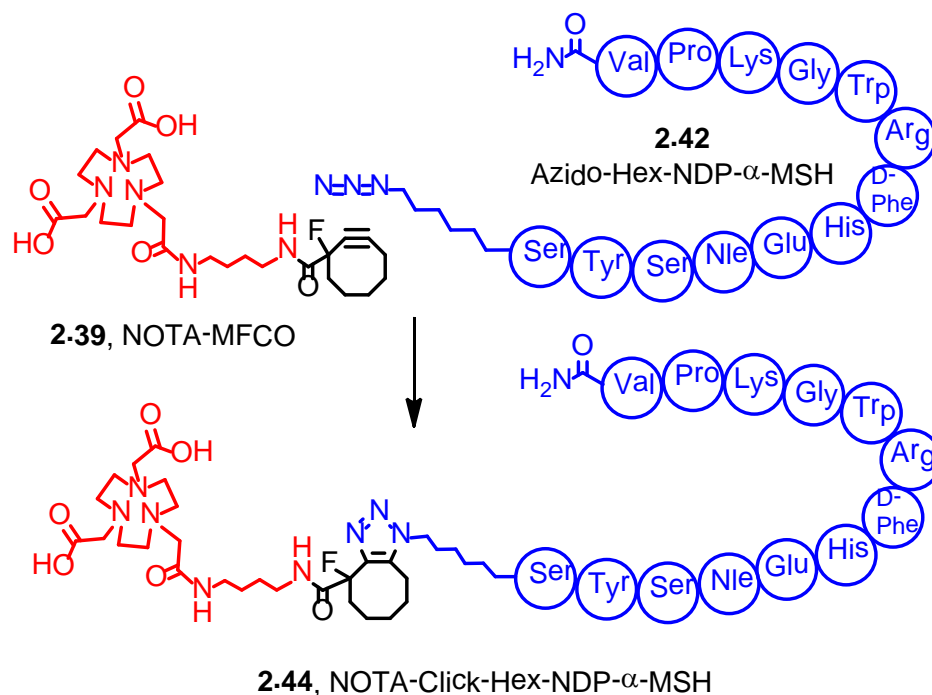
Scheme 2.10. Synthesis of Chelator-MFCO-amine conjugates

Next, the reactivity of these chelator-MFCO compounds was examined in click reactions with biologically significant molecules for eventual applications in cancer diagnosis and therapy. For this study, NDP- $\alpha$ -MSH, an analogue of  $\alpha$ -melanocortin-stimulating hormone ( $\alpha$ -MSH) which exhibits increased affinity for

MC1R, a cell surface receptor known to be expressed in melanoma cells, was chosen as the biomolecule component. DOTA-MFCO (**2.40**) and NOTA-MFCO (**2.39**) were conjugated to an azide-modified-NDP- $\alpha$ -MSH derivative (**2.42**) via copper free click reaction under aqueous conditions at room temperature to afford DOTA-click-hex-NDP- $\alpha$ -MSH product (**2.43**, 57%) (Scheme 2.11) and NOTA-click-hex-NDP- $\alpha$ -MSH (**2.43a**, 70%) (Scheme 2.12) respectively, in good isolated yield after HPLC purification. Radiolabelling with  $^{64}\text{Cu}$  and  $^{68}\text{Ga}$  was also successful and the corresponding radionuclide conjugates were obtained with very high radiochemical purity and specific activity (Figure 2.1).



Scheme 2.11. Synthesis of DOTA-click-hex-NDP- $\alpha$ -MSH derivative (**2.43**)



Scheme 2.12. Synthesis of NOTA-click-hex-NDP- $\alpha$ -MSH derivative (**2.44**)

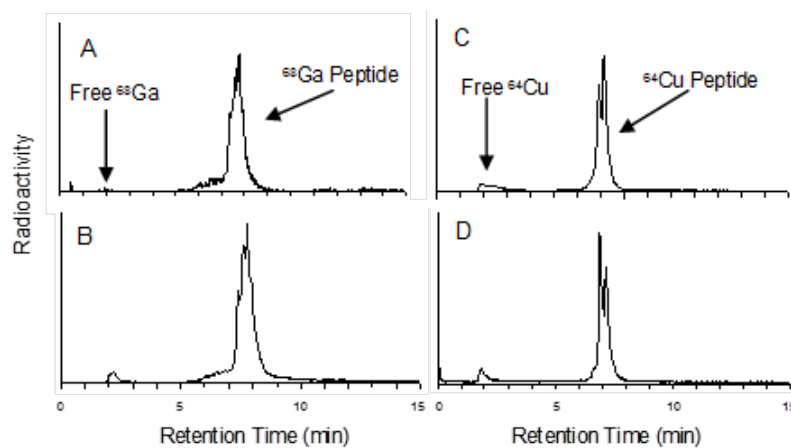


Figure 2.1. Radio-HPLC chromatogram for  $^{68}\text{Ga}$  and  $^{64}\text{Cu}$  labeled DOTA-click-hex-NDP- $\alpha$ -MSH (A and C) and NOTA-click-hex-NDP- $\alpha$ -MSH (B and D)

In vitro binding studies on B16-F10 mouse melanoma cells using  $^{125}\text{I}$ -NDP- $\alpha$ -MSH as the competitor were carried out to determine the effect of fused triazole-MFCO linkage on the stability and variation in binding affinity of the DOTA-click-hex-NDP- $\alpha$ -MSH (**2.43**) (D,  $\text{IC}_{50} = 0.76$  nM) and NOTA-click-hex-NDP- $\alpha$ -MSH (**2.44**) (E,  $\text{IC}_{50} = 0.82$  nM) relative to the NDP- $\alpha$ -MSH (A,  $\text{IC}_{50} = 0.21$  nM), azido-hex-NDP- $\alpha$ -MSH (B,  $\text{IC}_{50} = 0.25$  nM) and DOTA-amide-NDP- $\alpha$ -MSH derivatives (C,  $\text{IC}_{50} = 0.59$  nM) (Figure 2.2). It was found that  $\text{IC}_{50}$  values obtained for click chemistry-triazole products **2.43** and **2.44** were within the statistical uncertainty of DOTA-amide-NDP- $\alpha$ -MSH derivative which was prepared using standard amide coupling. *In vitro* binding assays suggested that the fused-triazole conjugation provides a stable coupling and does not significantly alter the binding affinity of the peptide for its cognate MC1R receptor (see experimental details).

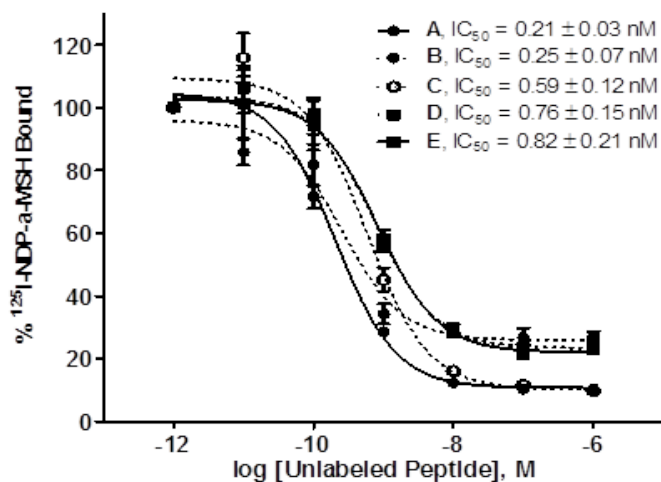


Figure 2.2. *In vitro* competitive binding studies of NDP- $\alpha$ -MSH derivatives. A = NDP- $\alpha$ -MSH; B = **2.42**; C = DOTA-amide-NDP- $\alpha$ -MSH; D = **2.43**; E = **2.44**.

Bio distribution and PET/CT imaging studies were performed using both  $^{68}\text{Ga}$ -DOTA-Hex-NDP- $\alpha$ -MSH and  $^{64}\text{Cu}$ -DOTA-Hex-NDP- $\alpha$ -MSH (see experimental details). Higher relative tumor accumulation and lower liver and blood accumulation was observed in the triazole conjugates as compared to results obtained using a simpler radiolabelled DOTA-amide-NDP- $\alpha$ -MSH variant (Figure 2.3). These results demonstrate biostability of our radioimaging click conjugates and augur well for the use of this methodology in design of more selective imaging and therapy agents.

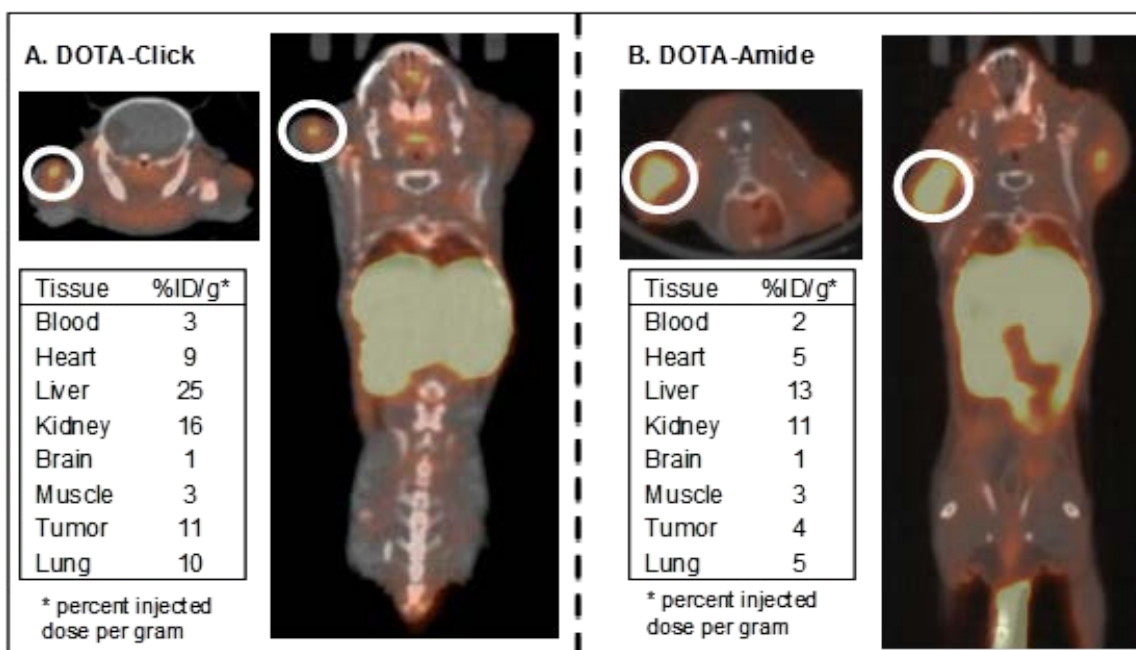
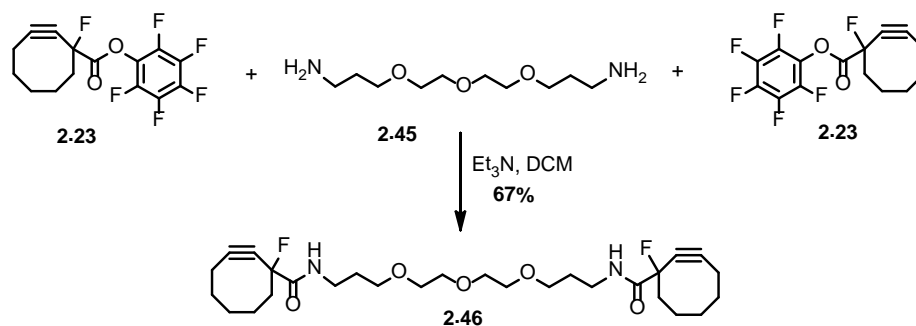


Figure 2.3. Bio distribution studies of  $^{68}\text{Ga}$ -DOTA-click-Hex-NDP- $\alpha$ -MSH (A) and  $^{68}\text{Ga}$ -DOTA-amide-Hex-NDP- $\alpha$ -MSH (B)

### Bis-MFCO derivative synthesis

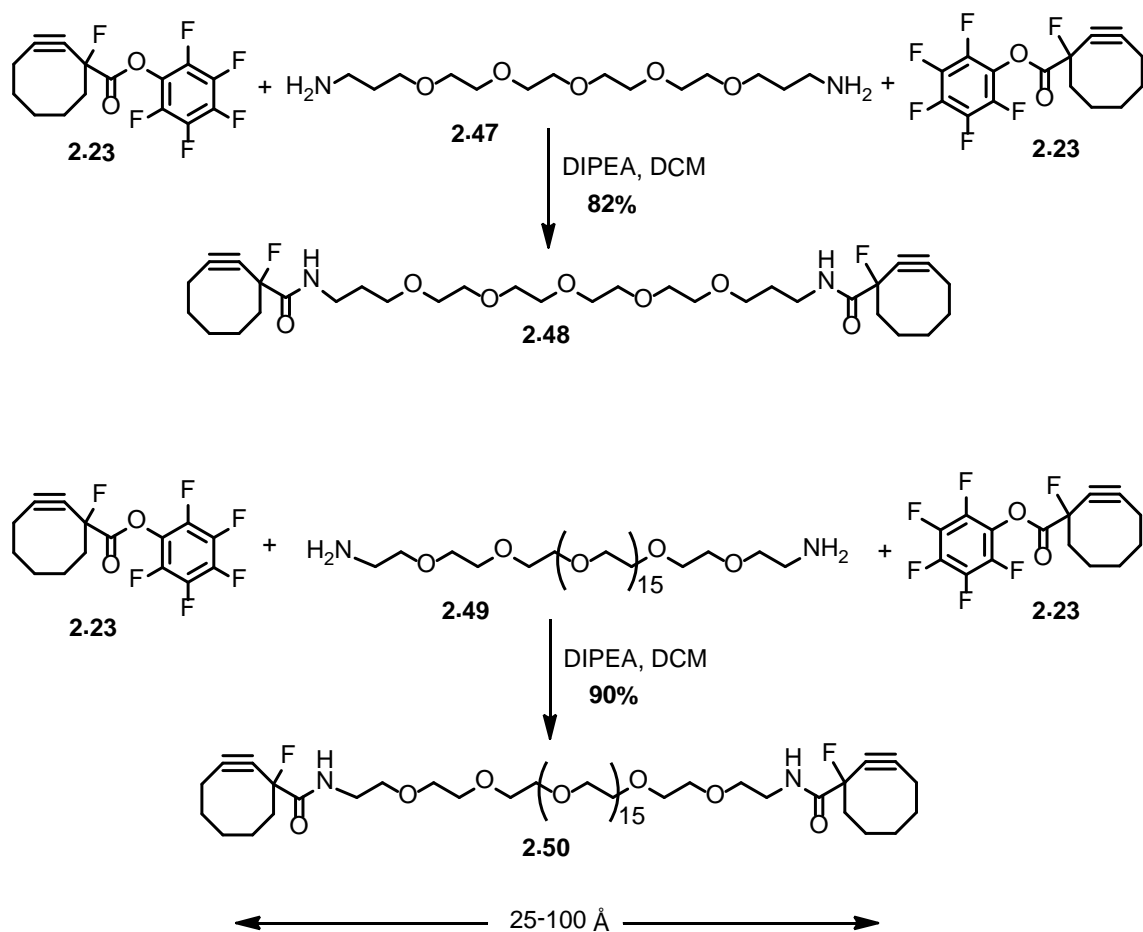
It has been reported in the literature that G protein-coupled receptors (GPCRs) form dimers or higher order oligomers on cell receptors. Melanocortin

receptors (such as MC1R) belong to the GPCR family of receptors and are potential targets for drugs of therapeutic value. It is hypothesized that dimeric or multimeric ligands capable of simultaneously binding to two or more members of a GPCR oligomeric assembly will exhibit increased binding affinity relative to monomeric analogues. Thus, homo-multivalent and hetero-multivalent radioimaging or radiotherapy ligands that target GPCR's expressed in cancer cells may exhibit greater selectivity and avidity for tumors over healthy cells. This hypothesis has been tested by Gillies and co-workers with promising results.<sup>56,57,59</sup> Significantly, our MFCO reagent seemingly offers a rapid means of assembling di- or multivalent ligand constructs. Our studies using monovalent  $\alpha$ -MSH-DOTA derivatives have shown promising results for the detection of metastatic melanoma cells in mice. To probe the potential of a multivalent ligand approach for the diagnosis and therapy of metastatic melanoma, we synthesized a series of bivalent cyclooctyne linkers that could be used to construct homo-divalent GPCR ligands. An example of a model reaction showing construction of bis(MFCO) construct **2.46** is shown in Scheme 2.13. A functional bivalent ligand could then be constructed from **2.46** via click reaction of each cyclooctyne with an azide-modified bio-molecule (such as azido-NDP- $\alpha$ -MSH).



Scheme 2.13. Synthesis of bis-MFCO-PEG-3-amide (**2.46**)

Modeling studies of GPCR dimers indicate that the distance between the two adjacent binding sites is in the range of 25-50 Å, and may increase up to 100 Å.<sup>59</sup> The linker structure and properties are also very important variables for successful bivalent ligand synthesis. The linker should have solubility, low toxicity and low nonspecific binding affinity. The linkers must also be flexible in order to accommodate multivalent interactions across variable distances while incurring minimal entropic penalties. Given the design criteria described above, the tris(PEG)-amine linker in **2.46** is clearly too short for use in divalent GPCR ligands. Thus, we have prepared additional bis(MFCO) analogues using longer PEG-amine linkers as shown in Scheme 2.14. Bis-MFCO-PEG-5 (**2.48**) and bis-MFCO-PEG-20 (**2.50**) were synthesized by treating MFCO-PFP ester (**2.23**) with corresponding PEG-amines (**2.47** and **2.49**, respectively) in good yields. The studies using these bivalent bis-MFCO linkers for bivalent homo and hetero ligand synthesis and their application in cancer diagnosis and therapy are underway in the laboratory of our collaborators. Preliminary results indicate that bivalent ligands derived from **2.50** targeting MC1R and endothelin-b (another GPCR expressed in melanoma cells) both display increased binding affinity as compared to monomeric ligands in *in vitro* cell binding assays.



Scheme 2.14. Synthesis of bis-MFCO linkers **2.47** and **2.49**

### 2.4 Conclusion

We have designed and synthesized a novel bifunctional monofluorinated cyclooctyne (MFCO) for copper free click chemistry. The synthesis of MFCO was achieved in three steps from commercial starting material in high overall yield (47%). Reasonable second order rate constant for the 1,3-dipolar cycloaddition reaction of MFCO with benzyl azide was determined in kinetic studies in CD<sub>3</sub>CN at room temperature. Conjugation of radiochelators to biomolecules was carried out using MFCO as a lynchpin. This allowed us to synthesize many chelator-biomolecule conjugates in straightforward fashion without additional tedious



protection, deprotection and purification steps. The chelator-biomolecules synthesized were radiolabelled with  $^{68}\text{Ga}$ ,  $^{64}\text{Cu}$  and  $^{111}\text{In}$  in very high radiochemical purity and specific activity. DOTA-click-Hex-NDP- $\alpha$ -MSH and NOTA-click-Hex-NDP- $\alpha$ -MSH were synthesized and radiolabelled with  $^{68}\text{Ga}$  and  $^{64}\text{Cu}$  successfully. *In vitro* binding assays using murine B16-F10 melanoma cells showed that the fused triazole products did not alter binding affinity of the peptides toward MC1R receptors expressed in these cells. Bio-distribution studies in mice showed promising results. Bis-MFCO-PEG molecules with different linker lengths were also synthesized for utilization in construction of flexible homo and hetero bivalent ligands for diagnosis and therapy of cancer cells. Finally, it is noteworthy that our MFCO reagent has been used for copper free click chemistry by other groups for various applications in bio-organic and material chemistry.<sup>80,81</sup> Additionally, activated MFCO derivatives are also available commercially.<sup>82</sup>

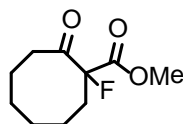
## 2.5 Experimental section

### **General experimental**

All commercially available starting materials and reagents were used as received unless otherwise noted. All the reactions were performed under argon atmosphere. Solvents were dried and purified by passage through activated alumina columns. Proton nuclear magnetic resonance ( $^1\text{H-NMR}$ ) spectra and carbon nuclear magnetic resonance ( $^{13}\text{C-NMR}$ ) spectra were recorded at 300 MHz and 75 MHz respectively. Chemical shifts are reported as  $\delta$  values in parts per million (ppm) relative to tetramethylsilane for  $^1\text{H-NMR}$  in  $\text{CDCl}_3$  and residual undeuterated solvent for all other spectra. IR spectra were recorded on a FT-IR spectrometer as thin films on sodium chloride discs. High resolution mass

spectra were obtained using electrospray ionization (ESI). Melting points were recorded using capillary melting point apparatus and are uncorrected.

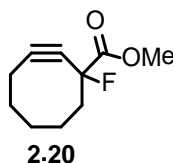
### Experimental procedures and characterization



**2.18**

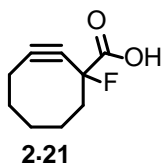
To a stirred solution of methyl-2-oxocyclooctane-1-carboxylate (12.5 g, 67.9 mmol, 1 equiv) in dry CH<sub>3</sub>CN at 0 °C was added Selectfluor<sup>®</sup> (28.9 g, 81.5 mmol, 1.2 equiv). The resulting mixture was then heated in a 55 °C oil bath for 8 h (of which time TLC indicated completion of the reaction). After cooling to room temperature the reaction mixture was quenched with water (200 mL) and extracted with ethyl acetate (4 x 100 mL). The combined organics were dried (anhydrous Na<sub>2</sub>SO<sub>4</sub>), filtered, and evaporated in vacuum to yield a clear oil which was then dissolved in CH<sub>2</sub>Cl<sub>2</sub> and passed through a silica plug to collect pure product **2.18** as white solid (12.0 g, 87.5%).

M.p. 42-45 °C. <sup>1</sup>H NMR (300 MHz, CDCl<sub>3</sub>), δ (ppm): 3.81 (s, 3H), 2.78-2.48 (m, 3H), 2.31-2.21 (m, 1H), 2.04-1.89 (m, 2H), 1.76-1.63 (m, 3H), 1.53-1.45 (m, 3H). <sup>13</sup>C NMR (75 MHz, CDCl<sub>3</sub>), δ (ppm): 208.9 (d,  $J_{C-F}^2 = 22.5$  Hz), 167.6 (d,  $J_{C-F}^2 = 24.8$  Hz), 99.3 (d,  $J_{C-F} = 199.3$  Hz), 53.4, 39, 33.5 (d,  $J_{C-F}^2 = 21.9$  Hz), 27.6, 26.6, 24.5, 21.4. IR (film): 2923, 2853, 1751, 1713 cm<sup>-1</sup>. HRMS (ESI): calculated for C<sub>10</sub>H<sub>15</sub>FO<sub>3</sub>Na [M + Na]<sup>+</sup>, 225.0903; found 225.0886.



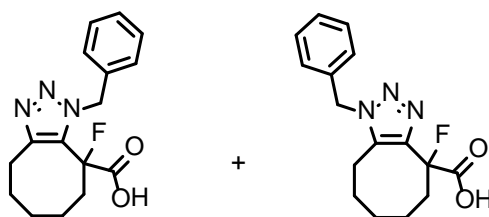
A solution of KHMDS (0.5 M in toluene, 44.6 mL, 22.3 mmol, 2.25 equiv) was added dropwise to the stirred solution of **2.18** (2.00 g, 9.9 mmol, 1 equiv) in THF (125 mL) at -78 °C. After the addition was complete, the reaction mixture was stirred for 30 min at the same temperature. Then Tf<sub>2</sub>NPh (3.89 g, 10.89 mmol, 1.1 equiv) in THF (25 mL) was added slowly via syringe. The reaction was stirred at -78 °C for an hour, and then slowly warmed to room temperature and stirred for an additional 5 h. CH<sub>3</sub>OH was then added and reaction mixture was concentrated in vacuum. The crude residue was purified by column chromatography on silica gel using 2-5% EtOAc in hexanes to afford **2.20** as pale yellow liquid (1.10 g, 60%).

<sup>1</sup>H NMR (300 MHz, CDCl<sub>3</sub>), δ (ppm): 3.83(s, 3H), 2.41-2.20 (m, 4H), 2.06-1.85 (m, 4H), 1.77-1.66 (m, 1H), 1.50-1.43(m, 1H). <sup>13</sup>C NMR (75 MHz, CDCl<sub>3</sub>), δ (ppm): 169.0 (d,  $J_{C-F}^2 = 29.9$  Hz), 108.7 (d,  $J_{C-F}^3 = 10.1$  Hz), 92 (d,  $J_{C-F} = 184.8$  Hz), 86.9 (d,  $J_{C-F}^2 = 31.6$  Hz), 53.4, 46.4 (d,  $J_{C-F}^2 = 24.8$  Hz), 33.9, 29.2, 25.6, 20.7. IR (film): 2929, 2853, 2223, 1751 cm<sup>-1</sup>. HRMS (ESI): calculated for C<sub>10</sub>H<sub>13</sub>FO<sub>2</sub>Na [M + Na]<sup>+</sup>, 207.0797, found 207.0786.



Ester substrate **2.20** (0.65 g, 3.53 mmol, 1 equiv) and Lithium hydroxide (0.17 g, 7.07 mmol, 2 equiv) were combined in ~10 mL of 50% aqueous methanol. The reaction mixture was heated in a 50 °C oil bath for 10 min. Then the reaction was stirred at room temperature for an additional 2 h. The reaction mixture was cooled to 0 °C and diluted with water, acidified to pH ~ 2 with dilute aq. HCl solution. The mixture was extracted with EtOAc (3 X 50 mL) and the combined organic layer was dried over anhydrous Na<sub>2</sub>SO<sub>4</sub>, filtered and evaporated in vacuum. The crude product was purified by silica gel column chromatography using 50% EtOAc in hexanes to afford yellow liquid **2.21** (0.48 g, 80%).

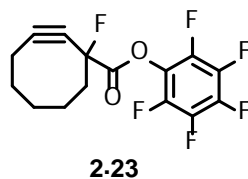
<sup>1</sup>H NMR (300 MHz, CDCl<sub>3</sub>), δ (ppm): 2.45-2.30 (m, 4H), 2.07-1.86 (m, 4H), 1.78-1.68 (m, 1H), 1.52-1.45 (m, 1H). <sup>13</sup>C NMR (75 MHz, CDCl<sub>3</sub>), δ (ppm): 173.7 (d,  $J_{C-F}^2 = 29.1$  Hz), 109.6 (d,  $J_{C-F}^3 = 9.9$  Hz), 91.6 (d,  $J_{C-F} = 185.8$  Hz), 86.2 (d,  $J_{C-F}^2 = 31.7$  Hz), 46.4 (d,  $J_{C-F}^2 = 24.6$  Hz), 33.9, 29.1, 25.6, 20.7. IR (film): 3474, 2932, 2850, 2220, 1732 cm<sup>-1</sup>. HRMS (ESI): calculated for C<sub>9</sub>H<sub>10</sub>FO<sub>2</sub> [M - H]<sup>-</sup>, 169.0665, found 169.0671.



**2.22, Mixture of regioisomers (~1:1)**

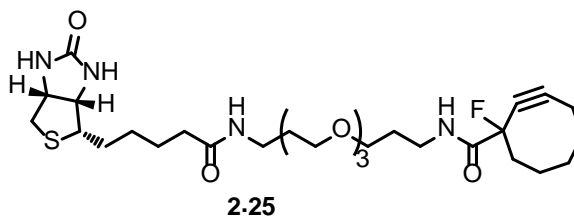
Benzyl azide (59 mg, 0.44 mmol, 1.25 equiv) and cyclooctyne **2.21** (60 mg, 0.353 mmol, 1 equiv) were stirred at room temperature in methanol (3 mL) for 2 h. The reaction mixture was then evaporated under vacuum and the crude product was purified on silica gel column chromatography using 50% ethyl acetate in methanol to obtain a white gummy solid **2.22** as an inseparable mixture of regioisomers (93 mg, 87%).

$^1\text{H}$  NMR (300 MHz, MeOD, mixture of regioisomers),  $\delta$  (ppm): 7.34-7.16 (m, 5H), 5.62-5.59 (m, 2H), 3.20-3.12 (m, 1H), 3.01-2.90 (m, 1H), 2.74-2.37 (m, 2H), 1.91-1.26 (m, 6H).  $^{13}\text{C}$  NMR (75 MHz,  $\text{CD}_3\text{OD}$ , mixture of regioisomers),  $\delta$  (ppm): 171.9 (d,  $J_{\text{C-F}} = 28.2$  Hz), 146.4, 137.1, 136.8, 133.0 (d,  $J_{\text{C-F}} = 23.2$  Hz), 130.2, 129.7, 129.5, 129.2, 128.7, 128.3, 91.8 (d,  $J_{\text{C-F}} = 184$  Hz), 54.2, 54.1, 52.8, 35 (d,  $J_{\text{C-F}} = 22$  Hz), 34.4, 27.6, 26.1, 25.8, 24.8, 24.3, 23.6, 22.1. IR (film): 3417, 2929, 2856, 1736  $\text{cm}^{-1}$ . HRMS (ESI): calculated for  $\text{C}_{16}\text{H}_{19}\text{FN}_3\text{O}_2$   $[\text{M} + \text{H}]^+$ , 304.1461, found 304.1449.



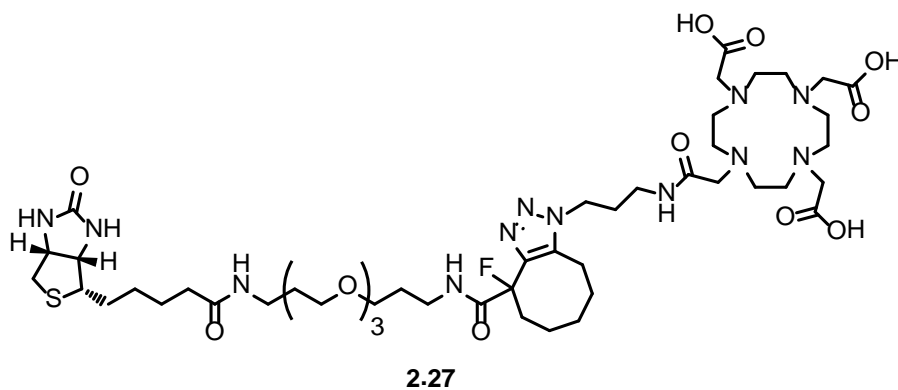
Pentafluorophenyltrifluoroacetate (0.61 mL, 3.53 mmol, 1.2 equiv) was added to the stirred solution of freshly prepared MFCO-acid (**2.21**) (0.55 g, 2.94 mmol, 1 equiv) in CH<sub>2</sub>Cl<sub>2</sub> (10 mL) at 0 °C. Diisopropylethylamine (0.58 mL, 3.53 mmol, 1.2 equiv) was then added and the reaction was stirred at 0 °C for 30 min, then allowed to warm to rt and maintained an additional 2 h. The reaction mixture was then filtered through a short silica gel column eluted with 2-5% EtOAc in hexanes. Column fractions containing product were combined and concentrated *in vacuo* to yield the desired PFP ester (**2.23**) as yellow oil (0.98 g, 90%).

<sup>1</sup>H NMR (300 MHz, CDCl<sub>3</sub>), δ (ppm): 2.58-2.33 (m, 4H), 2.13-1.89 (m, 4H), 1.87-1.76 (m, 1H), 1.58-1.48 (m, 1H). <sup>13</sup>C NMR (75 MHz, CDCl<sub>3</sub>), δ (ppm): 165.0 (d,  $J_{C-F} = 31.3$  Hz), 142.8, 141.9, 139.6, 138.4, 136.4, 124.8, 110.7 (d,  $J_{C-F} = 10.0$  Hz), 91.7 (d,  $J_{C-F} = 188.2$  Hz), 85.4 (d,  $J_{C-F} = 31.4$ ), 46.8 (d,  $J_{C-F} = 24.6$  Hz), 33.9, 29.2, 25.6, 20.7. The signals corresponding to the pentafluorophenyl carbons (142.8-124.8) exhibited considerable broadening due to extensive C-F coupling.



Diisopropylethylamine (31  $\mu$ l, 0.18 mmol, 1.2 equiv) was added to a stirred solution of **2.24**<sup>43</sup> (90 mg, 0.20 mmol, 1.25 equiv) and MFCO–PFP ester **2.23** (50 mg, 0.16 mmol, 1 equiv) in DMF (2 mL) at 0 °C. The reaction was warmed to room temperature and stirred for 2 h. The solvent was then removed under vacuum and the residue was purified by silica gel column chromatography using 10% ethyl acetate in methanol to afford **2.25** as pale yellow gummy liquid.

<sup>1</sup>H NMR (300 MHz, CD<sub>3</sub>OD, mixture of diastereomers),  $\delta$  (ppm): 4.56 (dd,  $J = 7.8, 4.5, 1\text{H}$ ), 4.37 (dd,  $J = 7.9, 4.4, 1\text{H}$ ), 3.71–3.56 (m, 12H), 3.40–3.24 (m, 5H), 2.99 (dd,  $J = 12.7, 4.9, 1\text{H}$ ), 2.77 (d,  $J = 12.7, 1\text{H}$ ), 2.42–2.24 (m, 6H), 2.17–1.62 (m, 13H), 1.54–1.44 (m, 3H). <sup>13</sup>C NMR (75 MHz, CD<sub>3</sub>OD, mixture of diastereomers),  $\delta$  (ppm): 176.0, 175.9, 170.7 (d,  $J_{C-F} = 24.6$  Hz), 166.0, 110.2, 110.1, 95.2 (d,  $J_{C-F} = 185.2$  Hz), 88.5 (d,  $J_{C-F} = 31.5$  Hz), 71.6, 71.4, 71.3, 70.2, 70.0, 63.4, 61.7, 57.1, 47.7 (d,  $J_{C-F} = 24.7$  Hz), 41.1, 38.4, 38.0, 37.9, 36.9, 35.1, 30.5, 30.2, 29.9, 29.6, 27, 26.8, 21.2. IR (film): 3303, 2920, 2863, 1694, 1669, 1539  $\text{cm}^{-1}$ . HRMS (ESI): calculated for C<sub>29</sub>H<sub>48</sub>FN<sub>4</sub>O<sub>6</sub>S [M + H]<sup>+</sup>, 599.3279, found 599.3271.



Separate solutions of **2.25** (76.0 mg, 0.13 mmol in 1.0 mL DMF) and **2.26** (70.3 mg, 0.1 mmol in 1.0 mL H<sub>2</sub>O) were combined and stirred at room temperature overnight. The reaction mixture was then evaporated to dryness and the residue was dissolved in ~0.7 mL DMF. Purification was performed using analytical RP-HPLC (C-18) with gradient elution. Fractions containing product were combined and concentrated in vacuo to give **2.27** (61.6 mg, 44%). HRMS (ESI): calculated for C<sub>48</sub>H<sub>81</sub>FN<sub>12</sub>O<sub>13</sub>S [M + H]<sup>+</sup>, 1085.5829, found 1085.5825.

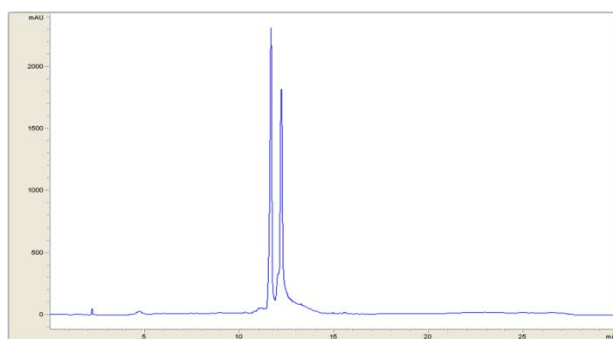


Figure 2.4. RP-HPLC chromatogram of **2.27** indicating the presence of two regioisomers



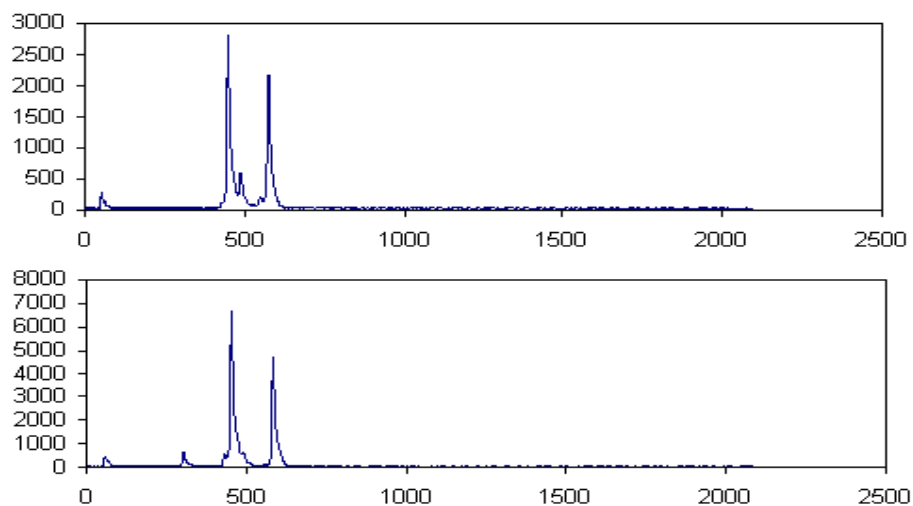
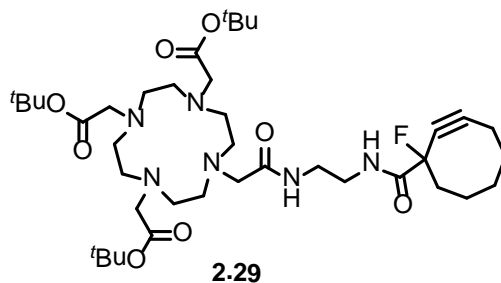
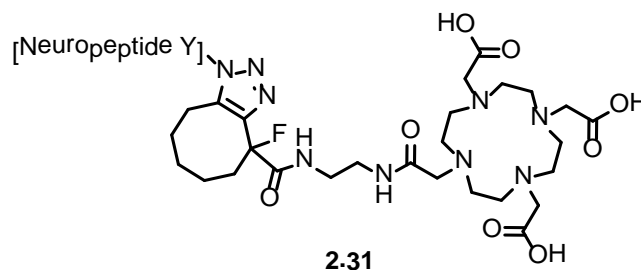


Figure 2.5. Radio-HPLC chromatogram of  $^{68}\text{Ga}$  labeled **2.27** in 5  $\mu\text{mol}$  (top) and 5 nmol (bottom)



MFCO (**2.21**, 1 equiv) was dissolved in dichloromethane and triethylamine (1 equiv) and benzotriazole-1-yl-oxy-tris-pyrrolidino-phosphonium hexafluorophosphate (1 equiv) were added and the mixture was stirred at 25 °C.  $\text{DO}_3\text{AtBu-N-(2-aminoethyl)ethanamide}$  (1.1 equiv; CheMatech, France), an amine modified and t-butyl protected DOTA derivative, was added to the mixture along with more triethylamine (1.1 equiv) and the reaction continued mixing for 24 hours. The solvent was removed by rotary evaporation, the product (**2.29**)

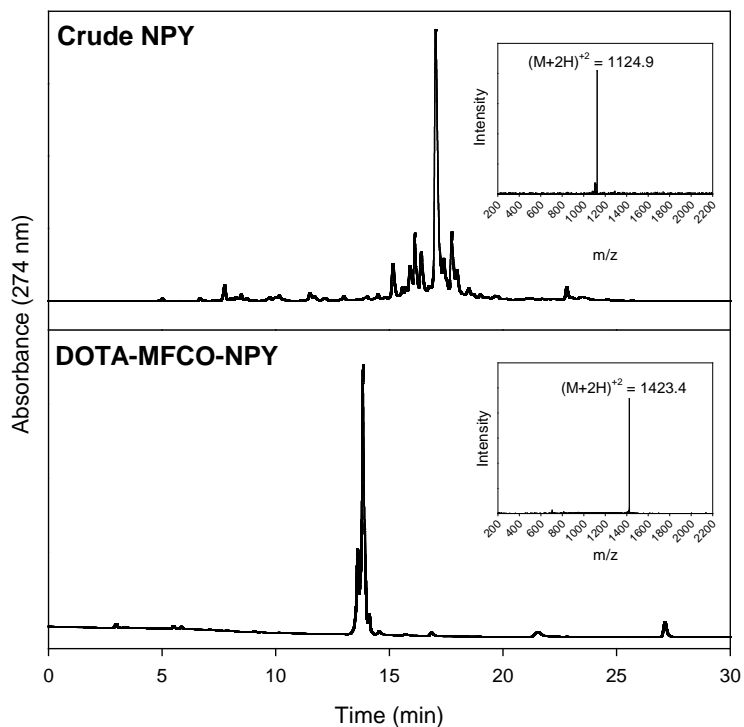
was characterized by mass spectrometry, and the DOTA-MFCO was used in the subsequent steps without further purification. LRMS (ESI): calculated for  $C_{39}H_{67}FN_6O_8$   $[M + H]^+$ , 767 found 767.



Compound **2.31** was prepared by Dr. Molly E. Martin, Department of Padiatrics, University of Iowa Carver College of Medicine.

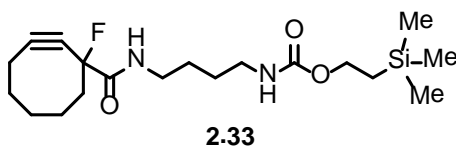
$[Lys(N_3)^4, Ahx^{5-24}]NPY$  (**2.30**) was synthesized at a 0.10 mmol scale on Rink resin using standard Fmoc procedures with 2-(1H-benzotriazol-1-yl)-1,1,3,3-tetramethyluronium hexafluorophosphate (HBTU) single couplings. The lysine at position 4 was replaced with an azide derivative for reaction with DOTA-MFCO by “click” chemistry. DOTA-MFCO (**2.29**) was conjugated to the azide side chain of  $Lys^4$  (**2.30**) using a 10:1 molar ratio of DOTA-MFCO:NPY (**2.29**) in DMF for 24 hours at 25 °C. The bioconjugate was simultaneously cleaved from the resin and deprotected by 95:2.5:2.5 trifluoroacetic acid (TFA)/triisopropylsilane (TIS)/water (v/v/v) and then precipitated with ice cold ether. DOTA-MFCO-NPY (**2.31**) was purified (final yield of 0.13 mole, 13%) by semipreparative HPLC eluted at 5 mL/min with 0.1% TFA and a 5-45% gradient of acetonitrile over 30 minutes while monitoring absorbance at 274 nm. Purified bioconjugates were characterized on an Agilent 1100 LC-ESI-ion trap eluted at 0.7 mL/min with 0.1%

TFA and a 5-65% gradient of acetonitrile gradient over 30 minutes with mass spectral data obtained in the positive mode.



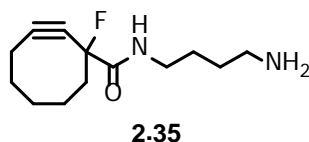
LC-MS characterization of crude NPY (**2.30**) and purified DOTA-MFCO-NPY (**2.31**): The chromatogram of crude NPY (**2.30**) (top) and purified DOTA-MFCO-NPY (**2.31**) (bottom) on RP-HPLC eluted with 0.1% TFA and acetonitrile is illustrated. The chromatogram was monitored by absorbance at 274 nm and by ESI-MS. The crude NPY peptide (top) eluted at 17.0 minutes producing a doubly charged positive ion at  $m/z$  1124.9 (inset) corresponding to an observed mass of 2247.8 amu (theoretical mass 2246.6 amu). Purified DOTA-MFCO-NPY (bottom) eluting as a major peak (>92%) at 13.8 min produced a doubly charged positive ion at  $m/z$  1423.4 (inset) corresponding to an observed mass of 2844.8 amu

(theoretical mass 2845.2 amu). The small front shoulder peak gives the same mass, suggesting its identity as a regioisomer of the DOTA-MFCO-NPY.

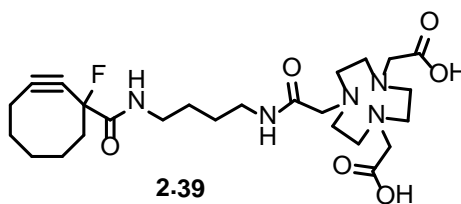


A solution of MFCO-PFP ester **2.23** (50 mg, 0.15 mmol, 1 equiv) in dichloromethane (1 mL) was added to a stirred solution of N-TeOc-1,4-diaminobutane derivative **2.32** (69 mg, 0.30 mmol, 2 equiv) and DIPEA (0.04 mL, 0.22 mmol, 1.5 equiv) in dichloromethane (2 mL) at 0 °C. The reaction was allowed to warm to rt and was stirred for 30 min. The reaction was then directly loaded on to a silica gel column and eluted with 80-90% ethyl acetate in hexanes to get colorless gummy product (50 mg, 88%).

$^1\text{H}$  NMR (300 MHz,  $\text{CD}_3\text{OD}$ ),  $\delta$  (ppm): 4.12 (t,  $J = 8.4$  Hz, 2H), 3.23 (t,  $J = 6.4$  Hz, 2H), 3.13-3.08 (m, 2H), 2.36-2.22 (m, 4H), 2.10-1.81 (m, 4H), 1.71-1.43 (m, 6H), 0.98 (t,  $J = 8.3$  Hz, 2H), 0.05 (s, 9H).  $^{13}\text{C}$  NMR (75 MHz,  $\text{CDCl}_3$ ),  $\delta$  (ppm): 171.1 (d,  $J_{\text{C-F}}^2 = 24.8$  Hz), 159.4, 110.1 (d,  $J_{\text{C-F}}^3 = 10.1$  Hz), 95.3 (d,  $J_{\text{C-F}} = 185.3$  Hz), 88.6 (d,  $J_{\text{C-F}}^2 = 31.3$  Hz), 63.8, 47.8 (d,  $J_{\text{C-F}}^2 = 24.8$  Hz), 41.4, 40.3, 35.1, 30.3, 28.4, 27.7, 26.9, 21.2, 18.8, -1.3. HRMS (ESI): calculated for  $\text{C}_{19}\text{H}_{33}\text{FN}_2\text{O}_3\text{SiNa}$   $[\text{M} + \text{Na}]^+$ , 407.2142, found 407.2150.

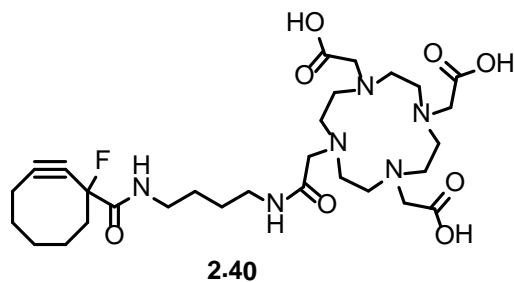


A solution of MFCO-PFP ester **2.23** (0.50 g, 1.49 mmol) in dichloromethane (20 mL) was added to a stirred solution of 1,4-diaminobutane (0.66 g, 7.44 mmol) and triethylamine (2.0 mL, 14.9 mmol) in dichloromethane (20 mL) at 0 °C. The reaction was allowed to warm to rt and was stirred for 20 min. The reaction was then diluted with water (50 mL) and extracted with dichloromethane (3 x 20 mL). The combined organic layer was washed with water (5 x 10 mL) and brine (10 mL), and dried over anhydrous Na<sub>2</sub>SO<sub>4</sub>. Filtration and evaporation of the solvent gave the desired MFCO amine **2.35** as a pale yellow colored gummy solid (0.33 g, 92%, crude yield). This crude material was found suitable for use in subsequent coupling reactions directly without further purification. <sup>1</sup>H NMR (300 MHz, CD<sub>3</sub>OD), δ (ppm): 3.24 (t, *J* = 6.5 Hz, 2H), 2.72 (t, *J* = 7.0 Hz, 2H), 2.36-2.23 (m, 4H), 2.10-1.81 (m, 4H), 1.68-1.44 (m, 6H). <sup>13</sup>C NMR (75 MHz, CDCl<sub>3</sub>), δ (ppm): 171.2 (d, *J*<sub>C-F</sub> = 24.1 Hz), 110.1 (d, *J*<sub>C-F</sub> = 10.0 Hz), 95.3 (d, *J*<sub>C-F</sub> = 185.3 Hz), 88.5 (d, *J*<sub>C-F</sub> = 31.4 Hz), 48.2 (d, *J*<sub>C-F</sub> = 24.9 Hz), 41.8, 40.2, 35.1, 30.3, 29.7, 26.9, 21.2. HRMS (ESI): calculated for C<sub>13</sub>H<sub>22</sub>FN<sub>2</sub>O [M + H]<sup>+</sup>, 241.1716, found 241.1724.

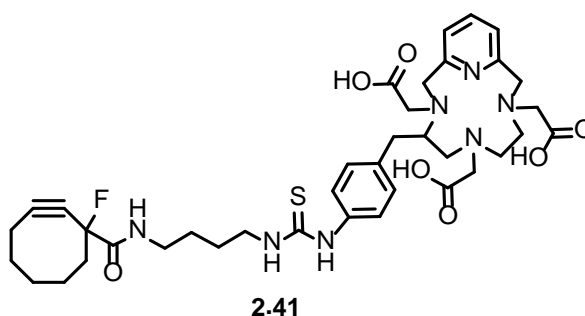


NOTA-MFCO **2.39** was prepared by reacting NOTA-NHS ester **2.36** (25 mg, 62.5  $\mu\text{mol}$ ) with MFCO-amine **2.35** (15 mg, 62  $\mu\text{mol}$ ) for 5 h at rt in a solvent mixture of DMF (0.5 mL), DMSO (1 mL), and triethylamine (88  $\mu\text{L}$ ). The MFCO modified chelator (**2.39**) was purified on an Agilent 1200 Series RP-HPLC to get isolated yield of 70%. LRMS (ESI): calculated for  $\text{C}_{25}\text{H}_{41}\text{FN}_5\text{O}_6$   $[\text{M}+\text{H}]^+$ , 526.3, found 526.33.

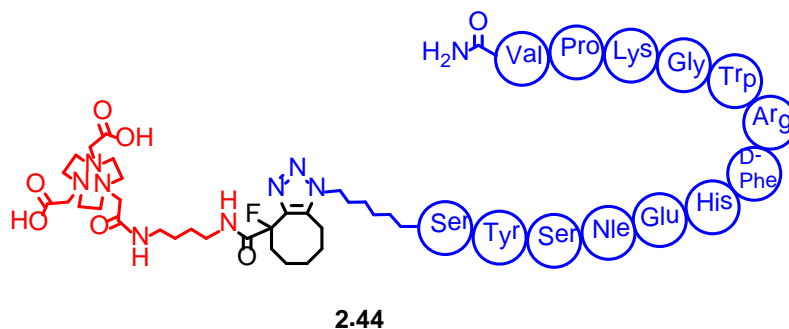
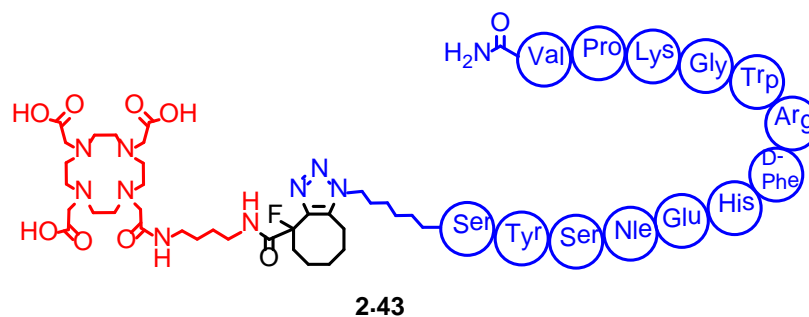
Purification of MFCO-modified chelators (**2.39**, **2.40** and **2.41**) was performed by injecting the reaction mixture on an Agilent semi-preparative C18 analytical column (9.4 x 25 cm) eluted at 3 mL/min with 50 mM triethylamine acetate buffer (pH 7.0) with 0.1 v/v % acetonitrile and acetonitrile gradient of 1-30 v/v % over 20 m while monitoring Abs at 214 nm. The major peak was collected and pooled from multiple runs, lyophilized, and stored at  $-20^\circ\text{C}$ . The products were characterized by ESI-MS in the positive and negative mode by preparing samples in a solution of acetonitrile/water (50/50 v/v %). Chelator MFCO's were analyzed by RP-HPLC using an Agilent C18 analytical column (4.6 x 15 cm) eluted at 1 mL/min with 50 mM triethylamine acetate buffer (pH 7.0) with 0.1 v/v % acetonitrile and acetonitrile gradient of 1-30 v/v% over 20 min while monitoring absorbance at 214 nm.



DOTA-MFCO **2.40** was prepared by reacting DOTA-NHS ester **2.37** (33.9 mg, 61  $\mu\text{mol}$ ) with MFCO-amine **2.35** (15 mg, 62  $\mu\text{mol}$ ) for 2 h at rt in a solvent mixture of DMF (0.5 mL), DMSO (1 mL), and triethylamine (88  $\mu\text{L}$ ). The MFCO modified chelator (**2.40**) was purified on an Agilent 1200 Series RP-HPLC to get 57% isolated yield of product. LRMS (ESI): calculated for  $\text{C}_{29}\text{H}_{48}\text{FN}_6\text{O}_8$   $[\text{M} + \text{H}]^+$ , 627, found 627.



PCTA-MFCO **2.41** was prepared by reacting PCTA-isothiocyanate **2.38** (37.4 mg, 62.5  $\mu\text{mol}$ , 1 equiv) with MFCO-amine **2.35** (15 mg, 62.5  $\mu\text{mol}$ , 1 equiv) for 2 h at rt in a solvent mixture of DMF (0.5 mL), DMSO (1 mL), and triethylamine (88  $\mu\text{L}$ ). The MFCO modified chelator (**2.41**) was purified on an Agilent 1200 Series RP-HPLC to get isolated yield of 52%. LRMS (ESI): calculated for  $\text{C}_{38}\text{H}_{51}\text{FN}_7\text{O}_7\text{S}$   $[\text{M} + \text{H}]^+$ , 768, found 768.



This experiment was performed by N. Baumhover and M. K. Schultz in the Department of Radiology, University of Iowa Carver College of Medicine.

DOTA-Click-Hex-NDP- $\alpha$ -MSH (**2.43**) and NOTA-Click-Hex-NDP- $\alpha$ -MSH (**2.44**) were synthesized by reacting 100 nmol of Azido-Hex-NDP- $\alpha$ -MSH (**2.42**) with a 10-fold excess of DOTA-MFCO (**2.40**) or a 20-fold excess of NOTA-MFCO (**2.39**) in 0.5 mL of H<sub>2</sub>O. Reaction progress was monitored by observing the disappearance of starting material using RP-HPLC (214 nm). The click reaction between DOTA-MFCO (**2.40**) and azido-Hex-NDP- $\alpha$ -MSH (**2.42**) was complete in 2 h while the NOTA-Click-Hex-NDP- $\alpha$ -MSH (**2.39**) required 5.5 h. The peptide conjugates were purified on an Agilent 1200 Series RP-HPLC by injecting the reaction mixture on an Agilent semi-preparative C18 analytical column (9.4 x 25 cm) eluted at 3 mL/min with 0.1 v/v % TFA and acetonitrile gradient of 5-45 v/v % over 20 min while monitoring tryptophan + tyrosine absorbance at 280 nm. The major peak was collected and pooled from multiple runs, lyophilized, and stored



at  $-20^{\circ}\text{C}$ . The peptides were prepared as the acetate salt by TFA salt exchange by employing multiple freeze drying cycles with 10 v/v % acetic acid. Purified peptides in the acetate salt form were reconstituted in water and quantified by tryptophan + tyrosine Abs ( $\epsilon$  280 nm =  $6930 \text{ M}^{-1} \text{ cm}^{-1}$ ) to determine isolated yield. Purified peptides were characterized on an Agilent 1100 series LC-ESI-MS by injecting 2 nmol onto a Vydac C18 analytical column (0.47 x 25 cm) eluted at 0.7 mL/min with 0.1 v/v % TFA and an acetonitrile gradient of 5-55 v/v% over 30 min.

### HPLC traces and mass spectra of DOTA and NOTA-click-hex-NDP- $\alpha$ -MSH (2.43 & 2.44)

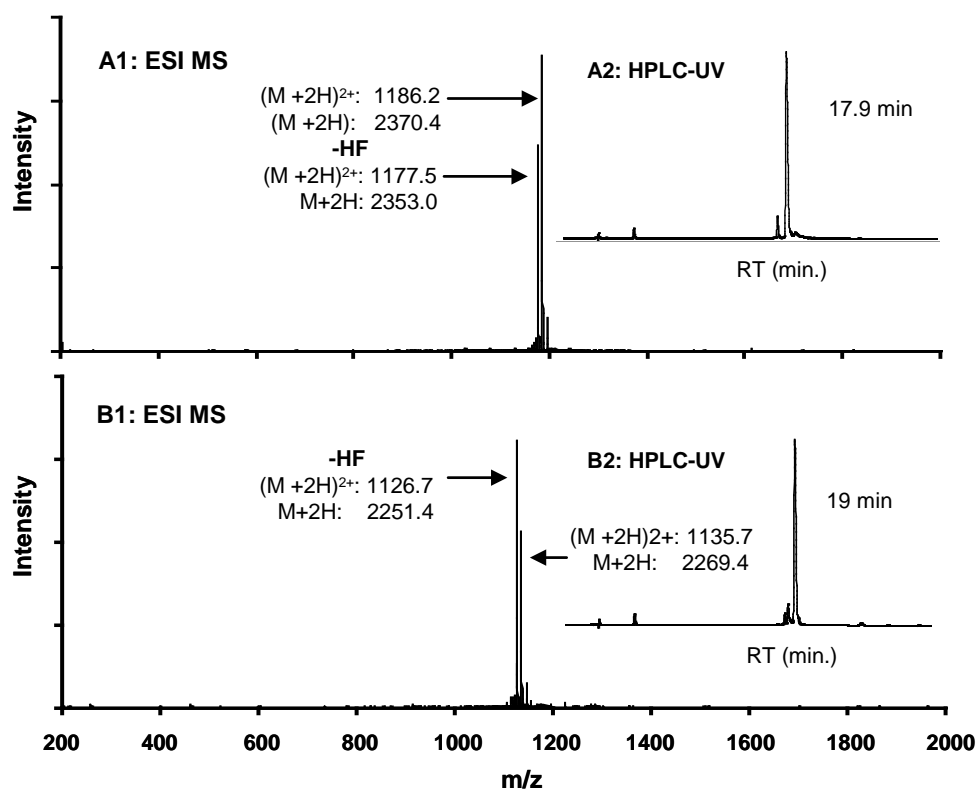


Figure 2.6. HPLC and Mass spectra of **2.43** (top) and **2.44** (bottom)

RP-HPLC-UV and ESI-MS analysis of purified DOTA and NOTA peptide

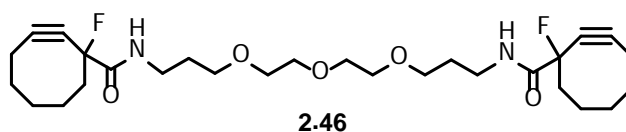
conjugates: (A1) DOTA-click-Hex-NDP- $\alpha$ -MSH (**2.43**) produces a doubly charged ion of  $m/z$  1186.2 corresponding to an observed mass of 2370.4 amu; theoretical 2370.7 amu and loss of HF from the triazole ring is observed as a doubly charged ion of  $m/z$  1177.5: observed 2353.0; theoretical 2352.7. (B1) observed masses of desired NOTA-click-Hex-NDP- $\alpha$ -MSH (**2.44**) produces a doubly charged ion of 1135.7  $m/z$  producing an observed mass of 2269.4; theoretical 2370.7 amu; and mass corresponding to loss of HF from the triazole ring interestingly produces the major doubly charged ion of  $m/z$  1126.7, producing an observed mass of 2251.4; agreeing with the theoretical mass of 2251.6 amu. (A2 and B2 insets); HPLC-UV traces of purified compounds.

### **In Vitro Competitive Binding Assays**

This experiment was performed by K. C. Kloeping and M. K. Schultz in the Department of Radiology, University of Iowa Carver College of Medicine.

B16-F10 murine melanoma cells were cultured in high glucose DMEM supplemented with 10% (v/v) FBS, 100 U/mL penicillin, and 100  $\mu$ g/mL streptomycin in 150 cm<sup>2</sup> culture flasks at 37°C in a humidified 5% CO<sub>2</sub> incubator. Cells were grown to 70% confluency and used in competitive binding assays similar to the methods developed by Eberle et al.<sup>83</sup> Cells were scraped from the culture flasks, counted on a Beckman Coulter cell counter, and resuspended in binding media (MEM containing 25 mM HEPES, 0.2% BSA, and 0.3 mM 1,10-phenanthroline). For binding assays, a total volume of 500  $\mu$ L was used in 1.5 mL Eppendorf tubes. The cell suspension (50  $\mu$ L containing approximately 4 million cells) was incubated with approximately 30,000 cpm of [<sup>125</sup>I]-[Nle<sup>4</sup>,D-Phe<sup>7</sup>]- $\alpha$ -MSH and increasing concentrations of  $\alpha$ -MSH or peptide analog ranging from 10<sup>-6</sup> to 10<sup>-11</sup> M. The tubes were mixed at 25 °C, 600 rpm on an Eppendorf Thermomixer for 1.5 h. Following incubation, cells were pelleted by centrifugation, the media was aspirated, pellets were transferred to 12 x 75 mm

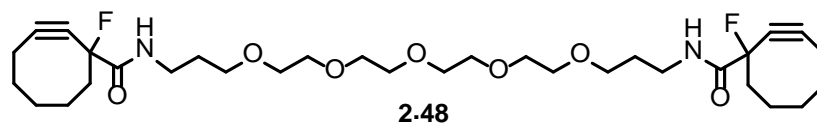
glass tubes, and the radioactivity of the cell pellet was determined using a PerkinElmer Cobra II gamma counter (PerkinElmer, Fremont, CA). All handling of radioactive materials was conducted using procedures and protocols approved through the University of Iowa Environmental Health and Safety Committee and Health Protection Office, adhering to ALARA principles. Each experiment was performed in quadruplicate and binding curves were plotted;  $IC_{50}$  values and their associated standard errors were calculated with GraphPad Prism 5 curve-fitting software (GraphPad Prism version 5.01 for Windows, GraphPad Software, San Diego, CA).



A solution of MFCO-PFP ester **2.23** (50 mg, 0.15 mmol, 2 equiv) in  $CH_2Cl_2$  (20 mL) was added to a stirred solution of PEG-3-amine **2.45** (16 mg, 0.074 mmol, 1 equiv) and triethylamine (0.05 mL, 0.37 mmol, 5 equiv) in dichloromethane (2 mL) at 0 °C. The reaction was allowed to warm to rt and was stirred for 30 min. The reaction was then diluted with water (5 mL) and extracted with dichloromethane (3 x 5 mL). The combined organic layer was washed with water (4 x 1 mL) and brine (2 mL), and dried over anhydrous  $Na_2SO_4$ . The mixture was filtered and evaporated in vacuo and purified using silica gel column chromatography using 80-90% EtOAc in hexanes to afford **2.46** as pale yellow oil (26 mg, 67%).

$^1H$  NMR (300 MHz,  $CDCl_3$ ),  $\delta$  (ppm): 7.18 (br s, 2H), 3.67-3.58 (m, 12H), 3.42 (q,  $J = 5.9$  Hz, 4H), 2.49-2.20 (m, 8H), 2.09-1.78 (m, 12H), 1.70-1.60 (m,

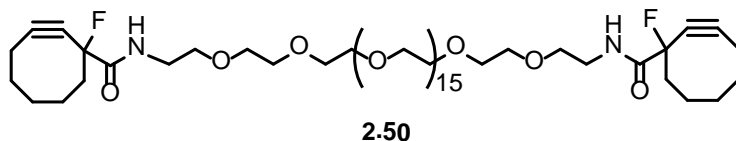
3H), 1.48-1.40 (m, 3H).  $^{13}\text{C}$  NMR (75 MHz,  $\text{CDCl}_3$ ),  $\delta$  (ppm): 168.9 (d,  $J_{\text{C-F}} = 22.6$  Hz), 109.6 (d,  $J_{\text{C-F}} = 11.3$  Hz), 94.6 (d,  $J_{\text{C-F}} = 185.0$  Hz), 87.5 (d,  $J_{\text{C-F}} = 31.5$  Hz), 70.7, 70.6, 70.5, 46.6 (d,  $J_{\text{C-F}} = 24.8$  Hz), 38.6, 34.1, 29.0, 28.7, 25.8, 20.8. HRMS (ESI): calculated for  $\text{C}_{28}\text{H}_{42}\text{F}_2\text{N}_2\text{O}_5\text{Na}$   $[\text{M} + \text{Na}]^+$ , 547.2959, found 547.2947.



A solution of MFCO-PFP ester **2.23** (0.10 g, 0.30 mmol, 2.2 equiv) in dichloromethane (20 mL) was added to a stirred solution of PEG-5-amine **2.47** (42 mg, 0.14 mmol, 1 equiv) and DIPEA (0.06 mL, 0.34 mmol, 2.5 equiv) in dichloromethane (2 mL) at 0 °C. The reaction was allowed to warm to rt and was stirred for 30 min. The reaction was then diluted with water (5 mL) and extracted with dichloromethane (3 x 5 mL). The combined organic layer was washed with water (2 x 1 mL) and brine (2 mL), and dried over anhydrous  $\text{Na}_2\text{SO}_4$ . The mixture was filtered and evaporated in vacuo and purified using silica gel column chromatography using 80-90% ethyl acetate in hexanes to obtain **2.48** as colorless gummy liquid (68 mg, 82%).

$^1\text{H}$  NMR (300 MHz,  $\text{CDCl}_3$ ),  $\delta$  (ppm): 7.04 (br s, 2H), 3.66-3.56 (m, 20H), 3.41 (q,  $J = 5.9$  Hz, 4H), 2.50-2.20 (m, 8H), 2.13-1.77 (m, 12H), 1.74-1.62 (m, 2H), 1.51-1.41 (m, 2H).  $^{13}\text{C}$  NMR (75 MHz,  $\text{CDCl}_3$ ),  $\delta$  (ppm): 168.4 (d,  $J_{\text{C-F}} = 24.0$  Hz), 109.1 (d,  $J_{\text{C-F}} = 10.5$  Hz), 94.5 (d,  $J_{\text{C-F}} = 185.5$  Hz), 87.7 (d,  $J_{\text{C-F}} = 31.4$  Hz), 70.7, 70.6, 70.3, 46.5 (d,  $J_{\text{C-F}} = 24.3$  Hz), 38.3, 34.0, 29.0, 28.9, 25.8, 20.7.

HRMS (ESI): calculated for  $C_{32}H_{50}F_2N_2O_7Na$   $[M + Na]^-$ , 635.3484, found 635.3471.



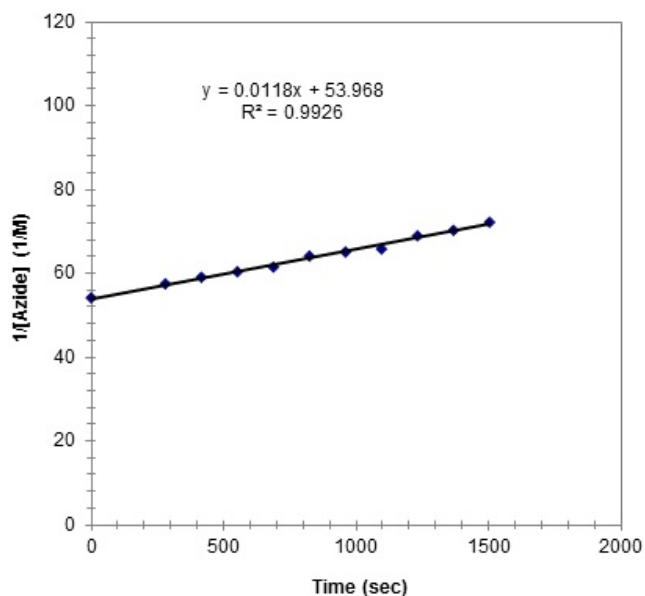
A solution of MFCO-PFP ester **2.23** (0.10 g, 0.30 mmol, 2.2 equiv) in  $CH_2Cl_2$  (1 mL) was added to a stirred solution of PEG-20-amine **2.49** (121 mg, 0.14 mmol, 1 equiv) and DIPEA (0.06 mL, 0.34 mmol, 2.5 equiv) in  $CH_2Cl_2$  (2 mL) at 0 °C. The reaction was allowed to warm to rt and was stirred for 16 h. The reaction was then diluted with water (5 mL) and extracted with  $CH_2Cl_2$  (3 x 2 mL). The combined organic layer was washed with water (3 x 5 mL) and brine (5 mL), and dried over anhydrous  $Na_2SO_4$ . The mixture was filtered and evaporated in vacuo and purified using silica gel column chromatography using 90% EtOAc in  $CH_2Cl_2$  to yield **2.50** as pale yellow gummy liquid (146 mg, 90%).

$^1H$  NMR (300 MHz,  $CDCl_3$ ),  $\delta$  (ppm): 6.89 (br s, 2H), 3.88-3.41 (m, 80H), 2.50-2.23 (m, 8H), 2.11-1.83 (m, 8H), 1.72-1.62 (m, 2H), 1.51-1.40 (m, 2H).  $^{13}C$  NMR (75 MHz,  $CDCl_3$ ),  $\delta$  (ppm): 168.6 (d,  $J_{C-F} = 24.4$  Hz), 109.2 (d,  $J_{C-F} = 10.4$  Hz), 94.4 (d,  $J_{C-F} = 185.4$  Hz), 87.4 (d,  $J_{C-F} = 31.6$  Hz), 70.6, 70.4, 69.4, 46.4 (d,  $J_{C-F} = 24.4$  Hz), 39.3, 33.9, 28.9, 25.7, 20.6. HRMS (ESI): calculated for  $C_{58}H_{102}F_2N_2O_{21}Na$   $[M + Na]^+$ , 1223.6841, found 1223.6841.

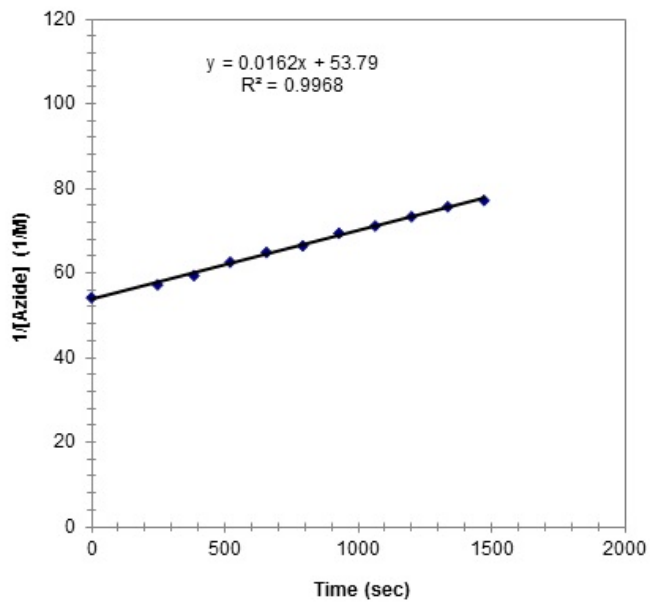
### Determination of rate constant for click reaction between MFCO (**2.21**) and benzyl azide

The rate constant was determined by monitoring the disappearance of benzyl azide over time using  $^1H$  NMR ( $CD_3CN$ ). Solutions of **2.21** and benzyl

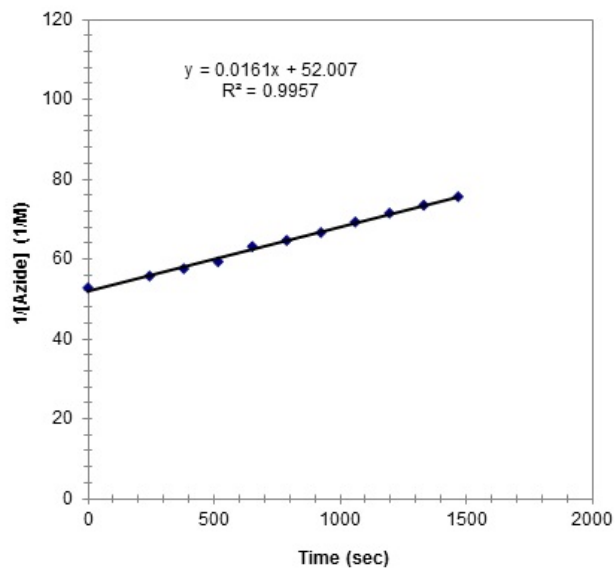
azide (in  $\text{CD}_3\text{CN}$ ) were combined in an NMR tube and spectra recorded at various regular time intervals. Disappearance of benzyl azide was monitored by noting the diminution of the singlet at  $\sim 4.4$  ppm corresponding to the benzylic hydrogens coupled with the appearance of a multiplet at  $\sim 5.5$  ppm corresponding to the benzyl triazole product. A plot of  $1/[\text{benzyl azide}]$  vs time was constructed and analyzed by linear regression methods. The second order rate constant was determined from the slope of the resulting line. The reported rate constant ( $1.47 \pm 0.21$ )  $\times 10^{-2} \text{ M}^{-1} \text{ s}^{-1}$  represents the average and standard deviation of three independent experiments (plots shown below).



Trial 2.1. Initial concentrations: **2.21** (20 mM): benzyl azide (18.4 mM)



Trial 2.2. Initial concentrations: **2.21** (20 mM): benzyl azide (18.4 mM)



Trial 2.3. Initial concentrations: **2.21** (20.1 mM): benzyl azide (18.9 mM)

## CHAPTER THREE

### PART A: SUMMARY AND FUTURE DIRECTIONS

#### 3.1 Summary

The initial objective of the research described in the previous chapter was to develop novel cyclooctyne reagents to facilitate efficient conjugation of radionuclide chelators to biomolecules. Ring strain-induced copper-free click chemistry using an activated cyclooctyne was envisioned for the coupling process. We have designed and successfully synthesized a new bifunctional monofluorinated cyclooctyne (MFCO) in three steps (47% overall yield) using commercially available starting material. Kinetic studies revealed that MFCO has a reasonable kinetic profile, and the second order rate constant for reaction between MFCO and benzyl azide is comparable to other cyclooctynes used in click chemistry. Proof of concept for conjugating biomolecules to chelator of choice via copper-free click reaction was demonstrated using MFCO as the lynchpin. Attachment of MFCO to bioligands such as biotin was accomplished by manipulating the carboxylic acid group of MFCO. Successful coupling of this MFCO-biotin adduct to an azide modified DOTA-chelator using copper-free click reaction gave a DOTA-MFCO-biotin conjugate that was then radiolabelled with  $^{68}\text{Ga}$  in high radiochemical purity and specific activity. In a separate experiment, an activated ester of MFCO was coupled to an amine-modified DOTA chelator and then subjected to click reaction with resin-bound azide modified Neuropeptide Y. The DOTA-MFCO-Neuropeptide Y substrate was then cleaved from the resin and radiolabelled with  $^{111}\text{In}$  in very high radiochemical purity and specific activity. We have also synthesized an amine-modified MFCO in very high yield and used this reagent to prepare chelator-modified MFCO via reaction with NHS esters and isothiocyanates. DOTA-MFCO-amide and NOTA-MFCO-amide prepared in



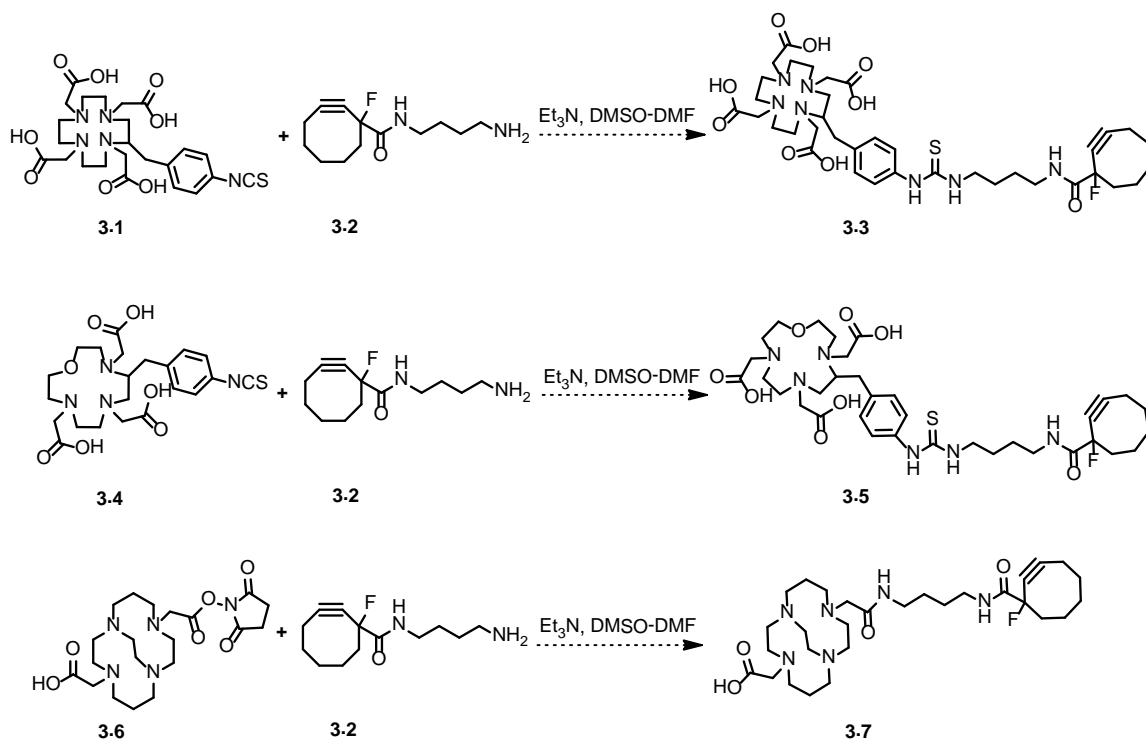
this way were then coupled to an azide modified  $\alpha$ -MSH analogue via click reaction in high yield and then radiolabelled with  $^{64}\text{Cu}$  and  $^{68}\text{Ga}$  in very high radiochemical purity and specific activity. *In vitro* binding assays performed on B16-F10 murine melanoma cells involving DOTA-click-Hex-NDP- $\alpha$ -MSH and NOTA-click-Hex-NDP- $\alpha$ -MSH established that the triazole ring did not affect the binding affinity of the peptides. Additionally, biodistribution studies performed in mice bearing xenografted melanoma tumors showed encouraging tumor-to-blood ratios upon injection with radiolabelled DOTA or NOTA-click-hex-NDP- $\alpha$ -MSH.

Finally, hetero- and homo-multivalent ligands may represent a viable strategy for achieving effective targeted radionuclide imaging and therapy of cancer. To test this hypothesis, MFCO-based bivalent ligands were prepared. This was accomplished by linking two MFCO units through an  $\alpha,\omega$ -diamine spacer. Click reaction between bis-MFCO units and azide-modified peptide ligands then afforded bivalent conjugates in good yield. Further studies involving these bis-MFCO-biomolecule vectors are underway.

### 3.2 Future directions

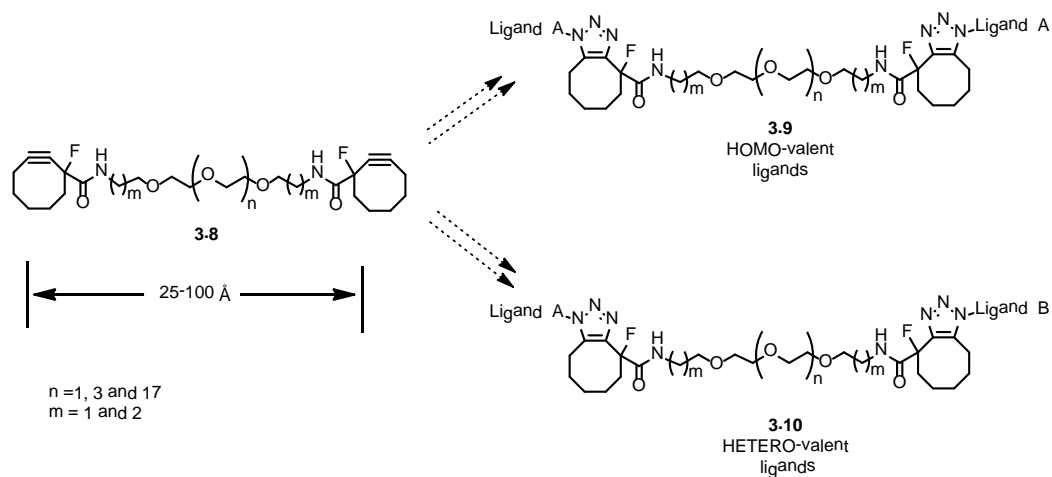
#### **Synthesis of MFCO-chelator molecules for radionuclide chemistry**

We have demonstrated that MFCO is a suitable bifunctional molecule for conjugation of radionuclide chelators to biomolecules using copper-free click chemistry. Several DOTA and NOTA chelators have been coupled to MFCO and then to biomolecules for application in radionuclide chemistry. To extend this chemistry, reaction between MFCO-amine and other activated chelator reagents, such as DOTA (**3.1**), N,O-chelator (**3.4**) and TE2A (**3.6**) could be examined as shown in Scheme 3.1. This will provide a wider pool of MFCO-chelator derivatives for subsequent applications in biomedical radiochemistry.



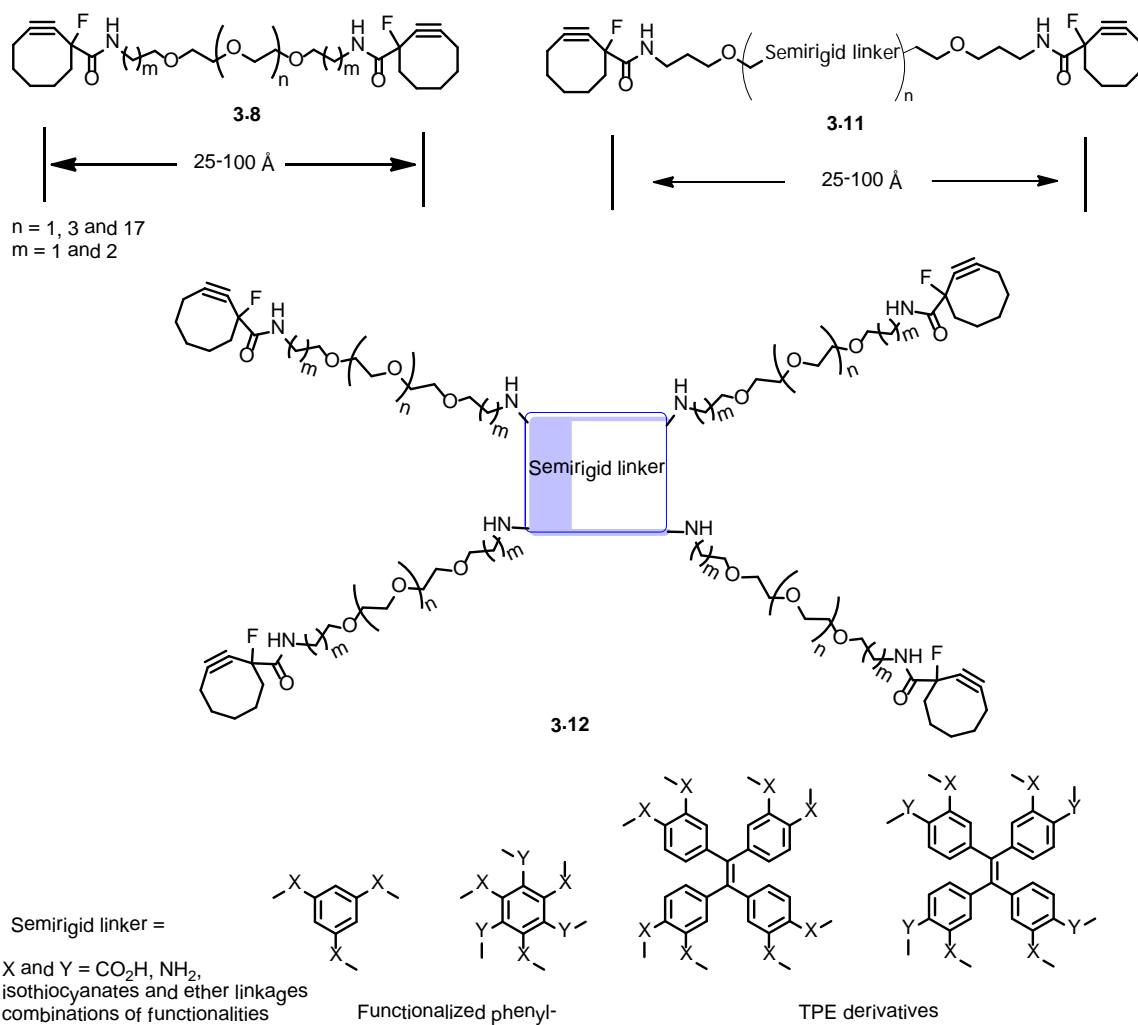
Scheme 3.1. Synthesis of MFCO-chelators

### Synthesis of bis-MFCO molecules for assembly of bivalent ligands



Scheme 3.2. Bis-MFCO for bivalent ligands synthesis

We have synthesized a few bis-MFCO compounds for use in development of multivalent ligands. These bis-MFCO substrates can be conjugated to identical ligands on both ends to yield homo-bivalent ligands or can be coupled to two different ligands to afford hetero-bivalent ligands (Scheme 3.2). Both homo and hetero bivalent ligands could potentially be used as more effective diagnosis and therapy agents for cancer. This bivalent approach may enable us to target overexpressed cell receptors in cancer cells with greater specificity than monovalent ligands. Linker length and flexibility are important variables in bivalent ligand synthesis. We have already synthesized bis-MFCO-PEG-3, bis-MFCO-PEG-5 and bis-MFCO-PEG-20 for these studies (see Chapter Two). Future work can be directed toward the synthesis of bis-MFCO as well as multi-MFCO constructs with various linker lengths using poly-PEG-amines. Biocompatible semi-rigid spacers such as [Pro-Gly], TPE (tetraphenylethylene), and multi-substituted phenyl rings could also be included to vary linker characteristics (Scheme 3.3).



Scheme 3.3. Synthesis of multivalent-MFCO with varying linker length and spacers

PART B

4-ALKYLPYRIDINE DERIVATIVES IN INTRAMOLECULAR  
DEAROMATIZATION AND HETEROCYCLE SYNTHESIS

## CHAPTER FOUR

### DEAROMATIZATION STRATEGIES IN ORGANIC SYNTHESIS

#### 4.1 Introduction

Aromatic compounds are widely available and represent versatile synthetic building blocks in organic chemistry. The utility of arenes is further enhanced by development of dearomatization reaction manifolds.

Dearomatization reactions result in conversion of planar arenes into non-planar alicyclic products. Several stereoselective and chemoselective approaches to complex molecules involving dearomatization of aromatic substrates have been reported, especially in the context of heterocyclic compound construction.

Heterocyclic frameworks are ubiquitous in natural products that exhibit potent bioactivity. Various heterocyclic motifs are also found in many pharmaceuticals.

While many routes are available for the synthesis of heterocycles, new approaches based on dearomatization of carbocyclic and heterocyclic arenes may offer concise and practical alternatives.

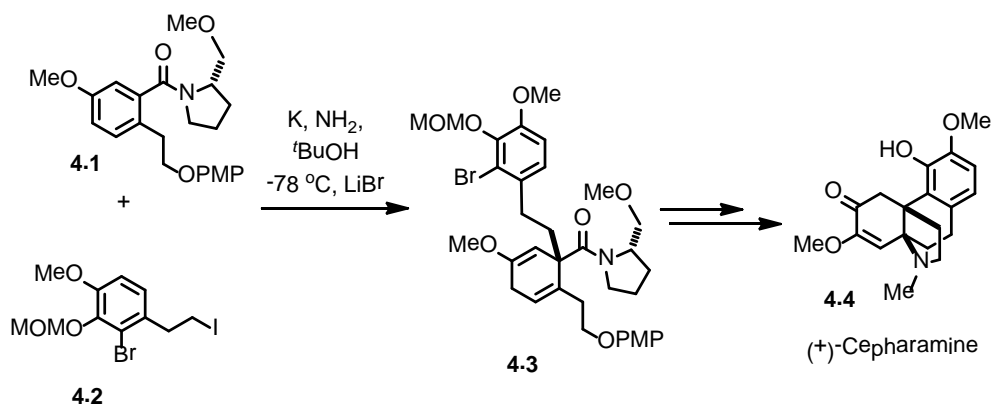
A number of strategies are available to achieve dearomatization reactions to produce fused rings, spirocycles, azaspirocycles and polycyclic systems from easily accessible aromatic substrates. These transformations include new C-C bond formations, C-heteroatom bond formations, and metal-mediated transformations that deliver valuable building blocks for synthetic purposes.

Oxidative and reductive dearomatizations using enzyme-catalyzed reactions have also been utilized in organic synthesis.<sup>84-86</sup> In the context of heterocyclic compound synthesis, photochemical and thermal cycloadditions,<sup>87-90</sup> nucleophilic additions,<sup>91</sup> radical cyclizations,<sup>92,93</sup> transition metal-mediated strategies<sup>94,95</sup> and oxidative dearomatization using hypervalent iodine reagents<sup>96,97</sup> have all been successfully applied for conversion of arenes or heteroarenes into various aza-or

oxa-cyclic materials. Despite these accomplishments, dearomatization remains an under-utilized tactic in organic synthesis, and developing new and broadly applicable dearomatization strategies would significantly expand the field of synthetic organic chemistry.

#### 4.2 General methods for heterocyclic synthesis via dearomatization

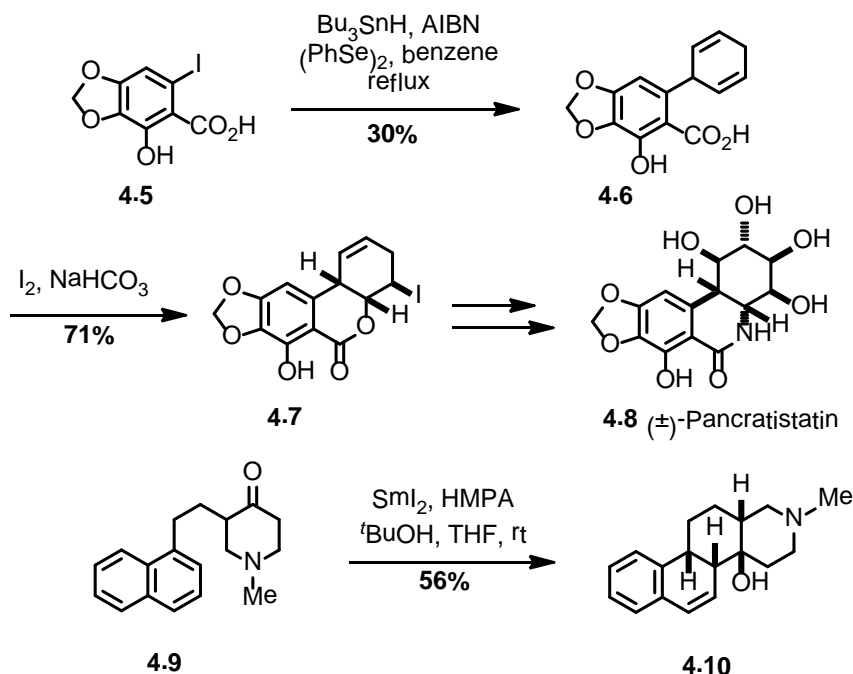
Several types of transformations have been used to convert aromatic substrates into alicyclic heterocycles. Birch reduction using dissolved alkali metal in liquid ammonia is a classic method of dearomatization. The reaction involves use of solvated electrons generated *in situ* to reduce aromatic compounds regioselectively to yield 1,4-dihydro cyclohexadienes, and this reaction still enjoys widespread use. For example, Schultz and coworkers utilized this reaction in their enantioselective synthesis of the alkaloid (+)-cepharamine (Scheme 4.1).<sup>98</sup> Diastereoselective Birch reduction of aromatic substrate **4.1** in the presence of alkyl iodide substrate **4.2** yielded 1,4-cyclohexadiene **4.3** as a single diastereomer which was further manipulated into (+)-cepharamine (**4.4**).



Scheme 4.1. Diastereoselective Birch reduction in synthesis of (+)-cepharamine (**4.4**)

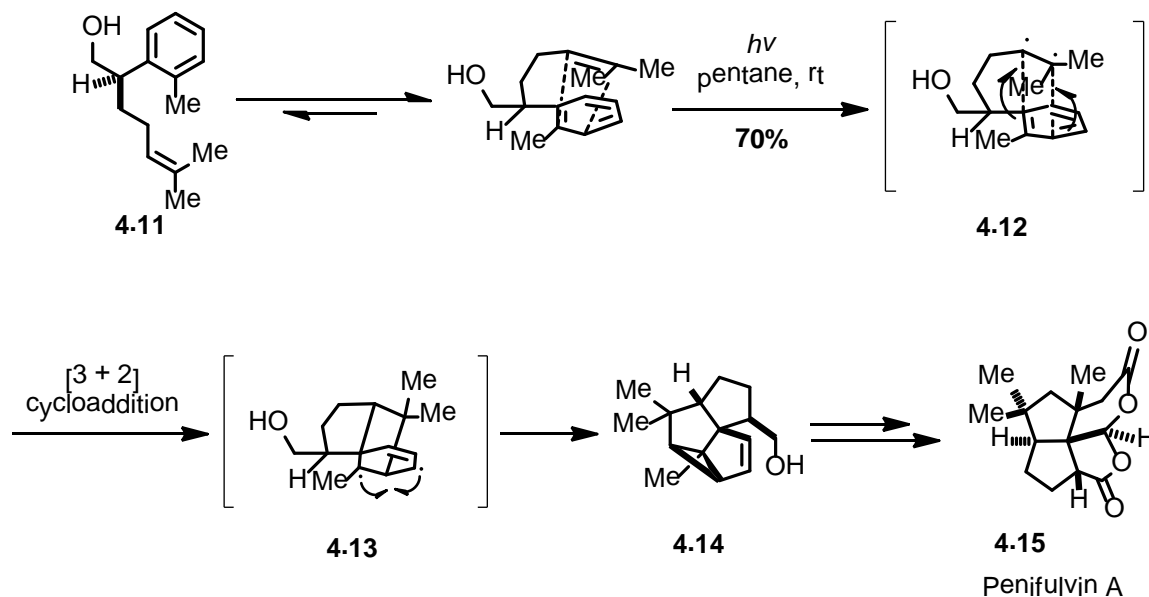
Related radical-based methods have been used to effect dearomatization. Inter- and intramolecular additions of aryl radicals to substituted arenes yield cyclohexadienyl radicals which generally are not reactive enough to propagate chain reactions. Consequently electron transfer occurs resulting in rearomatization to yield biaryl products. Crich and coworkers have shown that addition of catalytic quantities of diphenyl diselenide to stannane-mediated radical addition of aryl iodides such as **4.5** to arenes assists in trapping of cyclohexadienyl radicals and aids isolation of aryl substituted cyclohexadienes (e.g., **4.6**).<sup>99,100</sup> This radical-mediated dearomatization was utilized in their synthesis of bioactive phenanthridinone alkaloid (±)-pancratistatin (**4.8**) as shown scheme 4.2.<sup>101</sup> A second radical-based dearomatization is also shown in scheme 4.2. Samarium iodide has gained much importance in organic synthesis involving radical chemistry because of its unique electron transfer ability. This reagent has been used to promote reductive coupling of carbonyl groups and C-C multiple bonds with high stereoselectivity and efficiency. Aulenta and coworkers utilized this approach to synthesize steroids and azasteroid frameworks such as **4.10** from naphthyl-substituted aryl ketones (**4.9**) (Scheme 2).<sup>102</sup>





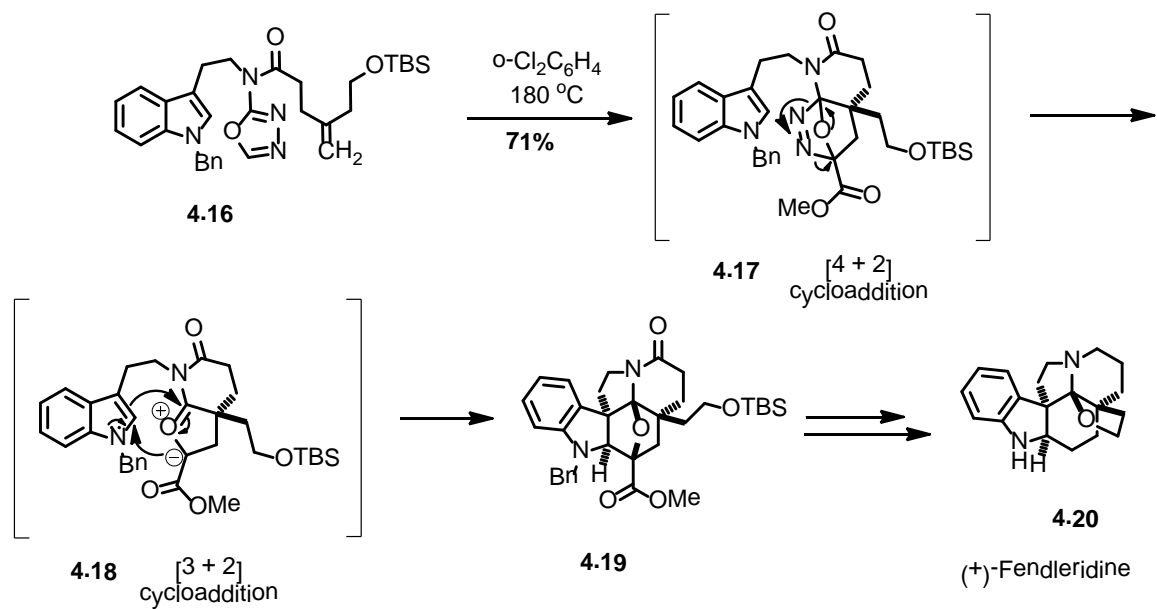
Scheme 4.2. Dearomatization using radical addition

Cycloaddition is extensively used in organic synthesis to form cyclic systems with stereo- and regioselectivity. Dearomatizations involving cycloadditions facilitate complex structural motifs, both in inter- and intramolecular fashion. Mulzer and coworkers have employed Wender's marvelous photoinduced [3+2] cycloaddition of arenes and olefins as a key step in the synthesis of the sesquiterpenoid penifulvin A (**4.15**) (Scheme 4.3).<sup>103</sup> Compound **4.11** was irradiated to generate excimer (**4.12**) which underwent formal cycloaddition to produce exciplex **4.13**. Radical recombination to form a cyclopropane ring yielded **4.14** as mixture of regioisomers. The stereochemical outcome was controlled by the A<sup>1,3</sup> strain between the aryl methyl and hydroxymethyl groups.



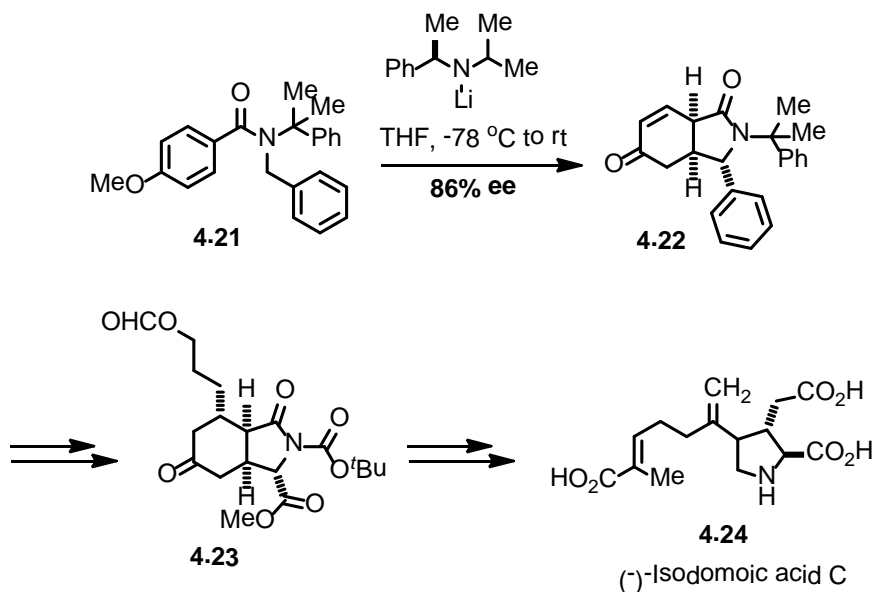
Scheme 4.3. Synthesis of penifulvin A (**4.15**) via radical cyclization

Boger and coworkers implemented powerful tandem [4+2] and [3+2] cycloaddition cascade reaction of 1,3,4-oxadiazoles in their attempts to synthesize aspidosperma alkaloids such as (+)-fendleridin (**4.20**) (Scheme 4.4).<sup>104</sup> This strategy enabled them to establish a pentacyclic ring system with all the stereocenters of the natural product in a reaction that forms three rings, four C-C bonds, and five stereocenters. The key reaction cascade starts with intramolecular [4+2] cycloaddition of 1,3,4-oxadiazole (**4.16**) substituted with a dienophile in the side chain to form cycloadduct (**4.17**) which loses  $N_2$  to give a 1,3-dipole **4.18**. Subsequent intramolecular [3+2] cycloaddition with dipolarophile tethered in the side chain afford the regioselective, endo cycloaddition intermediate **4.19** in excellent yield which, on further manipulation, yielded the natural product.



Scheme 4.4. Synthesis of (+)-fendleridine (**4.20**) using cycloaddition cascade reaction

Dearomatization using diastereoselective carbanion addition to aromatic rings is well documented.<sup>105-107</sup> This strategy was used by Clayden and coworkers in their enantioselective synthesis of an insecticidal cyclic kainoid amino acid, (-)-isodomoic acid C (**4.24**) (Scheme 4.5).<sup>108</sup> A significant step in the synthesis involved the asymmetric dearomatization of the N-benzyl benzamide intermediate **4.21** to give bicyclic product (**4.22**) with desired stereochemistry.



Scheme 4.5. Dearomatization via anionic cyclization

### 4.3 Transition metal-mediated dearomatization

Transition metal-mediated reactions are widely used in organic chemistry, including various C-C and C-heteroatom bond forming reactions. Particularly, transition metal-mediated dearomatization of aryl substrates has proven to be a powerful tool for conversion of aromatics into functionalized alicyclic compounds in controlled fashion.<sup>91</sup> Transition metal-mediated dearomatization is divided generally into two distinct parts: electrophilic and nucleophilic dearomatization. The operative mode is determined by the coordination of the metal to the arene ring (Figure 4.1). In  $\eta^6$ -coordination, the metal coordinates to all  $\pi$ -bonds in the arene ring and renders the ring electron-deficient and thus susceptible to nucleophilic addition [e.g.,  $(\eta^6\text{-arene})\text{Cr}(0)(\text{CO})_3$ ,  $(\eta^6\text{-arene})\text{Mn}(\text{I})(\text{CO})_3$ ,  $(\eta^6\text{-arene})\text{Fe}(\text{II})\text{Cp}$  complexes].<sup>95,109,110</sup> In  $\eta^2$ -arene complexes, the metal coordinates to only one bond of the arene ring and activates the ring by donating electron density by back-bonding through metal d  $\pi$ -arene  $\pi^*$  interactions. So,  $\eta^2$ -

metal complexes participate in electrophilic addition reactions (e.g.,  $\text{Os}(\text{NH}_3)_5^{2+}$ ).<sup>111,112</sup> Both  $\eta^6$  and  $\eta^2$  coordinated metal complexes provide regioselectivity and stereo-control and have been applied in many complex molecule syntheses.

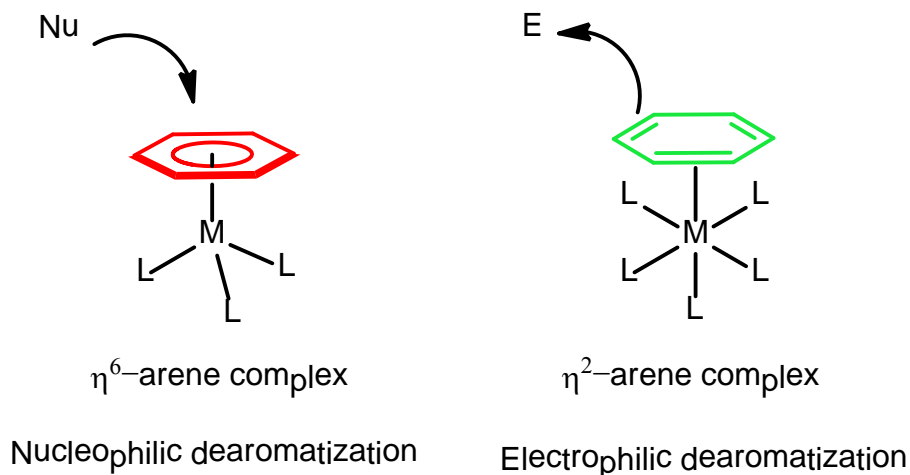
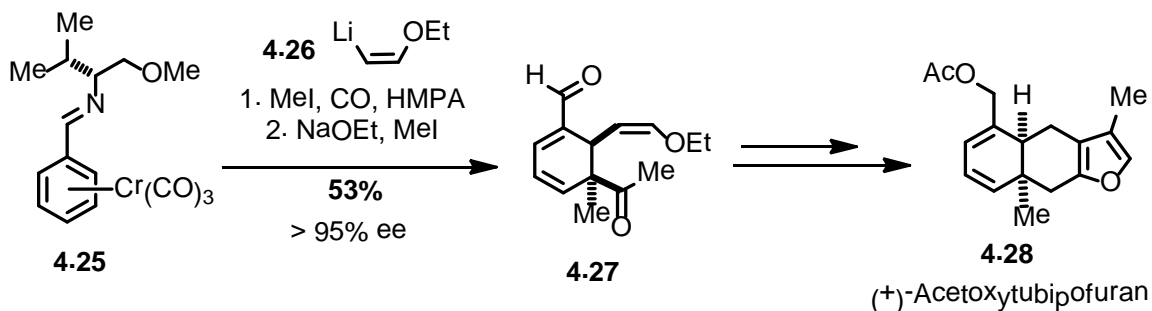
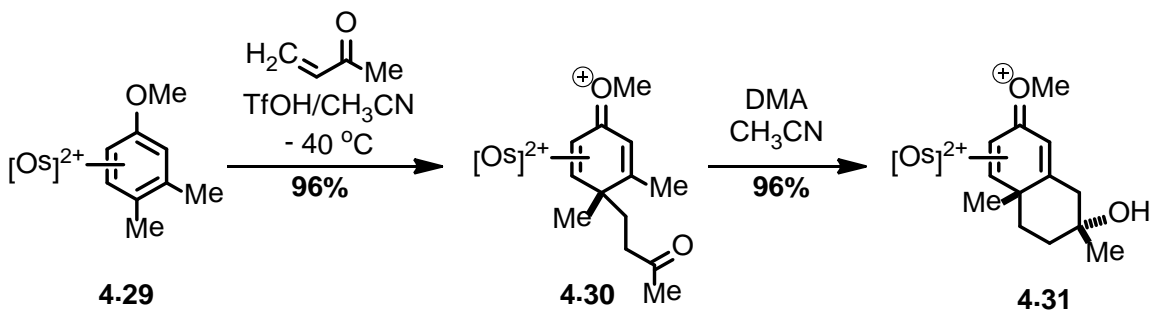


Figure 4.1. Representation of reactivity of transition metal-arene complexes

Kuding and coworkers developed asymmetric methods involving  $\text{Cr}(\text{CO})_3$ -mediated dearomatization in the synthesis of both enantiomers of acetyltubipofuran (**4.28**).<sup>113</sup> They have shown that  $\eta^6$ -coordinated benzaldehyde derived imine-chromium complex **4.25** directs addition of ethoxyvinyl lithium (**4.26**) to the *ortho* position, which was subsequently followed by alkylation/acylation and imine hydrolysis to afford compound **4.27** possessing the desired relative configuration (Scheme 4.6). This, on further manipulation, yielded the anticipated *cis*-decalin skeleton of the target natural product.



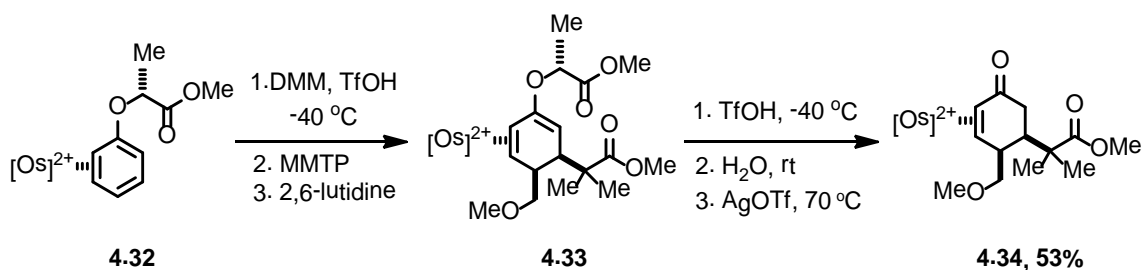
Scheme 4.6. Nucleophilic dearomatization using  $\eta^6$ -coordinated chromium metal-arene complex in natural product synthesis



Scheme 4.7.  $\eta^2$ -coordinated osmium metal-arene complex in electrophilic dearomatization

Harman and coworkers utilized  $\eta^2$ -coordinated pentaammineosmium(II)-arene complexes to study the benzylic carbon activation for functionalized decalin framework synthesis. They successfully dearomatized the 3-alkylated anisole complexes of  $\text{Os}(\text{NH}_3)_5^{2+}$  (**4.29**) using Michael addition to methyl vinyl ketone in presence of triflic acid to yield 4*H*-anisolum Michael adducts such as **4.30** (scheme 4.7).<sup>114</sup> This underwent regioselective deprotonation in the presence of weak base resulting in an intramolecular aldol reaction with a pendant ketone to form bicyclic decalin system **4.31**. The same group has also explored diastereoselective addition of  $\eta^2$ -coordinated pentaammineosmium(II)-

arene complexes to various electrophiles.<sup>111,115</sup> Chiral auxiliary attached enantiopure phenyl ether–osmium complex **4.32** underwent electrophilic addition with dimethoxymethane (DMM) followed by silyl ketene acetal addition to afford functionalized cyclohexadiene **4.33** (Scheme 4.8). Useful cyclohexenone **4.34** was obtained after removal of chiral auxiliary and decomplexation of the transition metal from **4.33**. Harman and coworkers have also developed methods to utilize tungsten complexes [e.g., {TpW(NO)(PMe<sub>3</sub>)}] to activate benzene and other hetero aromatics for Michael type addition under neutral or basic conditions.<sup>116,117</sup>

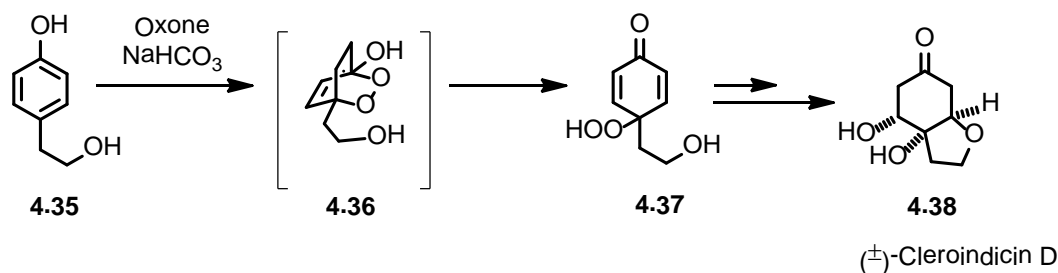


Scheme 4.8. Functionalized cyclohexenones (**4.34**) from electrophilic dearomatization using  $\eta^2$ -coordinated osmium metal-arene complex

#### 4.4 Oxidative dearomatization

Oxidative dearomatization offers economically and environmentally benign dearomatization methods for accessing complex structural motifs. Generally, electron rich aryl substrates such as phenols and phenyl ethers undergo facile oxidation on treatment with electrophilic hypervalent iodine reagents such as phenyliodine diacetate (PIDA) and phenyliodine trifluoroacetate (PIFA) and other oxidizing reagents.<sup>118</sup> Both inter and intramolecular oxidative dearomatization methods are reported and this strategy is useful in obtaining both *ortho*- and

*para*-cyclohexadienones.<sup>119,120</sup> Carreno and Urbano employed oxidative dearomatization to synthesize *para*-peroxyquinol and *para*-quinols from the corresponding *para*-alkyl phenols using Oxone as their oxidizing reagent.<sup>121</sup> They used this strategy to synthesize (±)-cleroindicin D diastereoselectively from *para*-(2-hydroxyethyl)phenol **4.35** (Scheme 4.9). Oxidation with Oxone of **4.35** resulted in dearomatized cyclic endoperoxide **4.36** which, on ring opening yielded *para*-peroxyquinol **4.37** and further manipulation afforded the natural product **4.38**.

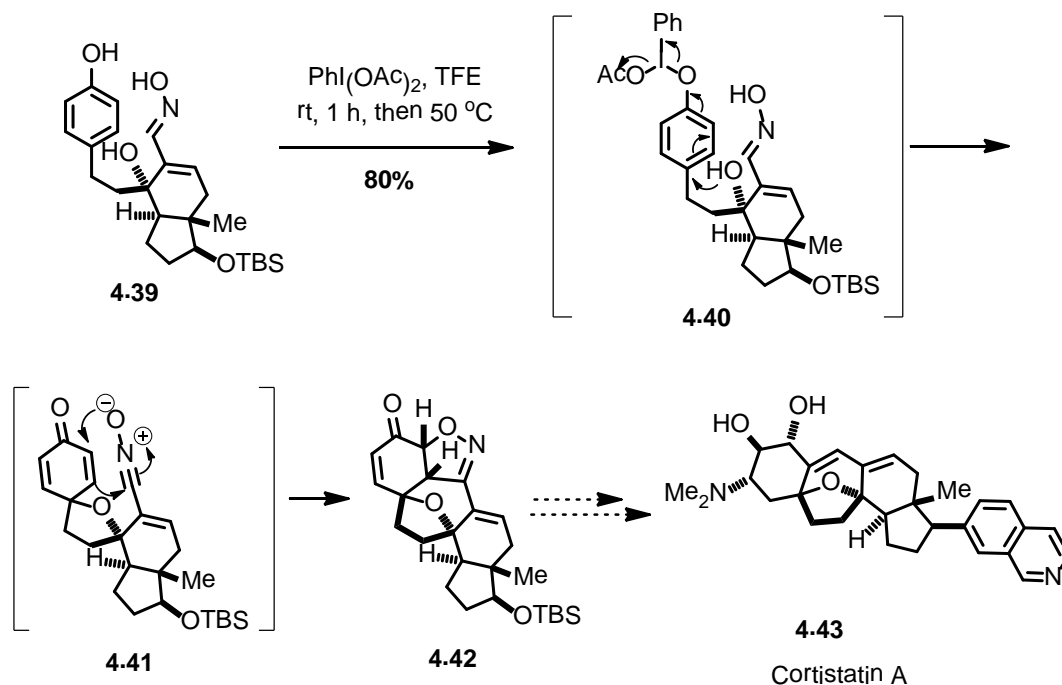


Scheme 4.9. Synthesis of (±)-cleroindicin D (**4.38**) using oxidative dearomatization

Hypervalent iodine reagent-mediated oxidative dearomatizations are widely used at various stages of natural product synthesis and in complex settings.<sup>122,123</sup> Sorensen and coworkers engaged a cascade process initiated by intramolecular hypervalent iodine reagent mediated oxidative dearomatization to construct the pentacyclic core of cortistatin A (**4.43**) (Scheme 4.10).<sup>124</sup> A substituted phenol (**4.39**) with a hydroxyl group in the side chain underwent tandem cyclization at the *ipso* position by nucleophilic attack of the hydroxyl group on the electrophilic aromatic ring generated upon treatment with PIDA to give **4.40** as shown in Scheme 4.10. This, on further oxidation, yielded nitrile oxide **4.41** which underwent [3+2] dipolar cycloaddition and generated a single

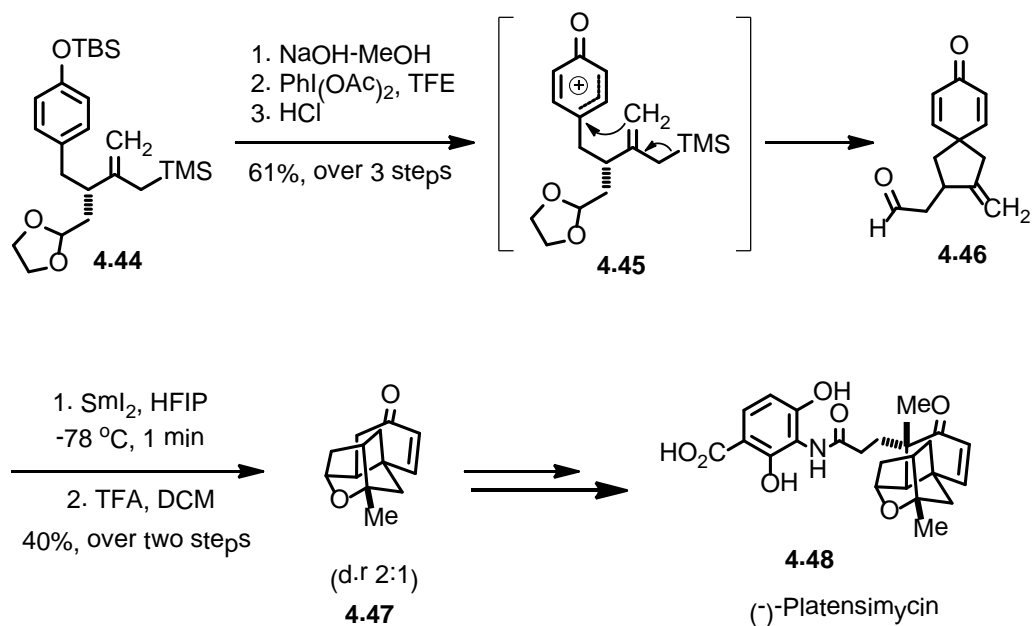


diastereomer **4.42** in one pot which displays the pentacyclic core structure of cortistatin A (**4.43**).



Scheme 4.10. Synthesis of cortistatin A (**4.43**) using hypervalent iodine mediated oxidative dearomatization

Nicolaou and coworkers have demonstrated elegant dearomatization via spirocyclization of phenol derivative involving carbon nucleophiles to form new C-C bonds in the presence of hypervalent iodine reagents (Scheme 4.11).<sup>125</sup> The free phenol obtained by TBS deprotection of **4.44** was activated by PIDA for nucleophilic attack. Allyl silane, a carbon nucleophile present in the side chain, attacked the *ipso* position of **4.45** to yield the spiro product **4.46** in polar solvent which, on further functionalization, afforded tetracyclic core structure (**4.47**) of (-)-platensimycin (**4.48**).

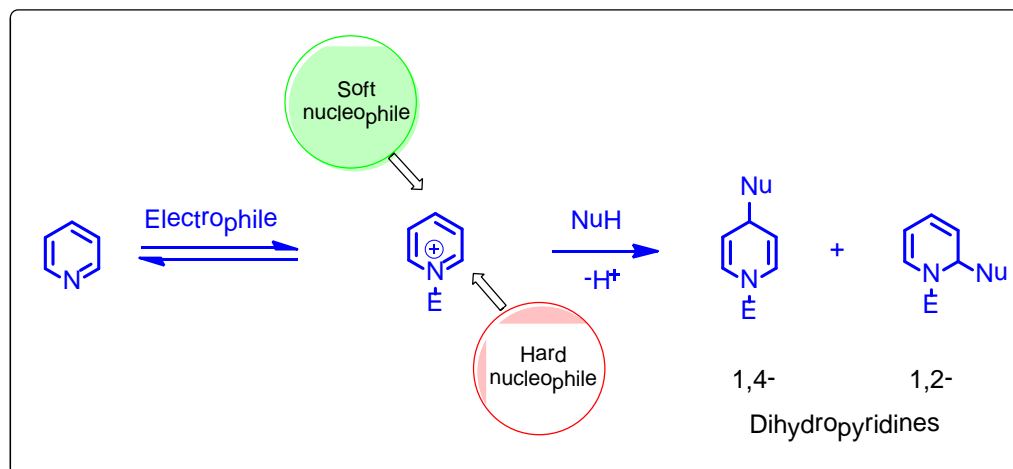


Scheme 4.11. Synthesis of (-)-platensimycin (**4.48**).using oxidative dearomatization

#### 4.5 Pyridine based dearomatization

Six-membered heterocycles containing a nitrogen atom are abundant in bioactive natural products. Pyridine derivatives provide a pool of starting materials for the synthesis of alicyclic aza-heterocycles via dearomatization. Pyridines participate in regioselective reactions with nucleophiles after conversion to pyridinium salts by treatment with alkylating or acylating reagents. Both inter and intramolecular additions of different types of nucleophiles to pyridinium intermediates using various electrophiles as pyridine activating groups have been reported. Particularly, intermolecular nucleophilic additions are extensively studied for the synthesis of functionalized heterocycles. In general, it was found that soft nucleophiles such as organocuprates, metal-enolates (e.g., zinc enolates) and enol ethers (e.g., silyl enol ethers) add to pyridinium intermediates preferentially at C-4 positions to afford 1,4-dihydropyridines

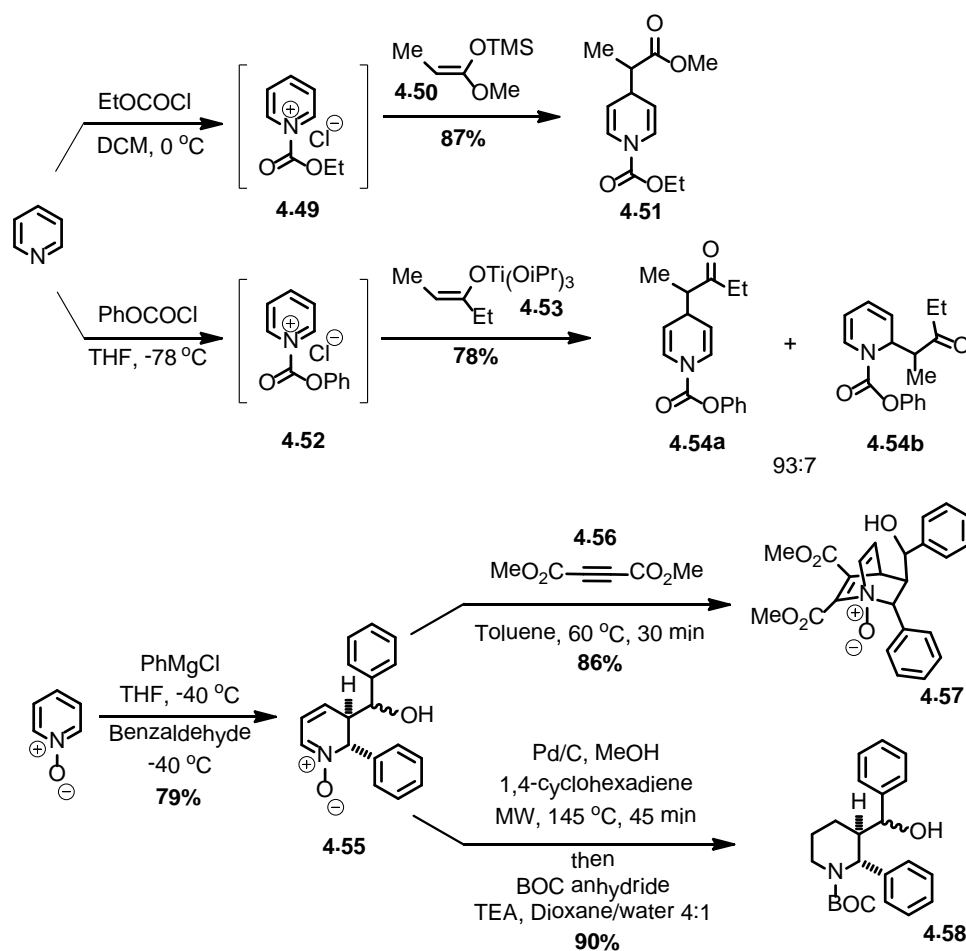
(Scheme 4.12).<sup>126-129</sup> On the other hand, hard nucleophiles such as organolithium and organomagnesium reagents add to the pyridinium intermediate at the C-2 position preferentially to give 1,2-dihydropyridines (Scheme 4.12).<sup>130-133</sup>



Scheme 4.12. General representation of nucleophilic additions to activated pyridine ring

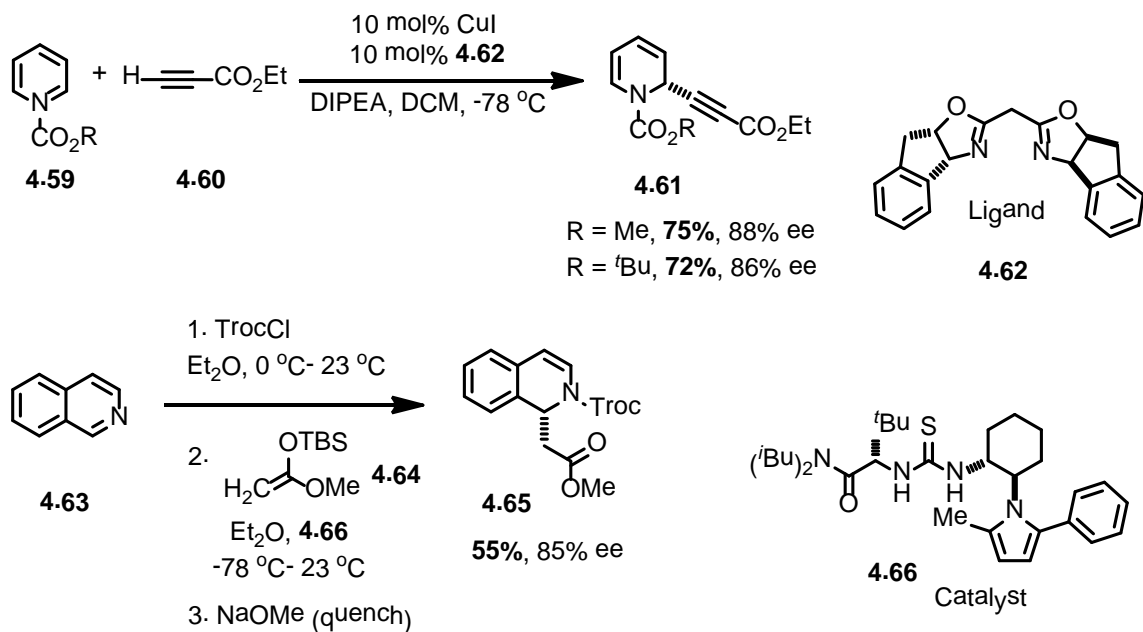
Examples of intermolecular additions to pyridinium salts are illustrated in Scheme 4.13. Akiba and coworkers reported that addition of silyl ketene acetal (**4.50**) to the pyridinium salt (**4.49**) resulted in 1,4-dihydropyridine regioisomer (**4.51**) in good yield.<sup>134</sup> Comins and coworkers, as part of efforts to direct nucleophiles to the 4-position, examined the addition of titanium enolates (**4.53**) to pyridinium salt (**4.52**).<sup>135</sup> They obtained a mixture of inseparable regioisomers (**4.54a-b**) with the 1,4-dihydropyridine being the major isomer. It has been reported that addition of organolithium reagents to pyridine N-oxide results in pyridine ring opening to yield dienyl oxime products. Almquist and coworkers, however, developed a methodology to add organo-magnesium reagents to

pyridine N-oxides selectively at the C-2 position in the presence of suitable electrophiles (e.g., benzaldehyde) to obtain functionalized *trans*-2,3-dihydropyridines (**4.55**) in a completely regio- and stereoselective process (scheme 4.13).<sup>136</sup> These *trans*-2,3-dihydropyridines were stable and participated in Diels-Alder cycloaddition reactions with dimethyl acetylene dicarboxylate (**4.56**) to afford **4.57** in excellent yield. They could also be converted into N-Boc protected piperidine derivative (**4.58**).



Scheme 4.13. Nucleophilic additions to pyridinium salts and their regioselectivity

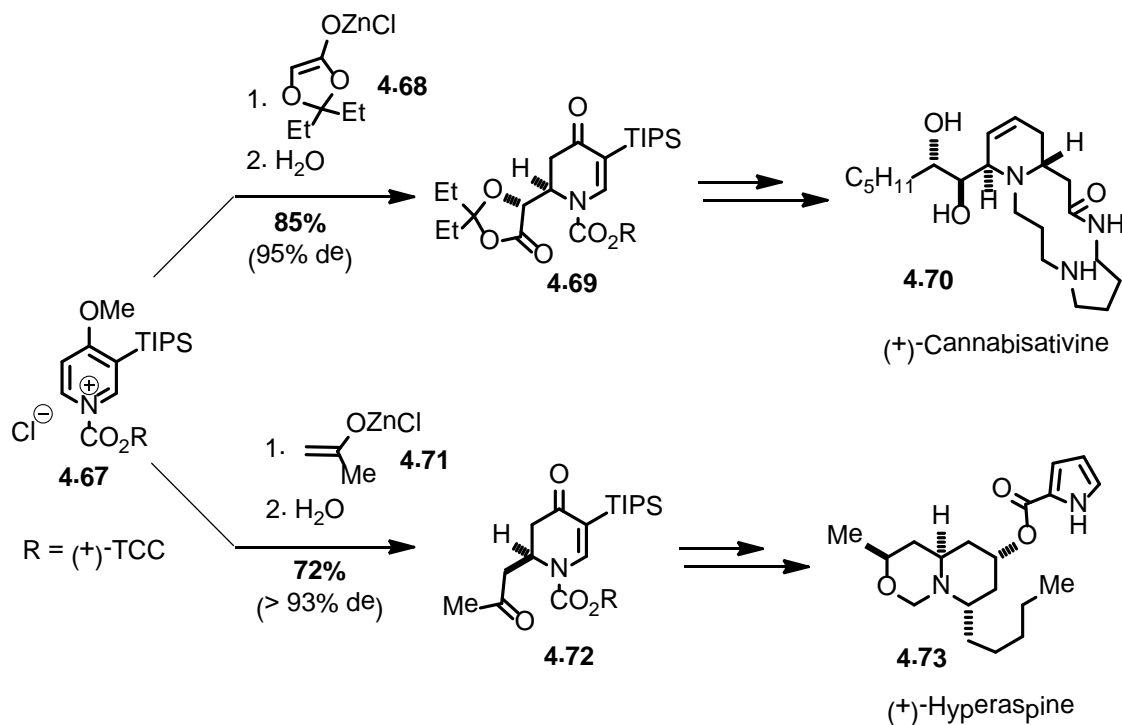
The asymmetric addition of nucleophiles to activated pyridines is a potentially powerful tool for stereocontrolled heterocycle synthesis. While chiral auxiliary technology has proven effective in promoting such additions. There are only a few reports describing catalytic asymmetric nucleophilic additions to pyridinium salts.<sup>137,138</sup> Ma and coworkers developed the asymmetric addition of activated terminal alkynes (e.g., **4.60**) to acylpyridinium intermediate (**4.59**) using copper complexes with bis(oxazoline) ligands (**4.62**) (Scheme 4.14).<sup>139</sup> Arndtsen and coworkers also reported that various terminal alkynyl reagents (not necessarily substituted with electron withdrawing groups) could be added to C-2 position of the pyridinium salt using copper catalysts and (R)-QUINAP ligands.<sup>140</sup> In another approach, Jacobsen and coworkers utilized asymmetric acyl-Mannich reaction involving chiral thiourea catalysts (e.g., **4.66**) for enantioselective addition of silyl ketene acetal (**4.64**) to acylated isoquinolinium intermediate to obtain dearomatized product (**4.65**) (Scheme 4.14).<sup>141</sup> They found enantioselectivity depends upon the nature of the activating group (TrocCl gave better selectivity), solvent (ether proved to be the best solvent), and substitution on the hydrogen bonding thiourea catalyst. While these transformations hint at the synthetic potential of catalytic asymmetric additions to pyridinium electrophiles, additional research needs to be performed to more fully develop this reaction type.<sup>137</sup>



Scheme 4.14. Asymmetric induction in nucleophilic addition to activated pyridine ring

In contrast, the use of chiral auxiliaries to mediate diastereoselective additions to pyridine has been widely used in synthesis. Comins and coworkers have extensively studied nucleophilic additions to activated pyridines and similar substrates.<sup>142,143</sup> They have used pyridine dearomatization strategies in total synthesis of many biologically important natural products. As a representative example, substrate controlled asymmetric induction during zinc enolate (**4.68**) addition to activated pyridine intermediate (**4.67**) was used to obtain 1,2-dihydropyridine (**4.69**).<sup>144</sup> Further manipulation yielded the desired natural product (+)-cannabisativine (**4.70**) (Scheme 4.15). The same starting material (**4.67**) has been utilized in the synthesis of several other alkaloid natural products, such as (+)-hyperaspine **4.73** by dearomatization strategy.<sup>145</sup> Addition of zinc enolate (**4.71**) was useful in obtaining dearomatized **4.72** in a highly

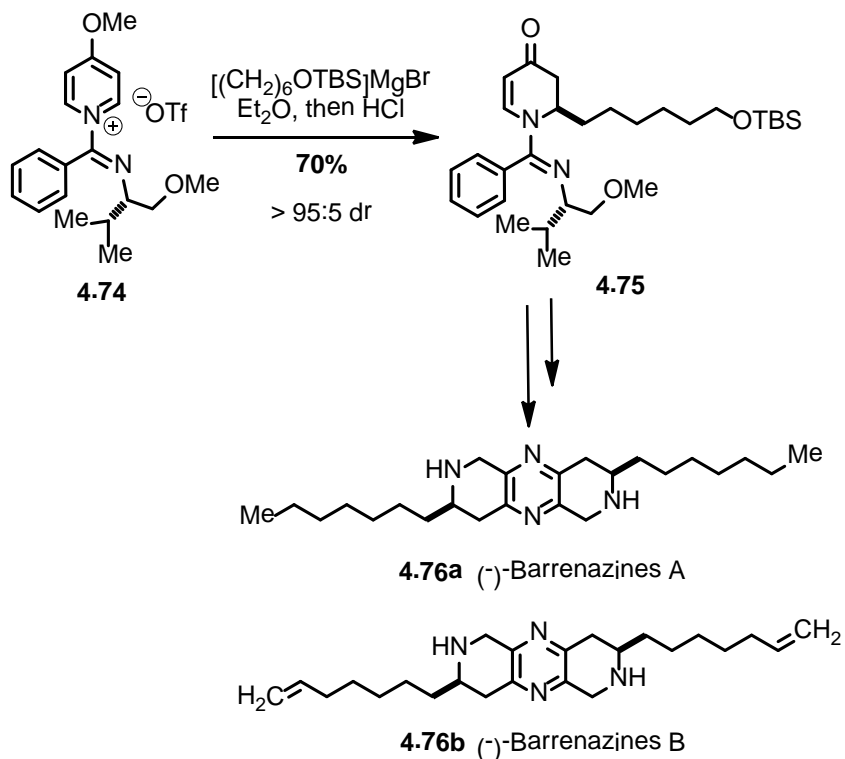
stereoselective manner, which was then further elaborated to the target natural product (Scheme 4.15).



Scheme 4.15. Intramolecular pyridine dearomatization in natural product synthesis (Comins *et al* approach)

Charette and coworkers have also comprehensively studied pyridine dearomatization to synthesize enantiopure, poly-substituted piperidines from readily available materials. They have synthesized chiral pyridinium salts such as **4.74** from substituted pyridines, secondary amides and triflic anhydride.<sup>146,147</sup> These pyridinium derivatives participate in highly diastereoselective and regioselective addition of carbon nucleophiles to produce dihydropyridines. For example, addition of Grignard reagent to the chiral pyridinium salt (**4.74**) produced 1,2-dihydropyridine **4.75** in good yield with excellent stereocontrol

(Scheme 4.16). Barrenazines A (**4.76a**) and B (**4.76b**) were then synthesized after a few additional chemical transformations in good overall yield (30% and 28% respectively).<sup>148</sup>



Scheme 4.16. Synthesis of (-)-barrenazines by Charette *et al* using intramolecular pyridine dearomatization

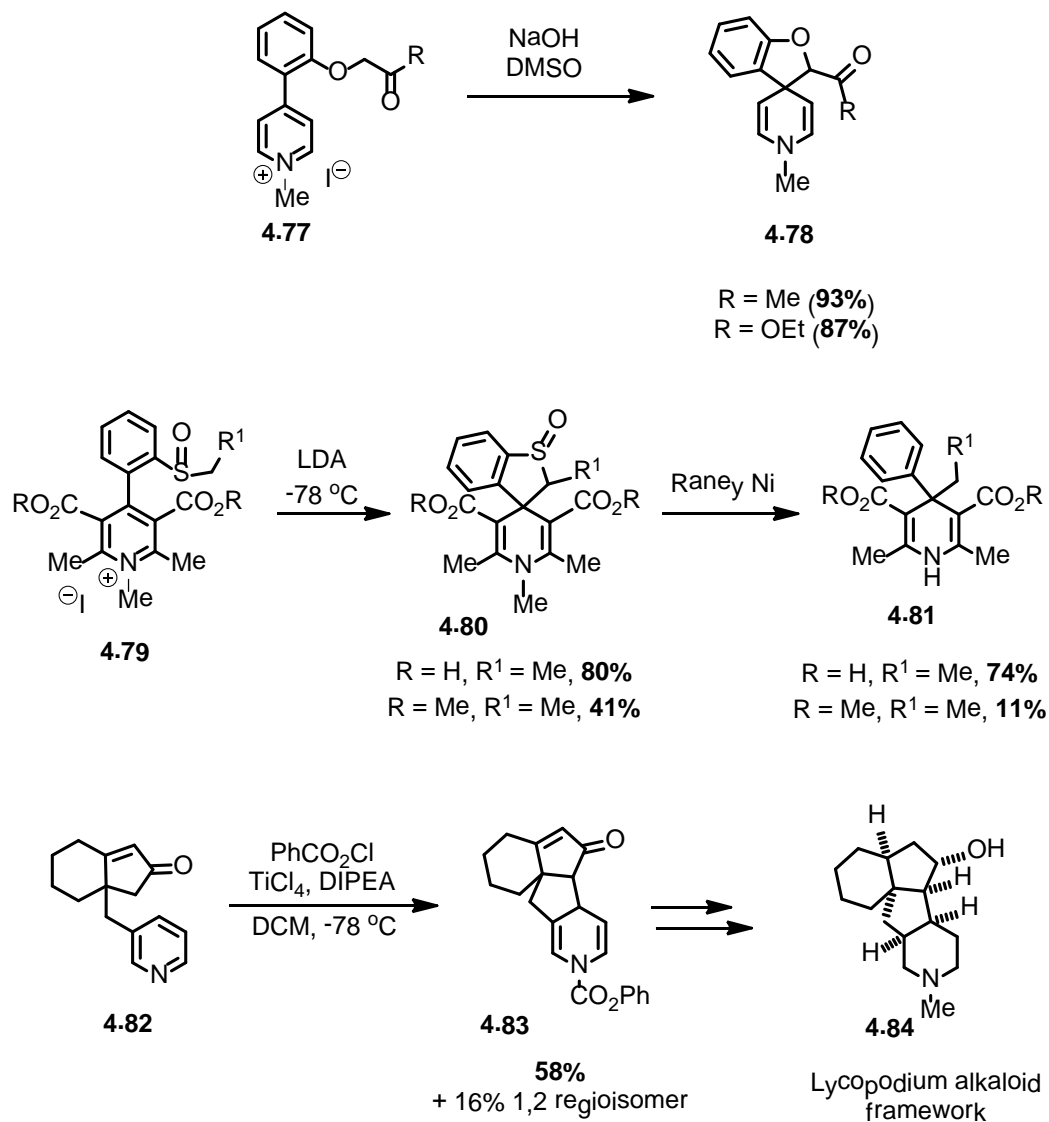
Intramolecular nucleophilic addition to pyridine derivatives offers potential entry to azaspirocycles and piperidine based fused-ring systems. Surprisingly, reports related to intramolecular dearomatization of pyridine substrates are less common relative to intermolecular reactions. Weller and coworkers have synthesized azaspirocycles using substituted pyridines with carbon nucleophiles in the side chains (scheme 4.17).<sup>149</sup> Treatment of alkyl pyridinium salts such as **4.77** with NaOH yielded the spirocyclic product (**4.78**) in DMSO in good yield, but



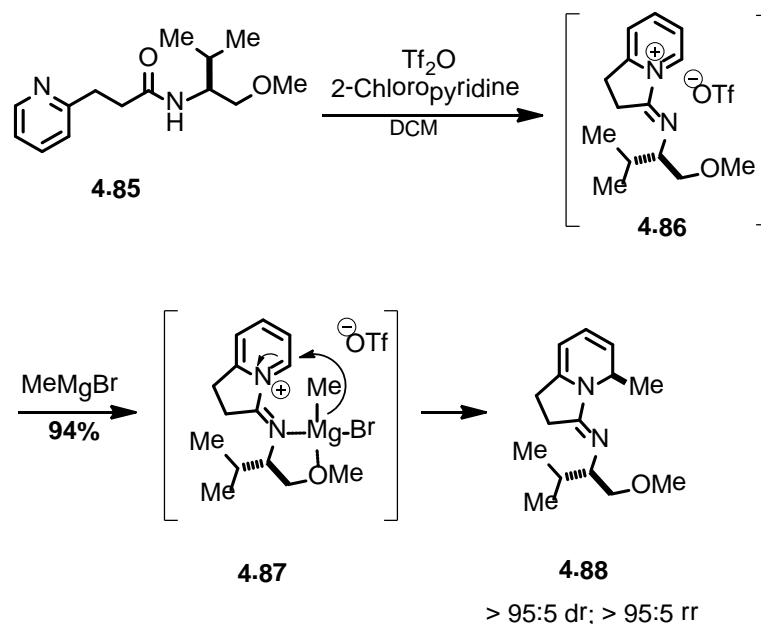
the spirocycles were only stable at -20 °C and decomposed at room temperature. In another experiment, Goldmann and coworkers synthesized 4,4'-disubstituted-1,4-dihydropyridines via dearomatization (Scheme 4.17).<sup>150</sup> Sulfinyl carbanion generated by treatment of **4.79** with LDA reacted in intramolecular fashion at the 4-position to afford spiro-1,4-dihydropyridine **4.80** which was further functionalized to obtain **4.81** as part of an effort to develop new antihypertension agents. Moreover, starting materials such as **4.79** were synthesized from Hantzsch esters, thus limiting the generality of this strategy. Meyers and coworkers were able to successfully add a titanium enolate to the 4-position of a pyridinium salt generated by treating **4.82** with phenyl chloroformate in the presence of DIPEA (Scheme 4.17).<sup>151</sup> This transformation resulted in a 5:1 mixture of regioisomers (**4.83**) (desired 3,4-regioisomer being major and 2,3-regioisomer was minor) and provided a key intermediate in construction of the tetracyclic core of *Lycopodium* alkaloids (**4.84**).

Intramolecular pyridine activation and asymmetric dearomatization was performed by Charette and coworkers to obtain 5-substituted indolizidines and 6-quinolizidines with high regio and diastereoselectivity (Scheme 4.18).<sup>152</sup> These researchers synthesized an activated chiral pyridinium salt **4.86** by reacting **4.85** with triflic anhydride in the presence of 2-chloro pyridine. Grignard reagent addition to **4.86** resulted in formation of unsaturated indolizidine **4.88** as single regio and diastereomer. Even though pyridinium salt (**4.85**) was base sensitive, the undesired deprotonation due to basicity of the Grignard reagent was not observed. Stereo- and regio-control is attributed to precomplexation (represented as **4.87**) of the Grignard reagent with *E*-imidate lone pair and also coordination with ether functionality, thus directing nucleophilic addition to the 6-position while minimizing 1,3-allylic strain with the auxiliary.

4.6 Intramolecular dearomatization of pyridine derivatives



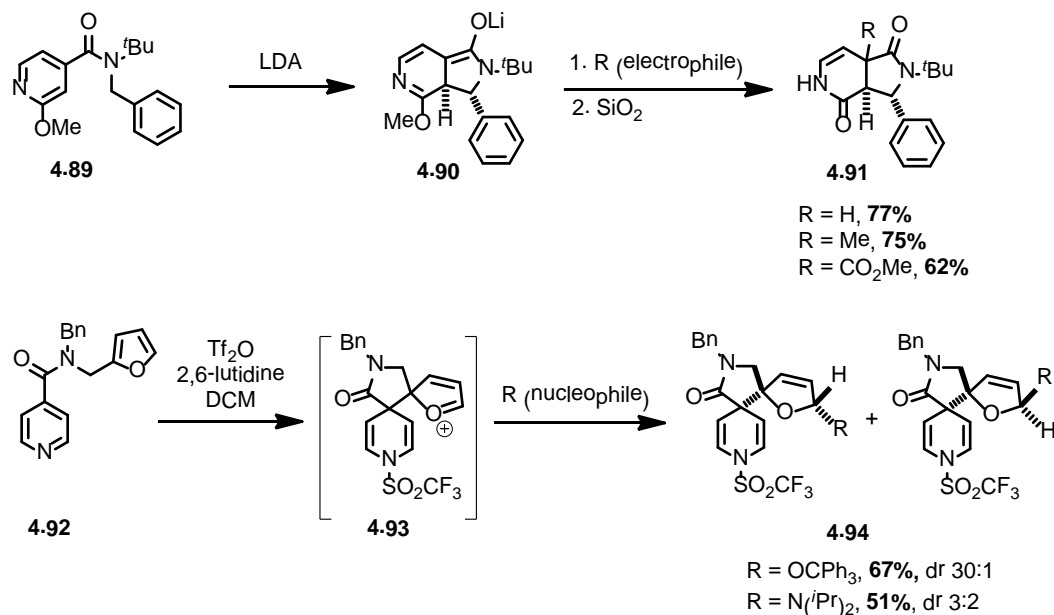
Scheme 4.17. Examples of intramolecular pyridine dearomatization



Scheme 4.18. Asymmetric induction in intramolecular pyridine dearomatization

Clayden and coworkers have investigated intramolecular pyridine dearomatization in great detail to access functionalized piperidines. They have successfully demonstrated that anions generated by lithiation of N-benzyl pyridine derivatives add directly to the pyridine ring or to the activated pyridine derivatives.<sup>153</sup> Lithiated isonicotinamide derivative **4.89** was added in an intramolecular manner to the pyridine ring and yielded dearomatized **4.90** which on alkylation or acylation with electrophiles, yielded **4.91** in good yield as a single diastereomer (Scheme 4.19). In a separate experiment, the same group has exploited double dearomatization of electrophilic and nucleophilic arene pairs tethered to each other via tandem intramolecular cyclizations (Scheme 4.19).<sup>154,155</sup> The pyridine ring in **4.92** was activated by acylation and nucleophilic attack by the electron rich furan ring resulted in spirocycle **4.93**. The oxonium intermediate **4.93** was successfully trapped by added nucleophiles to yield **4.94** with high diastereoselectivity. Even though a few additional reports describing

pyridine intramolecular dearomatization reactions are available, intramolecular dearomatization of pyridine-based substrates still remains relatively unexplored and thereby offers researchers an opportunity to access complex molecular architectures.<sup>156-158</sup>



Scheme 4.19. Examples of intramolecular pyridine dearomatization from the Clayden group

#### 4.7 Conclusion

Several methods to achieve dearomatization in the context of natural product synthesis and heterocyclic chemistry have been reported. Strategies benefit from readily available starting materials that can be converted to complex materials in a minimum of synthetic operations. Development of new dearomatization methods may facilitate discovery of concise, efficient, regioselective, and stereo-controlled routes to important synthetic building blocks in environmentally and economically friendly fashion.

## CHAPTER FIVE

## DIAZASPIRO[4.5]DECANES FROM 4-ALKYLPYRIDYL-BETA-AMIDO ESTER SPIROCYCLIZATION

5.1 Introduction

Heterocycles are one of the most important classes of ring systems found in many naturally occurring and biologically active compounds. Azaspirocycles and N-containing fused ring systems are abundant in many pharmacologically active molecules (Figure 1).<sup>159-161</sup> The structural complexity of azaspirocycles is interesting from a synthetic standpoint and the most notable feature is the presence of spirocyclic quaternary carbon center. These spirocyclic centers pose unique synthetic challenges.<sup>162-164</sup>

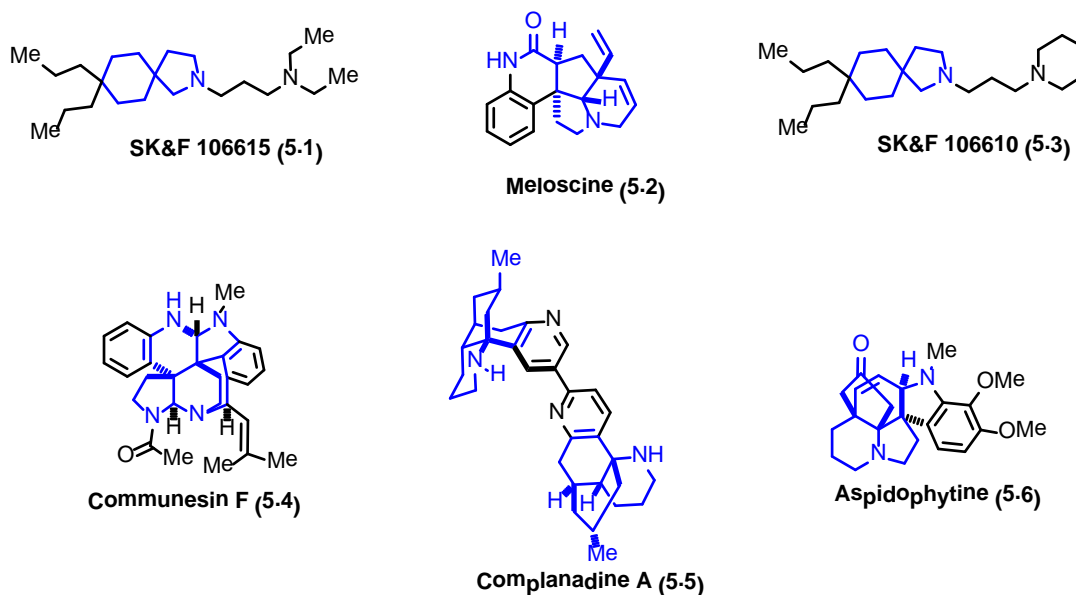
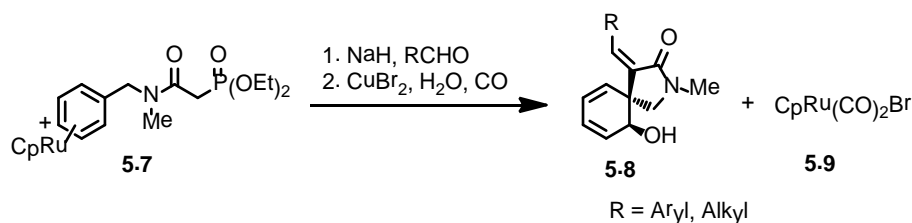


Figure 5.1. Azaspirocycles and fused ring systems in natural products and pharmacologically active compounds

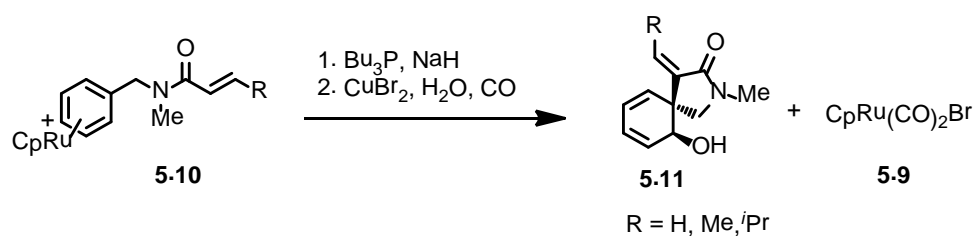
There are many synthetic approaches for the synthesis of these heterocycles in the literature. These often involve the use of toxic metals and expensive reagents. Dearomatization of aromatic substrates is one method that provides a unique pathway to synthesize these spirocycles.

Various groups have reported the synthesis of complex molecular architectures via dearomatization of aromatic substrates using both intra as well as intermolecular reactions. Previous work in the Pigge group has demonstrated that ruthenium mediated dearomatization strategies could be utilized to synthesize azaspirocycles.<sup>165-170</sup>  $\eta^6$ -Arene-ruthenium complexes substituted with stabilized carbon nucleophiles were synthesized and utilized as dearomatization substrates. Nucleophilic addition of the side chain to the arene ring resulted in generation of azaspirocycles. Particularly,  $\beta$ -amido phosphonate derived benzyl substrates were coordinated to a Ru(II)Cp fragment to give  $\eta^6$ -arene complexes (e.g. **5.7**). The electronically deficient benzene ring in the arene-ruthenium complex then suffered intramolecular attack by the side chain carbon nucleophile in the presence of base and aldehyde to yield azaspirocycle **5.8** with exocyclic olefin after demetallation with complete diastereoselectivity (Scheme 5.1).<sup>165</sup> Asymmetric variants were also developed to obtain enantiopure azaspirocycles.



Scheme 5.1. Azaspirocycles of arene-ruthenium complexes of  $\beta$ -amido phosphonates

In another approach, arene-ruthenium acrylamides underwent tandem conjugate addition in a Morita-Baylis-Hillman manner to yield functionalized spirocycles (**5.11**) and fused ring benzapine derivatives (Scheme 5.2).<sup>166</sup> Even though experimental procedures were developed to recover the cyclopentadienyl ruthenium(II) byproduct (**5.9**), the arene-ruthenium approach was limited because of the need to use stoichiometric amounts of expensive ruthenium reagents.



Scheme 5.2. Morita-Baylis-Hillman cyclization of arene-ruthenium acrylamides

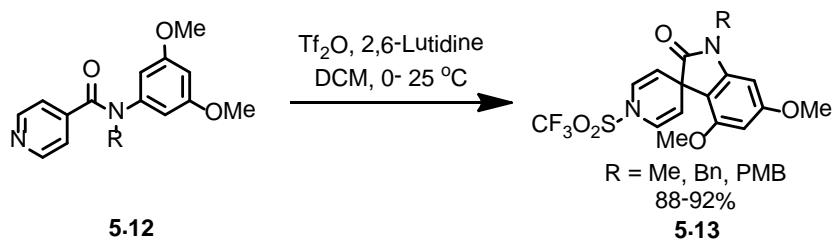
The Pigge group has also demonstrated that oxidative dearomatization strategies mediated by hypervalent iodine reagents could be utilized to synthesize azaspirocycles and the details of this approach are described in Chapter 7. In continuing efforts to uncover new synthetic methods based on dearomatization of aromatic compounds, we shifted our focus to pyridine derivatives. Pyridine ring systems offer a convenient source for the synthesis of substituted nitrogen containing heterocycles.

Intramolecular dearomatizations of pyridine derivatives can potentially rapidly produce complex molecular frameworks. Asymmetric variations of such methods could then provide access to enantiopure heterocyclic compounds. Unique 1,2 or 1,4-dihydropyridines formed upon nucleophilic addition into N-acyl

or N-alkyl pyridinium salts would serve as synthetic intermediates in these processes.

## 5.2 Background

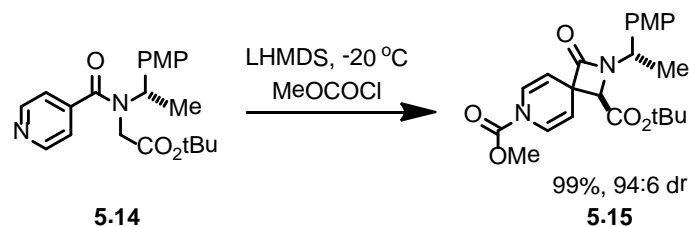
Even though numerous reports of intermolecular nucleophilic addition to pyridinium salts are known, reports pertaining to intramolecular cyclization to yield spirocycles are less common. Clayden and coworkers reported that the treatment of N-arylisonicotinamide (**5.12**) with triflic anhydride and a hindered base in CH<sub>2</sub>Cl<sub>2</sub> afforded the benzo fused spiro 1,4-dihydropyridines (**5.13**) (Scheme 5.3).<sup>171</sup>



Scheme 5.3. Intramolecular cyclization of pyridine derivatives

In another example, these same researchers found that 4,6-diazaspirocyclic lactams can be synthesized diastereoselectively using substrate control. On pyridine activation via N-acylation, enolates of N-isonicotinoyl glycine and alanine side chains attacked the *ipso* position with high diastereoselectivity (Scheme 5.4).<sup>155</sup>





Scheme 5.4. Diastereoselective synthesis of azaspirocycles

In general, all reported intramolecular spirocyclization reactions involving pyridine derivatives have a nucleophilic group on the side chain substituted at C4 position of the pyridine ring. Once the pyridine ring becomes activated by N-alkylation or acylation to yield an electrophilic pyridinium cation, the nucleophile in the side chain undergoes cyclization to give 1,4-dihydropyridines (Figure 5.2).

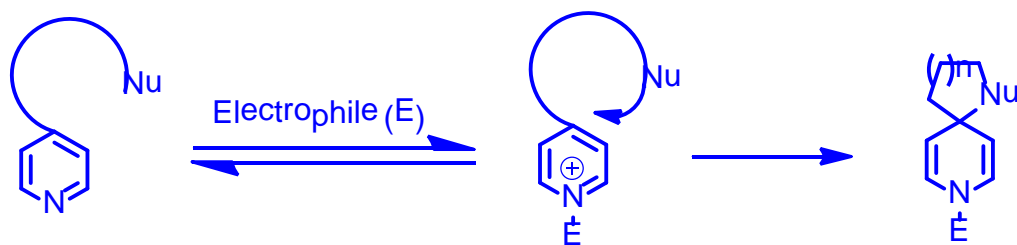
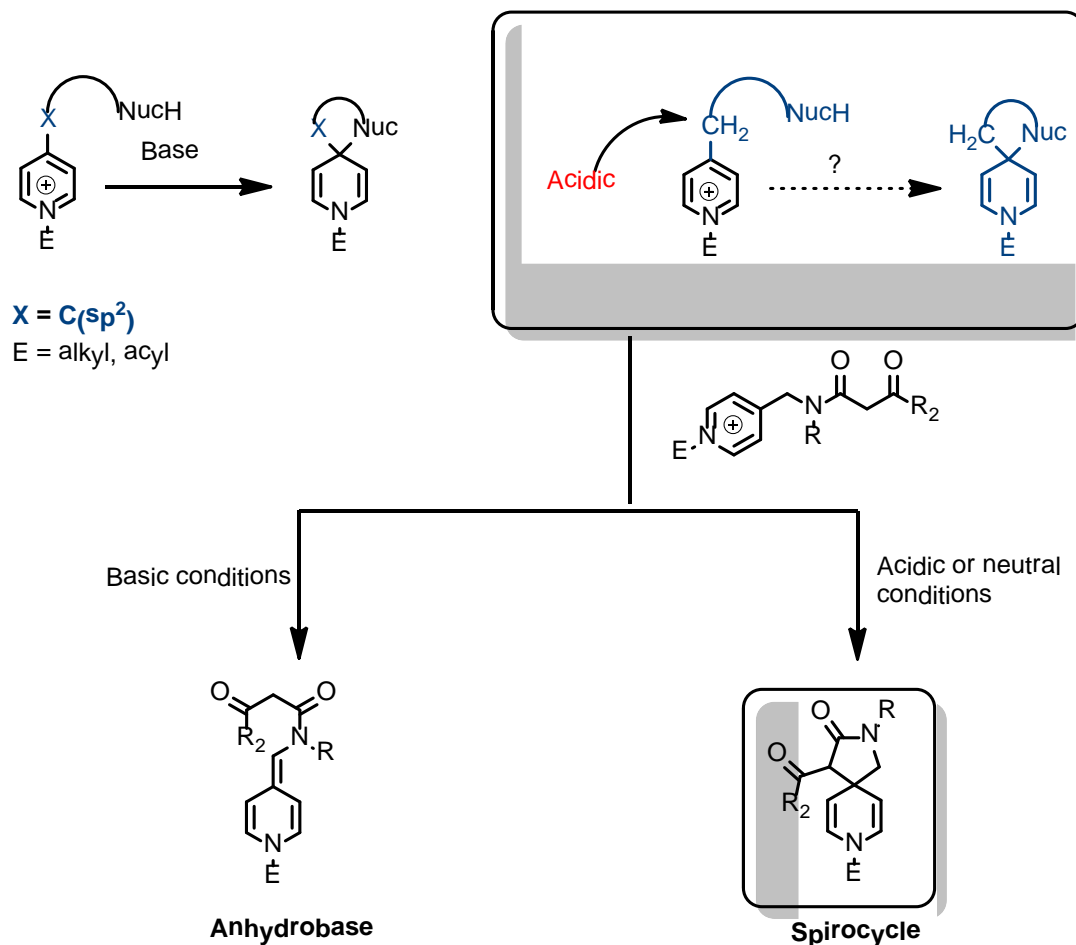


Figure 5.2. General approach for pyridine based spirocyclization

In all examples of this reaction reported thus far, the benzylic position of 4-pyridyl substrates involved in these transformations is always occupied with a heteroatom or a  $sp^2$  carbon (as in carbonyl or aryl groups). This feature enables the use of acidic or basic conditions for the cyclization process. Benzylic hydrogens at the C4 position experience an increase in acidity on pyridinium intermediate formation. Under basic conditions, undesired deprotonation of these

benzylic hydrogens leads to the formation of anhydrobases. The absence of benzylic hydrogens not only eliminates the possibility of anhydrobase formation but also limits the scope of the spirocyclization (Scheme 5.5). While there are no reports of any derivatives of 4-alkylpyridines involved in spirocyclizations in the literature, we envisioned that under near neutral or acidic conditions intramolecular nucleophilic addition of stabilized nucleophiles to pyridinium intermediates to yield spiroproducts from 4-alkylpyridines should be feasible. The resulting 1,4-dihydropyridines could be utilized further for the synthesis of more complex heterocyclic frameworks. Functionalization of these versatile building blocks could provide an interesting and useful entry into pharmacologically important azaspirocycle scaffolds. To evaluate our strategy, we decided to attach stabilized  $\beta$ -dicarbonyl carbon nucleophiles to 4-alkylpyridine substrates. To begin with, we used the  $\beta$ -amido ester as a model pro-carbon nucleophile for this study. These substrates were intended to afford diazaspiro[4.5]decanes upon cyclization.



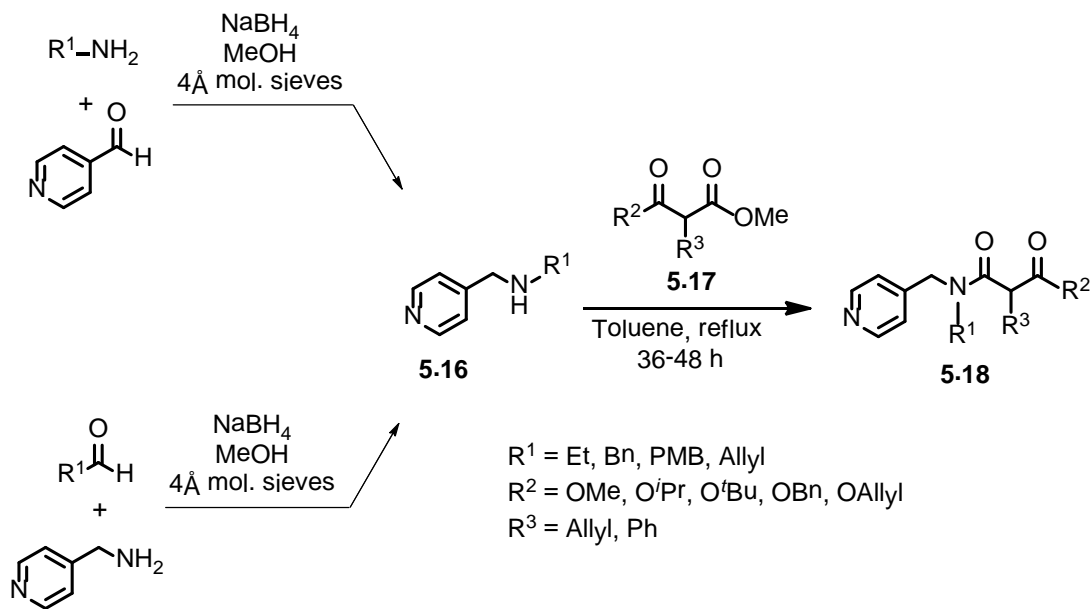
Scheme 5.5. Our approach to alkylpyridine dearomatization

### 5.3 Results and discussion

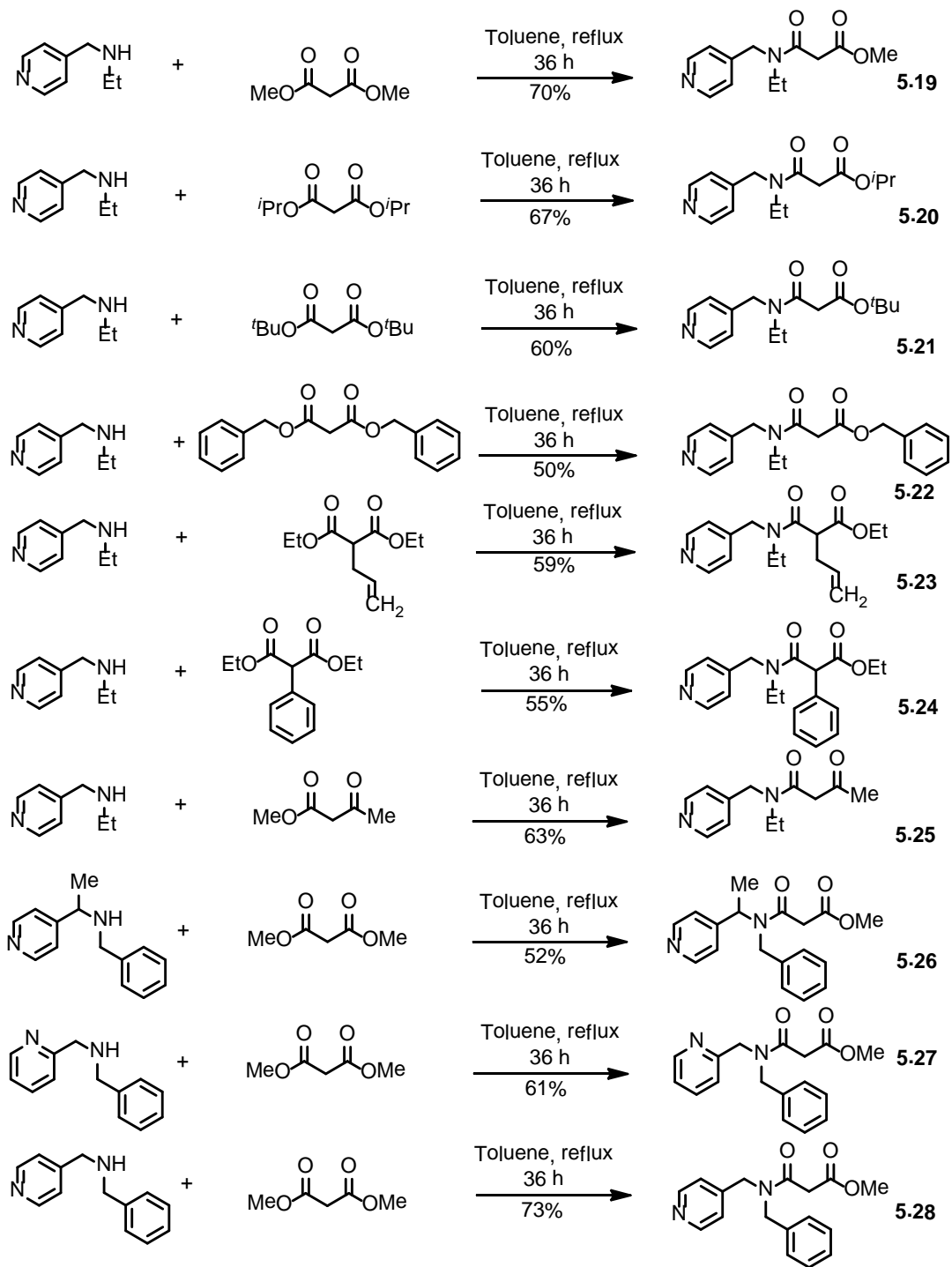
The 4-alkyl pyridine substrates with  $\beta$ -amido ester side chains (**5.18**) were designed and synthesized as shown in the Scheme 5.6. While designing these substrates, several factors were considered. 1) Successful incorporation of  $sp^3$  hybridized benzylic positions into spirocyclization substrates would expand the scope of pyridine dearomatization reactions. 2) Diazaspiro[4.5]decane frameworks that would result from successful cyclization are abundant in pharmacologically important molecules. 3) The ability to vary the substituent on nitrogen in the side chain would allow us to study the influence of different N-

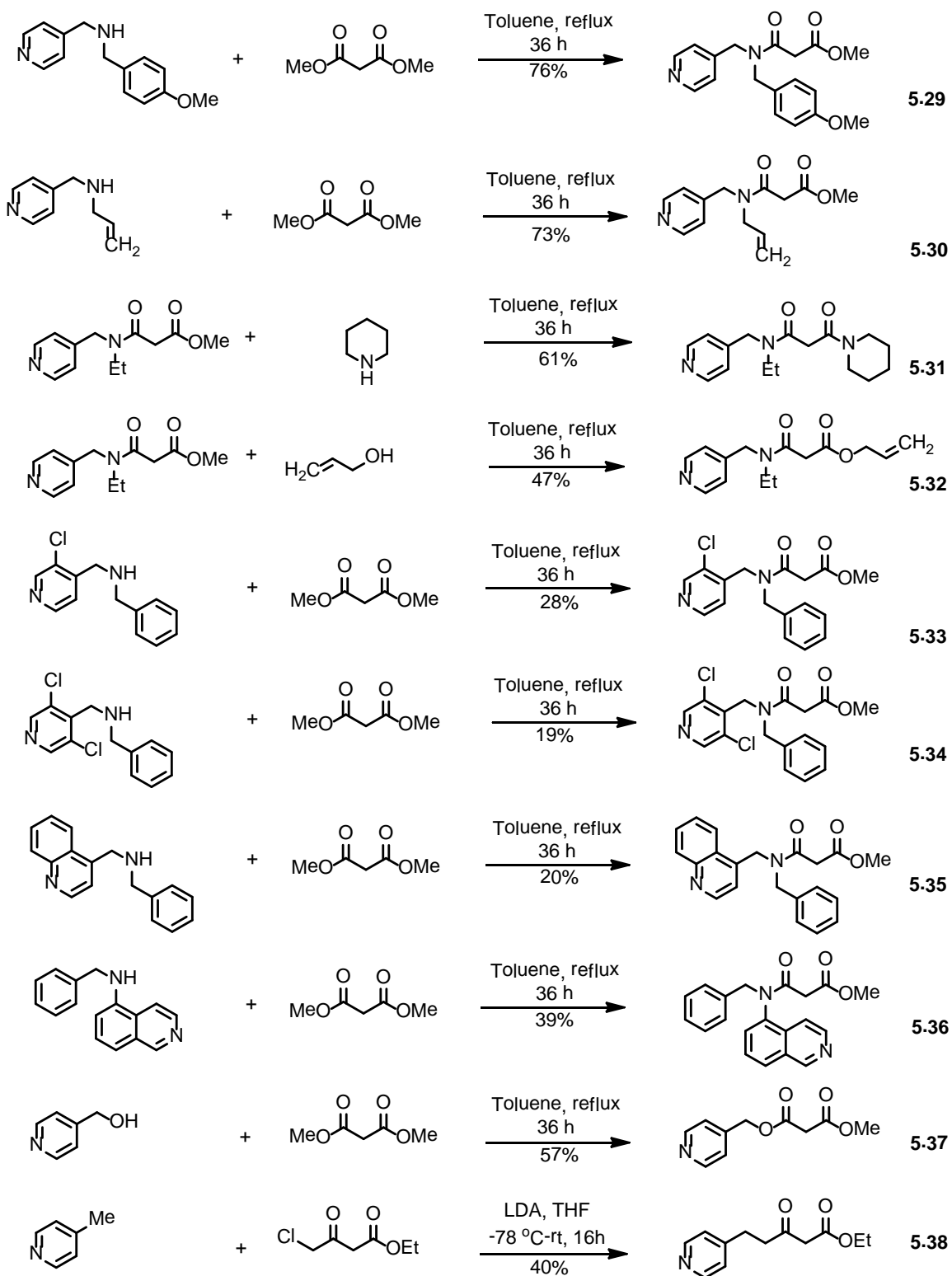
protecting groups on spirocyclization. 4) The pro-carbon nucleophile  $\beta$ -amido ester features an activated methylene group which would be helpful in nucleophilic addition in the presence of neutral or acidic reaction conditions. Furthermore, the ester functionality may act as a handle for additional manipulation of spirocyclic products. The lactam carbon of the spirocycle also may be potentially exploited synthetically. Finally, the envisioned spirocyclic precursors could be prepared from inexpensive, commercially available materials in only a few steps.

The cyclization precursor **5.19** was synthesized from commercially available 4-(ethylaminomethyl) pyridine with dimethyl malonate through a transamidation reaction in refluxing toluene for 36 h (Scheme 5.6). The other 4-alkylpyridine-derived secondary amines (**5.16**) were synthesized through reductive amination reactions of imines using  $\text{NaBH}_4$ . Imines were produced *in situ* from corresponding aldehydes and 4-aminomethyl pyridines (Scheme 5.6). The transamidation reactions were again performed to afford the initial cyclization substrates. Compounds **5.19-5.32** were prepared using these procedures (Scheme 5.7). Substituted pyridines **5.33-5.34** were obtained similarly starting with the corresponding chloro-substituted pyridine carboxaldehyde. Likewise, quinolone carboxaldehyde was used to prepare substrate **5.35** and amino-isoquinolone for **5.36**. 4-Alkyl pyridines with ester linkages (**5.37**) and methylene linkages (**5.38**) were also synthesized as shown in Scheme 5.7. The substituted pyridines shown in Scheme 5.7 were all obtained in moderate to good yield and all the precursors were stable to silica gel flash column chromatography. These substrates were characterized using NMR spectroscopy and mass spectrometry.



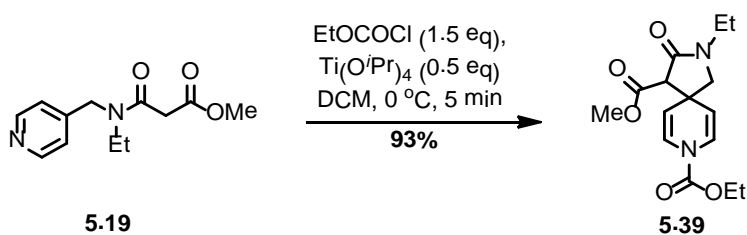
Scheme 5.6. General synthesis of 4-alkyl substituted pyridine with nucleophile  $\beta$ -amido ester side chains

Scheme 5.7. Synthesis of alkylpyridine- $\beta$ -amido ester substrates



Scheme 5.7. (Continued)

Pyridine derivative **5.19** was chosen as the model substrate for initial cyclization studies and results are summarized in Table 5.1. First, **5.19** was treated with ethyl chloroformate in dichloromethane at 0 °C.<sup>172</sup> The formation of putative acylated pyridinium intermediate accompanied by only a trace amount of product was observed using thin layer chromatography (TLC). Warming the reaction mixture to room temperature had no apparent effect as monitored by TLC. Subsequently different Lewis acid additives and solvents were screened in the presence of ClCO<sub>2</sub>Et in an effort to induce nucleophilic addition to acyl pyridinium intermediates. Titanium isopropoxide proved to be the best additive resulting in a faster reaction and complete conversion to the spirocyclic product. Other Lewis acids such as TiCl<sub>4</sub>, SnCl<sub>4</sub>, InCl<sub>3</sub>, MgBr<sub>2</sub>, Mg(ClO<sub>4</sub>)<sub>2</sub>, B(OMe)<sub>3</sub>, and Pd(OAc)<sub>2</sub> failed to promote the spirocyclization. Addition of substoichiometric quantities of Ti(O<sup>*i*</sup>Pr)<sub>4</sub> resulted in instantaneous conversion into the spirocycle in excellent isolated yield, but lower loadings of Ti(O<sup>*i*</sup>Pr)<sub>4</sub> were not helpful for the spirocyclization. This reaction was also successfully performed on 10 mmol scale with equal efficiency.



Scheme 5.8. Intramolecular dearomatization of **5.19**



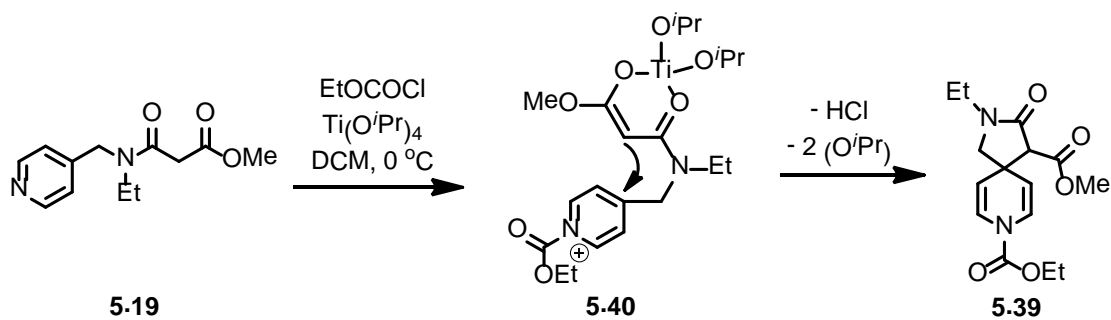
Table 5.1. Initial screening of the reaction conditions.

Entry	Solvent	Additive <sup>a</sup>	t(min)	% Yield <sup>b</sup>
1	DCM <sup>c</sup>	None	30	trace <sup>d</sup>
2	DCM	Ti(O <sup>i</sup> Pr) <sub>4</sub>	5	93
3	DCM	Ti(O <sup>i</sup> Pr) <sub>4</sub> <sup>e</sup>	5	trace
4	DCM	TiCl <sub>4</sub>	30	0
5	DCM	SnCl <sub>4</sub>	30	Trace
6	DCM	InCl <sub>3</sub>	30	Trace
7	DCM	B(OMe) <sub>3</sub>	30	Trace
8	DCM	Mg(ClO <sub>4</sub> ) <sub>2</sub>	30	0
9	DCM	Pd(OAc) <sub>2</sub>	30	0
10	DCM	MgBr <sub>2</sub>	30	Trace
11	THF	Ti(O <sup>i</sup> Pr) <sub>4</sub>	30	Trace
12	DMF	Ti(O <sup>i</sup> Pr) <sub>4</sub>	30	0
13	MeCN	Ti(O <sup>i</sup> Pr) <sub>4</sub>	5	79
14	PhMe	Ti(O <sup>i</sup> Pr) <sub>4</sub>	5	77

<sup>a</sup>0.5 equiv. used unless otherwise indicated.

<sup>b</sup>Isolated yield. <sup>c</sup>Dichloromethane.

<sup>d</sup>detected by TLC. <sup>e</sup>0.15 equiv. used.



Scheme 5.9. Possible mechanism for the Ti(O<sup>i</sup>Pr)<sub>4</sub> catalyzed 4-alkylpyridyl spirocyclization

A possible mechanism for this reaction (Scheme 5.9) entails enolization of the  $\beta$ -dicarbonyl side chain by  $\text{Ti}(\text{O}^i\text{Pr})_4$  (**5.40**) thereby facilitating the nucleophilic addition of the side chain to the activated pyridinium intermediate. It is unclear why other Lewis acids fail to promote this spirocyclization despite their ability to enolize the  $\beta$ -dicarbonyl side chain. It was reasoned that the  $\beta$ -dicarbonyl-Ti adduct may result in controlled release of isopropoxide anions which may be the important factor of this reaction. The presence of isopropoxide also resulted in the formation of trace amounts of spirocycle **5.45** along with **5.39** (Figure 5.3). The spirocyclization reaction was also found to occur in acetonitrile and toluene, but DMF and THF were not suitable for the transformation.

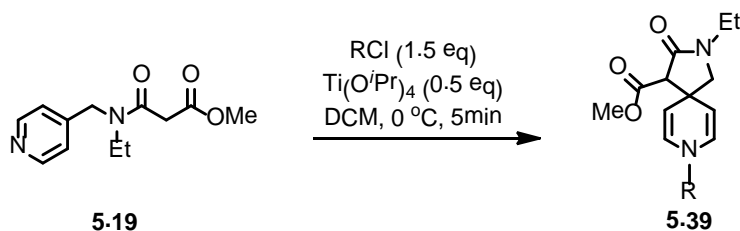


Table 5.2. Electrophiles examined for the spirocyclization

Entry	R	Yield <sup>a</sup>
1	$^i\text{PrO}_2\text{C}$	80 ( <b>5.39a</b> )
2	$\text{BnO}_2\text{C}$	86 ( <b>5.39b</b> )
3	$\text{PhO}_2\text{C}$	66 ( <b>5.39c</b> )
4	$\text{CH}_3\text{C(O)}$	20 ( <b>5.39d</b> )
5	$\text{PhSO}_2$	13 ( <b>5.39e</b> )
6	$\text{CF}_3\text{SO}_2^{\text{b}}$	0
7	$\text{Me}^{\text{c}}$	0

<sup>a</sup>Isolated yield. <sup>b</sup> $\text{Tf}_2\text{O}$  was used.

<sup>c</sup> $\text{MeI}$  was used.

Since the activation of the pyridine ring is required for spirocyclization, electrophiles other than ClCO<sub>2</sub>Et were examined and the results are summarized in Table 5.2. Both alkyl and aryl chloroformates behaved similarly to ethyl chloroformate, and the corresponding spirocycles **5.39a-c** were obtained in good yields. Acetyl chloride and phenylsulfonyl chloride were less effective and afforded the spirocycles **5.39d** and **5.39e** respectively, in lower yields. Pyridine activation using triflic anhydride or methyl iodide failed to produce any isolable products.

Next, the generality of the reaction was investigated by varying the substitution at the amide nitrogen as well as at the ester functionality in the pyridine derivatives (Figure 5.3). The optimized conditions indicated in Table 5.1 were employed, which involved treatment of substrate with 1.5 equivalents of ethyl chloroformate in the presence of 0.5 equivalents of titanium isopropoxide in DCM at 0 °C. The corresponding products **5.43**, **5.44** and **5.45** were obtained in good yield from their respective starting materials (Figure 5.3). These results demonstrated that substitution of the amide nitrogen with removable groups such as benzyl, allyl and PMB can be accommodated without affecting the efficiency of the cyclization. Even ester group variants behaved well for this transformation and yielded the corresponding 1,4-dihydropyridines **5.41**, **5.42**, **5.46** and **5.47** in excellent yield.

The scope of the reaction was also examined under the optimal reaction conditions with variation in 4-alkyl and carbon nucleophilic side chain (Scheme 5.10). The 4-alkylpyridine derivative with a benzylic substituent **5.26** was subjected to cyclization conditions and afforded the desired product **5.49** as the mixture of diastereomers in good yield. Substrate **5.31** with β-diamide as the pro-nucleophile also gave the desired spirocyclization product, but the β-diester derivative **5.37** resulted in low yield for the transformation with only 7% isolable

yield of **5.51**. A  $\beta$ -keto amide derivative **5.25** was also found to undergo cyclization in low yield. In general, the substrates containing  $\beta$ -dicarbonyl carbon nucleophiles other than  $\beta$ -amido esters were found to be poor substrates for this reaction. We speculate that the amide linkage provides beneficial conformational effect on chelation with the Lewis acid for the nucleophilic addition compared to other  $\beta$ -dicarbonyl-Lewis acid adducts. Conformational flexibility might be one reason for the attenuated reactivity of these spirocyclization precursors.

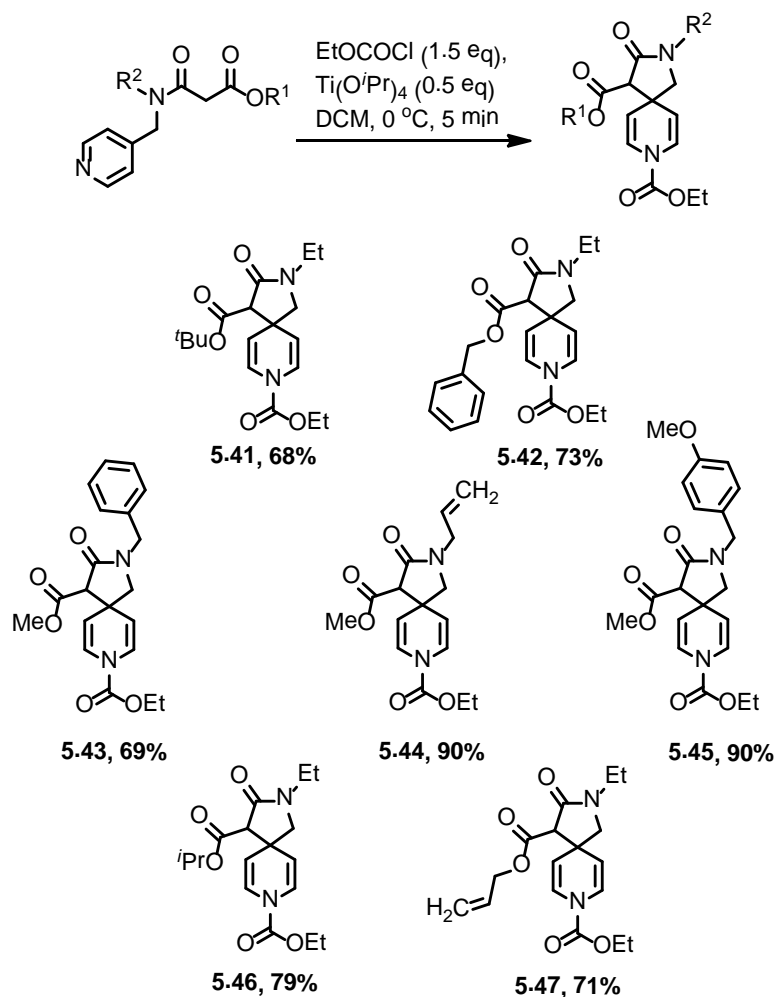
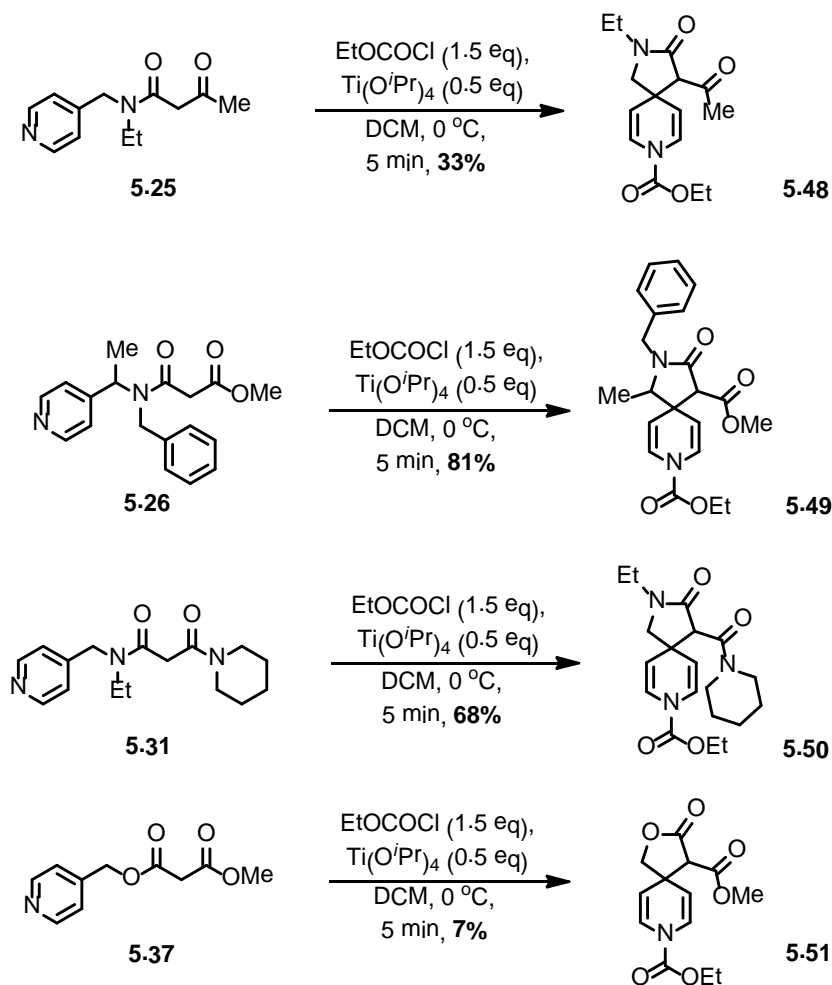


Figure 5.3. Examination of the scope of 4-alkylpyridine spirocyclization



Scheme 5.10. Additional examination of 4-alkylpyridine cyclizations

We also investigated substrates with substitution on the pyridine ring, as well as other heterocycles possessing  $\beta$ -amido ester side chains for titanium isopropoxide-mediated spirocyclization (Figure 5.4). Quinoline and isoquinoline derived substrates are widely used in dearomatization strategies in heterocyclic chemistry. Thus, quinoline derivative **5.35** and isoquinoline derivative **5.36** were synthesized (Scheme 5.7). Both substrates, however, failed to produce any isolable spirocyclization products. Similarly, upon exposure to reaction conditions successful for their pyridine counterparts, 3-chloro substituted pyridine derivative

**5.33** produced an intractable reaction mixture and 3,5-dichloro derivative **5.34** failed to form a pyridinium intermediate with  $\text{ClCO}_2\text{Et}$ . Efforts to utilize 2-substituted pyridine derivative **5.27** for the synthesis of a spirocyclic 1,2-dihydropyridine analogue also failed, perhaps due to unfavorable steric interactions between side chain and the chloroformate reagent that prevented acylation. Our attempts to cyclize substrates bearing a substituent at the active methylene group (**5.23** and **5.24**) also failed probably due to unfavorable steric effects imposed by these substituents during the nucleophilic addition event. Attempted spirocyclization of  $\beta$ -keto ester derivative **5.38**, a substrate lacking an amide linkage also failed to give any desired product (Figure 5.4).

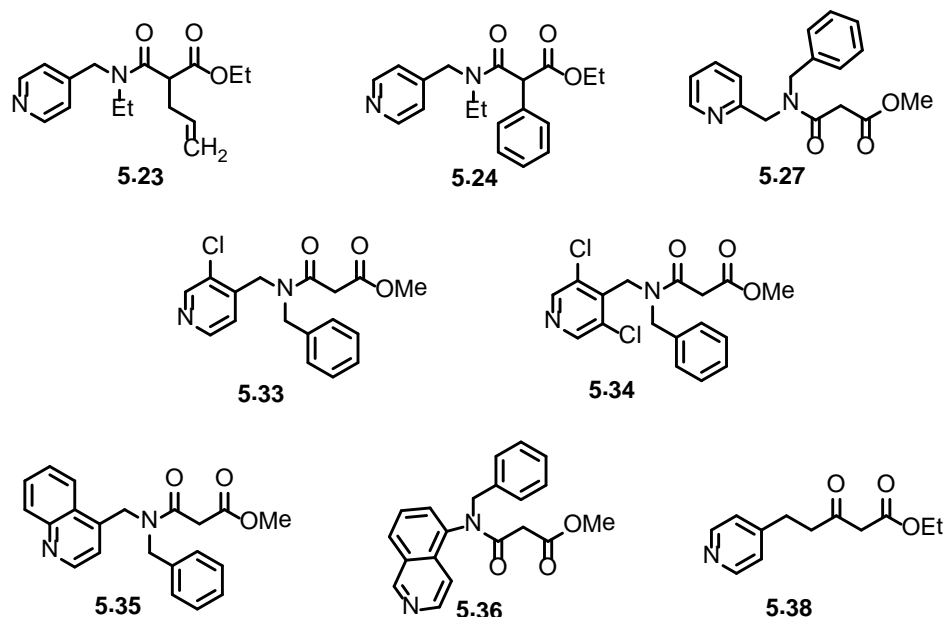


Figure 5.4. Substrates that failed to undergo spirocyclization

Similar observations were made by the Pigge group during dearomatization reactions of arene-ruthenium complexes. (Figure 5.5).<sup>173</sup> It was

found that arene ruthenium complexes **5.7**, tethered with  $\beta$ -amido phosphonate nucleophile and **5.53**, with a  $\beta$ -keto phosphonate nucleophile participated in spirocyclization reactions, however, the acyclic carbon analogue **5.52** failed to undergo cyclization under similar conditions. The beneficial conformational effect of amide derivative (**5.7**) and  $\beta$ -keto phosphonate (**5.53**) is the main reason for the difference in their reactivity compared to conformationally flexible **5.52**.

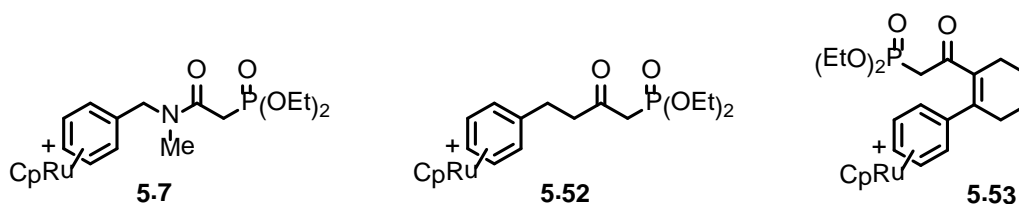
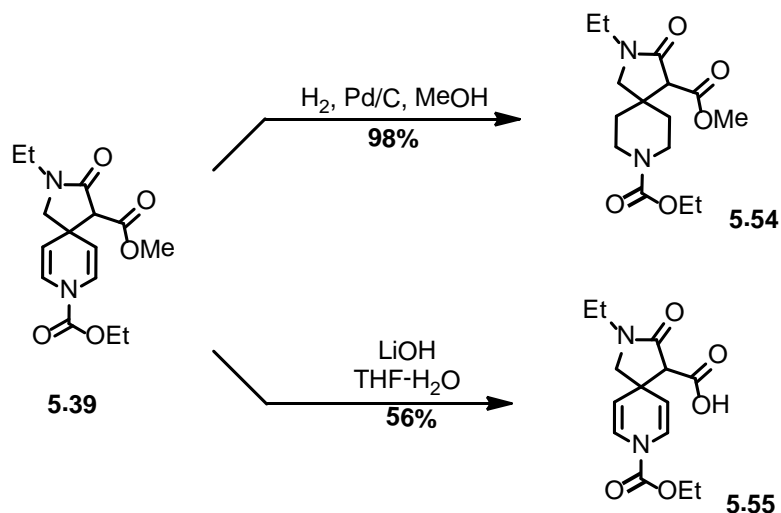


Figure 5.5. Examples from arene-ruthenium approach to spirocyclization

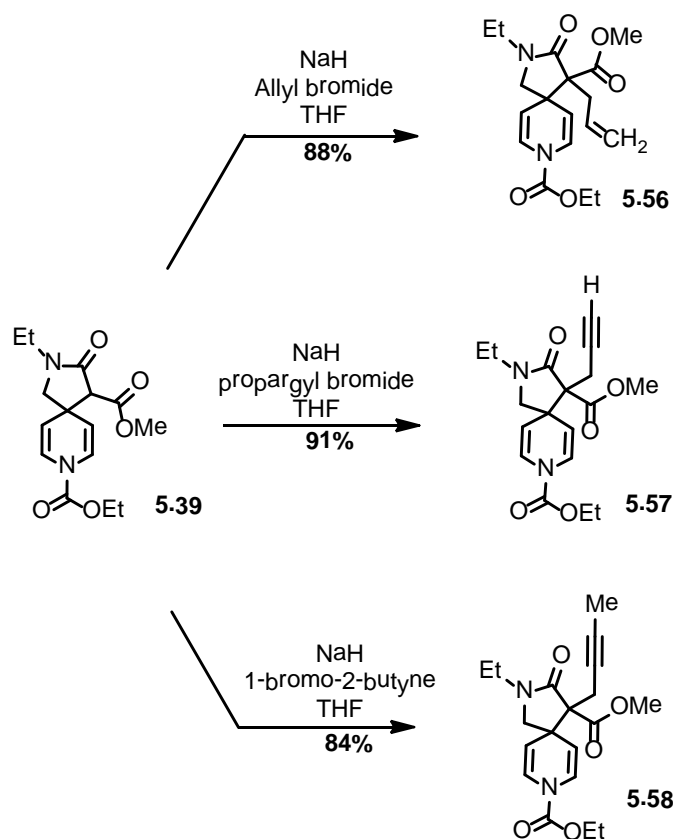
The experimentally simple titanium isopropoxide-mediated spirocyclization developed in this study affords structurally unique 1,4-dihydropyridines in good yields. Next, the reactivity of these 1,4-dihydropyridines was briefly examined. Toward this end, spirocycle **5.39** was hydrogenated under heterogeneous conditions in the presence of catalytic amount of Pd/C at 100 psi of hydrogen to afford spiro piperidine analogue **5.54** in excellent yield (Scheme 5.11). This method is a straightforward approach for synthesis of these frameworks that are found in many biologically important pharmacologically active drug molecules.



Scheme 5.11. Functionalization of the spirocycle **5.39**

The saponification of the ester functionality present in the lactam ring of **5.39** gave the corresponding acid derivative **5.55** in moderate yield (Scheme 5.11). The free acid **5.55** could potentially be used to conjugate these heterocyclic scaffolds to other molecules. The lactam ring was also successfully alkylated in the presence of NaH and an alkyl bromide electrophile (Scheme 5.12). This alkylation circumvents the apparent limitation concerning the inability of substituted  $\beta$ -dicarbonyls to participate in spirocyclization reactions. The intermediate **5.39** was alkylated with allyl bromide, propargyl bromide and butynyl bromide to give **5.56**, **5.57** and **5.58** in excellent yield. The products **5.57** and **5.58** possess 1,6-enyne moieties in their structures which were elaborated further via gold(III)-catalyzed cycloisomerization.

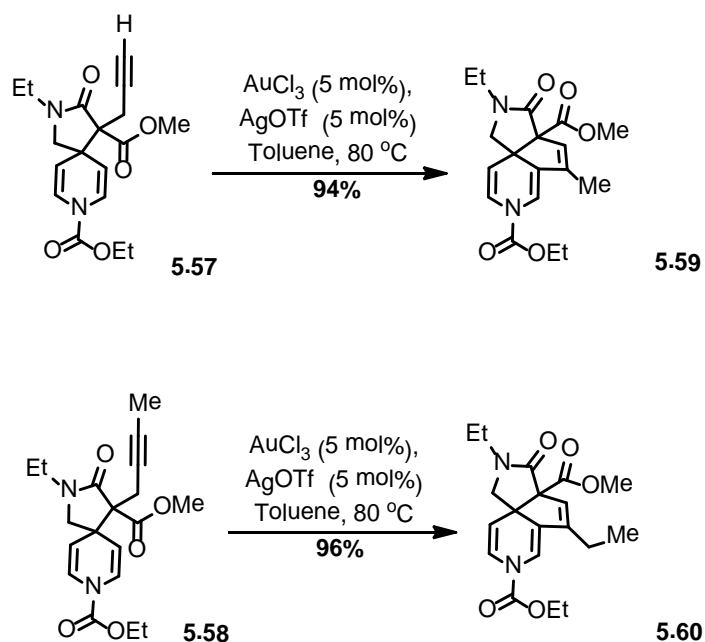




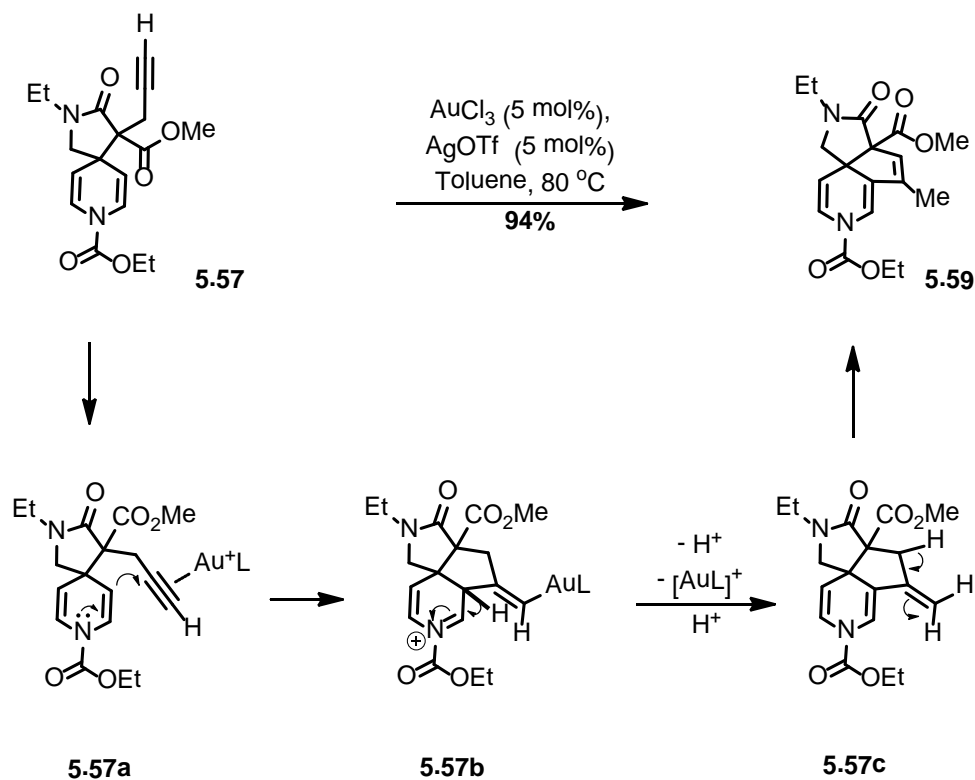
Scheme 5.12. Alkylation of the lactam carbon of the spirocycle **5.39**

On treatment with 5 mol%  $\text{AuCl}_3$  and 5 mol%  $\text{AgOTf}$  in toluene at 80 °C, **5.57** and **5.58** both were converted to tricyclic ring systems **5.59** and **5.60** respectively, in 2 h (Scheme 5.13).<sup>174,175</sup> A mechanistic rationale for this reaction involves alkyne activation by the Au(III) catalyst followed by nucleophilic addition of one of the enamide bonds to form a cationic intermediate. The loss of  $\text{H}^+$ , proto-demetalation and isomerization of the initially formed exocyclic olefin yields observed tricyclic products as shown in Scheme 5.14. Control experiments were carried out to determine the role of Au(III) as well as  $\text{AgOTf}$  catalyst. Treatment of **5.58** with  $\text{AuCl}_3$  or  $\text{AgOTf}$  alone returned unreacted starting material as the major product. This experiment established that both Au(III) and Ag(II) catalysts

were required for tricyclic product formation. Additionally, no reaction was observed in the presence of TfOH alone, which further supports the formation of an alkyne-Au(III) complex intermediate. The tricyclic product **5.60** was synthesized in three steps from its pyridine starting material **5.19** in ~80% overall yield. These transformations established a novel route to access complex heterocyclic frameworks from simple pyridine derivatives in only a few synthetic operations and in very high overall yield.

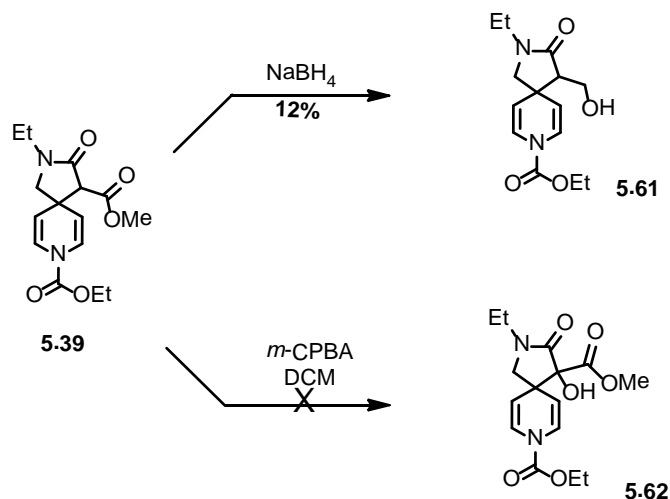


Scheme 5.13. Gold(III)-catalyzed cycloisomerization



Scheme 5.14. Mechanism of gold(III)-catalyzed cycloisomerization

Shown in Scheme 5.15 are two additional transformations of **5.39** that did not proceed in synthetically useful yields. First, attempted reduction of the methyl ester with  $\text{NaBH}_4$  gave the corresponding 1° alcohol (**5.61**) in only 12% yield. Second, attempted  $\alpha$ -hydroxylation and enamide epoxidation using *m*-CPBA failed to produce any product.



Scheme 5.15. Attempts to manipulate the spirocycle **5.39** into building blocks

#### 5.4. Conclusion

A novel titanium isopropoxide-catalyzed intramolecular dearomatization reaction of 4-alkylpyridine derivatives functionalized with stabilized carbon nucleophiles has been developed. This spirocyclization method allowed us to synthesize many diazaspiro[4.5]decanes under mild reaction conditions. Starting materials with varying substitution patterns were synthesized using straightforward routes and utilized in this mild spirocyclization reaction. Optimized conditions were determined through variation of pyridine activating electrophiles, Lewis acid additives, and solvents. Studies showed that we could easily synthesize 1,4-dihydropyridines with a range of substituents on the amide nitrogen and different ester groups. Our efforts demonstrated that  $\beta$ -amido esters were the better  $\beta$ -dicarbonyl carbon nucleophiles for this spirocyclization than  $\beta$ -keto esters and  $\beta$ -keto amides. However, studies describing other reaction manifolds related to these substrates are discussed in Chapter Six. The versatility of the spirocyclic building blocks obtained was further demonstrated through the preparation of spiropiperidines as well as complex tricyclic ring

systems. It was found that quionoline derivative, isoquinoline derivative and pyridine derivatives with substitution on the pyridine ring and at the active methylene group failed to undergo this spirocyclization. Efforts directed toward extending this strategy to synthesize diazaspiro[5.5]undecanes are discussed in the next chapter (five) as well. This approach provides a reasonably general and convenient way to synthesize diazaspirocycles in simple steps in high overall yields from 4-alkylpyridine derivatives.

## 5.5. Experimental section

### **General experimental**

All commercially available starting materials and reagents were used as received unless otherwise noted. All the reactions were performed under argon atmosphere. Solvents were dried and purified by passage through activated alumina columns. Proton nuclear magnetic resonance ( $^1\text{H-NMR}$ ) spectra and carbon nuclear magnetic resonance ( $^{13}\text{C-NMR}$ ) spectra were recorded at 300 MHz and 75 MHz respectively. Chemical shifts are reported as  $\delta$  values in parts per million (ppm) relative to tetramethylsilane for  $^1\text{H-NMR}$  in  $\text{CDCl}_3$  and residual undeuterated solvent for all other spectra. The NMR spectra for many of the compounds used in this study reveal the presence of amide rotamers.

Resonances corresponding to major and minor isomers are identified when appropriate. IR spectra were recorded on a FT-IR spectrometer as thin films on sodium chloride discs. High resolution mass spectra were obtained using electrospray ionization (ESI). Melting points were recorded using a capillary melting point apparatus and are uncorrected.

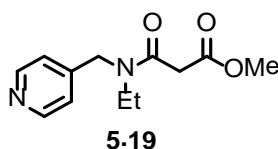
### **Experimental procedures and characterization for 4-alkylpyridyl substrates**

General procedure: The preparation of **5.19** is representative. A reaction mixture containing 4-(ethylaminomethyl)pyridine (5.0 g, 37 mmol, 1 equiv) and

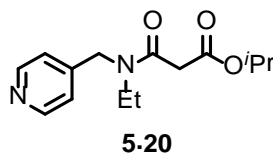
dimethyl malonate (7.3 g, 55 mmol, 1.5 equiv) in toluene (100 mL) was refluxed for 36 h. The reaction mixture was cooled to room temperature and concentrated *in vacuo*. The crude product was purified by silica gel column chromatography using 50-70% ethyl acetate in hexanes to obtain **5.19**, brown colored liquid (6.1 g, 70%).

The above general procedure was used to synthesize the spirocyclization precursors using corresponding secondary amines and di-ester starting materials.

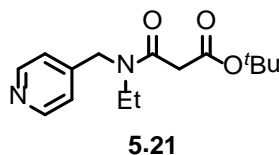
### **$\beta$ -amido ester 5.19**



Brown liquid, 70%,  $^1\text{H}$  NMR (300 MHz,  $\text{CDCl}_3$ ),  $\delta$  (ppm), Major rotamer: 8.56-8.55 (m, 2H), 7.21-7.19, (m, 2H), 4.62 (s, 2H), 3.79 (s, 3H), 3.58 (s, 2H), 3.33 (q,  $J = 7.2$  Hz, 2H), 1.19 (t,  $J = 7.2$  Hz, 3H). Minor rotamer: 8.63-8.61 (m, 2H), 7.16-7.14 (m, 2H), 4.56 (s, 2H), 3.71 (s, 3H), 3.4 (s, 2H), 3.47 (q,  $J = 7.1$  Hz, 2H), 1.15 (t,  $J = 7.2$  Hz, 3H).  $^{13}\text{C}$  NMR (75 MHz,  $\text{CDCl}_3$ , mixture of rotamers),  $\delta$  (ppm): 168.2, 167.9, 166.3, 166.2, 150.5, 150.2, 146.4, 145.9, 122.5, 121.4, 52.8, 52.7, 50.5, 47.4, 43.3, 41.8, 41.3, 40.8, 13.9, 12.6. IR (film): 1731, 1638  $\text{cm}^{-1}$ . HRMS (ESI): calculated for  $\text{C}_{12}\text{H}_{17}\text{N}_2\text{O}_3$   $[\text{M} + \text{H}]^+$ , 237.1239; found 237.1234.

**$\beta$ -amido ester 5.20**

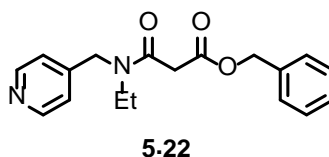
Pale Brown liquid, 67%,  $^1\text{H}$  NMR (300 MHz,  $\text{CDCl}_3$ ),  $\delta$  (ppm), Major rotamer: 8.56-8.54 (m, 2H), 7.23-7.20 (m, 2H), 5.15-5.0 (m, 1H), 4.62 (s, 1H), 3.54 (s, 2H), 3.32 (q,  $J = 7.2$  Hz, 2H), 1.30 (d,  $J = 6.3$  Hz, 6H), 1.19 (t,  $J = 7.2$  Hz). Minor rotamer: 8.62-8.60 (m, 2H), 7.17-7.16 (m, 2H), 5.15-5.0 (m, 1H), 4.55 (s, 2H), 3.46 (q,  $J = 7.1$  Hz, 2H), 3.36 (s, 2H), 1.25 (d,  $J = 6.3$  Hz, 6H), 1.15 (t,  $J = 7.1$  Hz, 3H).  $^{13}\text{C}$  NMR (75 MHz,  $\text{CDCl}_3$ , mixture of rotamers),  $\delta$  (ppm): 167.3, 166.5, 150.5, 150.1, 146.6, 122.5, 121.5, 69.6, 50.4, 47.3, 43.2, 41.8, 41.6, 41.4, 21.9, 21.8, 13.9, 12.5. IR (film): 1727, 1642  $\text{cm}^{-1}$ . HRMS (ESI): calculated for  $\text{C}_{14}\text{H}_{21}\text{N}_2\text{O}_3$   $[\text{M} + \text{H}]^+$ , 265.1552; found 265.1562.

 **$\beta$ -amido ester 5.21**

Yellow liquid, 60%,  $^1\text{H}$  NMR (300 MHz,  $\text{CDCl}_3$ ),  $\delta$  (ppm), Major rotamer: 8.56-8.54 (m, 2H), 7.23-7.21 (m, 2H), 4.62 (s, 1H), 3.49 (s, 2H), 3.32 (q,  $J = 7.23$  Hz, 2H), 1.50 (s, 9H), 1.18 (t,  $J = 10.9$  Hz, 3H). Minor rotamer: 8.62-8.60 (m, 2H), 7.17-7.15 (m, 2H), 4.54 (s, 2H), 3.45 (q,  $J = 7.14$  Hz, 2H), 3.30 (s, 2H), 1.46 (s,

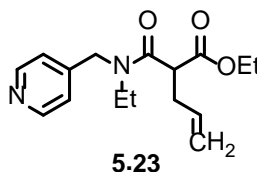
9H), 1.13 (t,  $J = 10.8$  Hz, 3H).  $^{13}\text{C}$  NMR (75 MHz,  $\text{CDCl}_3$ , mixture of rotamers),  $\delta$  (ppm): 166.9, 166.8, 150.6, 150.1, 146.7, 122.6, 121.5, 82.5, 50.4, 47.3, 43.2, 42.7, 42.4, 41.6, 28.2, 14.0, 12.6. IR (film): 1731, 1642  $\text{cm}^{-1}$ . HRMS (ESI): calculated for  $\text{C}_{15}\text{H}_{23}\text{N}_2\text{O}_3$   $[\text{M} + \text{H}]^+$ , 279.1709; found 279.1705.

### $\beta$ -amido ester 5.22



Dark yellow liquid, 50%,  $^1\text{H}$  NMR (300 MHz,  $\text{CDCl}_3$ ),  $\delta$  (ppm), Major rotamer: 8.48-8.46 (m, 2H), 7.40-7.35 (m, 5H), 7.15-7.13 (m, 2H), 5.22 (s, 2H), 4.60 (s, 2H), 3.62 (s, 2H), 3.29 (q,  $J = 7.2$  Hz, 2H), 1.15 (t,  $J = 7.1$  Hz, 3H). Minor rotamer: 8.58- 8.56 (m, 2H), 7.39- 7.35 (m, 5H), 7.12- 7.10 (m, 2H), 5.15 (s, 2H), 4.49 (s, 2H), 3.44 (q,  $J = 7.5$  Hz, 2H), 3.43 (s, 2H), 1.13 (t,  $J = 7.1$  Hz, 3H).  $^{13}\text{C}$  NMR (75 MHz,  $\text{CDCl}_3$ , mixture of rotamers),  $\delta$  (ppm): 167.6, 166.2, 150.6, 150.2, 146.4, 145.8, 135.3, 128.9, 128.8, 128.6, 122.5, 121.4, 67.7, 50.5, 47.4, 43.3, 41.8, 41.6, 41.1, 13.9, 12.6. IR (film): 1727, 1638  $\text{cm}^{-1}$ . HRMS (ESI): calculated for  $\text{C}_{18}\text{H}_{21}\text{N}_2\text{O}_3$   $[\text{M} + \text{H}]^+$ , 313.1552; found 313.1550.

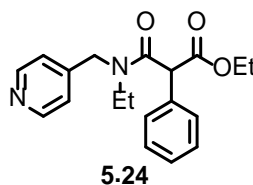
### $\beta$ -amido ester 4.23



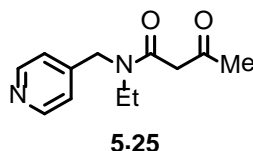


Dark brown liquid, 82%,  $^1\text{H}$  NMR (300 MHz,  $\text{CDCl}_3$ , mixture of rotamers),  $\delta$  (ppm): 8.60-8.52 (m, 2H), 7.18-7.15 (m, 2H), 5.88-5.64 (m, 1H), 5.20-5.06 (m, 2H), 4.88-4.36 (m, 2H), 4.23 (q,  $J = 7.1$  Hz, 1.5H), 4.16-4.08 (m, 0.5H), 3.72 (t,  $J = 7.3$  Hz, 0.76H), 3.56-3.23 (m, 2.3H), 2.78-2.65 (m, 2H), 1.31-1.11 (m, 6H).  $^{13}\text{C}$  NMR (75 MHz,  $\text{CDCl}_3$ , mixture of rotamers),  $\delta$  (ppm): 169.5, 169.2, 168.8, 168.4, 150.4, 150.1, 146.8, 146.2, 134.8, 134.6, 122.5, 121.6, 118.0, 117.9, 61.7, 50.0, 49.1, 48.7, 47.9, 42.8, 42.0, 33.6, 14.3, 12.5. IR (film): 1740, 1638  $\text{cm}^{-1}$ . HRMS (ESI): calculated for  $\text{C}_{16}\text{H}_{23}\text{N}_2\text{O}_3$   $[\text{M} + \text{H}]^+$ , 291.1709; found 291.1702.

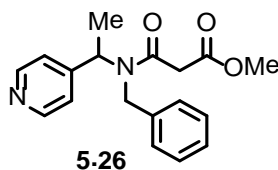
### $\beta$ -amido ester 5.24



Brown liquid, 55%,  $^1\text{H}$  NMR (300 MHz,  $\text{CDCl}_3$ , mixture of rotamers),  $\delta$  (ppm): 8.58-8.49 (m, 2H), 7.44-7.28 (m, 5H), 7.10-7.05 (m, 2H), 4.91 (s, 0.7H), 4.66-4.34 (m, 2.3H), 4.28-4.11 (m, 2H), 3.62-3.55 (m, 0.3H), 3.39-3.23 (m, 1.7H), 1.31-1.24 (m, 3H), 1.13-1.06 (m, 3H).  $^{13}\text{C}$  NMR (75 MHz,  $\text{CDCl}_3$ , mixture of rotamers),  $\delta$  (ppm): 168.8, 168.6, 168.4, 168.2, 150.5, 150.1, 146.7, 145.9, 133.3, 133.0, 129.5, 129.3, 129.0, 128.9, 128.4, 122.5, 121.5, 62.0, 56.5, 56.0, 50.2, 47.8, 43.1, 42.0, 14.2, 14.0, 12.5. IR (film): 1740, 1638  $\text{cm}^{-1}$ . HRMS (ESI): calculated for  $\text{C}_{19}\text{H}_{23}\text{N}_2\text{O}_3$   $[\text{M} + \text{H}]^+$ , 327.1709; found 327.1709.

**$\beta$ -amido ester 5.25**

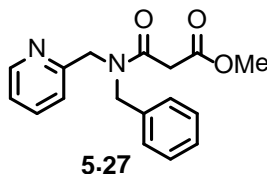
Brown liquid, 63%,  $^1\text{H}$  NMR (300 MHz,  $\text{CDCl}_3$ ),  $\delta$  (ppm), mixture of rotamers: 14.73-14.63 (m, 0.2H), 8.61-8.53 (m, 2H), 7.22-7.13 (m, 2H), 5.20-4.93 (m, 0.2H), 4.61-4.43 (m, 2H), 3.67 (s, 1H), 3.48-3.41 (m, 1H), 3.29 (q,  $J = 7.2$  Hz, 1.4H), 2.33-2.27 (m, 2.2H), 2.00-1.89 (m, 0.7H), 1.17 (t,  $J = 7.2$  Hz, 3H).  $^{13}\text{C}$  NMR (75 MHz,  $\text{CDCl}_3$ ),  $\delta$  (ppm): 202.4, 167.0, 150.5, 150.1, 146.6, 146.1, 123.8, 122.5, 121.4, 50.5, 50.2, 49.7, 47.4, 45.8, 43.3, 42.7, 41.7, 30.6, 22.2, 14.0, 12.7, 12.2. IR (film): 1717, 1628  $\text{cm}^{-1}$ . HRMS (ESI): calculated for  $\text{C}_{12}\text{H}_{17}\text{N}_2\text{O}_2$   $[\text{M} + \text{H}]^+$ , 221.1290; found 221.1301.

 **$\beta$ -amido ester 5.26**

Brown liquid, 52%,  $^1\text{H}$  NMR (300 MHz,  $\text{CDCl}_3$ , mixture of rotamers),  $\delta$  (ppm): 8.59-8.57 (m, 2H), 7.37-7.12 (m, 7H), 6.05 (q,  $J = 7.2$  Hz, 0.8H), 5.12-4.98 (m, 0.4H), 4.52 (d,  $J = 18.2$  Hz, 0.8H), 4.22 (d,  $J = 18.2$  Hz, 0.8H), 4.01 (d,  $J = 15.4$  Hz, 0.2H), 3.77-3.74 (m, 2.9H), 3.61 (s, 0.4H), 3.49-3.37 (m, 1.6H), 1.53-1.34 (m, 3H).  $^{13}\text{C}$  NMR (75 MHz,  $\text{CDCl}_3$ , mixture of rotamers),  $\delta$  (ppm): 168.3,

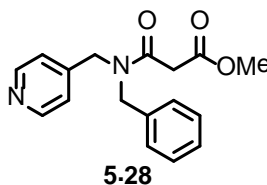
167.9, 150.6, 150.3, 149.8, 137.1, 129.2, 128.6, 127.9, 127.3, 125.9, 122.4, 121.8, 52.7, 51.7, 48.4, 41.8, 16.6. IR (film): 1740, 1647  $\text{cm}^{-1}$ . HRMS (ESI): calculated for  $\text{C}_{18}\text{H}_{21}\text{N}_2\text{O}_3$   $[\text{M} + \text{H}]^+$ , 313.1552; found 313.1543.

**$\beta$ -amido ester 5.27**



Brown liquid, 61%,  $^1\text{H}$  NMR (300 MHz,  $\text{CDCl}_3$ , mixture of rotamers),  $\delta$  (ppm): 8.60-8.50 (m, 1H), 7.67 (tt,  $J = 7.7$  Hz, 1.8 Hz, 1H), 7.43-7.11 (m, 7H), 4.75 (s, 1H), 4.67 (s, 1H), 4.63 (s, 1H), 4.52 (s, 1H), 3.75-3.74 (m, 3H), 3.68 (s, 1H), 3.56 (s, 1H).  $^{13}\text{C}$  NMR (75 MHz,  $\text{CDCl}_3$ , mixture of rotamers),  $\delta$  (ppm): 168.4, 168.3, 167.3, 167.0, 157.0, 156.1, 150.3, 149.4, 137.1, 136.8, 135.9, 129.2, 128.9, 128.5, 128.0, 127.7, 126.6, 123.0, 122.6, 122.5, 121.3, 52.73, 52.68, 52.6, 52.0, 51.2, 49.2, 41.5, 41.2. IR (film): 1735, 1647  $\text{cm}^{-1}$ . HRMS (ESI): calculated for  $\text{C}_{17}\text{H}_{19}\text{N}_2\text{O}_3$   $[\text{M} + \text{H}]^+$ , 299.1396; found 299.1395.

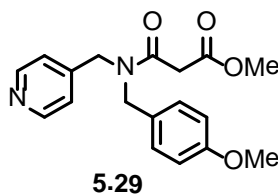
**$\beta$ -amido ester 5.28**



Brown liquid, 73%,  $^1\text{H}$  NMR (300 MHz,  $\text{CDCl}_3$ ),  $\delta$  (ppm), Major rotamer: 8.57-8.55 (m, 2H), 7.41-7.09 (m, 7H), 4.62 (s, 2H), 4.49 (s, 2H), 3.78 (s, 3H),

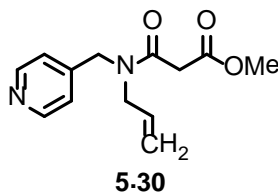
3.61 (s, 2H). Minor rotamer: 8.62- 8.60 (m, 2H), 7.41-7.09 (m, 7H), 4.65 (s, 2H), 4.46 (s, 2H), 3.75 (s, 3H), 3.50 (s, 2H).  $^{13}\text{C}$  NMR (75 MHz,  $\text{CDCl}_3$ , mixture of rotamers),  $\delta$  (ppm): 168.2, 167.1, 150.7, 150.3, 145.9, 135.4, 129.4, 129.0, 128.4, 128.0, 126.6, 122.8, 121.5, 52.9, 51.6, 49.9, 49.0, 47.9, 41.3, 41.1. IR (film): 1731, 1642  $\text{cm}^{-1}$ . HRMS (ESI): calculated for  $\text{C}_{17}\text{H}_{19}\text{N}_2\text{O}_3$   $[\text{M} + \text{H}]^+$ , 299.1396; found 299.1399.

### $\beta$ -amido ester 5.29



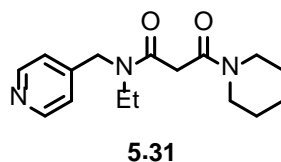
Brown liquid, 76%,  $^1\text{H}$  NMR (300 MHz,  $\text{CDCl}_3$ ),  $\delta$  (ppm), Mixture of rotamers: 8.62-8.55 (m, 2H), 7.18-7.05 (m, 4H), 6.91-6.84 (m, 2H), 4.59-4.58 (m, 2H), 4.43-4.42 (m, 2H), 3.82-3.79 (m, 5H), 3.74 (s, 1H), 3.63 (s, 1.3H), 3.48 (s, 0.7H).  $^{13}\text{C}$  NMR (75 MHz,  $\text{CDCl}_3$ , mixture of rotamers),  $\delta$  (ppm): 168.2, 166.9, 159.7, 150.7, 150.3, 146.0, 145.4, 129.9, 128.0, 127.1, 122.8, 121.5, 114.7, 114.3, 55.5, 52.8, 51.1, 49.6, 48.4, 47.6, 41.3, 41.1. IR (film): 1735, 1660  $\text{cm}^{-1}$ . HRMS (ESI): calculated for  $\text{C}_{18}\text{H}_{21}\text{N}_2\text{O}_4$   $[\text{M} + \text{H}]^+$ , 329.1501; found 329.1502.

### $\beta$ -amido ester 5.30



Brown liquid, 59%,  $^1\text{H}$  NMR (300 MHz,  $\text{CDCl}_3$ ),  $\delta$  (ppm), Major rotamer: 8.57-8.55 (m, 2H), 7.21-7.19 (m, 2H), 5.83-5.71 (m, 1H), 5.3-5.14 (m, 2H) 4.62 (s, 2H), 3.89-3.87 (m, 2H), 3.79 (s, 3H), 3.56 (s, 2H). Minor rotamer: 8.63-8.61 (m, 2H), 7.15-7.13 (m, 2H), 5.83-5.71 (m, 1H), 5.3-5.14 (m, 2H), 4.54 (s, 2H), 4.06-4.04 (m, 2H), 3.72 (s, 3H), 3.44 (s, 2H).  $^{13}\text{C}$  NMR (75 MHz,  $\text{CDCl}_3$ , mixture of rotamers),  $\delta$  (ppm): 168.2, 166.9, 150.7, 150.3, 146.1, 131.9, 122.7, 121.4, 118.6, 117.9, 52.8, 50.7, 50.0, 48.7, 48.0, 41.3, 41.0. IR (film): 1735, 1641  $\text{cm}^{-1}$ . HRMS (ESI): calculated for  $\text{C}_{13}\text{H}_{17}\text{N}_2\text{O}_3$   $[\text{M} + \text{H}]^+$ , 249.1239; found 249.1243.

### $\beta$ -diamide **5.31**

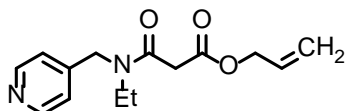


A reaction mixture containing **5.19** (1.0 g, 4.2 mmol, 1 equiv) and piperidine (0.55 mL, 5.5 mmol, 1.3 equiv) in toluene (30 mL) was refluxed for 48 h. The reaction mixture was cooled to room temperature and concentrated *in vacuo*. The crude product was purified by silica gel column chromatography using 70-90% ethyl acetate in hexanes to get **5.31**, pale brown liquid as the desired product (0.75 g, 61%).

$^1\text{H}$  NMR (300 MHz,  $\text{CDCl}_3$ ),  $\delta$  (ppm), Major rotamer: 8.56-8.54 (m, 2H), 7.25-7.23 (m, 2H), 4.61 (s, 2H), 3.62-3.39 (m, 8H), 1.66-1.58 (m, 6H), 1.2 (t,  $J = 7.1$  Hz, 3H). Minor rotamer: 8.61-8.59 (m, 2H), 7.16-7.14 (m, 2H), 4.74 (s, 2H), 3.62-3.39 (m, 8H), 1.66-1.58 (m, 6H), 1.15 (t,  $J = 7.2$  Hz, 3H)  $^{13}\text{C}$  NMR (75 MHz,  $\text{CDCl}_3$ , mixture of rotamers),  $\delta$  (ppm): 167.7, 165.2, 165.0, 150.4, 150.1, 146.7, 122.4, 121.5, 50.5, 47.7, 47.5, 43.3, 41.8, 41.3, 40.6, 26.5, 25.7, 24.5, 14.0, 12.6.

IR (film): 1735, 1628  $\text{cm}^{-1}$ . HRMS (ESI): calculated for  $\text{C}_{16}\text{H}_{24}\text{N}_3\text{O}_2$   $[\text{M} + \text{H}]^+$ , 290.1869; found 290.1867.

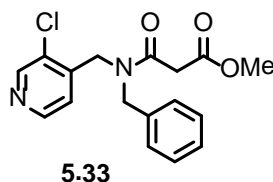
**$\beta$ -amido ester 5.32**



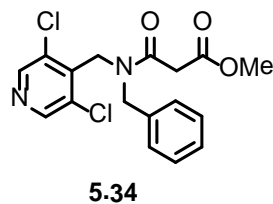
**5.32**

A reaction mixture containing **5.19** (1.0 g, 4.23 mmol, 1 equiv) and allyl alcohol (0.35 mL, 5.1 mmol, 1.2 equiv) in toluene (30 mL) was refluxed for 36 h. The reaction mixture was cooled to room temperature and concentrated *in vacuo*. The crude product was purified by silica column chromatography using 50-70% ethyl acetate in hexanes to get **5.32**, brown colored liquid as the desired product (0.40 g, 47%) and recovered starting material **5.19** (0.23 g).

$^1\text{H}$  NMR (300 MHz,  $\text{CDCl}_3$ ),  $\delta$  (ppm), mixture of rotamers: 8.62-8.54 (m, 2H), 7.21-7.14 (m, 2H), 6.01-5.83 (m, 1H), 5.41-5.24 (m, 2H), 4.71-4.55 (m, 4H), 3.79-3.71 (m, 0.2H), 3.60 (s, 1.5H), 3.50-3.42 (m, 1H), 3.33 (q,  $J = 7.1$  Hz, 1.6H), 1.22-1.13 (m, 3H).  $^{13}\text{C}$  NMR (75 MHz,  $\text{CDCl}_3$ , mixture of rotamers),  $\delta$  (ppm): 167.5, 167.2, 166.3, 150.6, 150.2, 146.5, 145.9, 131.6, 122.5, 121.4, 119.4, 119.1, 66.5, 66.4, 50.5, 47.5, 43.3, 41.8, 41.5, 41.0, 14.0, 12.6. IR (film): 1731, 1651  $\text{cm}^{-1}$ . HRMS (ESI): calculated for  $\text{C}_{14}\text{H}_{19}\text{N}_2\text{O}_3$   $[\text{M} + \text{H}]^+$ , 263.1396; found 263.1391.

**$\beta$ -amido ester 5.33**

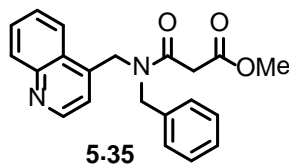
Brown liquid, 28%,  $^1\text{H}$  NMR (300 MHz,  $\text{CDCl}_3$ , mixture of rotamers),  $\delta$  (ppm): 8.58-8.48 (m, 2H), 7.40-7.17 (m, 7H), 4.71-4.66 (m, 2H), 4.57-4.53 (m, 2H), 3.80 (s, 2H), 3.74 (s, 1H), 3.63 (s, 1.4H), 3.46 (s, 0.6H).  $^{13}\text{C}$  NMR (75 MHz,  $\text{CDCl}_3$ , mixture of rotamers),  $\delta$  (ppm): 168.3, 167.3, 149.9, 149.4, 148.4, 143.3, 135.3, 131.2, 129.4, 129.1, 128.4, 128.1, 126.5, 122.7, 121.5, 52.9, 52.3, 49.4, 48.3, 46.4, 41.0. IR (film): 1735, 1660  $\text{cm}^{-1}$ . HRMS (ESI): calculated for  $\text{C}_{17}\text{H}_{18}\text{N}_2\text{O}_3\text{Cl}$   $[\text{M} + \text{H}]^+$ , 333.1006; found 333.1006.

 **$\beta$ -amido ester 5.34**

Brown liquid, 19%,  $^1\text{H}$  NMR (300 MHz,  $\text{CDCl}_3$ , mixture of rotamers),  $\delta$  (ppm): 8.41-8.31 (m, 2H), 7.36-7.06 (m, 5H), 5.02-4.98 (m, 1.5H), 4.78-4.58 (m, 1H), 4.51-4.49 (m, 2H), 3.86-3.51 (m, 4H).  $^{13}\text{C}$  NMR (75 MHz,  $\text{CDCl}_3$ , mixture of rotamers),  $\delta$  (ppm): 167.7, 166.8, 148.3, 148.1, 140.3, 135.6, 133.7, 133.5, 129.2, 128.4, 128.2, 127.4, 126.1, 53.6, 52.8, 51.6, 48.5, 47.5, 44.4, 41.9, 41.3.

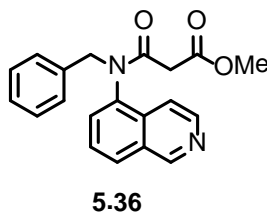
IR (film): 1744, 1655  $\text{cm}^{-1}$ . HRMS (ESI): calculated for  $\text{C}_{17}\text{H}_{17}\text{N}_2\text{O}_3\text{Cl}_2$   $[\text{M} + \text{H}]^+$ , 367.0616; found 367.0615.

**$\beta$ -amido ester 4.35**



Brown liquid, 20%,  $^1\text{H}$  NMR (300 MHz,  $\text{CDCl}_3$ , mixture of rotamers),  $\delta$  (ppm): 8.95-8.89 (m, 1H), 8.21-8.13 (m, 1H), 7.94- 7.91 (m, 0.6H), 7.77-7.71 (m, 1.4H), 7.60-7.53 (m, 1H), 7.42-7.16 (m, 6H), 5.30-4.53 (m, 4H), 3.79 (s, 2H), 3.74-3.47 (m, 3H).  $^{13}\text{C}$  NMR (75 MHz,  $\text{CDCl}_3$ , mixture of rotamers),  $\delta$  (ppm): 168.2, 167.3, 167.1, 150.7, 150.5, 148.5, 141.8, 136.5, 135.4, 130.8, 130.5, 130.0, 129.7, 129.4, 129.1, 128.4, 128.1, 127.4, 127.1, 126.9, 126.4, 126.0, 123.2, 122.1, 119.8, 117.3, 52.9, 51.4, 49.6, 47.8, 45.7, 41.2, 41.1. IR (film): 1744, 1650  $\text{cm}^{-1}$ . HRMS (ESI): calculated for  $\text{C}_{21}\text{H}_{21}\text{N}_2\text{O}_3$   $[\text{M} + \text{H}]^+$ , 349.1552; found 349.1569.

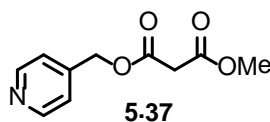
**$\beta$ -amido ester 5.36**





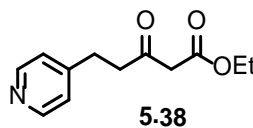
Brown liquid, 39%,  $^1\text{H}$  NMR (300 MHz,  $\text{CDCl}_3$ , mixture of rotamers),  $\delta$  (ppm): 9.33 (br s, 1H), 8.60 (d,  $J = 5.91$  Hz, 1H), 8.01 (d,  $J = 9.1$  Hz, 1H), 7.55-7.48 (m, 2H), 7.27-7.16 (m, 6H), 5.62 (d,  $J = 14.0$  Hz, 1H), 4.36 (d,  $J = 14.0$  Hz, 1H), 3.60 (s, 3H), 3.07 (d,  $J = 1.5$  Hz, 2H).  $^{13}\text{C}$  NMR (75 MHz,  $\text{CDCl}_3$ , mixture of rotamers),  $\delta$  (ppm): 167.9, 166.6, 153.3, 144.9, 136.7, 136.6, 133.3, 131.8, 129.4, 129.1, 128.7, 128.1, 127.3, 115.1, 52.9, 52.5, 41.7. IR (film): 1744, 1659  $\text{cm}^{-1}$ . HRMS (ESI): calculated for  $\text{C}_{20}\text{H}_{19}\text{N}_2\text{O}_3$   $[\text{M} + \text{H}]^+$ , 335.1396; found 335.1387.

### $\beta$ -amido ester 5.37



Yellow liquid, 57%,  $^1\text{H}$  NMR (300 MHz,  $\text{CDCl}_3$ ),  $\delta$  (ppm): 8.60-8.60 (m, 2H), 7.28-7.26 (m, 2H), 5.21 (s, 2H), 3.77 (s, 3H), 3.51 (s, 2H).  $^{13}\text{C}$  NMR (75 MHz,  $\text{CDCl}_3$ ),  $\delta$  (ppm): 166.8, 166.2, 150.3, 144.3, 122.0, 65.3, 52.9, 41.3. IR (film): 1739  $\text{cm}^{-1}$ . HRMS (ESI): calculated for  $\text{C}_{10}\text{H}_{12}\text{NO}_4$   $[\text{M} + \text{H}]^+$ , 210.0766; found 210.0757.

### $\beta$ -amido ester 5.38



4-Picoline (1.25 g, 13.4 mmol, 1 equiv) was added to a solution of LDA at -78 °C [1.5 equiv, freshly prepared from n-BuLi (8.1 mL, 2.5M solution in hexanes, 1.5 equiv) and diisopropylamine (2.82 mL, 20.1 mmol, 1.5 equiv) in THF (20 mL) at -78 °C)].<sup>176</sup> Reaction mixture was stirred for 30 min. To this was slowly added the stirred solution of ethyl 4-chloro acetoacetate (1.83 mL, 16 mmol, 1.2 equiv) and potassium *tert*-butoxide (1.8 g, 16 mmol 1.2 equiv) in THF (20 mL). The reaction mixture was warmed slowly to room temperature and stirred for 16 h. Reaction mixture was cooled with ice and quenched with 50% aqueous acetic acid (4 mL), stirred for 10-15 min, diluted with water (50 mL) and then extracted with ethyl acetate (3 X 50 mL). The combined organic extracts were dried over sodium sulfate and evaporated. The crude product was purified by silica gel column chromatography using ethyl acetate in hexanes to obtain **5.38**, brown colored liquid as the desired product (0.7 g, 40%) and recovered 0.7 g of the starting material.

<sup>1</sup>H NMR (300 MHz, CDCl<sub>3</sub>), δ (ppm): 8.50 (d, *J* = 5.73 Hz, 2H), 7.13-7.11 (m, 2H), 4.18 (q, *J* = 7.1 Hz, 2H), 3.44 (s, 2H), 2.92 (s, 4H), 1.26 (t, *J* = 7.3 Hz, 3H). <sup>13</sup>C NMR (75 MHz, CDCl<sub>3</sub>), δ (ppm): 201.1, 167.1, 150.1, 149.7, 123.9, 61.7, 49.5, 43.1, 28.7, 14.3. IR (film): 1739, 1712 cm<sup>-1</sup>. HRMS (ESI): calculated for C<sub>12</sub>H<sub>16</sub>NO<sub>3</sub> [M + H]<sup>+</sup>, 222.1130; found 222.1123.

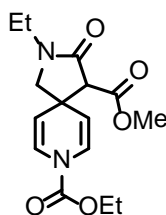
### Experimental procedures and characterization for spirodihydropyridines

General procedure (preparative scale): The preparation of **5.39** is representative. A reaction mixture of **5.19** (2.5 g, 10.6 mmol, 1 equiv) in dichloromethane (20 mL) was cooled to 0 °C. Titanium isopropoxide (1.6 mL, 5.3 mmol, 0.5 equiv) was added to the reaction mixture and stirred for 2 min. Ethyl chloroformate (1.52 mL, 15.9 mmol, 1.5 equiv) was added to reaction mixture which turned to dark brown color immediately. Resulting mixture was stirred for 5

min and then directly loaded on to the silica gel column and purified using 70-90% ethyl acetate in hexanes to give **5.39** (yellow liquid) as the desired product (3.5 g, 93%). The same reaction on 0.10 g scale gave 80% of the product.

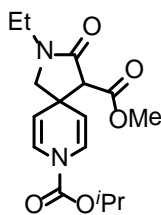
The above procedure has been used to synthesize all the spirocycles from 0.10 g of the corresponding 4-alkylpyridine precursors. In a few cases, the spirocyclized products are contaminated with trace amount of the corresponding isopropyl esters as a result of the trans-esterification in the presence of titanium isopropoxide.

### Spirocycle 5.39

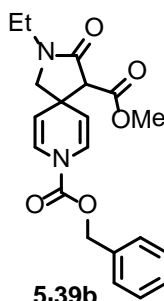


**5.39**

Yellow liquid, 93%,  $^1\text{H}$  NMR (300 MHz,  $\text{CDCl}_3$ ),  $\delta$  (ppm): 7.04 (br, 2H), 4.98 (br, 2H), 4.36 (q,  $J = 7.2$  Hz, 2H), 3.81 (s, 3H), 3.56 (d,  $J = 9.8$  Hz, 1H), 3.52-3.42 (m, 2H), 3.30 (s, 1H), 3.28 (d,  $J = 10$  Hz, 1H), 1.41 (t,  $J = 7.1$  Hz, 3H), 1.23 (t,  $J = 7.2$  Hz, 3H).  $^{13}\text{C}$  NMR (75 MHz,  $\text{CDCl}_3$ ),  $\delta$  (ppm): 168.0, 167.9, 151.0, 124.6, 122.7, 109.6, 105.4, 63.7, 63.1, 60.9, 60.4, 52.3, 39.4, 37.4, 21.9, 21.1, 14.4, 14.2, 12.3. IR (film): 1727, 1683, 1629  $\text{cm}^{-1}$ . HRMS (ESI): calculated for  $\text{C}_{15}\text{H}_{20}\text{N}_2\text{O}_5\text{Na}$   $[\text{M} + \text{Na}]^+$ , 331.1270; found 331.1262.

**Spirocycle 5.39a****5.39a**

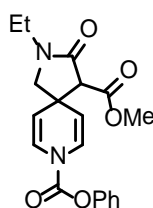
Brown liquid, 80%,  $^1\text{H}$  NMR (300 MHz,  $\text{CDCl}_3$ ),  $\delta$  (ppm): 7.0-6.89 (m, 2H), 5.05 (sep,  $J = 6.2$  Hz, 1H), 4.89 (br s, 2H), 3.73 (s, 3H), 3.49-3.35 (m, 3H), 3.23-3.19 (m, 2H), 1.32 (d,  $J = 6.3$  Hz, 6H), 1.15 (t,  $J = 7.3$  Hz, 3H).  $^{13}\text{C}$  NMR (75 MHz,  $\text{CDCl}_3$ ),  $\delta$  (ppm): 168.1, 168.0, 150.5, 124.6, 122.8, 109.5, 109.0, 105.4, 104.9, 71.2, 63.7, 60.9, 52.3, 39.4, 37.3, 22.0, 12.3. IR (film): 1723, 1678, 1634  $\text{cm}^{-1}$ . HRMS (ESI): calculated for  $\text{C}_{16}\text{H}_{22}\text{N}_2\text{O}_5\text{Na}$   $[\text{M} + \text{Na}]^+$ , 345.1426; found 345.1418.

**Spirocycle 5.39b****5.39b**

Brown liquid, 86%,  $^1\text{H}$  NMR (300 MHz,  $\text{CDCl}_3$ ),  $\delta$  (ppm): 7.38-7.37 (m, 5H), 7.04-6.87 (m, 2H), 5.23 (s, 2H), 4.96-4.86 (m, 2H), 3.71 (s, 3H), 3.48-

3.31(m, 3H), 3.22-3.17 (m, 2H), 1.13 (t,  $J = 7.2$  Hz, 3H).  $^{13}\text{C}$  NMR (75 MHz,  $\text{CDCl}_3$ ),  $\delta$  (ppm): 168.0, 167.9, 150.8, 135.1, 128.7, 128.4, 124.6, 124.3, 122.7, 122.5, 110.0, 109.5, 106.0, 105.5, 68.7, 63.5, 60.7, 52.3, 39.3, 37.3, 12.3. IR (film): 1723, 1683, 1634  $\text{cm}^{-1}$ . HRMS (ESI): calculated for  $\text{C}_{20}\text{H}_{22}\text{N}_2\text{O}_5\text{Na}$  [ $\text{M} + \text{Na}$ ] $^+$ , 393.1426; found 393.1430.

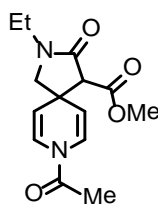
### Spirocycle 5.39c



5.39c

Brown liquid, 66%,  $^1\text{H}$  NMR (300 MHz,  $\text{CDCl}_3$ ),  $\delta$  (ppm): 7.43-7.37 (m, 2H), 7.29-7.24 (m, 1H), 7.16-7.02 (m, 4H), 5.09-4.98 (m, 2H), 3.75 (s, 3H), 3.52 (d,  $J = 9.9$  Hz, 1H), 3.47-3.33 (m, 2H), 3.28 (s, 1H), 3.25 (d,  $J = 9.9$  Hz, 1H), 1.16 (t,  $J = 7.3$  Hz, 3H).  $^{13}\text{C}$  NMR (75 MHz,  $\text{CDCl}_3$ ),  $\delta$  (ppm): 167.9, 150.4, 149.6, 129.6, 126.3, 124.6, 124.4, 122.7, 122.5, 121.4, 110.9, 110.4, 107.0, 106.4, 63.4, 60.6, 52.4, 39.3, 37.4, 12.3. IR (film): 1736, 1683, 1629  $\text{cm}^{-1}$ . HRMS (ESI): calculated for  $\text{C}_{19}\text{H}_{20}\text{N}_2\text{O}_5\text{Na}$  [ $\text{M} + \text{Na}$ ] $^+$ , 379.1270; found 379.1271.

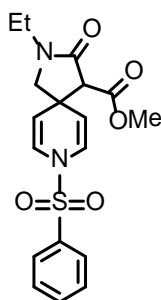
### Spirocycle 5.39d



5.39d

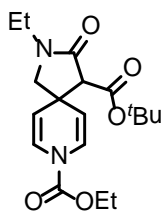
Brown liquid, 20%,  $^1\text{H}$  NMR (300 MHz,  $\text{CDCl}_3$ ),  $\delta$  (ppm): 7.34-7.28 (m, 1H), 6.73-6.66 (m, 1H), 5.08-4.93 (m, 2H), 3.73 (s, 3H), 3.52-3.33 (m, 3H), 3.25-3.19 (m, 2H), 2.26 (s, 3H), 1.15 (t,  $J = 7.3$  Hz, 3H).  $^{13}\text{C}$  NMR (75 MHz,  $\text{CDCl}_3$ ),  $\delta$  (ppm): 168.0, 166.4, 125.3, 123.5, 123.3, 121.4, 111.2, 110.6, 107.2, 106.7, 63.4, 63.3, 60.6, 52.5, 39.7, 37.5, 21.5, 12.4. IR (film): 1731, 1669, 1625  $\text{cm}^{-1}$ . HRMS (ESI): calculated for  $\text{C}_{14}\text{H}_{18}\text{N}_2\text{O}_4\text{Na}$   $[\text{M} + \text{Na}]^+$ , 301.1164; found 301.1183.

### Spirocycle 5.39e

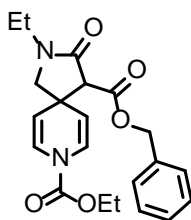


5.39e

Yellow liquid, 13%,  $^1\text{H}$  NMR (300 MHz,  $\text{CDCl}_3$ ),  $\delta$  (ppm): 7.80-7.77 (m, 2H), 7.68-7.63 (m, 1H), 7.60-7.54 (m, 2H), 6.71-6.67 (m, 2H), 4.96-4.91 (m, 2H), 3.54 (s, 3H), 3.38-3.29 (m, 3H), 3.12-2.98 (m, 2H), 1.10 (t,  $J = 7.3$  Hz, 3H).  $^{13}\text{C}$  NMR (75 MHz,  $\text{CDCl}_3$ ),  $\delta$  (ppm): 167.7, 167.6, 137.8, 133.9, 129.7, 127.0, 124.0, 122.8, 122.4, 111.1, 107.5, 63.6, 60.9, 52.3, 39.1, 37.5, 12.4. IR (film): 1740, 1678, 1643  $\text{cm}^{-1}$ . HRMS (ESI): calculated for  $\text{C}_{18}\text{H}_{20}\text{N}_2\text{O}_5\text{NaS}$   $[\text{M} + \text{Na}]^+$ , 399.0991; found 399.0973.

**Spirocycle 5.41****5.41**

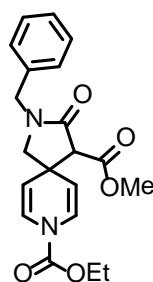
Pale yellow liquid, 68%,  $^1\text{H}$  NMR (300 MHz,  $\text{CDCl}_3$ ),  $\delta$  (ppm): 7.02-6.85 (m, 2H), 4.93-4.89 (m, 2H), 4.29 (q,  $J = 7.1$  Hz, 2H), 3.53-3.42 (m, 2H), 3.35-3.23 (m, 1H), 3.15 (d,  $J = 9.7$  Hz, 1H), 3.06 (s, 1H), 1.46 (s, 9H), 1.33 (t,  $J = 7.1$  Hz, 3H), 1.14 (t,  $J = 7.3$  Hz, 3H),  $^{13}\text{C}$  NMR (75 MHz,  $\text{CDCl}_3$ ),  $\delta$  (ppm): 168.7, 166.7, 151.2, 124.9, 122.3, 110.4, 110.0, 105.8, 105.4, 82.4, 64.6, 63.2, 60.9, 39.4, 37.4, 28.2, 14.6, 12.4. IR (film): 1735, 1676, 1629  $\text{cm}^{-1}$ . HRMS (ESI): calculated for  $\text{C}_{18}\text{H}_{26}\text{N}_2\text{O}_5\text{Na}$   $[\text{M} + \text{Na}]^+$ , 373.1739; found 373.1741.

**Spirocycle 5.42****5.42**

Yellow liquid, 73%,  $^1\text{H}$  NMR (300 MHz,  $\text{CDCl}_3$ ),  $\delta$  (ppm): 7.35-7.31 (m, 5H), 6.94-6.77 (m, 2H), 5.21 (d,  $J = 12.2$  Hz, 1H), 5.10 (d,  $J = 12.3$  Hz, 1H), 4.93-4.77 (m, 2H), 4.26 (q,  $J = 7.1$  Hz, 2H), 3.46-3.30 (m, 3H), 3.25 (s, 1H), 3.17 (d,  $J$

= 9.8 Hz, 1H), 1.32 (t,  $J = 7.1$  Hz, 3H), 1.11 (t,  $J = 7.2$  Hz, 3H).  $^{13}\text{C}$  NMR (75 MHz,  $\text{CDCl}_3$ ),  $\delta$  (ppm): 167.9, 167.3, 150.9, 135.4, 128.5, 128.48, 128.4, 124.6, 122.7, 109.6, 105.2, 67.0, 63.4, 63.1, 60.9, 39.6, 37.4, 14.5, 12.3. IR (film): 1724, 1684, 1629  $\text{cm}^{-1}$ . HRMS (ESI): calculated for  $\text{C}_{21}\text{H}_{24}\text{N}_2\text{O}_5\text{Na}$   $[\text{M} + \text{Na}]^+$ , 407.1583; found 407.1579.

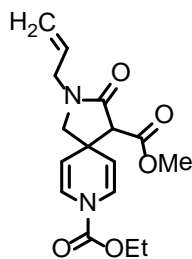
### Spirocycle 5.43



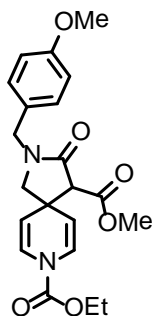
5.43

Brown liquid, 69%,  $^1\text{H}$  NMR (300 MHz,  $\text{CDCl}_3$ ),  $\delta$  (ppm): 7.38-7.26 (m, 5H), 6.95-6.85 (m, 2H), 4.83 (m, 2H), 4.59 (d,  $J = 14.8$  Hz, 1H), 4.44 (d,  $J = 14.8$  Hz, 1H), 4.25 (q,  $J = 7.1$  Hz, 2H), 3.74 (s, 3H), 3.34 (d,  $J = 10$  Hz, 1H), 3.29 (s, 1H), 3.06 (d,  $J = 10$  Hz, 1H), 1.31 (t,  $J = 7.4$  Hz, 3H).  $^{13}\text{C}$  NMR (75 MHz,  $\text{CDCl}_3$ ),  $\delta$  (ppm): 168.6, 168.0, 151.1, 135.8, 128.9, 128.3, 128.0, 124.9, 122.8, 109.7, 109.2, 105.1, 63.7, 63.3, 60.9, 52.5, 46.8, 39.4, 14.5. IR (film): 1731, 1684, 1629  $\text{cm}^{-1}$ . HRMS (ESI): calculated for  $\text{C}_{20}\text{H}_{22}\text{N}_2\text{O}_5\text{Na}$   $[\text{M} + \text{Na}]^+$ , 393.1426; found 393.1426.



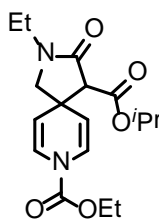
**Spirocycle 5.44****5.44**

Brown liquid, 90%,  $^1\text{H}$  NMR (300 MHz,  $\text{CDCl}_3$ ),  $\delta$  (ppm): 7.00-6.89 (m, 2H), 5.80-5.67 (m, 1H), 5.29-5.22 (m, 2H), 4.90 (br, 2H), 4.28 (q,  $J = 7.1$  Hz, 2H), 4.03-2.86 (m, 2H), 3.74 (s, 3H), 3.45 (d,  $J = 10$  Hz, 1H), 3.26 (s, 1H), 3.17 (d,  $J = 10$  Hz, 1H), 1.33 (t,  $J = 7.1$  Hz, 3H).  $^{13}\text{C}$  NMR (75 MHz,  $\text{CDCl}_3$ ),  $\delta$  (ppm): 168.3, 168.0, 151.1, 131.7, 124.7, 122.7, 118.8, 109.8, 109.3, 105.6, 105.2, 63.7, 63.2, 61.2, 52.4, 45.4, 39.5, 14.5. IR (film): 1727, 1688, 1629  $\text{cm}^{-1}$ . HRMS (ESI): calculated for  $\text{C}_{16}\text{H}_{20}\text{N}_2\text{O}_5\text{Na}$   $[\text{M} + \text{Na}]^+$ , 343.1270; found 343.1268.

**Spirocycle 5.45****5.45**

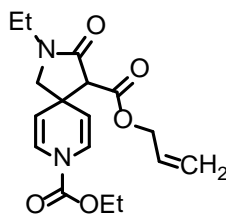
Brown liquid, 90%,  $^1\text{H}$  NMR (300 MHz,  $\text{CDCl}_3$ ),  $\delta$  (ppm): 7.21-7.18 (m, 2H), 6.95-6.86 (m, 4H), 4.82 (br, 2H), 4.51 (d,  $J = 14.7$  Hz, 1H), 4.38 (d,  $J = 14.4$  Hz, 1H), 4.25 (q,  $J = 7.2$  Hz, 2H), 3.80 (s, 3H), 3.73 (s, 3H), 3.31 (d,  $J = 10$  Hz, 1H), 3.27 (s, 1H), 3.04 (d,  $J = 10$  Hz, 1H), 1.30 (t,  $J = 7.1$  Hz, 3H).  $^{13}\text{C}$  NMR (75 MHz,  $\text{CDCl}_3$ ),  $\delta$  (ppm): 168.3, 167.9, 159.2, 150.9, 129.6, 127.7, 124.5, 122.5, 114.2, 109.6, 109.2, 105.4, 105.1, 63.6, 63.1, 60.7, 55.3, 52.3, 46.1, 39.3, 14.4. IR (film): 1724, 1680, 1629  $\text{cm}^{-1}$ . HRMS (ESI): calculated for  $\text{C}_{21}\text{H}_{24}\text{N}_2\text{O}_6\text{Na}$  [ $\text{M} + \text{Na}$ ] $^+$ , 423.1532; found 423.1535.

### Spirocycle 5.46

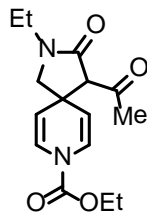


5.46

Yellow liquid, 79%,  $^1\text{H}$  NMR (300 MHz,  $\text{CDCl}_3$ ),  $\delta$  (ppm): 6.99-6.92 (m, 2H), 5.03 (sep,  $J = 6.3$  Hz, 1H), 4.90 (br s, 2H), 4.28 (q,  $J = 7.1$  Hz, 2H), 3.53-3.41 (m, 2H), 3.37-3.25 (m, 1H), 3.18 (d,  $J = 9.7$  Hz, 1H), 3.14 (s, 1H), 1.33 (t,  $J = 7.1$  Hz, 3H), 1.27 (d,  $J = 6.3$  Hz, 3H), 1.22 (d,  $J = 6.2$  Hz, 3H), 1.15 (t,  $J = 7.3$  Hz, 3H).  $^{13}\text{C}$  NMR (75 MHz,  $\text{CDCl}_3$ ),  $\delta$  (ppm): 168.3, 167.0, 151.0, 124.7, 122.6, 110.0, 109.6, 105.7, 105.4, 69.0, 63.7, 63.1, 60.9, 39.4, 37.3, 21.9, 14.5, 12.3. IR (film): 1727, 1687, 1629  $\text{cm}^{-1}$ . HRMS (ESI): calculated for  $\text{C}_{17}\text{H}_{24}\text{N}_2\text{O}_5\text{Na}$  [ $\text{M} + \text{Na}$ ] $^+$ , 359.1583; found 359.1576.

**Spirocycle 5.47****5.47**

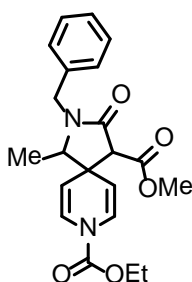
Brown liquid, 71%,  $^1\text{H}$  NMR (300 MHz,  $\text{CDCl}_3$ ),  $\delta$  (ppm): 6.94 (br s, 2H), 5.95-5.82 (m, 1H), 5.36-5.20 (m, 2H), 4.90 (br, 2H), 4.70-4.55 (m, 2H), 4.28 (q,  $J = 7.1$  Hz, 2H), 3.49-3.30 (m, 3H), 3.22-3.18 (m, 2H), 1.32 (t,  $J = 7.1$  Hz, 3H), 1.14 (t,  $J = 7.2$  Hz, 3H).  $^{13}\text{C}$  NMR (75 MHz,  $\text{CDCl}_3$ ),  $\delta$  (ppm): 168.1, 167.2, 151.1, 131.7, 124.7, 122.8, 118.9, 109.7, 105.5, 65.9, 63.7, 63.2, 61.0, 39.5, 37.5, 14.5, 12.3. IR (film): 1724, 1688, 1633  $\text{cm}^{-1}$ . HRMS (ESI): calculated for  $\text{C}_{17}\text{H}_{22}\text{N}_2\text{O}_5\text{Na}$   $[\text{M} + \text{Na}]^+$ , 357.1426; found 357.1424.

**Spirocycle 5.48****5.48**

Yellow liquid, 33%,  $^1\text{H}$  NMR (300 MHz,  $\text{CDCl}_3$ ),  $\delta$  (ppm), mixture of tautomers: 12.32 (s, 0.3H), 6.99-6.88 (m, 2H), 4.94-4.89 (m, 2H), 4.28 (q,  $J = 7.2$  Hz, 2H), 3.48-3.29 (m, 3.4H), 3.23-3.15 (m, 1.4H), 2.26 (s, 2H), 1.83 (s, 1H),

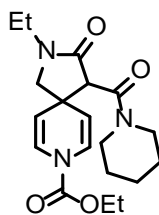
1.37-1.31 (m, 3H), 1.16-1.11 (m, 3H).  $^{13}\text{C}$  NMR (75 MHz,  $\text{CDCl}_3$ ),  $\delta$  (ppm): 204.0, 171.4, 168.8, 167.4, 151.4, 151.2, 124.9, 122.9, 121.3, 110.2, 105.9, 69.8, 63.3, 63.2, 61.0, 39.7, 37.4, 36.6, 33.4, 17.5, 14.6, 12.6, 12.5. IR (film): 3435, 1659, 1632  $\text{cm}^{-1}$ . HRMS (ESI): calculated for  $\text{C}_{15}\text{H}_{21}\text{N}_2\text{O}_4$   $[\text{M} + \text{H}]^+$ , 293.1501; found 293.1492.

### Spirocycle 5.49

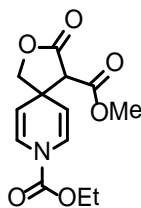


5.49

Brown liquid, 81%,  $^1\text{H}$  NMR (300 MHz,  $\text{CDCl}_3$ ),  $\delta$  (ppm), mixture of diastereomers: 7.37-7.23 (m, 5H), 7.01-6.93 (m, 2H), 5.17-4.98 (m, 1H), 4.82-4.57 (m, 2H), 4.31-4.22 (m, 2H), 4.05-3.91 (m, 1H), 3.74-3.71 (m, 3H), 3.51 (q,  $J = 6.7$  Hz, 0.7H), 3.35-3.32 (m, 1H), 3.16 (q,  $J = 6.7$  Hz, 0.3H), 1.31 (t,  $J = 6.9$  Hz, 3H), 1.11 (d,  $J = 6.7$  Hz, 0.9H), 1.04 (d,  $J = 6.8$  Hz, 2.1H).  $^{13}\text{C}$  NMR (75 MHz,  $\text{CDCl}_3$ ),  $\delta$  (ppm), mixture of diastereomers: 169.2, 168.7, 168.0, 167.8, 151.0, 137.2, 136.3, 135.8, 129.6, 128.8, 128.7, 128.4, 128.0, 127.7, 127.3, 125.8, 125.5, 124.5, 123.6, 108.4, 106.8, 106.3, 105.1, 104.7, 103.8, 63.7, 63.2, 63.0, 62.4, 61.8, 52.4, 49.6, 44.4, 44.3, 44.0, 40.9, 16.7, 14.5, 13.8, 13.5. IR (film): 1724, 1688, 1629  $\text{cm}^{-1}$ . HRMS (ESI): calculated for  $\text{C}_{21}\text{H}_{24}\text{N}_2\text{O}_5\text{Na}$   $[\text{M} + \text{Na}]^+$ , 407.1583; found 407.1583.

**Spirocycle 5.50****5.50**

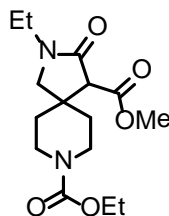
Brown liquid, 68%,  $^1\text{H}$  NMR (300 MHz,  $\text{CDCl}_3$ ),  $\delta$  (ppm): 6.95-6.88 (m, 2H), 4.98 (br s, 2H), 4.29 (q,  $J = 7.1$  Hz, 2H), 3.66-3.34 (m, 8H), 3.15 (d,  $J = 9.6$  Hz, 1H), 1.63-1.51 (m, 6H), 1.34 (t,  $J = 7.1$  Hz, 3H), 1.16 (t,  $J = 7.2$  Hz, 3H).  $^{13}\text{C}$  NMR (75 MHz,  $\text{CDCl}_3$ ),  $\delta$  (ppm): 170.3, 165.5, 151.1, 124.5, 121.5, 110.6, 106.7, 63.2, 61.4, 60.5, 47.8, 43.0, 38.7, 37.4, 26.4, 25.7, 24.4, 14.5, 12.4. IR (film): 1718, 1678, 1625  $\text{cm}^{-1}$ . HRMS (ESI): calculated for  $\text{C}_{19}\text{H}_{27}\text{N}_3\text{O}_4\text{Na}$   $[\text{M} + \text{Na}]^+$ , 384.1899; found 384.1898.

**Spirocycle 5.51****5.51**

Yellow liquid, 7%,  $^1\text{H}$  NMR (300 MHz,  $\text{CDCl}_3$ ),  $\delta$  (ppm): 7.02 (br s, 2H), 4.90-4.88 (m, 2H), 4.29 (q,  $J = 7.1$  Hz, 2H), 4.26 (d,  $J = 9.0$  Hz, 1H), 4.07 (d,  $J = 9.0$  Hz, 1H), 3.76 (s, 3H), 3.34 (s, 1H), 1.33 (t,  $J = 7.1$  Hz, 3H).  $^{13}\text{C}$  NMR (75

MHz, CDCl<sub>3</sub>),  $\delta$  (ppm): 170.7, 165.9, 151.0, 125.5, 124.5, 106.9, 103.5, 79.2, 63.6, 60.5, 52.9, 44.2, 14.6. IR (film): 1784, 1726, 1686, 1633 cm<sup>-1</sup>. HRMS (ESI): calculated C<sub>13</sub>H<sub>15</sub>NO<sub>6</sub>Na [M + Na]<sup>+</sup>, 304.0797; found 304.0796.

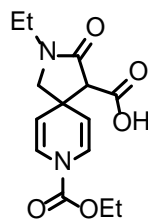
### Spirocycle 5.54



5.54

Spirocycle **5.39** (0.10 g, 0.32 mmol) was dissolved in methanol (5 mL) and 10% palladium on carbon (10 mg) was added. The mixture was hydrogenated at 100 psi for 14 h and then filtered through Celite. The filtrate was evaporated *in vacuo* and dried to get **5.54**, colorless liquid (0.10 g, 98%).

<sup>1</sup>H NMR (300 MHz, CDCl<sub>3</sub>),  $\delta$  (ppm): 4.13 (q,  $J = 7.1$  Hz, 2H), 3.76-3.74 (m, 3H), 3.57-3.30 (m, 7H), 3.21 (s, 1H), 3.16 (d,  $J = 9.6$  Hz, 1H), 1.68-1.57 (m, 4H), 1.26 (t,  $J = 7.1$  Hz, 3H), 1.15 (t,  $J = 7.2$  Hz, 3H). <sup>13</sup>C NMR (75 MHz, CDCl<sub>3</sub>),  $\delta$  (ppm): 169.0, 155.4, 61.5, 58.8, 55.4, 52.3, 40.6, 40.3, 38.8, 37.5, 36.0, 31.4, 14.7, 12.2. IR (film): 1731, 1699, 1677 cm<sup>-1</sup>. HRMS (ESI): calculated for C<sub>15</sub>H<sub>24</sub>N<sub>2</sub>O<sub>5</sub>Na [M + Na]<sup>+</sup>, 335.1583; found 335.1585.

**Spirocycle 5.55****5.55**

Spirocycle **5.39** (0.10 g, 0.3 mmol, 1 equiv) was taken in 4 mL of THF-water (1:1). LiOH (10 mg, 0.39 mmol, 1.2 equiv) was added and the reaction mixture was heated at 75 °C for 6 h. Reaction mixture was cooled to room temperature and extracted with ethyl acetate (2 X 3 mL). The aqueous layer was then acidified with 10% aq.HCl solution to pH ~2 and extracted with ethyl acetate (5 X 10 mL). The combined extract was then dried over anhydrous sodium sulfate and evaporated to afford **5.55**, pale brown liquid (53 mg, 56%).

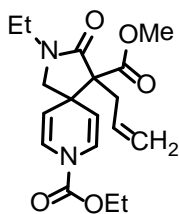
$^1\text{H}$  NMR (300 MHz,  $\text{CDCl}_3$ ),  $\delta$  (ppm): 10.1 (br s, 1H), 7.05-6.92 (m, 2H), 4.94-4.86 (m, 2H), 4.28 (q,  $J = 7.1$  Hz, 2H), 3.43-3.37 (m, 3H), 3.26 (d,  $J = 10.2$  Hz, 1H), 3.24 (s, 1H), 1.33 (t,  $J = 7.1$  Hz, 3H), 1.16 (t,  $J = 7.3$  Hz, 3H).  $^{13}\text{C}$  NMR (75 MHz,  $\text{CDCl}_3$ ),  $\delta$  (ppm): 169.8, 168.8, 151.1, 124.8, 123.9, 108.7, 108.2, 105.5, 105.0, 63.2, 60.9, 40.2, 37.8, 14.5, 12.3. IR (film): 3453, 1739, 1682, 1628  $\text{cm}^{-1}$ . HRMS (ESI): calculated for  $\text{C}_{14}\text{H}_{17}\text{N}_2\text{O}_5$   $[\text{M} - \text{H}]^-$ , 293.1137; found 293.1158.

**Experimental procedures and characterization for alkylation of spirocycle 5.39**

General procedure: Spirocycle **5.39** (0.5 g, 1.6 mmol, 1 equiv) was taken in dry THF (25 mL) at 0 °C. 50% suspension of NaH (0.10 g, 2.1 mmol, 1.3 equiv)

was added to it and stirred for 30 min. 1-bromo-2-butyne (0.18 mL, 2 mmol, 1.2 equiv) was then added to the reaction mixture and slowly warmed to room temperature and stirred for 16 h. Reaction was quenched with water and extracted with ethyl acetate (3 X 25 mL). The combined organics were dried over  $\text{Na}_2\text{SO}_4$  and evaporated *in vacuo*. Crude product was purified by silica gel column chromatography using 50-70% ethyl acetate in hexanes to obtain **5.58**, as yellow liquid (0.49 g, 84%).

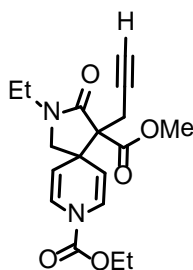
### Spirocycle 5.56



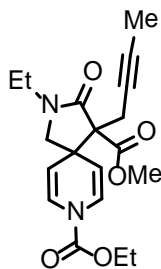
**5.56**

Yellow liquid, 88%,  $^1\text{H}$  NMR (300 MHz,  $\text{CDCl}_3$ ),  $\delta$  (ppm): 6.94 (br s, 2H), 6.02-5.88 (m, 1H), 5.13-4.99 (m, 2H), 4.83 (br s, 2H), 4.28 (q,  $J = 7.1$  Hz, 2H), 3.70 (s, 3H), 3.43-3.34 (m, 3H), 3.08 (d,  $J = 9.8$  Hz, 1H), 2.72-2.64 (m, 1H), 2.53-2.45 (m, 1H), 1.33 (t,  $J = 7.1$  Hz, 3H), 1.12 (t,  $J = 7.2$  Hz, 3H).  $^{13}\text{C}$  NMR (75 MHz,  $\text{CDCl}_3$ ),  $\delta$  (ppm): 170.6, 169.9, 151.2, 133.6, 124.6, 124.3, 118.2, 106.8, 64.9, 63.2, 59.8, 52.2, 43.6, 37.7, 34.9, 14.6, 12.2. IR (film): 1731, 1683, 1629  $\text{cm}^{-1}$ . HRMS (ESI): calculated for  $\text{C}_{18}\text{H}_{24}\text{N}_2\text{O}_5\text{Na}$   $[\text{M} + \text{Na}]^+$ , 371.1583; found 371.1596.



**Spirocycle 5.57****5.57**

Yellow liquid, 91%,  $^1\text{H}$  NMR (300 MHz,  $\text{CDCl}_3$ ),  $\delta$  (ppm): 7.03-6.95 (m, 2H), 5.00-4.86 (m, 2H), 4.28 (q,  $J = 7.1$  Hz, 2H), 3.72 (s, 3H), 3.46-3.38 (m, 3H), 3.25 (d,  $J = 9.7$  Hz, 1H), 2.89 (dd,  $J = 17.2, 2.7$  Hz, 1H), 2.61 (dd,  $J = 17.2, 2.8$  Hz, 1H), 1.90 (t,  $J = 2.6$  Hz, 1H), 1.33 (t,  $J = 7.1$  Hz, 3H), 1.15 (t,  $J = 7.3$  Hz, 3H).  $^{13}\text{C}$  NMR (75 MHz,  $\text{CDCl}_3$ ),  $\delta$  (ppm): 169.6, 169.3, 151.2, 124.7, 106.6, 80.2, 70.4, 64.5, 63.3, 60.6, 52.5, 43.0, 37.8, 20.6, 14.6, 12.3. IR (film): 1727, 1678, 1629  $\text{cm}^{-1}$ . HRMS (ESI): calculated for  $\text{C}_{18}\text{H}_{22}\text{N}_2\text{O}_5\text{Na}$   $[\text{M} + \text{Na}]^+$ , 369.1426; found 369.1433.

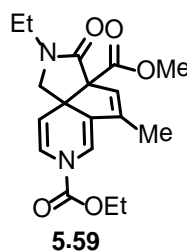
**Spirocycle 5.58****5.58**

Yellow liquid, 84%,  $^1\text{H}$  NMR (300 MHz,  $\text{CDCl}_3$ ),  $\delta$  (ppm): 7.09-6.87 (m, 2H), 5.07-4.89 (m, 2H), 4.28 (q,  $J = 7.1$  Hz, 2H), 3.84, 3.7 (2s, 3H), 3.54-3.28 (m, 4H), 2.89-2.83 (m, 1H), 2.60-2.53 (m, 1H), 1.68 (t,  $J = 2.6$  Hz, 3H), 1.33 (t,  $J = 7$  Hz, 3H), 1.15 (t,  $J = 7.3$  Hz, 3H).  $^{13}\text{C}$  NMR (75 MHz,  $\text{CDCl}_3$ ),  $\delta$  (ppm): 170.0, 169.7, 151.2, 124.7, 123.4, 107.9, 105.8, 74.7, 65.0, 63.2, 60.7, 52.5, 42.5, 37.7, 21.0, 14.6, 12.3, 3.7. IR (film): 1727, 1683, 1634  $\text{cm}^{-1}$ . HRMS (ESI): calculated for  $\text{C}_{19}\text{H}_{24}\text{N}_2\text{O}_5\text{Na}$  [ $\text{M} + \text{Na}$ ] $^+$ , 383.1583; found 383.1578.

### Procedure for Au(III)-catalyzed cycloisomerization

General procedure: The spirocycle **5.57** (0.10 g, 0.29 mmol, 1 equiv) was taken in dry toluene (3 mL) and 5 mol%  $\text{AuCl}_3$  and 5 mol%  $\text{AgOTf}$  was added. Reaction mixture was heated at 80  $^\circ\text{C}$  for 2 h and then cooled to room temperature and evaporated in vacuo. The crude product was purified on silica gel column chromatography using ethyl acetate in hexanes to obtain **5.59**, yellow liquid (94 mg, 94%).

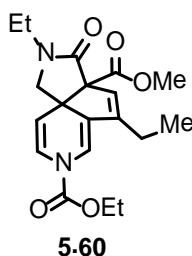
### Tricyclic molecule 5.59



Yellow liquid, 94%,  $^1\text{H}$  NMR (300 MHz,  $\text{CDCl}_3$ ),  $\delta$  (ppm): 7.01 (br s, 2H), 5.65 (s, 1H), 5.47 (d,  $J = 7.9$  Hz, 1H), 4.33 (q,  $J = 7.2$  Hz, 2H), 3.72 (s, 3H), 3.31 (q,  $J = 7.3$  Hz, 2H), 3.28 (d,  $J = 10.1$  Hz, 1H), 3.15 (d,  $J = 10.1$  Hz, 1H), 1.98 (t,  $J = 0.6$  Hz, 3H), 1.36 (t,  $J = 7.1$  Hz, 3H), 1.08 (t,  $J = 7.2$  Hz, 3H).  $^{13}\text{C}$  NMR (75

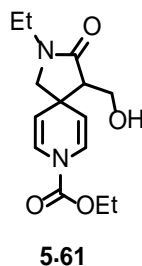
MHz, CDCl<sub>3</sub>),  $\delta$  (ppm): 169.8, 169.2, 151.9, 140.5, 129.1, 125.8, 123.7, 114.9, 107.3, 71.1, 63.4, 63.2, 52.5, 46.7, 37.5, 14.6, 12.7, 12.2. IR (film): 1730, 1682, 1624 cm<sup>-1</sup>. HRMS (ESI): calculated for C<sub>18</sub>H<sub>22</sub>N<sub>2</sub>O<sub>5</sub>Na [M + Na]<sup>+</sup>, 369.1426; found 369.1427.

### Tricyclic molecule 5.60



Yellow liquid, 96%, <sup>1</sup>H NMR (300 MHz, CDCl<sub>3</sub>),  $\delta$  (ppm): 7.06-6.98 (m, 2H), 5.66 (s, 1H), 5.47 (br s, 1H), 4.33 (q,  $J$  = 7.1 Hz, 2H), 3.72 (s, 3H), 3.32 (q,  $J$  = 7.3 Hz, 2H), 3.24 (d,  $J$  = 10.1 Hz, 1H), 3.14 (d,  $J$  = 10.0 Hz, 1H), 2.45- 2.26 (m, 2H), 1.36 (t,  $J$  = 7.1 Hz, 3H), 1.2 (t,  $J$  = 7.4 Hz, 3H), 1.08 (t,  $J$  = 7.3 Hz, 3H). <sup>13</sup>C NMR (75 MHz, CDCl<sub>3</sub>),  $\delta$  (ppm): 169.9, 169.3, 151.9, 146.8, 128.1, 123.6, 114.9, 107.1, 70.9, 63.4, 63.1, 52.6, 46.8, 37.5, 20.3, 14.6, 12.3, 12.1. IR (film): 1734, 1682, 1624 cm<sup>-1</sup>. HRMS (ESI): calculated for C<sub>19</sub>H<sub>24</sub>N<sub>2</sub>O<sub>5</sub>Na [M + Na]<sup>+</sup>, 383.1583; found 383.1605.

### Spirocycle 5.61



Spirocycle **5.39** (0.10 g, 0.3 mmol, 1 equiv) was taken in 2 mL of ethanol at 0 °C. NaBH<sub>4</sub> (14 mg, 0.36 mmol, 1.1 equiv) was added and the reaction mixture was stirred at room temperature for 16 h. Reaction mixture was diluted with water (20 mL) and extracted with ethyl acetate (10 X 3 mL). The combined extract was then dried over anhydrous Na<sub>2</sub>SO<sub>4</sub> and evaporated *in vacuo*. The crude product was purified by silica gel column chromatography using ethyl acetate in hexanes to afford **5.61**, Yellow liquid (11 mg, 12%) and recovered 50 mg of the starting material.

<sup>1</sup>H NMR (300 MHz, CDCl<sub>3</sub>), δ (ppm): 6.93 (br s, 2H), 4.87-4.80 (m, 2H), 4.28 (q, *J* = 7.11 Hz, 2H), 3.89-3.82 (m, 1H), 3.79-3.72 (m, 1H), 3.35 (q, *J* = 7.3 Hz, 2H), 3.34-3.31 (m, 1H), 3.24 (d, *J* = 10.0 Hz, 1H), 3.14 (d, *J* = 10.0 Hz, 1H), 2.37 (d, *J* = 8.3, 5.0 Hz, 1H), 1.33 (t, *J* = 7.1 Hz, 3H), 1.12 (t, *J* = 7.3 Hz, 3H). <sup>13</sup>C NMR (75 MHz, CDCl<sub>3</sub>), δ (ppm): 174.2, 151.3, 124.4, 123.5, 109.5, 107.0, 63.2, 61.3, 60.4, 55.8, 39.4, 37.1, 14.6, 12.6. IR (film): 3417, 1717, 1668 cm<sup>-1</sup>. HRMS (ESI): calculated for C<sub>14</sub>H<sub>20</sub>N<sub>2</sub>O<sub>4</sub>Na [M + Na]<sup>+</sup>, 303.1321; found 303.1324.

## CHAPTER SIX

### EXTENDED STUDY OF 4-ALKYLPYRIDINE SPIROCYCLIZATION

#### 6.1 Introduction

Azaspirocyclic systems are important structural motifs in pharmacological molecules. In particular, many piperidines incorporated into spirocyclic frameworks exhibit valuable biological activities. The previous chapter described a novel method to synthesize diazaspiro[4.5]decanes using titanium isopropoxide-mediated spirocyclization of 4-(aminomethyl) pyridines substituted with  $\beta$ -amido esters in the side chain. Extended studies were carried out to synthesize related diazaspiro[5.5]undecanes from 4-(ethylamino)pyridine derivatives substituted with  $\beta$ -keto amides. In addition, the scope and limitations of diazaspiro[4.5] decane synthesis has been investigated in greater detail, and results of this study are also reported in this chapter.

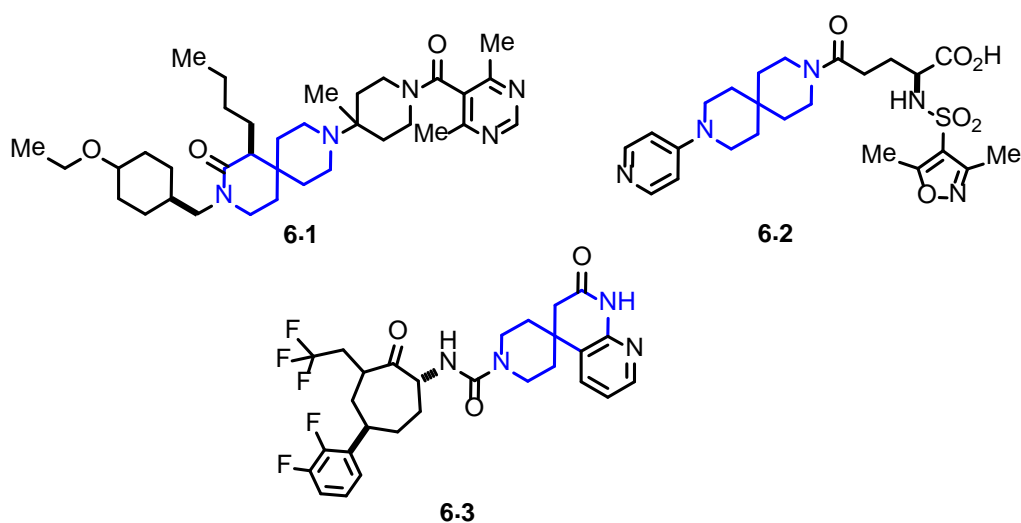


Figure 6.1. Few examples of diazaspiro[5.5]decanes in medicinal chemistry

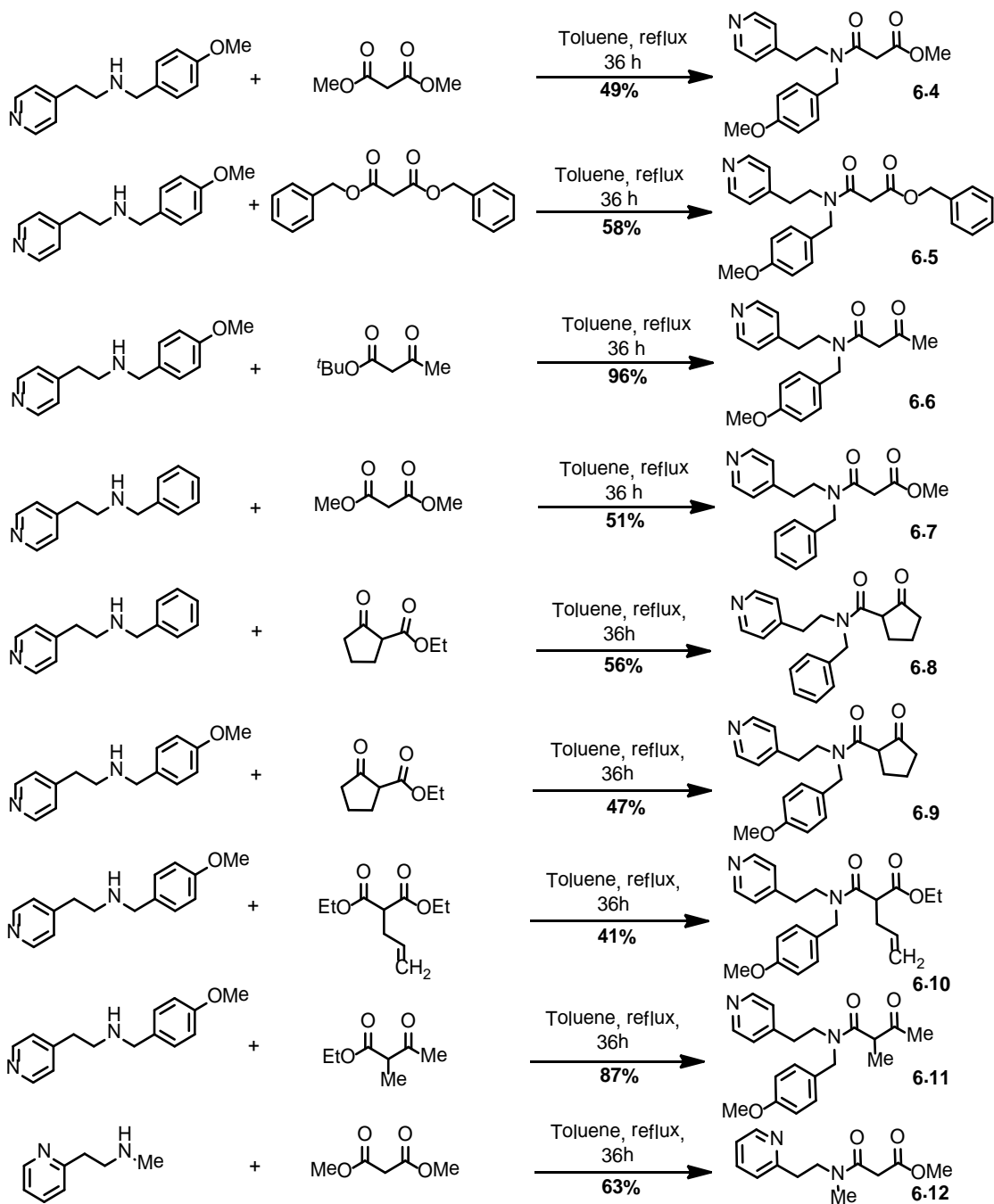
3,9-Diazaspiro[5.5]undecanes form the core structure of many therapeutic molecules and are used in structure-relationship screening for allergic diseases such as asthma.<sup>177</sup> Numerous applications of these heterocycles in medicinal chemistry exist in literature. For example, A functionalized spiro[5.5]undecane (**6.1**) was found to be a potent antagonist of chemokine GPCR receptor CCR5.<sup>178</sup> N-substituted azaspirocycle analogue (**6.2**) was shown to be an antagonist of platelet glycoprotein IIb-IIIa (Figure 6.1).<sup>179</sup> Studies have shown that spiropiperidine analogue (**6.3**) has the potential to become suitable oral drug for migraine with minimum associated cardiovascular side effects.<sup>180</sup> It is evident that heterocycles with spiro-skeleton are of pharmacological importance in many molecules. However, general methods to prepare diazaspiroundecanes have not been reported. In this context, the dearomatization strategy based on pyridine derivatives discussed in the previous chapter could be used to synthesize spiroundecane scaffolds.

## 6.2 Results and discussion

### **Synthesis of diazaspiro[5.5]undecanes via spirocyclization<sup>181</sup>**

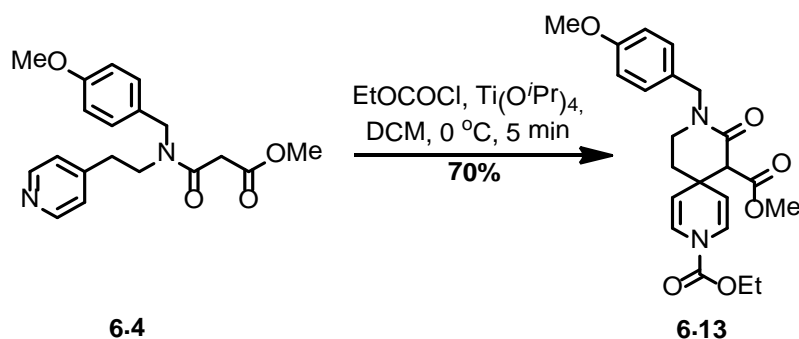
The 4-alkylpyridine precursors were synthesized using procedures similar to those described in the preceding chapter. In general, 4-(aminomethyl)pyridine was first converted to a secondary amine and then converted to a  $\beta$ -amido ester. The synthesis of 4-(ethylamino)pyridines **6.4-6.12**, substituted with  $\beta$ -dicarbonyl stabilized carbon nucleophiles were synthesized in good yields. The side chain contained different ester functionalities, as well as  $\beta$ -amido esters and  $\beta$ -keto amides. We also varied N-substitution of 4-pyridine derivatives with N-benzyl and N-PMB groups. These 4-(ethylamino)pyridine derivatives were found to undergo efficient spirocyclization to give 1,4-dihydro pyridines, which could be further manipulated into bis(piperidine) analogues. Importantly, all compounds prepared

in this study were stable and could be isolated and purified using conventional techniques.



Scheme 6.1. Synthesis of 4-alkylpyridyl substrates

As discussed in the previous chapter, spirocyclization was performed by initially treating the pyridine derived starting materials (**6.4**) with ethyl chloroformate in the presence of titanium isopropoxide at 0 °C in DCM (Scheme 6.2).<sup>181</sup> Spirocyclization was fast and yielded the corresponding spiroperidine derivative (**6.13**) in good yield.



Scheme 6.2. Synthesis of diazaspиро[5.5]decane system

This spirocyclization procedure was applied to pyridine substrates **6.5-6.9** to afford the expected dihydropyridine products as shown in Figure 6.2. Pyridine derivative **6.6** with acyclic  $\beta$ -keto amide in the side chain yielded the corresponding spirocycle **6.16** in lower yield. However,  $\beta$ -keto amides **6.8** and **6.9** with cyclopentanone side chain gave the products **6.17** and **6.18** in were better yield. The 2-pyridyl substrates (**6.12**) failed to produce any desirable product. Spirocyclizations using 4-pyridyl substrates with substitution at the active methylene position in the carbon nucleophile (**6.10** and **6.12**) also failed to undergo spirocyclization.

Titanium isopropoxide catalyzed spirocyclization was rapid, efficient and simple. Pyridine derivatives tethered with  $\beta$ -amido esters proved to be the best candidates for the spirocyclization under optimized condition. This trend is similar



to the observation noted in the synthesis of diazaspiro[4.5]decanes as mentioned in the preceding chapter.

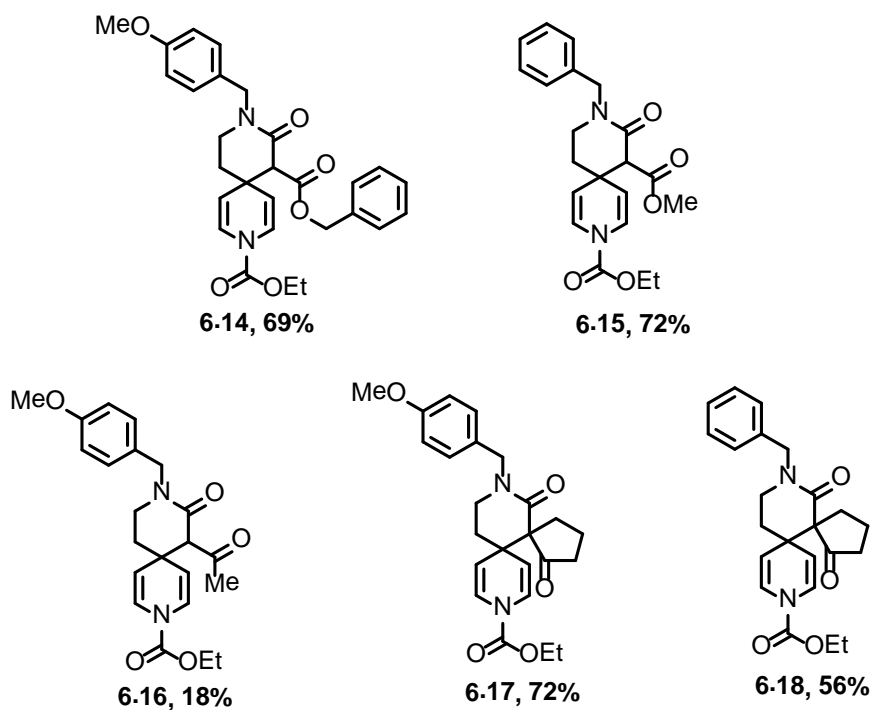
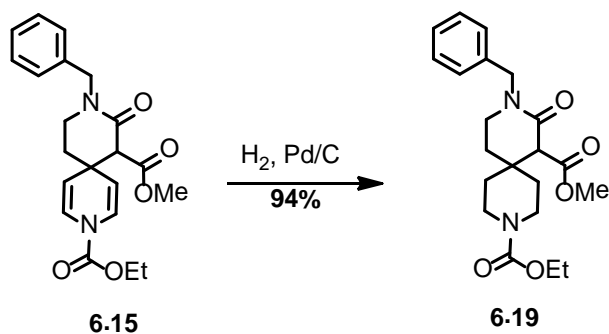


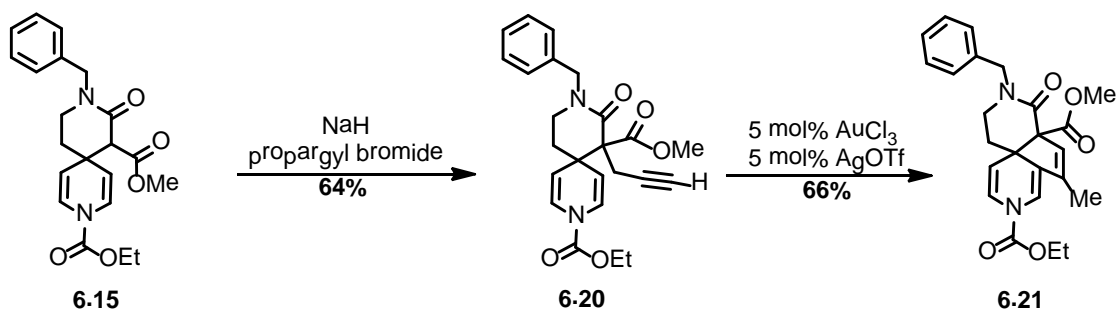
Figure 6.2. Examples of diazaspiro[5.5]undecane framework synthesis

The 1,4-dihydro pyridine products obtained by this procedure were then further functionalized to demonstrate the potential utility of these moieties in heterocyclic chemistry. Spirocycle **6.15** on hydrogenation in the presence of Pd/C at room temperature yielded the functionalized spiro-bis(piperidine) **6.19** in excellent yield (Scheme 6.3).



Scheme 6.3. Hydrogenation of 1,4-dihydropyridine **6.15**

Alkylation of the lactam ring in **6.15** using propargyl bromide in the presence of base gave **6.20** (Scheme 6.4). The complex tricyclic **6.21** was then obtained by a gold(III) catalyzed cycloisomerization of 1,6-enyne **6.20**. This overall 3 step sequence illustrates the construction of complex molecular structures starting from simple pyridine derivatives.



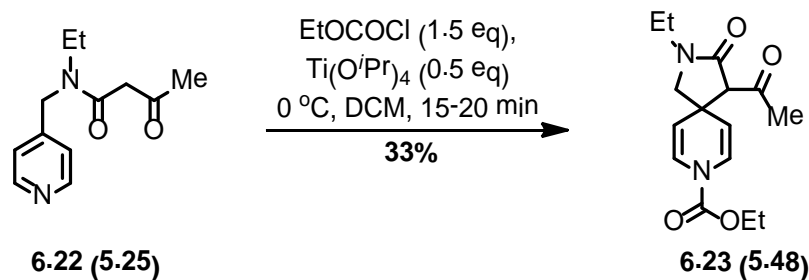
Scheme 6.4. Elaboration of spirocycle **6.15** into complex building blocks

### Scope and limitations of diazaspиро[4.5]decanes synthesis: spirocyclization of $\beta$ -keto amides

As discussed in the preceding chapter, a variety of  $\beta$ -amido carbonyl nucleophiles were found to participate in intramolecular cyclization under the

optimized reaction conditions. However, substrate **6.22 (5.25)** gave a poor yield for this transformation (Scheme 6.5). Hence we focused our efforts in this extended study to optimize the efficiency of spirocyclization involving alkylpyridines with  $\beta$ -keto amide side chains, as well as carbon nucleophiles other than  $\beta$ -dicarbonyls. Pyridine derivative **6.22 (5.25)** was chosen as the model substrate for this examination.

To begin with, various reaction conditions were screened for the spirocyclization of **6.22 (5.25)** to obtain **6.23 (5.48)** and the results are summarized in Table 6.1. At 0 °C, spirocyclization was found to occur in TFE alone, a strongly hydrogen bonding solvent, by treatment of **6.22 (5.25)** with ethyl chloroformate. In DCM, however, a Lewis acid additive was required for the spirocyclization. Titanium isopropoxide and  $\text{InCl}_3$  were found to be effective whereas other Lewis acid additives failed to promote the reaction. The presence of DIPEA (Hunig's base) was found to be beneficial in spirocyclization reactions performed in DMF both at 0 °C and at higher temperature (table 6.1, entries 18-19). Inclusion of Hunig's base (Table 6.1, entry 17) also improved the yield of reactions in DCM in the presence of excess of ethyl chloroformate. The presence of 2-chloro pyridine or proton sponge did not assist the transformation. Isopropyl chloroformate and phenyl chloroformate could be substituted for ethyl chloroformate and yielded **6.23a** and **6.23b** in moderate yield, respectively (Table 6.1, entries 20-21) (figure 6.3). An X-ray crystal structure was obtained for spirocycle **6.23 (5.48)** (see Appendix A). This structure confirmed the identity of the spirocyclic product.

Scheme 6.5. Spirocyclization of substrate **6.22 (5.25)**Table 6.1. Reaction conditions screened for spirocyclization of **6.22 (5.45)**

Entry	Reagents	Yield
1	CICO <sub>2</sub> Et (2 equiv), TFE, 0 °C, 20 min	19%
2	CICO <sub>2</sub> Et (1.5 equiv), Ti(O <sup>i</sup> Pr) <sub>4</sub> (1 equiv), DCM, 0 °C, 20 min	20%
3	CICO <sub>2</sub> Et (1.5 equiv), Ti(O <sup>i</sup> Pr) <sub>4</sub> (0.5 equiv), DCM, 0 °C, 20 min	33%
4	CICO <sub>2</sub> Et (1.5 equiv), Ti(O <sup>i</sup> Pr) <sub>4</sub> (0.25 equiv), DCM, 0 °C, 20 min	31%
5	CICO <sub>2</sub> Et (1.5 equiv), InCl <sub>3</sub> (1 equiv), DCM-water (1:1), 0 °C, 20 min	31%
6	CICO <sub>2</sub> Et (1.5 equiv), InCl <sub>3</sub> (1 equiv), THF, 0 °C, 20 min	0%
7	CICO <sub>2</sub> Et (1.5 equiv), TMSOTf (1 equiv), DCM, 0 °C, 20 min	0%
8	CICO <sub>2</sub> Et (1.5 equiv), Mg(OTf) <sub>2</sub> (1 equiv), DCM, 0 °C, 20 min	0%
9	CICO <sub>2</sub> Et (1.5 equiv), Cu(OTf) <sub>2</sub> (1 equiv), DCM, 0 °C, 20 min	0%
10	Tf <sub>2</sub> O (1.2 equiv), Ti(O <sup>i</sup> Pr) <sub>4</sub> (1 equiv), DCM, 0 °C, 20 min	0%
11	PhSO <sub>2</sub> Cl(1.5 equiv), Ti(O <sup>i</sup> Pr) <sub>4</sub> , DCM, 0 °C, 20 min	0%
12	CICO <sub>2</sub> Et (1.5 equiv), Ti(O <sup>i</sup> Pr) <sub>4</sub> , DMF, 0 °C, 20 min	trace
13	CICO <sub>2</sub> Et (1.5equiv), Ti(O <sup>i</sup> Pr) <sub>4</sub> , toluene, 0 °C, 20 min	0%
14	CICO <sub>2</sub> Et (1.5 equiv), Ti(O <sup>i</sup> Pr) <sub>4</sub> , acetone, 0 °C, 20 min	0%
15	CICO <sub>2</sub> Et (1.5 equiv), Ti(O <sup>i</sup> Pr) <sub>4</sub> (1.2 equiv), 2-chloro pyridine, DCM, 0 °C, 20 min	0%
16	CICO <sub>2</sub> Et (1.5 equiv), Ti(O <sup>i</sup> Pr) <sub>4</sub> (1.1 equiv), proton sponge, DCM, 0 °C, 20 min	0%
17	CICO <sub>2</sub> Et (5 equiv), Ti(O <sup>i</sup> Pr) <sub>4</sub> (0.5 equiv), DIPEA (1 equiv), DCM, 0 °C-rt, 15-20 min	44%
18	CICO <sub>2</sub> Et (1.5 equiv), Ti(O <sup>i</sup> Pr) <sub>4</sub> (0.5 equiv), DIPEA (1 equiv), DMF, 0 °C-rt, 15 min	29%
19	CICO <sub>2</sub> Et (5 equiv), Ti(O <sup>i</sup> Pr) <sub>4</sub> (0.5 equiv), DIPEA (1 equiv), DMF, 100 °C, 15 min	49%
20	CICO <sub>2</sub> <sup>i</sup> Pr (1.5 equiv), Ti(O <sup>i</sup> Pr) <sub>4</sub> (0.5 equiv), DIPEA (1.5 equiv), DCM, 0 °C-rt, 15-20 min	36%
21	CICO <sub>2</sub> Ph (1.5 equiv), Ti(O <sup>i</sup> Pr) <sub>4</sub> (0.5 equiv), DIPEA (1.5 equiv), DCM, 0 °C-rt, 15-20 min	50%

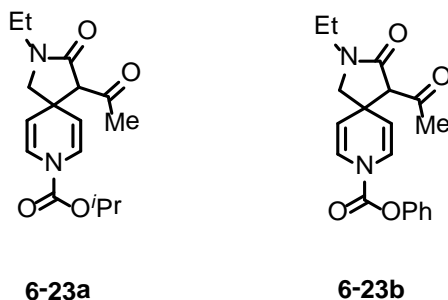
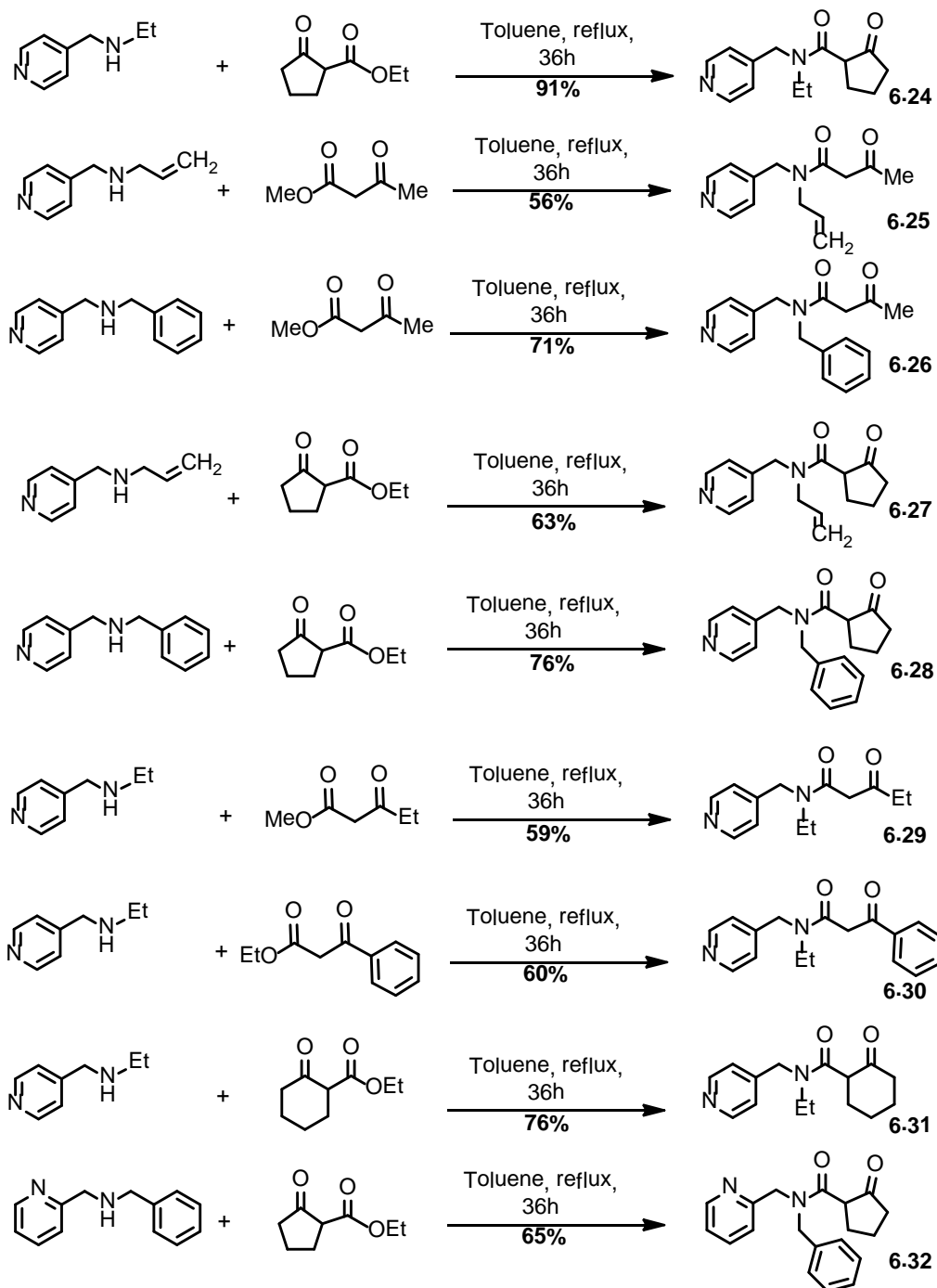
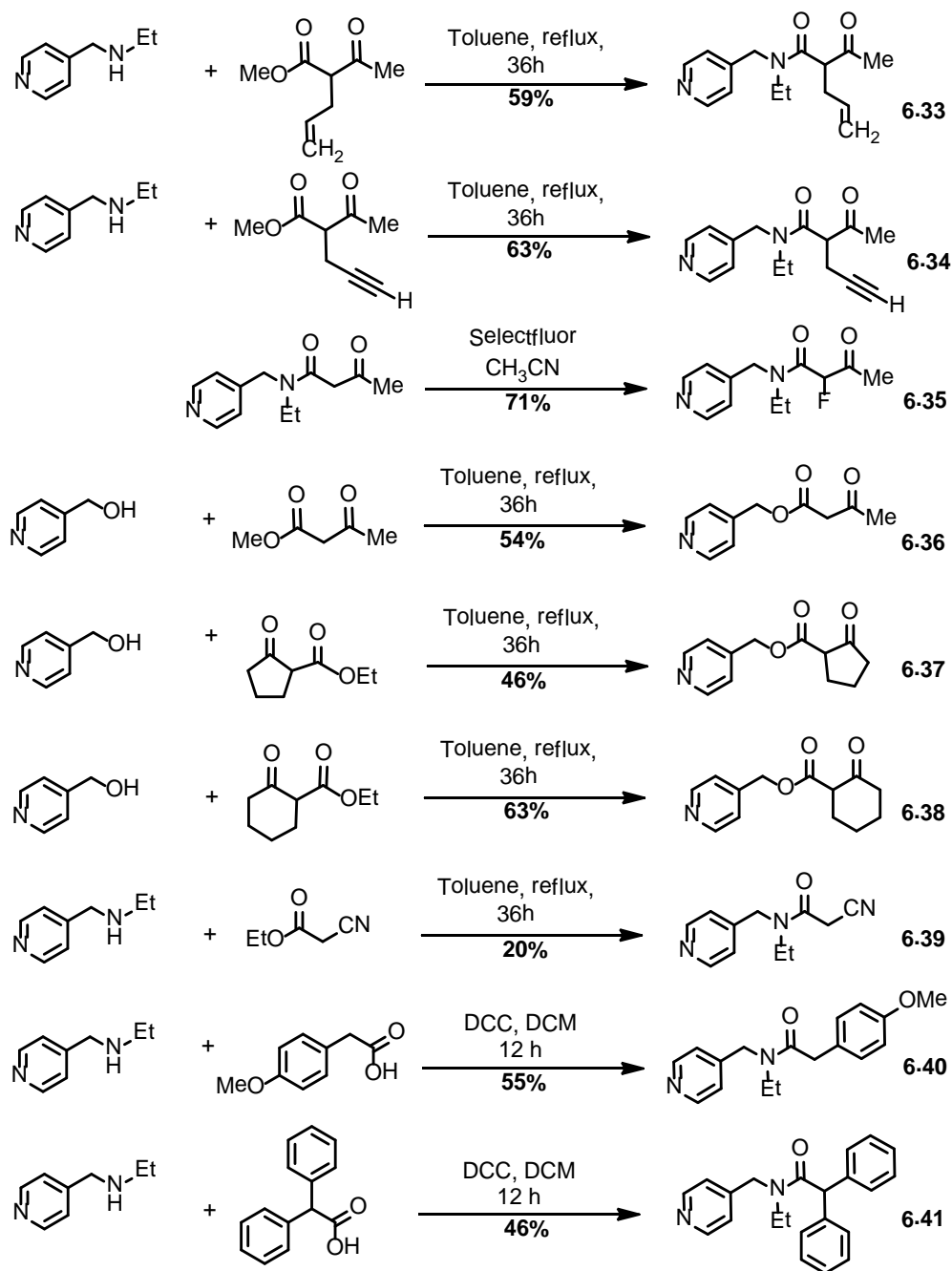


Figure 6.3. Carbamate analogues of the spirocycle **6.23**

Studies were also directed toward utilizing different 4-alkylpyridines with  $\beta$  keto amides for the construction of azaspirocycles. Starting materials were synthesized using the general protocol described earlier (Chapter Five, Scheme 5.6-5.7) and synthesis is summarized in Scheme 6.6. The  $\beta$ -keto amide substrates **6.24-6.31** were prepared with variable N-substitution such as N-ethyl, N-benzyl and N-allyl groups. Additionally, the nature of the  $\beta$ -keto side chain was varied from acyclic acetyl to cyclopentanone and cyclohexanone moieties. 2-Pyridyl analogue **6.32** was also prepared. Substrates **6.33** and **6.34** feature substituted  $\beta$ -keto amide side chains and were prepared to test the effect of substitution of the nucleophilic center upon cyclization. In addition, a fluorinated analogue (**6.35**) was also prepared via monofluorination of **6.22** with Selectfluor.<sup>71</sup> 4-Alkylpyridine substrates **6.36**, **6.37** and **6.38** with  $\beta$ -keto ester nucleophiles were examined in this study. Finally, cyclization precursors **6.39**, **6.40**, and **6.41** equipped with carbon nucleophiles other than  $\beta$ -dicarbonyls were also synthesized.

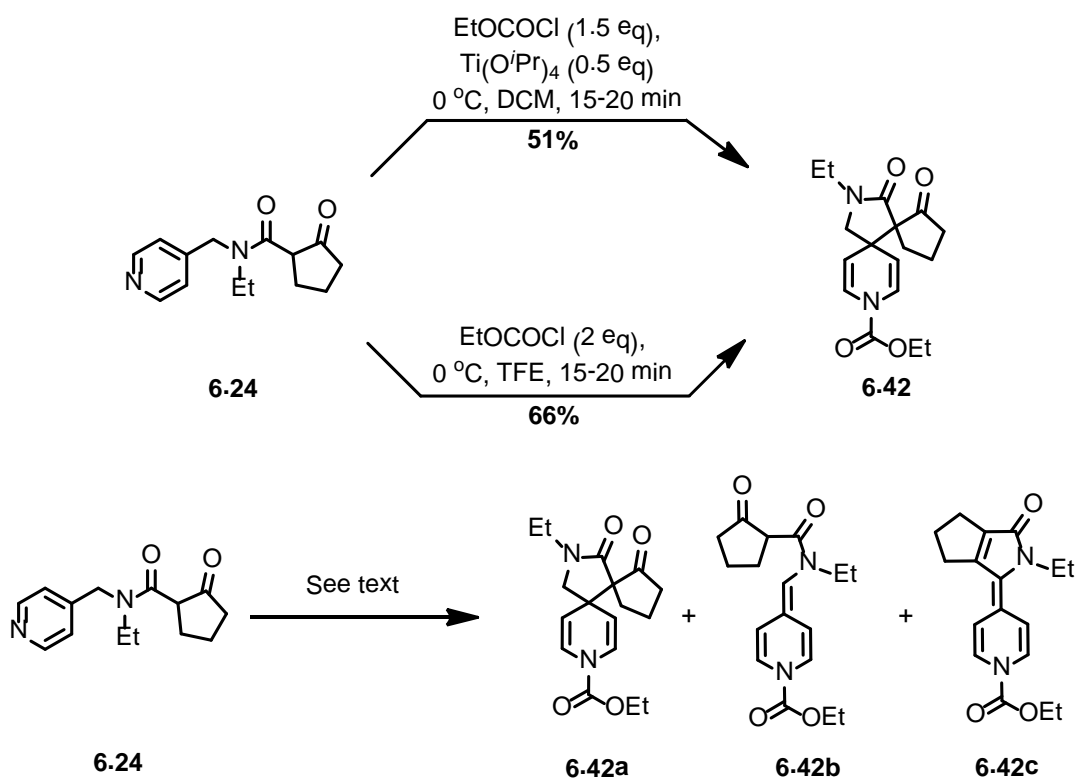
Scheme 6.6. Synthesis of alkylpyridines with  $\beta$ -keto amides



Scheme 6.6. (Continued)

With the substrates shown in scheme 6.6 in hand, compound **6.24** was subjected to different cyclization reaction conditions and results are depicted in table 6.2. Spirocycle **6.42** was obtained using ethyl chloroformate in TFE alone in

moderate yield (Scheme 6.7). This result is attributed to the strong enolization of  $\beta$ -keto amides by the non nucleophilic polar solvent TFE. Spirocyclization was not observed in DCM alone (Table 6.2, entry 11) but addition of Lewis acid such as titanium isopropoxide and magnesium bromide afforded product in moderate yield (Table 6.2, entry 3-4). But  $\text{TiCl}_4$  and  $\text{SnCl}_4$  did not promote the cyclization.



Scheme 6.7. Spirocyclization of **6.24**



Table 6.2. Spirocyclization reaction conditions screened for substrate **6.24**.

Entry	Reagents	% yield
1	ClCO <sub>2</sub> Et (2 equiv), TFE, 0 °C, 20 min	66%
2	ClCO <sub>2</sub> Et (1.5 equiv), Ti(O <sup>i</sup> Pr) <sub>4</sub> (1 equiv), DCM, 0 °C, 20 min- reflux 5 min	39% <sup>a</sup>
3	ClCO <sub>2</sub> Et (1.5 equiv), Ti(O <sup>i</sup> Pr) <sub>4</sub> (0.5 equiv), DCM, 0 °C, 20 min	51%
4	ClCO <sub>2</sub> Et (1.5 equiv), MgBr <sub>2</sub> (1 equiv), DCM, 0 °C, 20 min	47%
5	ClCO <sub>2</sub> Et (1.5 equiv), CuSO <sub>4</sub> ·5H <sub>2</sub> O (1 equiv), DCM, 0 °C, 20 min	0%
6	ClCO <sub>2</sub> Et (1.5 equiv), TiCl <sub>4</sub> (1 equiv), DCM, 0 °C-rt, 15-20 min	0%
7	ClCO <sub>2</sub> Et (1.5 equiv), SnCl <sub>4</sub> (1 equiv), DCM, 0 °C-rt, 15-20 min	0%
8	ClCO <sub>2</sub> Et (1.5 equiv), K <sub>2</sub> CO <sub>3</sub> (1 equiv), THF, 0 °C, 20 min	0%
9	ClCO <sub>2</sub> Et (1.5 equiv), Ti(O <sup>i</sup> Pr) <sub>4</sub> (0.5 equiv), DIPEA (1 equiv), DCM, 0 °C-rt, 15-20 min	37%
10	ClCO <sub>2</sub> Et (10 equiv), Ti(O <sup>i</sup> Pr) <sub>4</sub> (0.5 equiv), DCM, 0 °C-rt, 15-20 min	42%
11	ClCO <sub>2</sub> Et (1.5 equiv), DCM, 0 °C, 20 min- reflux 5 min	trace

<sup>a</sup>15% of **6.42c** was formed on heating.

An interesting product mixture was obtained upon treatment of **6.24** with ethyl chloroformate and base (K<sub>2</sub>CO<sub>3</sub>) (Table 6.2, entry 8). In this instance an unstable anhydrobase (**6.42b**) was formed at the expense of spirocyclization. In contrast, the formation of anhydrobase **6.42c** was observed along with the spirocycle (**6.42a**) when the reaction mixture was briefly heated in a rotary evaporator (Table 6.2, entry 2). Further details about the synthesis of the anhydrobase **6.42c** will be discussed in Chapter Seven. Hunig's base, a basic additive, along with titanium isopropoxide reduced the formation of spirocycle to 37% (Table 6.2, entry 9). The addition of excess ethyl chloroformate also decreased the efficiency of the spirocyclization (Table 6.2, entry 10). In general; the spirocyclization of  $\beta$ -keto amides was low yielding in comparison to cyclization of 4-alkylpyridine  $\beta$ -amido esters as described in Chapter Five.

Table 6.3. Generality of spirocyclization of 4-alkylpyridine with  $\beta$ -keto amides side chains.

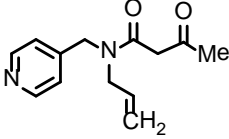
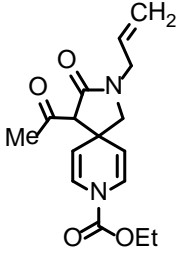
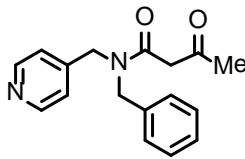
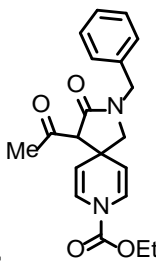
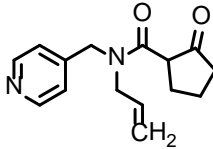
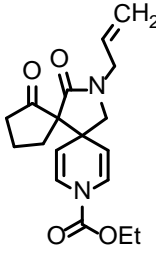
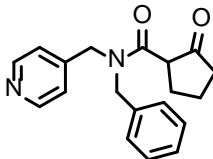
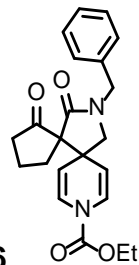
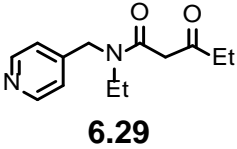
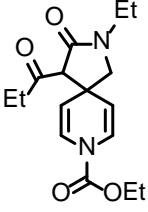
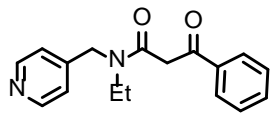
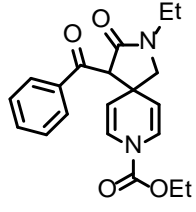
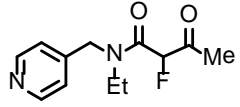
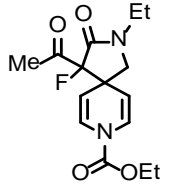
Entry	Substrate	Spirocycle	Yield	Reaction conditions
1	 <p><b>6.25</b></p>	 <p><b>6.43</b></p>	12%	A
2	 <p><b>6.26</b></p>	 <p><b>6.44</b></p>	18%	A
3	 <p><b>6.27</b></p>	 <p><b>6.45</b></p>	40%	B
4	 <p><b>6.28</b></p>	 <p><b>6.46</b></p>	44%	B
5	 <p><b>6.29</b></p>	 <p><b>6.47</b></p>	53%	A

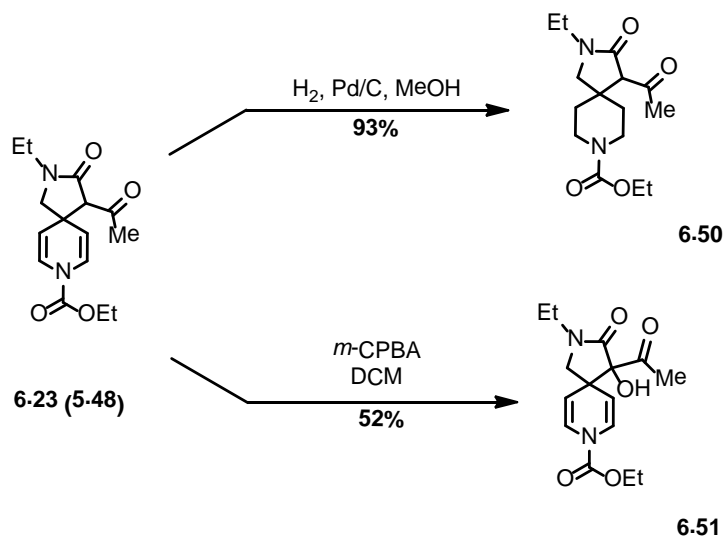
Table 6.3. (Continued)

6	 <p style="text-align: center;"><b>6.30</b></p>	 <p style="text-align: center;"><b>6.48</b></p>	43%	A
7	 <p style="text-align: center;"><b>6.35</b></p>	 <p style="text-align: center;"><b>6.49</b></p>	10%	A

Condition A: EtO<sub>2</sub>CCl (1.5 equiv), Ti(O<sup>i</sup>Pr)<sub>4</sub> (0.5 equiv), DCM.

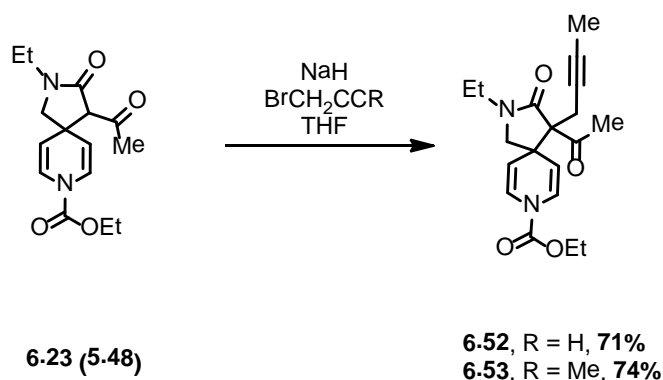
Condition B: EtO<sub>2</sub>CCl (2 equiv), TFE.

Nonetheless, other 4-alkylpyridine substrates **6.29-6.41** were subjected to cyclization conditions, and the results are summarized in table 6.3. 4-alkyl pyridine substrates **6.25** and **6.26** (analogues of **6.22**) gave **6.43** and **6.44** respectively, in poor yield for the transformation. Substrates with cyclic (cyclopentanone) nucleophile (**6.27-6.28**) yielded spirocycles **6.45** and **6.46** in moderate yield with excess of ethyl chloroformate in TFE. Substrates with acyclic β-dicarbonyl nucleophile **6.29** and **6.30** worked well when treated with ethyl chloroformate in the presence of titanium isopropoxide in DCM and gave **6.47** and **6.48** in good yield. Fluorinated substrate **6.35**, however, underwent cyclization to give **6.49** in poor yield. Substrates with β-keto ester nucleophiles **6.36**, **6.37** and **6.38** as well as substrates with other carbon nucleophiles **6.39**, **6.40** and **6.41** failed to undergo this transformation under optimized conditions. The extent of enolization, nucleophilicity, and conformational flexibility of the side chains may have a strong impact on the spirocyclization.



Scheme 6.8. Elaboration of the spirocycle **6.23**

Finally, as for the spirodihydropyridines discussed in the preceding chapter, products of spirocyclization were further elaborated. For example, the spirocycle **6.23 (5.48)** was hydrogenated using Pd/C at room temperature to afford spiropiperidine derivative **6.50** in excellent yield (Scheme 6.8). In contrast, attempted oxidation of the enamide groups in **6.23** using *m*-CPBA afforded only the  $\alpha$ -hydroxylated product **6.51**. Alkylation of **6.23** with propargyl bromide and butynyl bromide yielded **6.52** and **6.53** in good yields (Scheme 6.9).



Scheme 6.9. Alkylation of **6.23**

### 6.3 Conclusion

Extended studies of titanium isopropoxide mediated intramolecular dearomatization of 4-alkylpyridine derivatives has uncovered a new pathway for construction of azaspirocyclic frameworks. This methodology is simple, utilizes readily prepared pyridine derivatives, and provides access to a diverse array of heterocyclic building blocks. Both 4-(methylamino) and 4-(ethylamino)pyridine derivatives substituted with stabilized  $\beta$ -dicarbonyl carbon nucleophiles were synthesized and successfully used in intramolecular dearomatization to obtain diazapro[4.5]decanes and diazapro[5.5]undecanes in good yields. These spirocycles were further elaborated under several sets of reaction conditions to obtain important synthetic building blocks. It was observed that under optimal conditions these  $\beta$ -amido ester, 4-(ethylamino)pyridine starting materials behaved in a similar manner to 4-(aminomethyl)pyridine  $\beta$ -amido esters described in Chapter Five. These spirocycles were converted into more complex tricyclic moieties using gold catalyzed cycloisomerization. It was also demonstrated that 4-(aminomethyl)pyridine  $\beta$ -keto amides could be used to synthesize azaspirocyclics using this strategy. The efficiency of this transformation was lower in comparison to their  $\beta$ -amido ester counterparts.

### 6.4 Experimental section

#### **General experimental**

All commercially available starting materials and reagents were used as received unless otherwise noted. All the reactions were performed under argon atmosphere. Solvents were dried and purified by passage through activated alumina columns. Proton nuclear magnetic resonance ( $^1\text{H-NMR}$ ) spectra and carbon nuclear magnetic resonance ( $^{13}\text{C-NMR}$ ) spectra were recorded at 300 MHz and 75 MHz respectively. Chemical shifts are reported as  $\delta$  values in parts

per million (ppm) relative to tetramethylsilane for  $^1\text{H-NMR}$  in  $\text{CDCl}_3$  and residual undeuterated solvent for all other spectra. The NMR spectra for many of the compounds used in this study reveal the presence of amide rotamers.

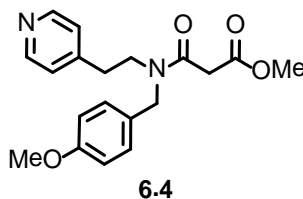
Resonances corresponding to major and minor isomers are identified when appropriate. IR spectra were recorded on a FT-IR spectrometer as thin films on sodium chloride discs. High resolution mass spectra were obtained using electron spray ionization (ESI). Melting points were recorded using capillary melting point apparatus and are uncorrected.

### Procedures and characterization of 4-(ethylamino)pyridine starting materials

General procedure: A reaction mixture containing secondary amine derived from 4-(aminoethyl) pyridine (1.00 g, 4.71 mmol, 1 equiv) and dimethyl malonate (0.72 g, 5.42 mmol, 1.3 equiv) in toluene (30 mL) was refluxed for 36 h. The reaction mixture was cooled to room temperature and concentrated in vacuo. The crude product was purified by silica gel column chromatography using 70-100% ethyl acetate in hexanes to afford the desired  $\beta$ -amido ester substrate **6.4** (0.70 g, 49%).

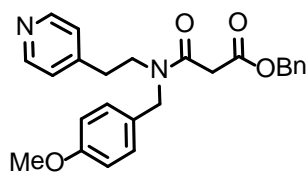
$\beta$ -amido ester substrates **6.4**, **6.5**, **6.7**, **6.10** and **6.12** were prepared using the above procedure and  $\beta$ -keto amide substrates **6.7**, **6.8**, **6.9** and **6.11** were prepared using secondary amines and corresponding  $\beta$ -keto ester starting materials (1.00 g-2.00 g scale).

#### $\beta$ -amido ester **6.4**



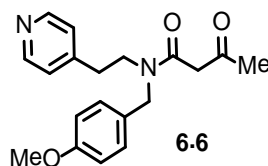
Yellow liquid, 49%,  $^1\text{H}$  NMR (300 MHz,  $\text{CDCl}_3$ ),  $\delta$  (ppm), mixture of rotamers: 8.54-8.48 (m, 2H), 7.21-7.03 (m, 4H), 6.90-6.85 (m, 2H), 4.59 (s, 0.7H), 4.32 (s, 1.3H), 3.80 (s, 3H), 3.76-3.75 (m, 3H), 3.58 (t,  $J = 7.2$  Hz, 1.3H), 3.49 (s, 1.3H), 3.44 (t,  $J = 7.3$  Hz, 0.7H), 3.37 (s, 0.7H), 2.88-2.77 (m, 2H)  $^{13}\text{C}$  NMR (75 MHz,  $\text{CDCl}_3$ , mixture of rotamers),  $\delta$  (ppm): 168.1, 166.6, 166.1, 159.6, 150.4, 150.1, 148.2, 129.6, 128.9, 127.9, 127.7, 124.4, 124.1, 114.7, 114.4, 55.5, 52.7, 52.3, 48.1, 47.6, 41.4, 41.1, 34.4, 33.3. IR (film): 1739, 1641  $\text{cm}^{-1}$ . HRMS (ESI): calculated for  $\text{C}_{19}\text{H}_{23}\text{N}_2\text{O}_4$   $[\text{M} + \text{H}]^+$ , 343.1658; found 343.1652.

### $\beta$ -amido ester 6.5

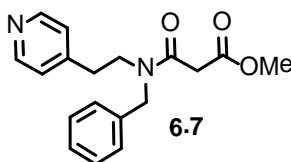


6.5

Brown liquid, 58%,  $^1\text{H}$  NMR (300 MHz,  $\text{CDCl}_3$ ),  $\delta$  (ppm), mixture of rotamers: 8.50- 8.46 (m, 2H), 7.37-7.34, (m, 5H), 7.18-7.00 (m, 4H), 6.87-6.80 (m, 2H), 5.19 (s, 2H), 4.57 (s, 0.7H), 4.28 (s, 1.3H), 3.79 (s, 3H), 3.58-3.52.(m, 2.6H), 3.43-3.36 (m, 1.4H), 2.84-2.71 (m, 2H)  $^{13}\text{C}$  NMR (75 MHz,  $\text{CDCl}_3$ , mixture of rotamers),  $\delta$  (ppm): 167.6, 166.5, 159.6, 150.4, 150.1, 148.2, 135.5, 129.6, 128.8, 128.6, 128.0, 127.4, 124.4, 124.1, 114.7, 114.3, 67.5, 55.5, 52.4, 48.1, 47.5, 41.6, 41.3, 34.4, 33.3. IR (film): 1735, 1642  $\text{cm}^{-1}$ . HRMS (ESI): calculated for  $\text{C}_{25}\text{H}_{27}\text{N}_2\text{O}_4$   $[\text{M} + \text{H}]^+$ , 419.1971; found 419.1978.

**$\beta$ -amido ester 6.6**

Yellow liquid, 96%,  $^1\text{H}$  NMR (300 MHz,  $\text{CDCl}_3$ ),  $\delta$  (ppm), mixture of rotamers: 14.80-14.73 (m, 0.3H), 8.54- 8.49 (m, 2H), 7.27-7.03 (m, 4H), 6.90-6.86 (m, 2H), 5.14-5.07 (m, 0.3H), 4.58-4.48 (m, 0.7H), 4.31 (s, 1.3H), 3.80-3.79 (m, 3H), 3.61-3.57 (m, 2.2H), 3.44-3.40 (m, 1.2H), 2.87-2.76 (m, 2H), 2.26-2.25 (s, 2.1H), 1.98-1.94 (m, 0.9H).  $^{13}\text{C}$  NMR (75MHz,  $\text{CDCl}_3$ , mixture of rotamers),  $\delta$  (ppm): 202.4, 167.3, 159.6, 159.4, 150.4, 150.0, 129.6, 128.9, 127.9, 124.5, 124.2, 114.7, 114.4, 55.5, 52.2, 50.2, 50.1, 48.1, 48.0, 47.3, 34.4, 33.4, 30.6. IR (film): 1717, 1633  $\text{cm}^{-1}$ . HRMS (ESI): calculated for  $\text{C}_{19}\text{H}_{22}\text{N}_2\text{O}_3$   $[\text{M} + \text{H}]^+$ , 327.1709; found 327.1709.

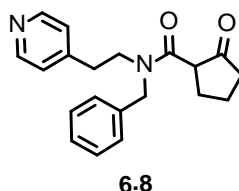
 **$\beta$ -amido ester 6.7**

Pale brown liquid, 51%,  $^1\text{H}$  NMR (300 MHz,  $\text{CDCl}_3$ ),  $\delta$  (ppm), mixture of rotamers: 8.54- 8.49 (m, 2H), 7.37-7.28, (m, 4H), 7.15-7.03 (m, 3H), 4.65 (s, 0.6H), 4.40 (s, 1.4H), 3.76-3.74.(m, 3H), 3.61 (t,  $J = 7.5$  Hz, 1.4H), 3.49-3.44 (m, 2H), 3.40 (s, 0.6H), 2.91-2.79 (m, 2H)  $^{13}\text{C}$  NMR (75 MHz,  $\text{CDCl}_3$ , mixture of

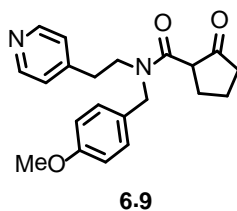


rotamers),  $\delta$  (ppm): 168.1, 166.7, 150.4, 150.1, 148.1, 146.9, 136.8, 135.9, 129.3, 129.0, 128.2, 127.9, 126.5, 124.4, 124.1, 52.8, 52.7, 48.7, 48.4, 47.8, 41.4, 41.0, 34.4, 33.3. IR (film): 1739, 1646  $\text{cm}^{-1}$ . HRMS (ESI): calculated for  $\text{C}_{18}\text{H}_{21}\text{N}_2\text{O}_3$   $[\text{M} + \text{H}]^+$ , 313.1552; found 313.1563.

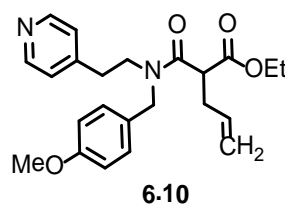
### $\beta$ -amido ester 6.8



Pale brown liquid, 56%,  $^1\text{H}$  NMR (300 MHz,  $\text{CDCl}_3$ ),  $\delta$  (ppm), mixture of rotamers: 8.53-8.49 (m, 2H), 7.38-7.23, (m, 4H), 7.14-7.04 (m, 3H), 4.94-4.88 (m, 1H), 4.44-4.26 (m, 1H), 4.02-3.93 (m, 0.7H), 3.84-3.76.(m, 0.3H), 3.56-3.46 (m, 0.3H), 3.38 (t,  $J = 8.7$  Hz, 0.7H), 3.28-3.18 (m, 1H), 2.89-2.83 (m, 2H), 2.55-2.46 (m, 1H), 2.35-2.29 (m,2H), 2.20-1.95(m, 2H), 1.83-1.78 (m, 1H).  $^{13}\text{C}$  NMR (75 MHz,  $\text{CDCl}_3$ , mixture of rotamers),  $\delta$  (ppm): 214.7, 169.6, 169.3, 150.3, 150.0, 148.2, 147.4, 137.1, 136.7, 129.2, 128.9, 128.0, 127.8, 127.6, 126.4, 124.5, 124.3, 52.3, 52.1, 52.0, 48.9, 48.2, 47.9, 38.8, 34.7, 33.6, 27.6, 21.3, 21.2. IR (film): 1735, 1637  $\text{cm}^{-1}$ . HRMS (ESI): calculated for  $\text{C}_{20}\text{H}_{23}\text{N}_2\text{O}_2$   $[\text{M} + \text{H}]^+$ , 323.1760; found 323.1767.

**$\beta$ -amido ester 6.9**

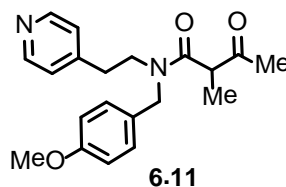
Pale brown liquid, 47%,  $^1\text{H}$  NMR (300 MHz,  $\text{CDCl}_3$ ),  $\delta$  (ppm), mixture of rotamers: 8.54- 8.49 (m, 2H), 7.19-7.05 (m, 4H), 6.90-6.86 (m, 2H), 4.85-4.77 (m, 1H), 4.39-4.21 (m, 1H), 3.97-3.88 (m, 0.7H), 3.80-3.72 (m, 3.3H), 3.54-3.38 (m, 1H), 3.28-3.16 (m, 1H), 2.87-2.82 (m, 2H), 2.53-2.45 (m, 1H), 2.36-2.29 (m, 2H), 2.19-2.14 (m, 2H), 1.98-1.78 (m, 1H).  $^{13}\text{C}$  NMR (75 MHz,  $\text{CDCl}_3$ , mixture of rotamers),  $\delta$  (ppm): 214.8, 169.5, 169.2, 159.4, 159.1, 150.3, 149.9, 148.4, 147.5, 129.2, 129.1, 128.4, 127.7, 124.5, 124.3, 114.5, 114.3, 55.5, 52.3, 52.0, 51.6, 48.2, 47.9, 47.6, 38.8, 34.6, 33.5, 27.7, 21.3, 21.2. IR (film): 1735, 1633  $\text{cm}^{-1}$ . HRMS (ESI): calculated for  $\text{C}_{21}\text{H}_{25}\text{N}_2\text{O}_3$   $[\text{M} + \text{H}]^+$ , 353.1865; found 353.1874.

 **$\beta$ -amido ester 6.10**

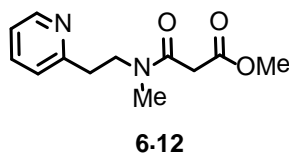
Brown liquid, 41%,  $^1\text{H}$  NMR (300 MHz,  $\text{CDCl}_3$ ),  $\delta$  (ppm), mixture of rotamers: 8.54-8.48 (m, 2H), 7.17-7.05 (m, 4H), 6.89-6.83 (m, 2H), 5.79-5.65 (m, 1H), 5.15-5.02 (m, 2H), 4.73-4.68 (m, 0.4H), 4.56-4.50 (m, 0.6H), 4.42-4.29 (m,

1H), 4.21-4.14 (m, 2H), 3.80-3.79 (m, 3H), 3.70-3.43 (m, 3H), 2.84 (t,  $J = 7.2$  Hz, 2H), 2.69 (t,  $J = 7.0$  Hz, 2H), 1.28-1.22 (m, 3H).  $^{13}\text{C}$  NMR (75 MHz,  $\text{CDCl}_3$ , mixture of rotamers),  $\delta$  (ppm): 169.5, 169.4, 168.8, 168.5, 159.6, 159.3, 150.4, 150.1, 148.2, 147.2, 147.1, 134.84, 134.8, 129.6, 129.3, 128.1, 124.4, 124.2, 117.9, 117.8, 114.5, 114.2, 61.8, 61.7, 55.53, 55.5, 51.7, 49.2, 48.5, 47.7, 47.6, 34.8, 33.7, 33.2, 14.3. IR (film): 1735, 1642  $\text{cm}^{-1}$ . HRMS (ESI): calculated for  $\text{C}_{23}\text{H}_{29}\text{N}_2\text{O}_4$   $[\text{M} + \text{H}]^+$ , 397.2127; found 397.2125.

### $\beta$ -amido ester 6.11



Brown liquid, 87%,  $^1\text{H}$  NMR (300 MHz,  $\text{CDCl}_3$ ),  $\delta$  (ppm), mixture of rotamers: 8.55- 8.48 (m, 2H), 7.19-7.04 (m, 4H), 6.91-6.85 (m, 2H), 4.73-4.68 (m, 0.3H), 4.52-4.44 (m, 1H), 4.31-4.26 (m, 0.7H), 3.80-3.78 (m, 3H), 3.76-3.71.(m, 0.6H), 3.63 (q,  $J = 6.9$  Hz, 0.7H), 3.57-3.44 (m, 1.7H), 2.87-2.77.(m, 2H), 2.12-2.11 (m, 3H), 1.37 (d,  $J = 7.0$  Hz, 2H), 1.32 (d,  $J = 6.9$  Hz, 1H).  $^{13}\text{C}$  NMR (75 MHz,  $\text{CDCl}_3$ , mixture of rotamers),  $\delta$  (ppm): 205.1, 171.0, 170.4, 159.6, 150.4, 150.1, 148.0, 146.9, 129.6, 129.3, 128.2, 127.8, 124.4, 124.2, 114.7, 114.4, 55.5, 52.1, 51.9, 51.6, 48.2, 47.5, 34.5, 33.4, 27.4, 27.0, 14.2. IR (film): 1726, 1633  $\text{cm}^{-1}$ . HRMS (ESI): calculated for  $\text{C}_{20}\text{H}_{25}\text{N}_2\text{O}_3$   $[\text{M} + \text{H}]^+$ , 341.1865; found 341.1858.

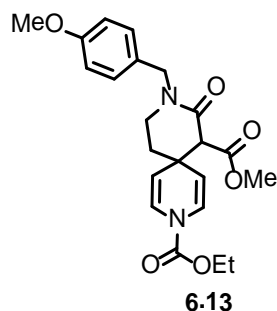
**$\beta$ -amido ester 6.12**

Yellow gummy liquid, 63%,  $^1\text{H}$  NMR (300 MHz,  $\text{CDCl}_3$ ),  $\delta$  (ppm), mixture of rotamers: 8.57- 8.52 (m, 1H), 7.66-7.59 (m, 1H), 7.24-7.13 (m, 2H), 3.80-3.72 (m, 5H), 3.44 (s, 1H), 3.34 (s, 1H), 3.08-3.03 (m, 2H), 2.97 (s, 1.5H), 1.98 (s, 1.5H).  $^{13}\text{C}$  NMR (75 MHz,  $\text{CDCl}_3$ , mixture of rotamers),  $\delta$  (ppm): 168.4, 168.2, 166.2, 166.1, 159.1, 157.9, 149.9, 149.5, 136.9, 136.7, 123.8, 122.1, 121.7, 52.6, 50.2, 48.7, 41.6, 40.7, 36.8, 36.0, 33.5. IR (film): 1731, 1625  $\text{cm}^{-1}$ . HRMS (ESI): calculated for  $\text{C}_{12}\text{H}_{17}\text{N}_2\text{O}_3$   $[\text{M} + \text{H}]^+$ , 237.1239; found 237.1235.

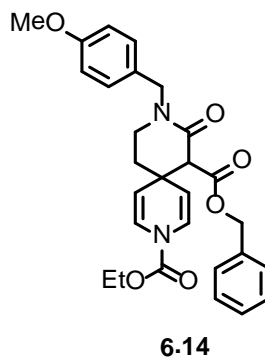
**Procedure and characterization of 3,9-diazaspiro[5.5]undecanes**

General procedure for spirocyclization: The preparation of **6.13** is representative. The reaction mixture of 4-alkylpyridine compound **6.4** (0.10 g, 0.30 mmol, 1 equiv) in dichloromethane (3 mL) was cooled to 0 °C. Titanium isopropoxide (44  $\mu\text{L}$ , 0.14 mmol, 0.5 equiv) was added to the reaction mixture and stirred for 2 min. Ethyl chloroformate (42  $\mu\text{L}$ , 0.44 mmol, 1.5 equiv) was then added to the reaction mixture. The resulting mixture was stirred for 5-7 min and then directly loaded on to the silica gel column and purified using 70-80% ethyl acetate in hexanes to give **6.13**, yellow gummy liquid as the desired product (85 mg, 70%).

The above procedure was used to synthesize all other spirocycles from 0.10 g of their corresponding starting materials.

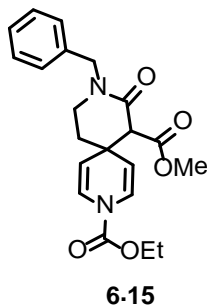
**Spirocycle 6.13**

$^1\text{H}$  NMR (300 MHz,  $\text{CDCl}_3$ ),  $\delta$  (ppm): 7.29 (d,  $J = 8.7$  Hz, 2H), 6.88-6.85 (m, 4H), 4.76-4.51 (m, 4H), 4.25 (q,  $J = 7.1$  Hz, 2H), 3.80 (s, 3H), 3.73 (s, 3H), 3.41 (s, 1H), 3.35-3.16 (m, 2H), 2.13-2.04 (m, 1H), 1.74-1.65 (m, 1H), 1.30 (t,  $J = 7.1$  Hz, 3H).  $^{13}\text{C}$  NMR (75 MHz,  $\text{CDCl}_3$ ),  $\delta$  (ppm): 169.2, 164.5, 159.2, 151.2, 129.6, 128.8, 123.4, 123.2, 114.2, 109.6, 109.3, 107.8, 107.2, 63.0, 61.0, 55.4, 55.2, 49.8, 41.4, 36.9, 35.2, 14.5. IR (film): 1722, 1686, 1637  $\text{cm}^{-1}$ . HRMS (ESI): calculated for  $\text{C}_{22}\text{H}_{27}\text{N}_2\text{O}_6$   $[\text{M} + \text{H}]^+$ , 415.1869; found 415.1862.

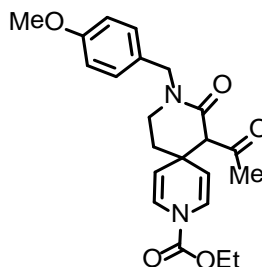
**Spirocycle 6.14**

Pale yellow gummy liquid, 69%,  $^1\text{H}$  NMR (300 MHz,  $\text{CDCl}_3$ ),  $\delta$  (ppm): 7.37-7.30 (m, 5H), 7.20 (d,  $J = 8.6$  Hz, 2H), 6.88-6.71 (m, 4H), 5.24-5.12 (m, 2H), 4.75-4.67 (m, 3H), 4.48-4.43 (m, 1H), 4.24 (q,  $J = 7.1$  Hz, 2H), 3.79 (s, 3H), 3.44 (s, 1H), 3.34-3.26 (m, 1H), 3.21-3.13 (m, 1H), 2.04-1.99 (m, 1H), 1.72-1.63 (m, 1H), 1.31 (t,  $J = 7.2$  Hz, 3H).  $^{13}\text{C}$  NMR (75 MHz,  $\text{CDCl}_3$ ),  $\delta$  (ppm): 168.6, 164.5, 159.1, 151.1, 135.7, 129.6, 128.8, 128.6, 128.5, 128.3, 123.3, 114.1, 109.8, 109.3, 107.5, 106.9, 67.1, 63.0, 61.0, 55.4, 49.7, 37.1, 35.6, 14.5. IR (film): 1721, 1686, 1646  $\text{cm}^{-1}$ . HRMS (ESI): calculated for  $\text{C}_{28}\text{H}_{30}\text{N}_2\text{O}_6\text{Na}$   $[\text{M} + \text{Na}]^+$ , 513.2002; found 513.2015.

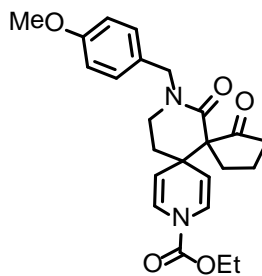
### Spirocycle 6.15



Yellow liquid, 72%,  $^1\text{H}$  NMR (300 MHz,  $\text{CDCl}_3$ ),  $\delta$  (ppm): 7.37-7.26 (m, 5H), 6.94-6.83 (m, 2H), 4.84-4.66 (m, 4H), 4.25 (q,  $J = 7.1$  Hz, 2H), 3.74 (s, 3H), 3.44 (s, 1H), 3.37-3.18 (m, 2H), 2.12-2.00 (m, 1H), 1.76-1.67 (m, 1H), 1.31 (t,  $J = 7.1$  Hz, 3H).  $^{13}\text{C}$  NMR (75 MHz,  $\text{CDCl}_3$ ),  $\delta$  (ppm): 169.2, 164.6, 151.1, 136.7, 128.8, 128.1, 127.7, 123.3, 109.6, 109.1, 107.7, 107.1, 63.0, 60.9, 52.3, 50.3, 41.6, 36.9, 35.1, 14.5. IR (film): 1722, 1686, 1646  $\text{cm}^{-1}$ . HRMS (ESI): calculated for  $\text{C}_{21}\text{H}_{24}\text{N}_2\text{O}_5\text{Na}$   $[\text{M} + \text{Na}]^+$ , 407.1583; found 407.1593.

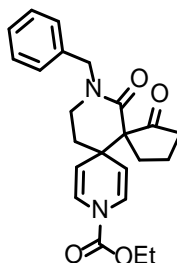
**Spirocycle 6.16****6.16**

Pale yellow liquid, 18%,  $^1\text{H}$  NMR (300 MHz,  $\text{CDCl}_3$ ),  $\delta$  (ppm), mixture of tautomers: 16.0 (s, 0.2H), 7.27-7.18 (m, 2H), 6.95-6.82 (m, 4H), 4.77-4.49 (m, 4H), 4.30-4.22 (m, 2H), 3.81-3.80 (m, 3H), 3.59 (s, 0.8H), 3.32-3.12 (m, 2H), 2.31 (s, 2.4H), 2.26-2.17 (m, 1H), 2.00 (s, 0.6H), 1.77-1.62 (m, 1H), 1.35-1.29 (m, 3H).  $^{13}\text{C}$  NMR (75 MHz,  $\text{CDCl}_3$ ),  $\delta$  (ppm), mixture of tautomers: 205.5, 176.7, 165.3, 159.3, 151.3, 129.6, 129.4, 129.2, 128.9, 123.9, 123.1, 120.9, 114.3, 109.6, 107.9, 67.1, 63.2, 55.5, 49.8, 41.7, 41.1, 40.4, 37.0, 35.4, 34.7, 33.8, 21.5, 14.6. IR (film): 1722, 1686, 1628  $\text{cm}^{-1}$ . HRMS (ESI): calculated for  $\text{C}_{22}\text{H}_{27}\text{N}_2\text{O}_5$  [ $\text{M} + \text{H}$ ] $^+$ , 399.1920; found 399.1934.

**Spirocycle 6.17****6.17**

Yellow gummy liquid, 72%,  $^1\text{H}$  NMR (300 MHz,  $\text{CDCl}_3$ ),  $\delta$  (ppm): 7.17 (d,  $J$  = 8.6 Hz, 2H), 6.96-6.83 (m, 4H), 4.64-4.43 (m, 4H), 4.26 (q,  $J$  = 7.1 Hz, 2H), 3.80 (s, 3H), 3.37 (td,  $J$  = 12.5, 5.2 Hz, 1H), 3.19 (dd,  $J$  = 12.8, 5.6 Hz, 1H), 2.81 (td,  $J$  = 12.9, 6.7 Hz, 1H), 2.57-2.43 (m, 2H), 2.25-2.13 (m, 3H), 2.01-1.94 (m, 1H), 1.62 (dd,  $J$  = 13.6, 4.0 Hz, 1H), 1.32 (t,  $J$  = 7.2 Hz, 3H).  $^{13}\text{C}$  NMR (75 MHz,  $\text{CDCl}_3$ ),  $\delta$  (ppm): 217.3, 168.3, 159.0, 151.2, 129.1, 129.0, 124.0, 114.1, 109.4, 108.8, 107.2, 106.7, 63.9, 63.1, 55.3, 50.1, 41.6, 41.2, 41.1, 33.4, 31.6, 20.8, 14.5. IR (film): 1726, 1686, 1624  $\text{cm}^{-1}$ . HRMS (ESI): calculated for  $\text{C}_{24}\text{H}_{28}\text{N}_2\text{O}_5\text{Na}$   $[\text{M} + \text{Na}]^+$ , 447.1896; found 447.1909.

### Spirocycle 6.18



6.18

Yellow gummy liquid, 56%,  $^1\text{H}$  NMR (300 MHz,  $\text{CDCl}_3$ ),  $\delta$  (ppm): 7.36-7.22 (m, 5H), 6.97-6.83 (m, 2H), 4.80-4.46 (m, 4H), 4.27 (q,  $J$  = 7.1 Hz, 2H), 3.39 (td,  $J$  = 12.5, 5.1 Hz, 1H), 3.20 (dd,  $J$  = 12.7, 5.6 Hz, 1H), 2.84 (td,  $J$  = 13.2, 6.7 Hz, 1H), 2.58-2.43 (m, 2H), 2.31-2.13 (m, 3H), 2.01-1.96 (m, 1H), 1.63 (dd,  $J$  = 13.5, 4.0 Hz, 1H), 1.33 (t,  $J$  = 7.2 Hz, 3H).  $^{13}\text{C}$  NMR (75 MHz,  $\text{CDCl}_3$ ),  $\delta$  (ppm): 217.2, 168.4, 151.2, 137.0, 128.8, 127.7, 127.5, 124.3, 124.0, 109.4, 108.9, 107.2, 106.7, 63.9, 63.1, 50.7, 41.9, 41.2, 41.1, 33.4, 31.6, 20.9, 14.5. IR (film): 1735,

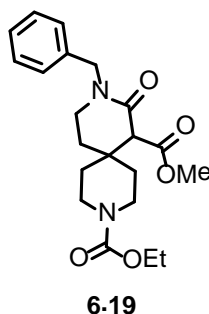


1682, 1624  $\text{cm}^{-1}$ . HRMS (ESI): calculated for  $\text{C}_{23}\text{H}_{26}\text{N}_2\text{O}_4\text{Na}$   $[\text{M} + \text{Na}]^+$ , 417.1790; found 417.1810.

### Experimental procedure for hydrogenation of spirocycle 6.15

Spirocycle **6.15** (0.10 g, 0.26 mmol) was taken in methanol (5 mL) and 10% palladium on carbon (10 mg) was added. The reaction mixture was then hydrogenated at 100 psi for 14 h and then filtered through Celite bed. The filtrate was evaporated in vacuo and dried to give **6.19**, as a colorless liquid (95 mg, 94%).

### Spirocycle 6.19

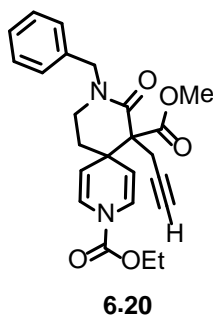


Colorless liquid, 94%,  $^1\text{H}$  NMR (300 MHz,  $\text{CDCl}_3$ ),  $\delta$  (ppm): 7.34-7.26 (m, 5H), 4.85-4.80 (m, 1H), 4.48-4.43 (m, 1H), 4.12 (q,  $J = 7.1$  Hz, 2H), 3.76 (s, 3H), 3.54-3.44 (m, 5H), 3.27-3.22 (m, 2H), 2.30-2.19 (m, 1H), 1.61-1.49 (m, 4H), 1.36-1.31 (m, 1H), 1.25 (t,  $J = 7.1$  Hz, 3H).  $^{13}\text{C}$  NMR (75 MHz,  $\text{CDCl}_3$ ),  $\delta$  (ppm): 170.1, 165.1, 155.5, 136.5, 128.8, 127.9, 127.6, 61.4, 56.9, 52.4, 50.1, 42.8, 39.2, 34.4, 34.3, 33.3, 27.4, 14.7. IR (film): 1734, 1685, 1637  $\text{cm}^{-1}$ . HRMS (ESI): calculated for  $\text{C}_{21}\text{H}_{29}\text{N}_2\text{O}_5$   $[\text{M} + \text{H}]^+$ , 389.2076; found 389.2097.

## Experimental procedure and characterization for alkylation of spirocycle 6.15

Spirocycle **6.15** (0.30 g, 0.78 mmol, 1 equiv) was taken in dry THF (20 mL) and cooled to 0 °C. NaH (50% suspension, 50 mg, 1.01 mmol, 1.3 equiv) was added and the reaction was stirred for 30 min. Propargyl bromide (80% solution in toluene, 0.11 mL, 1.01 mmol, 1.3 equiv) was then added to the reaction mixture and slowly warmed to room temperature and stirred for 16 h. The reaction was quenched with water and extracted with ethyl acetate (3 x 25 mL). The combined organics were dried over sodium sulfate, filtered and evaporated *in vacuo*. Crude product was purified by silica gel column chromatography using 50-70% ethyl acetate in hexanes to obtain **6.20**, as a pale yellow liquid (0.21 g, 64%).

### Spirocycle 6.20

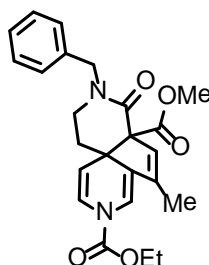


Pale yellow liquid, 64%,  $^1\text{H}$  NMR (300 MHz,  $\text{CDCl}_3$ ),  $\delta$  (ppm): 7.36-7.27 (m, 5H), 6.99-6.88 (m, 2H), 4.91-4.59 (m, 4H), 4.27 (q,  $J = 7.1$  Hz, 2H), 3.83 (s, 0.4H), 3.77 (s, 2.6H), 3.31-3.23 (m, 2H), 2.97-2.75 (m, 2H), 2.05 (t,  $J = 2.6$  Hz, 1H), 2.02-1.97 (m, 2H), 1.33 (t,  $J = 7.0$  Hz, 3H).  $^{13}\text{C}$  NMR (75 MHz,  $\text{CDCl}_3$ ),  $\delta$  (ppm): 170.5, 167.2, 151.2, 137.0, 128.8, 128.5, 127.7, 125.1, 124.8, 123.6,

108.7, 108.3, 106.3, 82.3, 70.7, 63.2, 62.5, 52.7, 50.8, 41.3, 40.6, 34.4, 34.3, 24.0, 14.6. IR (film): 1726, 1690, 1650  $\text{cm}^{-1}$ . HRMS (ESI): calculated for  $\text{C}_{24}\text{H}_{26}\text{N}_2\text{O}_5\text{Na}$   $[\text{M} + \text{Na}]^+$ , 445.1739; found 445.1737.

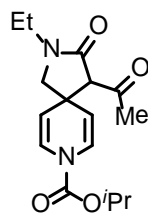
### Procedure for Au(III)-catalyzed cycloisomerization

The spirocycle **6.20** (50 mg, 0.12 mmol, 1 equiv) was taken in dry toluene (3 mL) and 5 mol%  $\text{AuCl}_3$  and 5 mol%  $\text{AgOTf}$  were added. The reaction mixture was heated at 100  $^\circ\text{C}$  for 2 h and then cooled to room temperature and evaporated *in vacuo*. The crude product was purified on silica gel column chromatography using 70% ethyl acetate in hexanes to get **6.21**, as a yellow liquid (33 mg, 66%).

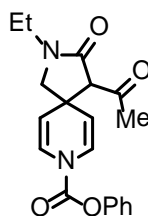


**6-21**

$^1\text{H}$  NMR (300 MHz,  $\text{CDCl}_3$ ),  $\delta$  (ppm): 7.38-7.27 (m, 5H), 6.98-6.76 (m, 2H), 5.79 (s, 1H), 5.37-5.30 (m, 1H), 4.83 (d,  $J = 14.8$  Hz, 1H), 4.54 (d,  $J = 14.8$  Hz, 1H), 4.30 (q,  $J = 7.0$  Hz, 2H), 3.86-3.69 (m, 3H), 3.53-3.45 (m, 1H), 2.93 (dt,  $J = 12.8, 3.6$  Hz, 1H), 1.96 (s, 3H), 1.78 (td,  $J = 12.9, 4.0$  Hz, 1H), 1.54 (td,  $J = 13.3, 2.7$  Hz, 1H), 1.35 (br s, 3H).  $^{13}\text{C}$  NMR (75 MHz,  $\text{CDCl}_3$ ),  $\delta$  (ppm): 171.1, 168.4, 152.1, 139.6, 136.9, 131.7, 128.9, 128.1, 127.7, 125.1, 113.8, 107.2, 69.3, 63.3, 52.6, 50.9, 47.0, 42.3, 37.6, 14.7, 12.9. IR (film): 1721, 1677, 1637  $\text{cm}^{-1}$ . HRMS (ESI): calculated for  $\text{C}_{24}\text{H}_{27}\text{N}_2\text{O}_5$   $[\text{M} + \text{H}]^+$ , 423.1920; found 423.1940.

**Spirocycle 6.23a****6.23a**

Yellow liquid, 36%,  $^1\text{H}$  NMR (300 MHz,  $\text{CDCl}_3$ ),  $\delta$  (ppm), mixture of rotamers: 12.31 (s, 0.3H), 6.97-6.87 (m, 2H), 5.09-5.01 (m, 1H), 4.93-4.82 (m, 2H), 3.48-3.14 (m, 4.7H), 2.26 (s, 2H), 1.84 (s, 1H), 1.34-1.28 (m, 6H), 1.13 (t,  $J = 7.3$  Hz, 3H).  $^{13}\text{C}$  NMR (75 MHz,  $\text{CDCl}_3$ , mixture of rotamers),  $\delta$  (ppm): 203.9, 171.4, 168.8, 167.3, 150.9, 150.6, 124.6, 122.8, 121.5, 110.2, 105.5, 71.5, 71.3, 71.1, 69.8, 63.4, 61.1, 39.7, 37.4, 36.6, 33.3, 22.1, 22.0, 17.5, 12.6, 12.4. HRMS (ESI): calculated for  $\text{C}_{16}\text{H}_{23}\text{N}_2\text{O}_4$   $[\text{M} + \text{H}]^+$ , 307.1658; found 307.1675.

**Spirocycle 6.23b****6.23b**

Yellow liquid, 56%,  $^1\text{H}$  NMR (300 MHz,  $\text{CDCl}_3$ ),  $\delta$  (ppm), mixture of rotamers: 12.4 (s, 0.3H), 7.43-7.37 (m, 2H), 7.29-7.24 (m, 1H), 7.18-7.05 (m, 4H), 5.07-4.92 (m, 2H), 3.53-3.18 (m, 4.7H), 2.29 (s, 2H), 1.89 (s, 1H), 1.14 (t,  $J$

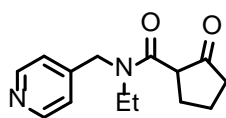
= 7.3 Hz, 3H).  $^{13}\text{C}$  NMR (75 MHz,  $\text{CDCl}_3$ , mixture of rotamers),  $\delta$  (ppm): 203.7, 171.3, 168.7, 167.4, 150.6, 150.5, 149.9, 149.7, 129.7, 126.4, 126.3, 124.7, 124.3, 122.8, 122.5, 121.5, 121.2, 111.8, 111.2, 110.8, 109.8, 107.3, 106.8, 69.5, 63.0, 60.7, 39.6, 37.4, 36.6, 33.2, 17.6, 12.6, 12.5. HRMS (ESI): calculated for  $\text{C}_{19}\text{H}_{21}\text{N}_2\text{O}_4$   $[\text{M} + \text{H}]^+$ , 341.1501; found 341.1518.

### Procedures and characterization of 4-alkylpyridine substrates

General procedure: A reaction mixture containing secondary amine derived from 4-(aminomethyl) pyridine (2.00 g, 14.67 mmol, 1 equiv) and ethyl-2-cyclopentanone carboxylate (2.98 g, 19.07 mmol, 1.3 equiv) in toluene (100 mL) was refluxed for 36 h. The reaction mixture was cooled to room temperature and concentrated *in vacuo*. The crude product was purified by silica gel column chromatography using 70-100% ethyl acetate in hexanes to afford the desired  $\beta$ -keto amide substrate **6.24** (3.30 g, 91%).

$\beta$ -keto amide substrates **6.24-6.34**, and **6.39**, were prepared using the above procedure using secondary amines and corresponding  $\beta$ -keto ester starting materials (1.00 g-2.00 g scale).

#### $\beta$ -keto amide **6.24**

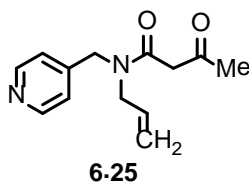


**6.24**

Brown liquid, 91%,  $^1\text{H}$  NMR (300 MHz,  $\text{CDCl}_3$ ),  $\delta$  (ppm), mixture of rotamers: 8.64- 8.52 (m, 2H), 7.19-7.14 (m, 2H), 5.05-4.95 (m, 1H), 4.47 (d,  $J$  = 18.4 Hz, 0.3H), 4.26 (d,  $J$  = 16.1 Hz, 0.7H), 3.81-3.67 (m, 1H), 3.57-3.51 (m, 0.7H), 3.31-3.11 (m, 1.3H), 2.62-2.49 (m, 1H), 2.39-2.04 (m, 4H), 1.96-1.83 (m,

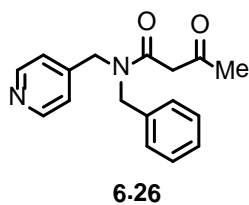
1H), 1.22-1.11 (m, 3H).  $^{13}\text{C}$  NMR (75 MHz,  $\text{CDCl}_3$ , mixture of rotamers),  $\delta$  (ppm): 214.7, 169.3, 150.5, 150.1, 146.9, 122.3, 121.5, 52.3, 52.0, 49.9, 47.9, 42.9, 42.1, 38.7, 27.7, 21.3, 14.3, 12.8. IR (film): 1735, 1628  $\text{cm}^{-1}$ . HRMS (ESI): calculated for  $\text{C}_{14}\text{H}_{19}\text{N}_2\text{O}_2$   $[\text{M} + \text{H}]^+$ , 247.1447; found 237.1462.

### $\beta$ -keto amide 6.25



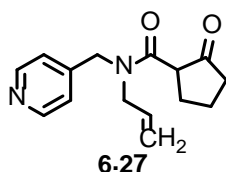
Brown liquid, 56%,  $^1\text{H}$  NMR (300 MHz,  $\text{CDCl}_3$ ),  $\delta$  (ppm), mixture of rotamers: 14.58-14.50 (m, 0.25H), 8.62- 8.55 (m, 2H), 7.23-7.11 (m, 2H), 5.82-5.70 (m, 1H), 5.29-5.15 (m, 2H), 4.61 (s, 1.4H), 4.51-4.47 (m, 0.6H), 4.04-4.02 (m, 0.5H), 3.85-3.82 (m, 1.5H), 3.65 (s, 1H), 3.52 (s, 0.4H), 2.31-2.28 (m, 2.2H), 1.98-1.90 (m, 0.8H).  $^{13}\text{C}$  NMR (75 MHz,  $\text{CDCl}_3$ , mixture of rotamers),  $\delta$  (ppm): 202.4, 167.6, 150.6, 150.2, 146.2, 132.2, 132.0, 122.6, 121.5, 118.5, 117.8, 86.9, 50.7, 50.0, 49.8, 48.6, 47.9, 30.7, 22.2. HRMS (ESI): calculated for  $\text{C}_{13}\text{H}_{17}\text{N}_2\text{O}_2$   $[\text{M} + \text{H}]^+$ , 233.1290; found 233.1308.

### $\beta$ -keto amide 6.26

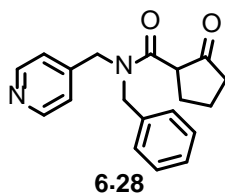


Brown liquid, 71%,  $^1\text{H}$  NMR (300 MHz,  $\text{CDCl}_3$ ),  $\delta$  (ppm), mixture of rotamers: 14.69-14.57 (m, 0.3H), 8.61- 8.53 (m, 2H), 7.41-7.07 (m, 7H), 5.29 (s, 0.2H), 5.03 (s, 0.1H), 4.64-4.60 (m, 2H), 4.44-4.41 (m, 2H), 3.71 (s, 0.9H), 3.58 (s, 0.5H), 2.30 (s, 2H), 1.96-1.92 (m, 1H).  $^{13}\text{C}$  NMR (75 MHz,  $\text{CDCl}_3$ , mixture of rotamers),  $\delta$  (ppm): 202.3, 167.8, 167.4, 150.6, 150.3, 145.9, 145.5, 135.6, 129.4, 129.2, 129.0, 128.3, 128.0, 126.8, 126.6, 122.7, 121.5, 86.8, 51.5, 50.6, 50.0, 49.9, 48.9, 47.9, 30.7, 22.3. HRMS (ESI): calculated for  $\text{C}_{17}\text{H}_{19}\text{N}_2\text{O}_2$  [ $\text{M} + \text{H}$ ] $^+$ , 283.1447; found 283.1462.

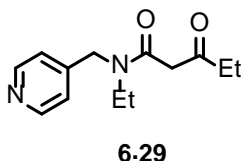
### $\beta$ -keto amide 6.27



Brown liquid, 63%,  $^1\text{H}$  NMR (300 MHz,  $\text{CDCl}_3$ ),  $\delta$  (ppm), mixture of rotamers: 8.61- 8.54 (m, 2H), 7.19-7.12 (m, 2H), 5.88-5.70 (m, 1H), 5.27-4.99 (m, 3H), 4.49-4.37 (m, 1.3H), 4.14-4.09 (m, 0.7H), 3.80-3.72 (m, 0.7H), 3.66-3.59 (m, 0.3H), 3.52-3.46 (m, 0.7H), 3.31-3.25 (m, 0.3H), 2.63-2.38 (m, 1H), 2.36-2.14 (m, 4H), 1.96-1.80 (m, 1H).  $^{13}\text{C}$  NMR (75 MHz,  $\text{CDCl}_3$ , mixture of rotamers),  $\delta$  (ppm): 214.8, 169.6, 150.6, 150.2, 146.4, 132.8, 132.2, 122.3, 121.4, 117.9, 117.1, 52.3, 50.0, 49.5, 48.9, 48.3, 38.7, 27.5, 21.2. IR (film): 1735, 1641  $\text{cm}^{-1}$ . HRMS (ESI): calculated for  $\text{C}_{15}\text{H}_{19}\text{N}_2\text{O}_2$  [ $\text{M} + \text{H}$ ] $^+$ , 259.1447; found 259.1461.

**$\beta$ -keto amide 6.28**

Brown liquid, 76%,  $^1\text{H}$  NMR (300 MHz,  $\text{CDCl}_3$ ),  $\delta$  (ppm), mixture of rotamers: 8.60- 8.54 (m, 2H), 7.41-7.08 (m, 7H), 5.26-4.94 (m, 2H), 4.42-4.33 (m, 1H), 4.18-4.01 (m, 1H), 3.56-3.51 (m, 0.7H), 3.36-3.31 (m, 0.3H), 2.66-2.54 (m, 1H), 2.39-2.33 (m, 2H), 2.26-2.15 (m, 2H), 1.92-1.79 (m, 1H).  $^{13}\text{C}$  NMR (75 MHz,  $\text{CDCl}_3$ , mixture of rotamers),  $\delta$  (ppm): 214.8, 169.9, 150.6, 150.3, 146.2, 136.5, 136.2, 129.3, 129.0, 128.1, 128.0, 126.4, 122.4, 121.4, 52.4, 51.0, 49.5, 48.4, 38.8, 27.5, 21.2. IR (film): 1739, 1646  $\text{cm}^{-1}$ . HRMS (ESI): calculated for  $\text{C}_{19}\text{H}_{21}\text{N}_2\text{O}_2$   $[\text{M} + \text{H}]^+$ , 309.1614; found 309.1615.

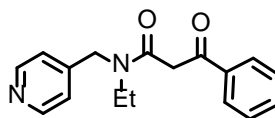
 **$\beta$ -keto amide 6.29**

Brown liquid, 59%,  $^1\text{H}$  NMR (300 MHz,  $\text{CDCl}_3$ ),  $\delta$  (ppm), mixture of rotamers: 14.71-14.62 (m, 0.2H), 8.62- 8.55 (m, 2H), 7.23-7.13 (m, 2H), 4.61-4.50 (m, 2H), 3.66 (s, 1.2H), 3.48-3.41 (m, 1.1H), 3.33-3.26 (m, 1.5H), 2.67-2.55 (m, 1.6H), 2.31-2.24 (m, 0.4H), 1.20-1.03 (m, 6H).  $^{13}\text{C}$  NMR (75 MHz,  $\text{CDCl}_3$ , mixture of rotamers),  $\delta$  (ppm): 205.1, 180.6, 167.2, 150.6, 150.2, 146.6, 122.5, 121.5,



85.1, 50.5, 49.0, 48.5, 47.4, 43.3, 41.7, 36.8, 29.2, 14.0, 12.7, 7.8. HRMS (ESI): calculated for  $C_{13}H_{19}N_2O_2$   $[M + H]^+$ , 235.1447; found 235.1460.

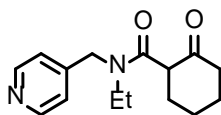
**$\beta$ -keto amide 6.30**



**6.30**

Brown liquid, 60%,  $^1H$  NMR (300 MHz,  $CDCl_3$ ),  $\delta$  (ppm), mixture of rotamers: 15.27-15.18 (m, 0.5H), 8.61- 8.54 (m, 2H), 8.05-7.95 (m, 1H), 7.82-7.37 (m, 4H), 7.25-7.13 (m, 2H), 5.86 (s, 0.3H), 5.58 (s, 0.1H), 4.68-4.61 (m, 2H), 4.23 (s, 0.8H), 4.04 (s, 0.3H), 3.57-3.31 (m, 2H), 1.27-1.13 (m, 3H).  $^{13}C$  NMR (75 MHz,  $CDCl_3$ , mixture of rotamers),  $\delta$  (ppm): 194.2, 172.5, 167.5, 150.6, 150.2, 147.1, 146.6, 136.3, 135.0, 134.1, 131.1, 129.04, 129.0, 128.8, 128.7, 126.2, 122.6, 122.5, 121.6, 84.8, 84.5, 50.6, 50.2, 47.9, 47.5, 46.1, 45.8, 43.4, 43.0, 41.7, 14.0, 12.6. IR (film): 1683, 1638  $cm^{-1}$ . HRMS (ESI): calculated for  $C_{17}H_{19}N_2O_2$   $[M + H]^+$ , 283.1447; found 283.1462.

**$\beta$ -keto amide 6.31**

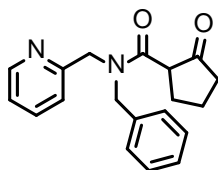


**6.31**

Brown liquid, 76%,  $^1H$  NMR (300 MHz,  $CDCl_3$ ),  $\delta$  (ppm), mixture of rotamers: 8.61- 8.54 (m, 2H), 7.30-7.29 (m, 1.6H), 7.13-7.11 (m, 0.4H), 5.04 (d, *J*

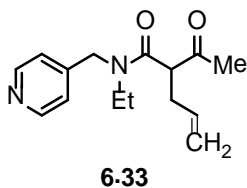
= 16.5 Hz, 0.8H), 4.52 (d,  $J = 18.1$  Hz, 0.2H), 4.36 (d,  $J = 18.1$  Hz, 0.2H), 4.23 (d,  $J = 16.2$  Hz, 0.8H), 3.68-3.61 (m, 1H), 3.36-3.04 (m, 2H), 2.64-1.69 (m, 8H), 1.15 (t,  $J = 7.2$  Hz, 3H).  $^{13}\text{C}$  NMR (75 MHz,  $\text{CDCl}_3$ , mixture of rotamers),  $\delta$  (ppm): 207.6, 169.9, 150.5, 150.1, 146.8, 146.6, 122.4, 121.5, 54.6, 54.5, 49.9, 47.5, 42.4, 42.2, 41.9, 41.7, 30.6, 30.4, 27.1, 26.9, 23.9, 23.5, 14.3, 12.6. HRMS (ESI): calculated for  $\text{C}_{15}\text{H}_{21}\text{N}_2\text{O}_2$   $[\text{M} + \text{H}]^+$ , 261.1603; found 261.1616.

### $\beta$ -keto amide 6.32

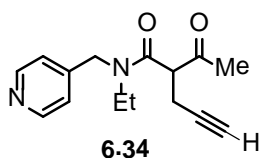


6.32

Brown liquid, 65%,  $^1\text{H}$  NMR (300 MHz,  $\text{CDCl}_3$ ),  $\delta$  (ppm), mixture of rotamers: 8.58- 8.49 (m, 1H), 7.71-7.63 (m, 1H), 7.40-7.13 (m, 7H), 5.31-5.00 (m, 2H), 4.54-4.39 (m, 1H), 4.29-4.20 (m, 1H), 3.74-3.68 (m, 0.5H), 3.53-3.47 (m, 0.5H), 2.59-2.51 (m, 1H), 2.37-2.31 (m, 2H), 2.25-2.12 (m, 2H), 1.89-1.82 (m, 1H).  $^{13}\text{C}$  NMR (75 MHz,  $\text{CDCl}_3$ , mixture of rotamers),  $\delta$  (ppm): 215.1, 214.9, 170.3, 170.0, 157.3, 156.9, 150.1, 149.4, 137.2, 137.0, 136.6, 129.2, 128.8, 128.1, 127.8, 127.5, 126.4, 122.8, 122.4, 121.7, 121.4, 52.6, 52.4, 51.6, 51.3, 49.5, 38.9, 27.9, 27.7, 21.2. IR (film): 1740, 1641  $\text{cm}^{-1}$ . HRMS (ESI): calculated for  $\text{C}_{19}\text{H}_{21}\text{N}_2\text{O}_2$   $[\text{M} + \text{H}]^+$ , 309.1603; found 309.1620.

**$\beta$ -keto amide 6.33**

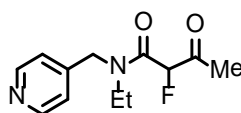
Brown liquid, 59%,  $^1\text{H}$  NMR (300 MHz,  $\text{CDCl}_3$ ),  $\delta$  (ppm), mixture of rotomers: 8.60 (d,  $J = 6.1$  Hz, 0.5H), 8.54 (d,  $J = 6.0$  Hz, 1.5H), 7.15-7.11 (m, 2H), 5.85-5.59 (m, 1H), 5.20-5.02 (m, 2H), 4.80-4.42 (m, 2H), 3.77-3.72 (m, 0.7H), 3.65-3.42 (m, 1.3H), 3.37-3.24 (m, 1H), 2.83-2.59 (m, 2H), 2.23 (s, 2.2H), 2.17 (s, 0.8H), 1.19 (t,  $J = 7.2$  Hz, 2.2H), 1.13 (t,  $J = 7.1$  Hz, 0.8H),  $^{13}\text{C}$  NMR (75 MHz,  $\text{CDCl}_3$ , mixture of rotomers),  $\delta$  (ppm): 204.7, 204.5, 169.0, 168.5, 150.4, 150.1, 146.6, 146.1, 134.5, 134.3, 122.5, 121.4, 118.0, 58.2, 57.6, 49.8, 48.0, 42.8, 42.0, 33.8, 33.6, 27.5, 27.1, 14.3, 12.6. HRMS (ESI): calculated for  $\text{C}_{15}\text{H}_{21}\text{N}_2\text{O}_2$   $[\text{M} + \text{H}]^+$ , 261.1603; found 261.1612.

 **$\beta$ -keto amide 6.34**

Brown liquid, 63%,  $^1\text{H}$  NMR (300 MHz,  $\text{CDCl}_3$ ),  $\delta$  (ppm), mixture of rotomers: 8.61 (d,  $J = 6.1$  Hz, 0.5H), 8.55 (d,  $J = 6.0$  Hz, 1.5H), 7.18 (d,  $J = 6.1$  Hz, 2H), 4.83-4.56 (m, 2H), 3.96-3.91 (m, 0.7H), 3.69-3.35 (m, 2.3H), 2.89-2.79 (m, 2H), 2.25 (s, 2.2H), 2.17 (s, 0.8H), 2.08 (t,  $J = 2.7$  Hz, 0.7H), 2.06-2.04 (m,

0.3H), 1.26 (t,  $J = 7.2$  Hz, 2.2H), 1.15 (t,  $J = 7.1$  Hz, 0.8H),  $^{13}\text{C}$  NMR (75 MHz,  $\text{CDCl}_3$ , mixture of rotamers),  $\delta$  (ppm): 202.4, 168.6, 167.9, 150.5, 150.1, 146.4, 146.0, 122.6, 121.5, 80.8, 71.1, 56.5, 55.8, 50.0, 48.1, 43.1, 42.2, 27.6, 27.1, 19.0, 14.3, 12.5. HRMS (ESI): calculated for  $\text{C}_{15}\text{H}_{19}\text{N}_2\text{O}_2$   $[\text{M} + \text{H}]^+$ , 259.1447; found 259.1454.

### $\beta$ -keto amide **6.35**



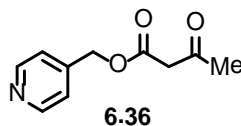
**6.35**

A reaction mixture containing **6.22** (0.30 g, 1.36 mmol, 1 equiv) in acetonitrile (10 mL) was cooled to 0 °C and Selectfluor<sup>®</sup> (0.48 g, 1.36 mmol, 1 equiv) was added. Resulting mixture was warmed to room temperature and stirred for 18 h. and then was quenched with sat. aq.  $\text{NaHCO}_3$  solution (10 mL), extracted with ethyl acetate (3 x 10 mL). The combined organics were dried over sodium sulfate, filtered and evaporated in vacuo. Crude product was purified by silica gel column chromatography using 50-90% ethyl acetate in hexanes to obtain **6.35**, as a brown liquid (0.23 g, 71%).

Brown liquid, 71%,  $^1\text{H}$  NMR (300 MHz,  $\text{CDCl}_3$ ),  $\delta$  (ppm), mixture of rotamers: 8.63-8.55 (m, 2H), 7.16-7.12 (m, 2H), 5.65 (s, 0.3H), 5.50-5.48 (m, 0.4H), 5.33-5.31 (m, 0.3H), 4.73-4.50 (m, 2H), 3.58-3.30 (m, 2H), 2.44-2.36 (m, 3H), 1.22 (t,  $J = 7.2$  Hz, 2.1H), 1.13 (t,  $J = 7.2$  Hz, 0.9H).  $^{13}\text{C}$  NMR (75 MHz,  $\text{CDCl}_3$ , mixture of rotamers),  $\delta$  (ppm): 202.5 (d,  $J^2_{\text{C-F}} = 24.9$  Hz), 164.5 (d,  $J^2_{\text{C-F}} = 20.2$  Hz), 150.6, 150.3, 145.7, 145.5, 122.4, 121.7, 92.1 (d,  $J^1_{\text{C-F}} = 196.2$  Hz), 91.4 (d,  $J^1_{\text{C-F}} = 194.7$  Hz), 53.6, 49.3, 48.1, 47.8, 42.6, 42.0, 26.5, 26.4, 14.1,

12.3. HRMS (ESI): calculated for  $C_{12}H_{16}N_2O_2F$   $[M + H]^+$ , 239.1196; found 239.1206.

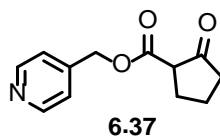
### $\beta$ -keto ester **6.36**



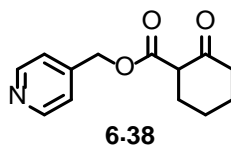
A reaction mixture containing 4-(hydroxymethyl) pyridine (2.20 g, 20.16 mmol, 1 equiv) and *t*-Butyl acetoacetate (4.78 g, 30.24 mmol, 1.5 equiv) in toluene (50 mL) was refluxed for 36 h. The reaction mixture was cooled to room temperature and concentrated in vacuo. The crude product was purified by silica gel column chromatography using 70-100% ethyl acetate in hexanes to afford yellow liquid as the desired  $\beta$ -keto ester **6.36** (2.1 g, 54%).

$\beta$ -keto ester substrates **6.36-6.38** were prepared using the above procedure using corresponding  $\beta$ -keto ester starting materials (1.00 g-2.00 g scale).

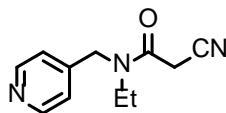
$^1H$  NMR (300 MHz,  $CDCl_3$ ),  $\delta$  (ppm), mixture of tautomers: 11.89 (s, 0.1H), 8.62-8.59 (m, 2H), 7.29-7.24 (m, 2H), 5.20-5.19 (m, 2H), 5.11 (s, 0.1H), 3.58 (s, 1.8H), 2.29 (s, 2.7H), 2.00 (s, 0.3H).  $^{13}C$  NMR (75 MHz,  $CDCl_3$ , mixture of tautomers),  $\delta$  (ppm): 200.1, 166.8, 150.3, 144.4, 122.1, 65.2, 50.0, 30.5. IR (film): 1744, 1708  $cm^{-1}$ . HRMS (ESI): calculated for  $C_{10}H_{12}NO_3$   $[M + H]^+$ , 194.0817; found 194.0834.

**$\beta$ -keto ester 6.37**

Brown liquid, 46%,  $^1\text{H}$  NMR (300 MHz,  $\text{CDCl}_3$ ),  $\delta$  (ppm): 8.61 (d,  $J = 6.1$  Hz, 2H), 7.29 (d,  $J = 5.9$  Hz, 2H), 5.28-5.14 (m, 2H), 3.29 (t,  $J = 9.3$  Hz, 1H), 2.59-1.85 (m, 6H).  $^{13}\text{C}$  NMR (75 MHz,  $\text{CDCl}_3$ ),  $\delta$  (ppm): 212.0, 169.0, 150.1, 144.7, 121.8, 65.0, 54.8, 38.2, 27.4, 21.1. IR (film): 1757, 1726  $\text{cm}^{-1}$ . HRMS (ESI): calculated for  $\text{C}_{12}\text{H}_{13}\text{NO}_3$   $[\text{M} + \text{H}]^+$ , 220.0974; found 220.0995.

 **$\beta$ -keto ester 6.38**

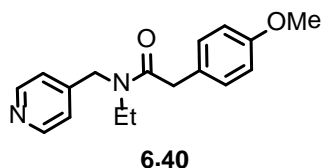
Brown liquid, 63%,  $^1\text{H}$  NMR (300 MHz,  $\text{CDCl}_3$ ),  $\delta$  (ppm), mixture of tautomers: 12.03 (s, 0.7H), 8.62-8.60 (m, 2H), 7.30-7.26 (m, 2H), 5.30-5.14 (m, 2H), 3.53-3.48 (m, 0.3H), 2.55-1.61 (m, 8H).  $^{13}\text{C}$  NMR (75 MHz,  $\text{CDCl}_3$ , mixture of tautomers),  $\delta$  (ppm): 206.1, 173.6, 172.2, 169.8, 150.2, 145.3, 144.8, 122.0, 121.8, 97.5, 64.9, 63.9, 57.4, 41.9, 30.1, 29.4, 27.3, 23.7, 22.5, 22.47, 23.0. HRMS (ESI): calculated for  $\text{C}_{13}\text{H}_{16}\text{NO}_3$   $[\text{M} + \text{H}]^+$ , 234.1130; found 234.1157.

**$\beta$ -amido nitrile 6.39****6.39**

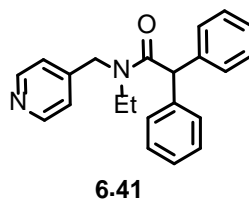
Brown liquid, 39%,  $^1\text{H}$  NMR (300 MHz,  $\text{CDCl}_3$ ),  $\delta$  (ppm):. 8.64 (d,  $J = 6.0$  Hz, 2H), 8.57 (d,  $J = 6.2$  Hz, 2H), 7.17-7.13 (m, 2H), 4.60 (s, 1.5H), 4.54 (s, 0.5H), 3.62 (s, 1.5H), 3.50 (q,  $J = 7.2$  Hz, 0.5H), 3.43 (s, 0.5H), 3.35 (q,  $J = 7.2$  Hz, 1.5H), 1.24 (t,  $J = 7.2$  Hz, 2.2H), 1.18 (t,  $J = 7.2$  Hz, 0.8H).  $^{13}\text{C}$  NMR (75 MHz,  $\text{CDCl}_3$ ),  $\delta$  (ppm): 162.2, 150.9, 150.4, 145.7, 144.9, 122.7, 121.2, 114.0, 50.6, 48.2, 43.5, 42.8, 25.4, 25.1, 13.9, 12.7. IR (film): 2260, 1655  $\text{cm}^{-1}$ . HRMS (ESI): calculated for  $\text{C}_{11}\text{H}_{14}\text{N}_3\text{O}$   $[\text{M} + \text{H}]^+$ , 204.1137; found 204.1164.

**Preparation of 6.40-6.41 (N-ethyl-4-aminomethyl)pyridines**

A reaction mixture containing the secondary amine derived from 4-(aminoethyl) pyridine (1.00 g, 7.3 mmol, 1 equiv) and 4-methoxy phenyl acetic acid (1.46 g, 8.81 mmol, 1.2 equiv) in DCM (25 mL) was cooled to 0  $^\circ\text{C}$ . DCC (2.27 g, 11.0 mmol, 1.5 equiv) was added in one portion and the reaction mixture was allowed to stir at room temperature for 16 h and then washed with sat. aq.  $\text{NaHCO}_3$  (2 X 5 mL), water (10 mL) and brine (5 mL). The organic layer was dried over sodium sulfate, filtered and evaporated in vacuo. The crude product was purified by silica gel column chromatography using 70-100% ethyl acetate in hexanes to obtain **6.40**, as a pale yellow colored liquid (1.20 g, 55%).

**$\beta$ -amido PMP 6.40**

55%,  $^1\text{H}$  NMR (300 MHz,  $\text{CDCl}_3$ ),  $\delta$  (ppm), mixture of rotamers: 8.56-8.48 (m, 2H), 7.23-7.21 (m, 1.4H), 7.10-7.03 (m, 2.6H), 6.90-6.81 (m, 2H), 4.6 (s, 1.3H), 4.50 (s, 0.7H), 3.80-3.74 (m, 4.3H), 3.57 (s, 0.7H), 3.43 (q,  $J=7.1$  Hz, 0.7H), 3.34 (q,  $J=7.1$  Hz, 1.3H), 1.14-1.07 (m, 3H).  $^{13}\text{C}$  NMR (75 MHz,  $\text{CDCl}_3$ , mixture of rotamers),  $\delta$  (ppm): 171.7, 171.5, 158.7, 150.3, 149.9, 147.2, 146.6, 129.9, 129.7, 127.0, 126.7, 122.6, 121.4, 114.3, 55.4, 50.2, 47.5, 42.9, 41.6, 40.4, 39.9, 13.9, 12.6. HRMS (ESI): calculated for  $\text{C}_{17}\text{H}_{21}\text{N}_2\text{O}_2$   $[\text{M} + \text{H}]^+$ , 285.1603; found 285.1620.

 **$\beta$ -amido diphenyl 6.41**

Yellow liquid, 46%,  $^1\text{H}$  NMR (300 MHz,  $\text{CDCl}_3$ ),  $\delta$  (ppm), mixture of rotamers: 8.62-8.60 (m, 0.7H), 8.51-8.49 (m, 1.3H), 7.35-7.23 (m, 8.5H), 7.17-7.09 (m, 3.5H), 5.27 (s, 0.7H), 4.92 (s, 0.3H), 4.61 (s, 1.3H), 4.47 (s, 0.7H), 3.51 (q,  $J=7.1$  Hz, 0.8H), 3.36 (q,  $J=7.1$  Hz, 1.2H).  $^{13}\text{C}$  NMR (75 MHz,  $\text{CDCl}_3$ , mixture of rotamers),  $\delta$  (ppm): 172.1, 150.6, 150.1, 147.2, 147.0, 139.4, 139.3, 129.1,



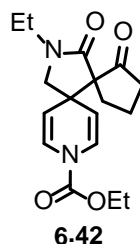
129.0, 128.8, 127.4, 122.7, 121.3, 55.1, 54.7, 50.1, 48.0, 42.9, 42.4, 14.4, 12.7.  
HRMS (ESI): calculated for  $C_{22}H_{23}N_2O$   $[M + H]^+$ , 331.1810; found 331.1824.

#### **Spirocyclization and characterization of diazaspiro[4.5]decanes:**

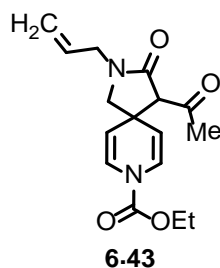
General procedure for spirocyclization (condition A): The preparation of **6.42** is representative. The reaction mixture of 4-alkylpyridine compound **6.29** (0.05 g, 0.20 mmol, 1 equiv) in dichloromethane (1 mL) was cooled to 0 °C. Titanium isopropoxide (30  $\mu$ L, 0.10 mmol, 0.5 equiv) was added to the reaction mixture and stirred for 2 min. Ethyl chloroformate (29  $\mu$ L, 0.31 mmol, 1.5 equiv) was then added to the reaction mixture. The resulting mixture was stirred for 5-7 min and then directly loaded on to the silica gel column and purified using 70-80% ethyl acetate in hexanes to give **6.42**, yellow gummy liquid as the desired product (33 mg, 51%).

General procedure for spirocyclization (condition B): The preparation of **6.42** is representative. Ethyl chloroformate (78  $\mu$ L, 0.81 mmol, 2 equiv) was added to a reaction mixture containing **6.24** (0.10 g, 0.41 mmol, 1 equiv) in TFE (2 mL) at room temperature. The resulting mixture was stirred for 15-20 min and then directly loaded on to the silica gel column and purified using 70-80% ethyl acetate in hexanes to give **6.42**, yellow gummy liquid as the desired product (85 mg, 66%).

The above procedures were used to synthesize all other spirocycles from 0.05-0.10 g of their corresponding starting materials.

**Spirocycle 6.42**

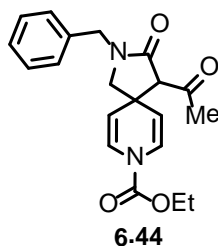
Pale yellowish liquid, 66%,  $^1\text{H}$  NMR (300 MHz,  $\text{CDCl}_3$ ),  $\delta$  (ppm), mixture of rotamers: 6.98 (br s, 2H), 4.85 (br s, 1H), 4.66 (br s, 1H), 4.29 (q,  $J = 7.1$  Hz, 2H), 3.76 (d,  $J = 9.5$  Hz, 1H), 3.44-3.28 (m, 2H), 3.02 (d,  $J = 9.5$  Hz, 1H), 2.37-2.24 (m, 2H), 2.12-2.06 (m, 3H), .1.90-1.87 (m, 1H), 1.34 (t,  $J = 7.1$  Hz, 3H), 1.14 (t,  $J = 7.2$  Hz, 3H).  $^{13}\text{C}$  NMR (75 MHz,  $\text{CDCl}_3$ , mixture of rotamers),  $\delta$  (ppm): 216.0, 171.0, 151.1, 125.9, 123.2, 108.2, 105.1, 69.0, 63.2, 59.1, 43.8, 39.8, 37.6, 28.6, 19.9, 14.5, 12.5. HRMS (ESI): calculated for  $\text{C}_{17}\text{H}_{22}\text{N}_2\text{O}_4\text{Na}$   $[\text{M} + \text{Na}]^+$ , 341.1477; found 341.1459.

**Spirocycle 6.43**

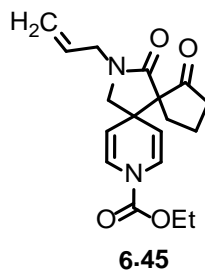
Brown liquid, 12%,  $^1\text{H}$  NMR (500MHz,  $\text{CDCl}_3$ ),  $\delta$  (ppm), mixture of rotamers: 12.27 (s, 0.3H), 7.00-6.88 (m, 2H), 5.78-5.70 (m, 1H), 5.28-5.19 (m,

2H), 4.97-4.81 (m, 2H), 4.30 (q,  $J = 7.0$  Hz, 2H), 4.00-3.89 (m, 2H), 3.47-3.45 (m, 1.3H), 3.21 (s, 0.7H), 3.16-3.14 (m, 0.7H), 2.28 (s, 2H), 1.86 (s, 1H), 1.37-1.33 (m, 3H).  $^{13}\text{C}$  NMR (125 MHz,  $\text{CDCl}_3$ , mixture of rotamers),  $\delta$  (ppm): 203.9, 171.6, 167.9, 151.2, 132.2, 131.9, 118.8, 118.5, 109.9, 69.8, 63.7, 63.4, 63.2, 61.3, 45.4, 44.7, 39.8, 36.7, 33.4, 29.9, 17.6, 14.6. HRMS (ESI): calculated for  $\text{C}_{16}\text{H}_{21}\text{N}_2\text{O}_4$   $[\text{M} + \text{H}]^+$ , 305.1501; found 305.1511.

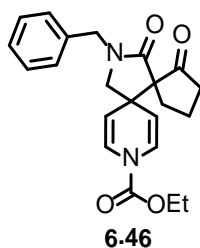
### Spirocycle 6.44



Yellow liquid, 19%,  $^1\text{H}$  NMR (300 MHz,  $\text{CDCl}_3$ ),  $\delta$  (ppm), mixture of rotamers: 12.32 (s, 0.4H), 7.38-7.22 (m, 5H), 6.95-6.83 (m, 2H), 4.82-4.75 (m, 2H), 4.51-4.48 (m, 1H), 4.44 (s, 1H), 4.26 (q,  $J = 7.1$  Hz, 2H), 3.49 (s, 0.6H), 3.33 (d,  $J = 9.9$  Hz, 1H), 3.11 (s, 0.8H), 3.02 (d,  $J = 9.9$  Hz, 0.6H), 2.28 (s, 2H), 1.85 (s, 1H), 1.35-1.29 (m, 3H).  $^{13}\text{C}$  NMR (75 MHz,  $\text{CDCl}_3$ , mixture of rotamers),  $\delta$  (ppm): 203.9, 171.7, 168.1, 151.4, 151.1, 136.2, 135.9, 129.0, 128.33, 128.3, 128.0, 127.9, 122.9, 110.0, 69.7, 63.3, 63.2, 60.1, 46.8, 46.1, 39.7, 36.6, 33.5, 17.6, 14.6. HRMS (ESI): calculated for  $\text{C}_{20}\text{H}_{23}\text{N}_2\text{O}_4$   $[\text{M} + \text{H}]^+$ , 355.1658; found 355.1675.

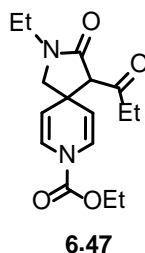
**Spirocycle 6.45**

Spirocyclization condition B was used to prepare **6.45** from **6.27**. Pale yellowish liquid, 40%,  $^1\text{H}$  NMR (300 MHz,  $\text{CDCl}_3$ ),  $\delta$  (ppm), mixture of rotamers: 6.99-6.96 (m, 2H), 5.79-5.66 (m, 1H), 5.31-5.19 (m, 2H), 4.85 (br s, 1H), 4.67 (br s, 1H), 4.28 (q,  $J = 7.1$  Hz, 2H), 3.95-3.86 (m, 2H), 3.73 (d,  $J = 9.7$  Hz, 1H), 3.01 (d,  $J = 9.7$  Hz, 1H), 2.39-2.25 (m, 2H), 2.13-2.07 (m, 3H), 1.90-1.87 (m, 1H), 1.34 (t,  $J = 7.1$  Hz, 3H).  $^{13}\text{C}$  NMR (75 MHz,  $\text{CDCl}_3$ , mixture of rotamers),  $\delta$  (ppm): 216.0, 171.3, 151.2, 132.1, 126.0, 123.3, 118.5, 108.3, 105.1, 69.1, 63.3, 59.5, 45.7, 43.9, 39.9, 28.8, 20.0, 14.6. HRMS (ESI): calculated for  $\text{C}_{18}\text{H}_{23}\text{N}_2\text{O}_4$  [ $\text{M} + \text{H}$ ] $^+$ , 331.1658; found 331.1644.

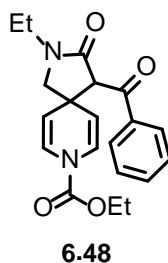
**Spirocycle 6.46**

Pale yellowish liquid, 44%,  $^1\text{H}$  NMR (300 MHz,  $\text{CDCl}_3$ ),  $\delta$  (ppm), mixture of rotamers: 7.38-7.26 (m, 5H), 6.97-6.88 (m, 2H), 4.83-4.78 (m, 1H), 4.62-4.51 (m, 3H), 4.26 (q,  $J = 7.1$  Hz, 2H), 3.65 (d,  $J = 9.7$  Hz, 1H), 2.90 (d,  $J = 9.6$  Hz, 1H), 2.44-2.32 (m, 2H), 2.17-2.10 (m, 3H), 1.92-1.89 (m, 1H), 1.32 (t,  $J = 7.1$  Hz, 3H).  $^{13}\text{C}$  NMR (75 MHz,  $\text{CDCl}_3$ , mixture of rotamers),  $\delta$  (ppm): 216.2, 171.5, 151.2, 136.1, 128.9, 128.3, 127.9, 125.8, 123.3, 107.9, 105.2, 104.8, 69.0, 63.3, 59.1, 47.1, 43.8, 39.9, 28.8, 20.1, 14.6. HRMS (ESI): calculated for  $\text{C}_{22}\text{H}_{25}\text{N}_2\text{O}_4$  [ $\text{M} + \text{H}$ ] $^+$ , 381.1814; found 381.1812.

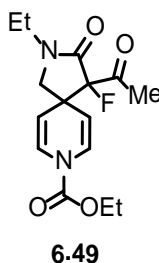
### Spirocycle 6.47



Yellow liquid, 60%,  $^1\text{H}$  NMR (300 MHz,  $\text{CDCl}_3$ ),  $\delta$  (ppm), mixture of rotamers: 12.40 (s, 0.2H), 6.95 (br s, 2H), 4.90 (br s, 2H), 4.28 (q,  $J = 7.2$  Hz, 2H), 3.51 (d,  $J = 9.7$  Hz, 0.8H), 3.44-3.28 (m, 2.8H), 3.21 (s, 0.4H), 3.14 (d,  $J = 9.7$  Hz, 0.8H), 2.72-2.43 (m, 1.6H), 2.16 (q,  $J = 7.4$  Hz, 0.4H), 1.37-1.31 (m, 3H), 1.16-1.08 (m, 3H), 1.06-1.00 (m, 3H).  $^{13}\text{C}$  NMR (75 MHz,  $\text{CDCl}_3$ , mixture of rotamers),  $\delta$  (ppm): 206.4, 171.7, 169.1, 151.2, 124.7, 122.5, 121.1, 110.5, 105.8, 69.5, 63.5, 63.3, 63.2, 61.1, 39.6, 37.5, 36.7, 24.4, 14.6, 12.5, 11.0, 7.1. HRMS (ESI): calculated for  $\text{C}_{16}\text{H}_{23}\text{N}_2\text{O}_4$  [ $\text{M} + \text{H}$ ] $^+$ , 307.1658; found 307.1675.

**Spirocycle 6.48**

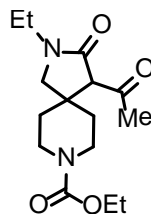
Brown liquid, 43%,  $^1\text{H}$  NMR (300 MHz,  $\text{CDCl}_3$ ),  $\delta$  (ppm), mixture of rotamers: 7.93-7.91 (m, 2H), 7.59-7.54 (m, 1H), 7.48-7.43 (m, 2H), 6.97-6.76 (m, 2H), 5.08 (br s, 2H), 4.88 (br s, 1H), 4.30 (s, 1H), 4.24 (q,  $J = 7.1$  Hz, 2H), 3.65 (d,  $J = 9.7$  Hz, 1H), 3.53-3.33 (m, 2H), 3.23 (d,  $J = 9.8$  Hz, 1H), 1.31-1.26 (m, 3H), 1.19 (t,  $J = 7.3$  Hz, 3H).  $^{13}\text{C}$  NMR (75 MHz,  $\text{CDCl}_3$ , mixture of rotamers),  $\delta$  (ppm): 196.0, 169.6, 151.1, 137.6, 133.7, 129.1, 128.7, 124.6, 122.3, 110.5, 106.1, 65.4, 63.2, 61.4, 40.2, 37.5, 14.5, 12.5. IR (film): 1723, 1678, 1669  $\text{cm}^{-1}$ . HRMS (ESI): calculated for  $\text{C}_{20}\text{H}_{23}\text{N}_2\text{O}_4$   $[\text{M} + \text{H}]^+$ , 355.1658; found 355.1679.

**Spirocycle 6.49**

Pale yellowish liquid, 10%,  $^1\text{H}$  NMR (500 MHz,  $\text{CDCl}_3$ ),  $\delta$  (ppm), mixture of rotamers: 7.11-7.01 (m, 2H), 4.88-4.79 (m, 2H), 4.29 (q,  $J = 7.1$  Hz, 2H), 3.50 (d,

$J = 9.5$  Hz, 1 H), 3.48-3.30 (m, 2H), 3.12 (d,  $J = 9.6$  Hz, 1H), 2.30 (d,  $J = 5.8$  Hz, 3H), 1.34 (t,  $J = 7.2$  Hz, 3H). 1.16 (t,  $J = 7.3$  Hz, 3H). HRMS (ESI): calculated for  $C_{15}H_{20}FN_2O_4$   $[M + H]^+$ , 311.1407; found 311.1415.

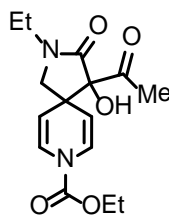
### Spirocycle 6.50



**6.50**

Spirocycle **6.23** (55 mg, 0.19 mmol) was taken in ethanol (5 mL) and 10% palladium on carbon (5 mg) was added. The resulting mixture was hydrogenated at 100 psi for 14 h and then filtered through Celite. The filtrate was evaporated in vacuo and dried to obtain **6.50**, as a colorless liquid (52 mg, 93%).

$^1H$  NMR (300 MHz,  $CDCl_3$ ),  $\delta$  (ppm): 4.13 (q,  $J = 7.1$  Hz, 2H), 3.69-3.64 (m, 1H), 3.57-3.49 (m, 1H), 3.51 (d,  $J = 9.6$  Hz, 0.7H), 3.45-3.22 (m, 4.3H), 3.17 (d,  $J = 9.6$  Hz, 1H), 2.32 (s, 3H), 1.74-1.59 (m, 3H), 1.26 (t,  $J = 7.1$  Hz, 3H), 1.13 (t,  $J = 7.2$  Hz, 3H).  $^{13}C$  NMR (75 MHz,  $CDCl_3$ ),  $\delta$  (ppm): 204.9, 169.8, 155.6, 65.3, 61.7, 55.1, 41.0, 40.3, 39.4, 37.6, 36.2, 33.0, 30.7, 14.8, 12.4. HRMS (ESI): calculated for  $C_{15}H_{25}N_2O_4$   $[M + H]^+$ , 297.1814; found 297.1823.

**Spirocycle 6.51****6.51**

*m*-CPBA (77 mg, 0.45 mmol, 1.3 equiv) was added to the reaction mixture containing spirocycle **6.23** (0.10 g, 0.34 mmol, 1 equiv) in DCM (5 mL) at 0 °C. The resulting mixture was stirred at room temperature for 9 h and then washed with sat. aq. NaHCO<sub>3</sub> (2 X 5 mL), water (10 mL) and brine (5 mL). The organic layer was dried over sodium sulfate, filtered and evaporated in vacuo. Crude product was purified by silica gel column chromatography using 50-100% ethyl acetate in hexanes to obtain **6.51**, as a colorless liquid (55 mg, 52%).

<sup>1</sup>H NMR (300 MHz, CDCl<sub>3</sub>), δ (ppm): 7.03 (br s, 2H), 4.80-4.25 (m, 3H), 4.28 (q, *J* = 7.1 Hz, 2H), 3.51 (d, *J* = 9.8 Hz, 1H), 3.47-3.28 (m, 2H), 3.09 (d, *J* = 9.8 Hz, 1H), 2.27 (s, 3H), 1.32 (t, *J* = 7.1 Hz, 3H), 1.15 (t, *J* = 7.3 Hz, 3H). <sup>13</sup>C NMR (75 MHz, CDCl<sub>3</sub>), δ (ppm): 209.8, 170.6, 151.1, 126.3, 124.2, 106.2, 103.6, 88.8, 63.3, 58.8, 46.0, 38.1, 28.7, 14.5, 12.2. HRMS (ESI): calculated for C<sub>15</sub>H<sub>21</sub>N<sub>2</sub>O<sub>5</sub> [M + H]<sup>+</sup>, 309.1450; found 309.1438.

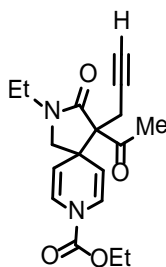
**Experimental procedures and characterization for alkylation of spirocycle 6.23**

Spirocycle **6.23** (0.50 g, 1.7 mmol, 1 equiv) was taken in dry THF (15 mL) at 0 °C and KO<sup>t</sup>Bu (0.25 g, 2.2 mmol, 1.3 equiv) was added to it and stirred for 30 min. 1-bromo-2-butyne (0.19 mL, 2.1 mmol, 1.2 equiv) was then added to the



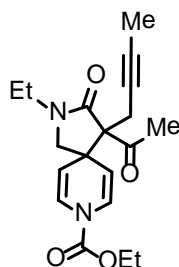
reaction mixture and slowly warmed to room temperature and stirred for 16 h. Reaction was quenched with water and extracted with ethyl acetate (3 X 25 mL). The combined organics were dried over sodium sulfate, filtered and evaporated in vacuo. Crude product was purified by silica gel column chromatography using 50-70% ethyl acetate in hexanes to obtain **6.53**, as yellow liquid (0.35 g, 74%) and recovered 0.1 g of the starting material.

### Spirocycle 6.52



**6.52**

The above procedure was used to prepare compound **6.52** from 0.20 g of **6.23** and propargyl bromide. Yellow liquid, 71%,  $^1\text{H}$  NMR (300 MHz,  $\text{CDCl}_3$ ),  $\delta$  (ppm): 6.97-6.86 (m, 2H), 5.04-4.85 (m, 2H), 4.28 (q,  $J = 7.1$  Hz, 2H), 3.47-3.36 (m, 3H), 3.25 (d,  $J = 9.6$  Hz, 1H), 2.96 (dd,  $J = 17.5, 2.7$  Hz, 1H), 2.62 (dd,  $J = 17.6, 2.6$  Hz, 1H), 1.94 (t,  $J = 2.3$  Hz, 1H), 1.33 (t,  $J = 7.1$  Hz, 3H), 1.15 (t,  $J = 7.2$  Hz, 3H).  $^{13}\text{C}$  NMR (75 MHz,  $\text{CDCl}_3$ ),  $\delta$  (ppm): 205.9, 170.5, 151.2, 124.8, 124.4, 106.6, 106.2, 80.0, 71.2, 68.8, 63.3, 60.4, 43.1, 37.8, 30.4, 28.2, 20.6, 14.6, 12.4. HRMS (ESI): calculated for  $\text{C}_{18}\text{H}_{22}\text{N}_2\text{O}_4\text{Na}$   $[\text{M} + \text{Na}]^+$ , 353.1477; found 353.1470.

**Spirocycle 6.53****6.53**

Yellow liquid, 74%,  $^1\text{H}$  NMR (300 MHz,  $\text{CDCl}_3$ ),  $\delta$  (ppm): 7.07-6.96 (m, 2H), 5.04-4.86 (m, 2H), 4.27 (q,  $J = 7.1$  Hz, 2H), 3.46-3.30 (m, 3H), 3.21 (d,  $J = 9.4$  Hz, 1H), 2.91 (dd,  $J = 17.4, 2.5$  Hz, 1H), 2.55 (dd,  $J = 17.4, 2.4$  Hz, 1H), 2.28 (s, 3H), 1.76 (t,  $J = 2.5$  Hz, 3H), 1.33 (t,  $J = 7.0$  Hz, 3H), 1.13 (t,  $J = 7.3$  Hz, 3H).  $^{13}\text{C}$  NMR (75 MHz,  $\text{CDCl}_3$ ),  $\delta$  (ppm): 206.5, 170.8, 151.3, 124.7, 124.2, 107.4, 106.6, 78.2, 74.7, 69.5, 63.2, 60.5, 43.0, 37.7, 30.3, 28.3, 21.1, 14.6, 12.4, 3.5. HRMS (ESI): calculated for  $\text{C}_{19}\text{H}_{25}\text{N}_2\text{O}_4$   $[\text{M} + \text{H}]^+$ , 345.1814; found 345.1803.

## CHAPTER SEVEN

BENZYLIC CYCLIZATION REACTIONS OF ACTIVATED 4-  
ALKYLPYRIDINES7.1 Introduction

In the preceding two chapters methodology based on titanium isopropoxide-catalyzed spirocyclization of 4-alkylpyridine substrates equipped with carbon nucleophiles in the side chain was discussed. Under these acidic and neutral reaction conditions, certain 4-alkylpyridine derivatives were efficiently converted to spirodihydropyridine products. As mentioned in Chapters Five and Six, it was anticipated that these same 4-alkylpyridine substrates under basic conditions will yield anhydrobases instead of spirocycles. Anhydrobases of pyridinium salts are generated by loss of proton from an alkyl substituent at C-2 or C-4 as illustrated in Figure 7.1. Only a few examples illustrating the use anhydrobases of pyridinium salts for heterocyclic synthesis have been reported in the literature. Construction of heterocycles utilizing anhydrobases of pyridines would provide another alternative for the synthesis of complex heterocyclic molecules.

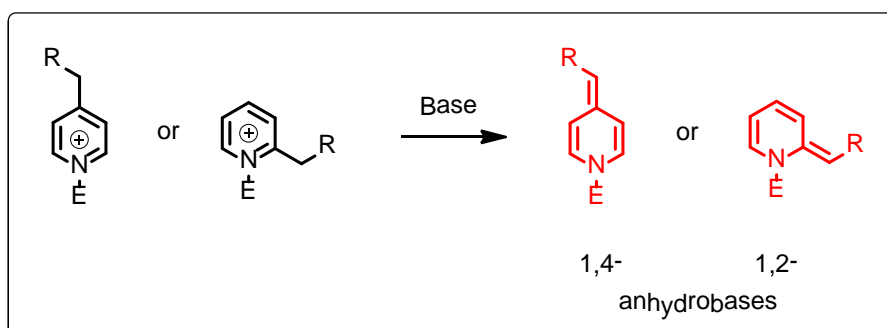
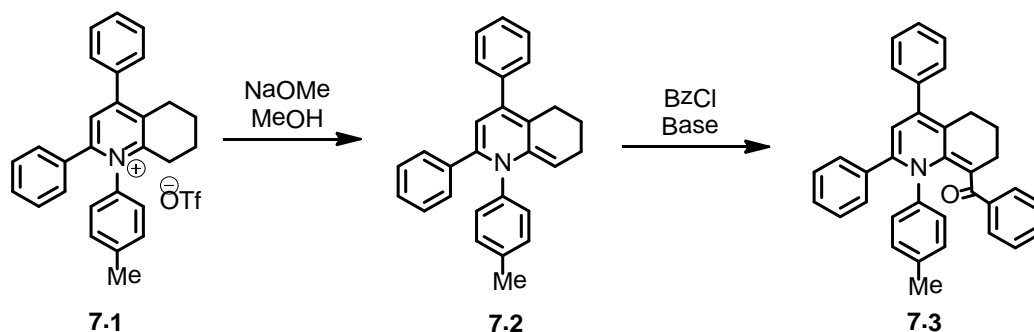
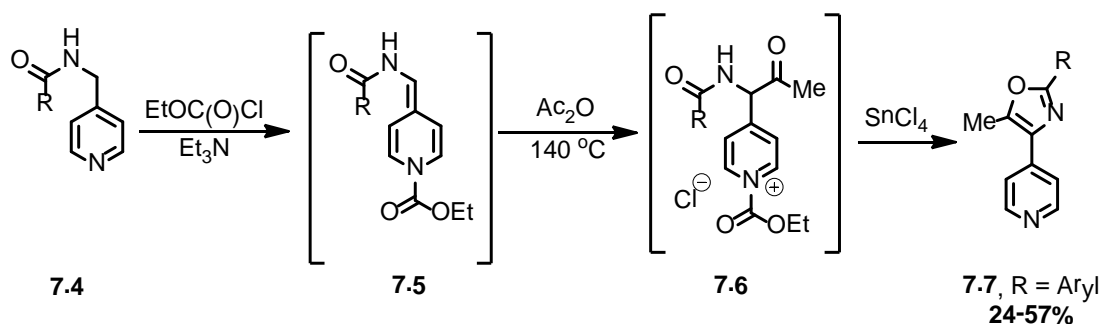


Figure 7.1. Anhydrobases of alkyl pyridines



Scheme 7.1. Synthesis of acylated anhydrobases

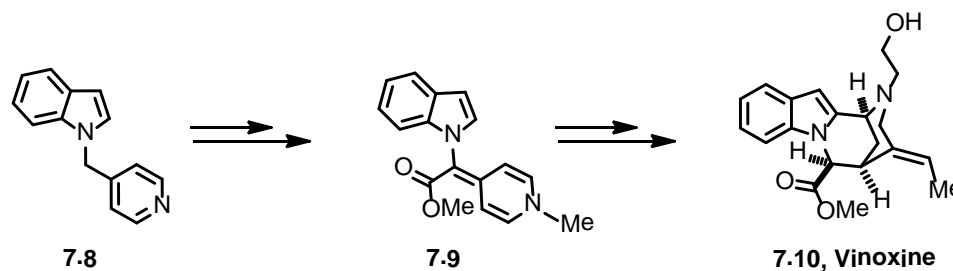
Katritzky and coworkers reported the synthesis of an orange colored anhydrobase (**7.2**) of quinolinium salt (**7.1**) using sodium methoxide in methanol at room temperature as shown in Scheme 7.1.<sup>182</sup> This anhydrobase was then treated with electrophiles such as benzoyl chloride under Schotten-Baumann conditions to generate the corresponding acylated anhydrobase (**7.3**). However, they found that few of the anhydrobases prepared in this manner were stable, and on heating regeneration of starting materials was observed.



Scheme 7.2. Synthesis of heterocycle **7.7** from anhydrobase **7.5**

In another example, Brana and coworkers found that 4-(4-pyridyl)oxazoles could be synthesized by heating 4-acylaminomethyl-1-alkyl pyridinium

salts (**7.5**) with acetic anhydride in the presence of triethylamine and  $\text{SnCl}_4$  (Scheme 7.2).<sup>183</sup> The unstable anhydrobase intermediate (**7.5**) reacts with the electrophile to give the acylated product (**7.6**) which, in turn, undergoes condensation reaction to yield the pyridine substituted oxazole (**7.7**) in low yield.



Scheme 7.3. Anhydrobase utilization in natural product synthesis

Bosch and coworkers utilized an anhydrobase approach in their attempt to synthesize vinoxine, a tetracyclic indole alkaloid (**7.10**) (Scheme 7.3).<sup>184</sup> In general, however, reports related to anhydrobases and their uses in natural product synthesis are rare. In this context, we became interested in investigating routes to bis(piperidine)s and related materials via intramolecular condensations of anhydrobase intermediates. Significantly, the bis(piperidine) ring system is encountered in several families of macrocyclic marine alkaloids such as halicyclamines (**7.11-7.12**), arenosclerin A (**7.13**), haliclonacyclamine C (**7.17**), neopetrosiamine A (**7.16**) and saraines (**7.18**) (Figure 7.2).<sup>185-189</sup> Even though these diaza-macrocyclic products exhibit a range of biological activities such as anticancer, antibacterial, antiviral, and anti-malarial properties, reports related to their synthesis are rare. Previous syntheses of macrocyclic alkaloids such as

haliclonyclamine C (**7.17**) and related natural products proved to be complex and required lengthy preparative sequences.<sup>190</sup>

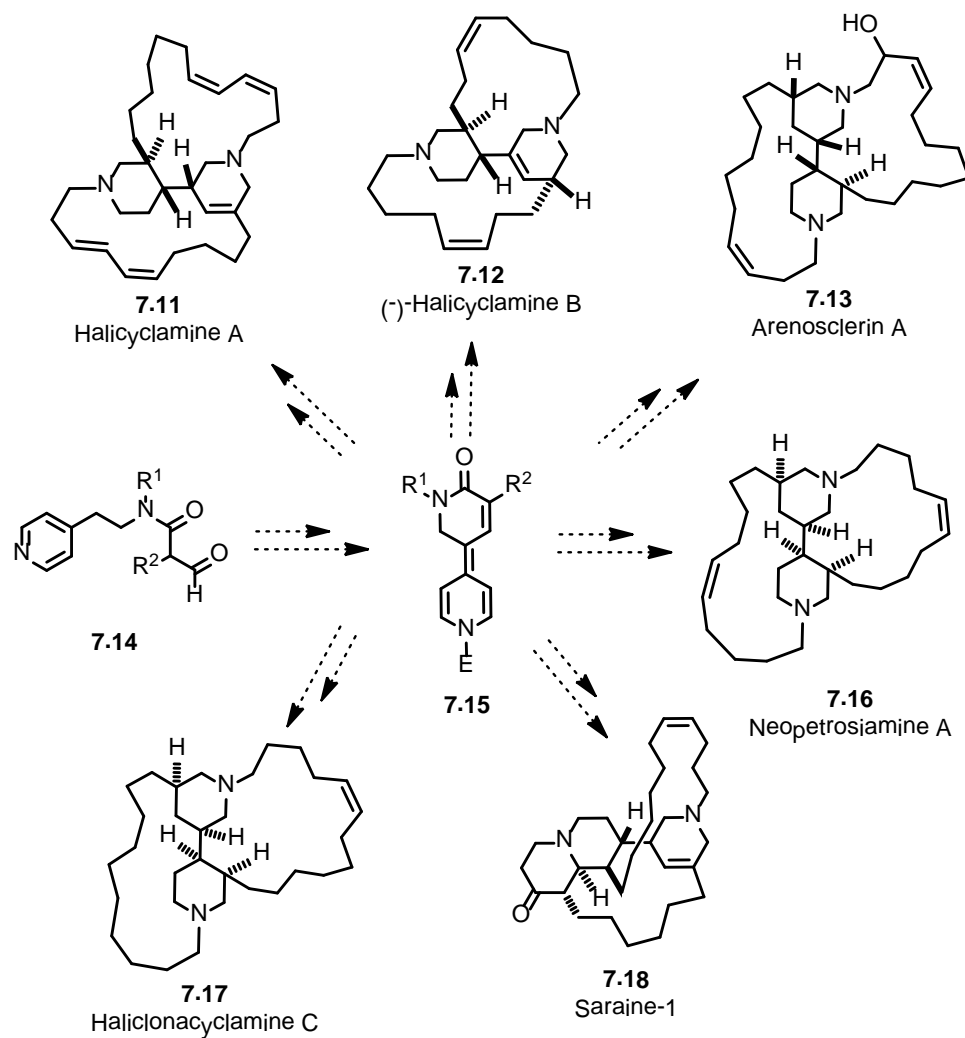


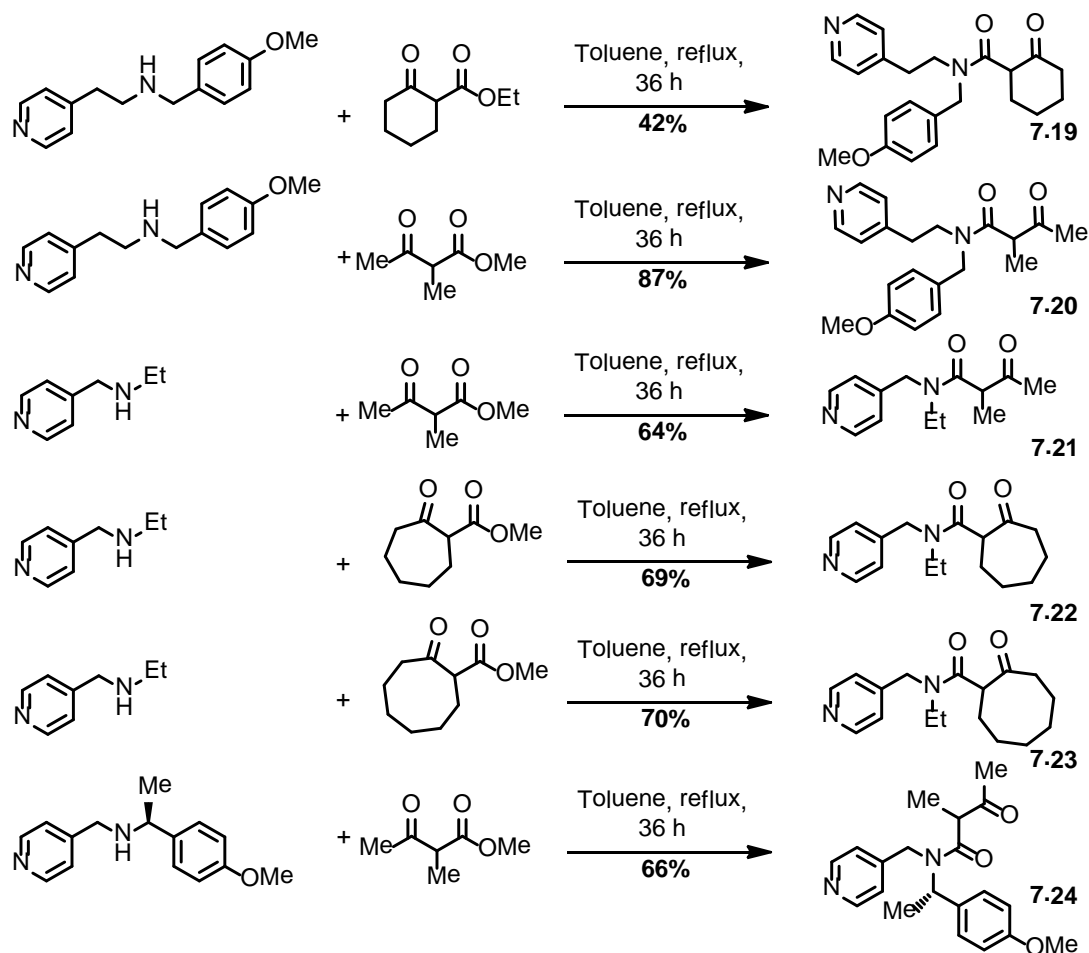
Figure 7.2. Examples of marine alkaloids bearing a bis(piperidine) core structure

Dearomatization of 4-alkylpyridine substrates substituted with appropriate functional groups and their application for the synthesis of natural products such as halicyclamines (**7.11-7.12**) may offer more concise routes to these alkaloid frameworks. To develop a route to synthesize the basic skeleton of these classes

of natural products, a general strategy needs to be established using model substrates. In this regard, 4-alkylpyridine derivatives synthesized for spirocyclization studies (see Chapter Five and Six) were considered as anhydrobase precursors. The preparation of functionalized heterocycles via this approach would then help demonstrate the validity of this synthetic strategy.

## 7.2 Results and discussion

Considering the information available on the synthesis and stability of anhydrobases, it was envisioned that treatment of 4-alkylpyridines substituted with  $\beta$ -keto amides,  $\beta$ -amido esters and other  $\beta$ -dicarbonyl systems should generate anhydrobases under basic conditions which could then be engaged further in intramolecular aldol-like condensation reactions with a tethered electrophilic center. Many of the 4-alkylpyridine substrates used in spirocyclization studies discussed in Chapter Five and Six were also used in the this study. The syntheses of a few new starting materials (**7.19-7.24**) are shown in Scheme 7.4.

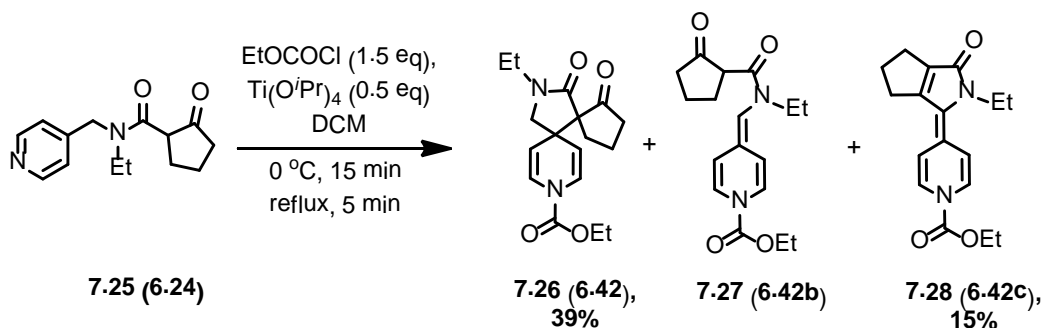


Scheme 7.4. Synthesis of 4-alkylpyridyl substrates

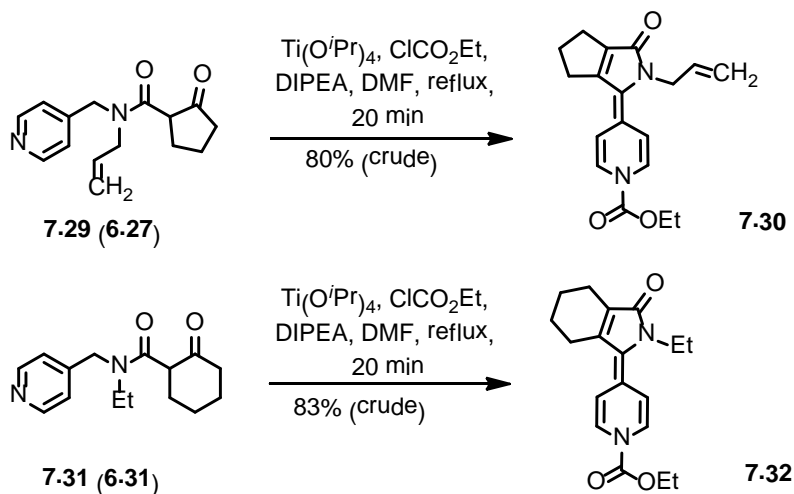
During the course of spirocyclization studies involving substrate **7.25** (**6.24**), it was observed that a new highly colored and less stable product was formed in 15% yield on heating the reaction mixture under vacuum in the rotary evaporator during work up (Scheme 7.5). The new compound formed was isolated and characterized by NMR and mass spectrometry, and was identified as the anhydrobase **7.28**. Initial attempts to exclusively form the anhydrobase **7.28** by increasing reaction time and temperature under reaction conditions shown in Scheme 7.5 were unsuccessful and were always associated with the



competing spirocycle (**7.26**, see also **6.42**) formation. Our attempts to use only basic conditions such as  $K_2CO_3$  or  $KO^tBu$  in THF resulted in formation of the highly unstable and brightly colored intermediate (presumed anhydrobase **7.27**), which gave the corresponding starting material and unidentifiable baseline materials over time and on water workup.

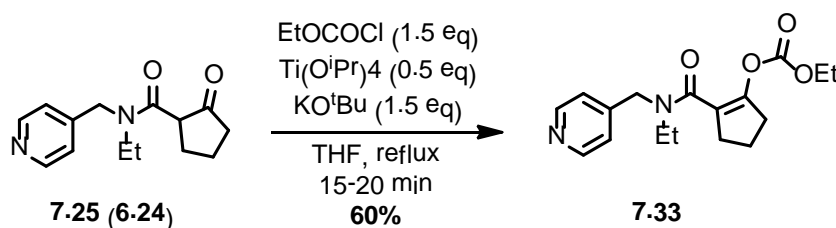


Scheme 7.5. First evidence of anhydrobase formation



Scheme 7.6. Synthesis of highly conjugated anhydrobases of **7.29 (6.27)** and **7.31 (6.31)**

During these studies, it was also observed that the treatment of substrates **7.29** (**6.27**) and **7.31** (**6.31**) with ethyl chloroformate in the presence of  $\text{Ti}(\text{O}^i\text{Pr})_4$  and Hunig's base in DMF as well as in THF at 100 °C yielded the highly colored anhydrobases **7.30** and **7.32**, respectively, in excellent yield as determined by NMR spectroscopy (Scheme 7.6). This result indicates that the presence of Lewis acid activates the carbonyl carbon for further nucleophilic attack from the benzylic position. Our attempts to purify these anhydrobase products (**7.30** and **7.32**) by silica gel and neutral alumina column chromatography, however, were unsuccessful. Hunig's base was also helpful for the formation of anhydrobase **7.28** (according to NMR spectroscopy), whereas  $\text{KO}^t\text{Bu}$  produced **7.33** as the major product on treatment of substrate **7.25** with ethyl chloroformate and titanium isopropoxide in refluxing THF (Scheme 7.7).

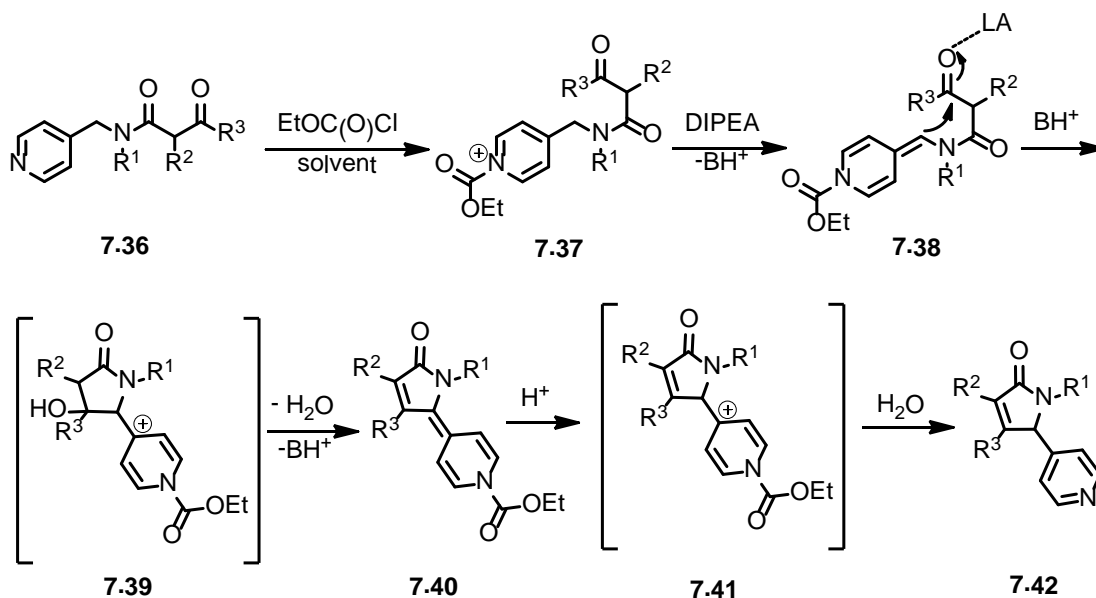


Scheme 7.7. Reactivity of **7.25** (**6.24**) under  $\text{KO}^t\text{Bu}$  condition

Based on these results, particularly, the instability of **7.30** and **7.32** toward conventional purification techniques, we decided to attempt to process anhydrobase intermediates *in situ*. It was envisioned that addition of a proton source to crude reaction mixtures containing benzylically cyclized intermediates would generate new pyridinium salts. Subsequent hydrolysis of the acyl pyridinium group would then give stable substituted pyridine products. It was also



Lewis acids (TMSOTf,  $\text{BF}_3\text{Et}_2\text{O}$  and  $\text{InCl}_3$ ) were successful in generating **7.35**, but isolated yields were lower compared to  $\text{Ti}(\text{O}^i\text{Pr})_4$ -mediated transformations. In examining the data in Table 7.1, optimal conditions for formation of **7.35** entail treatment of **7.34** (**6.33**) with an excess of ethyl chloroformate, a sub-stoichiometric amount of titanium isopropoxide and excess diisopropylamine in refluxing THF for 20 min (entry 1). The putative anhydrobase intermediate is then subjected to protonation by addition of TFA (trifluoroacetic acid) followed by carbamate hydrolysis promoted by addition of  $\text{H}_2\text{O}$ .



Scheme 7.9. Possible mechanism for benzylic condensation

A possible mechanism for this transformation is shown in Scheme 7.9. On activation of pyridine via N-acylation, the pyridinium intermediate (**7.37**) undergoes benzylic deprotonation in the presence of Hunig's base to produce the unstable anhydrobase **7.38**. The nucleophilic benzylic carbon now attacks the appropriately positioned carbonyl carbon activated by the Lewis acid and yields

the corresponding alcohol (**7.39**). Subsequent elimination of water and a second deprotonation offers the highly conjugated (hence colored) anhydrobase **7.40**. Addition of TFA generates a new pyridinium salt (**7.41**), which then undergoes hydrolysis to form functionalized lactam (**7.42**).

Table 7.2. Synthesis of functionalized lactams via benzylic condensation.

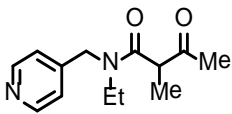
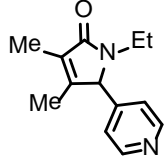
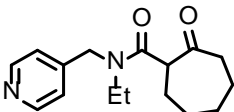
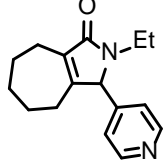
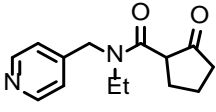
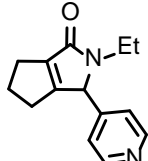
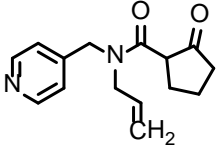
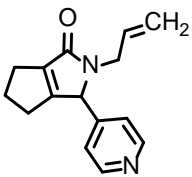
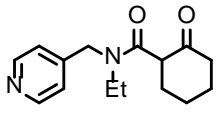
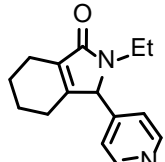
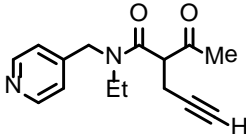
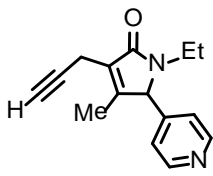
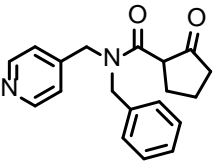
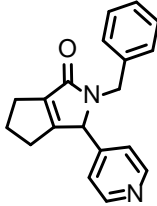
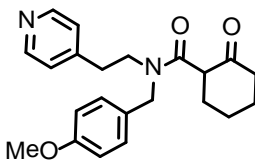
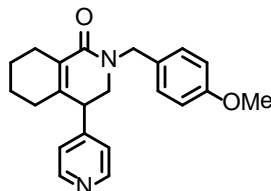
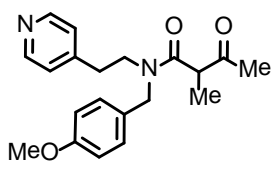
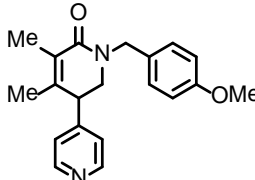
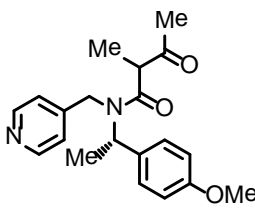
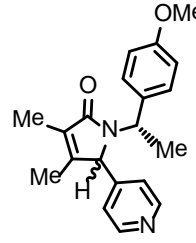
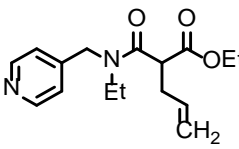
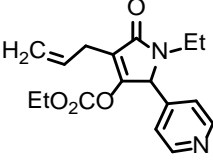
Entry	Substrate	Product	Yield
1	 <p><b>7.21</b></p>	 <p><b>7.43</b></p>	59%
2	 <p><b>7.22</b></p>	 <p><b>7.44</b></p>	42%
3	 <p><b>7.25 (6.24)</b></p>	 <p><b>7.45</b></p>	63%
4	 <p><b>7.29 (6.27)</b></p>	 <p><b>7.46</b></p>	44%
5	 <p><b>7.31 (6.31)</b></p>	 <p><b>7.47</b></p>	68%
6	 <p><b>7.48 (6.34)</b></p>	 <p><b>7.49</b></p>	86%

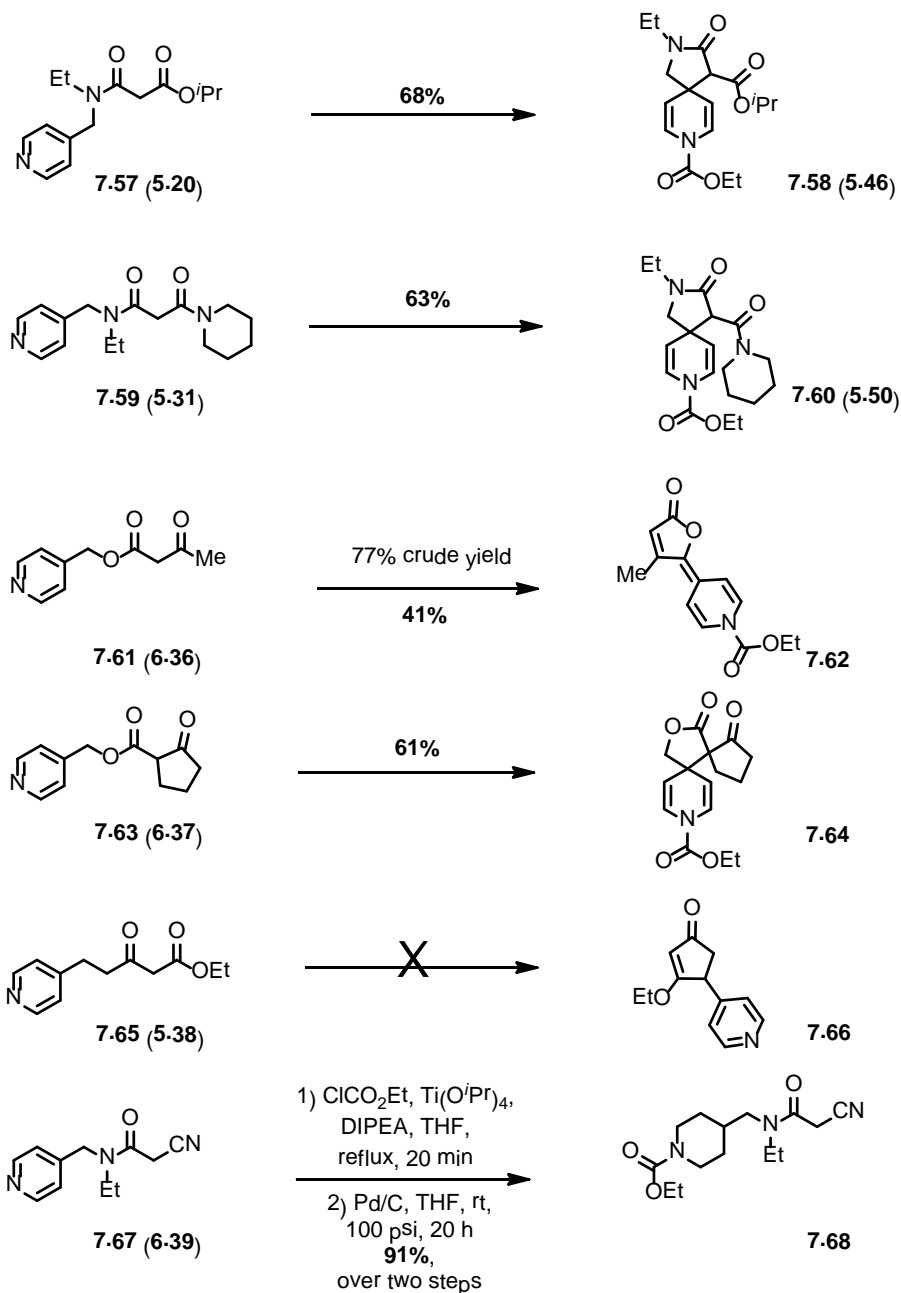
Table 7.2. (Continued)

7	 <p><b>7.50 (6.28)</b></p>	 <p><b>7.51</b></p>	48%
8	 <p><b>7.19</b></p>	 <p><b>7.52</b></p>	68%
9	 <p><b>7.20</b></p>	 <p><b>7.53</b></p>	48%
10	 <p><b>7.24</b></p>	 <p><b>7.54</b></p>	36%
11	 <p><b>7.55 (5.23)</b></p>	 <p><b>7.56</b></p>	62%

Reaction conditions: 1) EtO<sub>2</sub>CCl (1.5 equiv), DIPEA (1.5 equiv), Ti(O<sup>i</sup>Pr)<sub>4</sub> (0.5 equiv), THF, reflux, 20 min. 2) TFA, H<sub>2</sub>O.

The generality of this transformation was next explored by subjecting 4-alkylpyridine substrates substituted with β-dicarbonyl side chains to the optimized

reaction conditions described above and the results are summarized in Table 7.2. The benzylic condensation was found to be general and functionalized pyrrolidinones with different substitutions at  $\alpha$  and  $\beta$  positions of the lactam ring (**7.43-7.56**) were obtained in good yields. These conditions also enabled us to have a removable group such as allyl and benzyl at the nitrogen atom of the lactam. Additionally, under these conditions spirocyclic product formation was found to be minimal (< 10%) and so substrates prone to spirocyclization (such as **7.25**) also could be converted to pyridyl lactams in good yield. 4-(Aminoethyl)pyridine derivatives **7.19** and **7.20** also behaved well in this aldol-like condensation reaction to afford the corresponding substituted pyridines with functionalized  $\delta$ -lactam substituents (**7.52** and **7.53**) in good yield. Significantly, these products resemble the basic bis(piperidine) structural framework found in the macrocyclic marine alkaloids described earlier in this chapter. Substrate **7.24** was prepared to test the effect of a pre-existing chiral center on the diastereoselectivity of anhydrobase protonation. Treatment of **7.24** under optimized reaction conditions gave an inseparable 2.7:1 mixture of diastereomeric pyridyl lactams (**7.54**), although in modest isolated yield. This shows that a chiral substituent on the amide nitrogen has little influence on the protonation of the anhydrobase intermediate after benzylic cyclization. Finally, the ester substrate **7.55** (a compound which failed to undergo spirocyclization earlier) underwent smooth benzylic cyclization to ultimately yield tetramic acid derivative **7.56** in good yield. The enol carbonate moiety in **7.56** presumably arises from reaction of initial cyclization adduct with excess  $\text{EtO}_2\text{CCl}$  or a pyridinium carbamate.

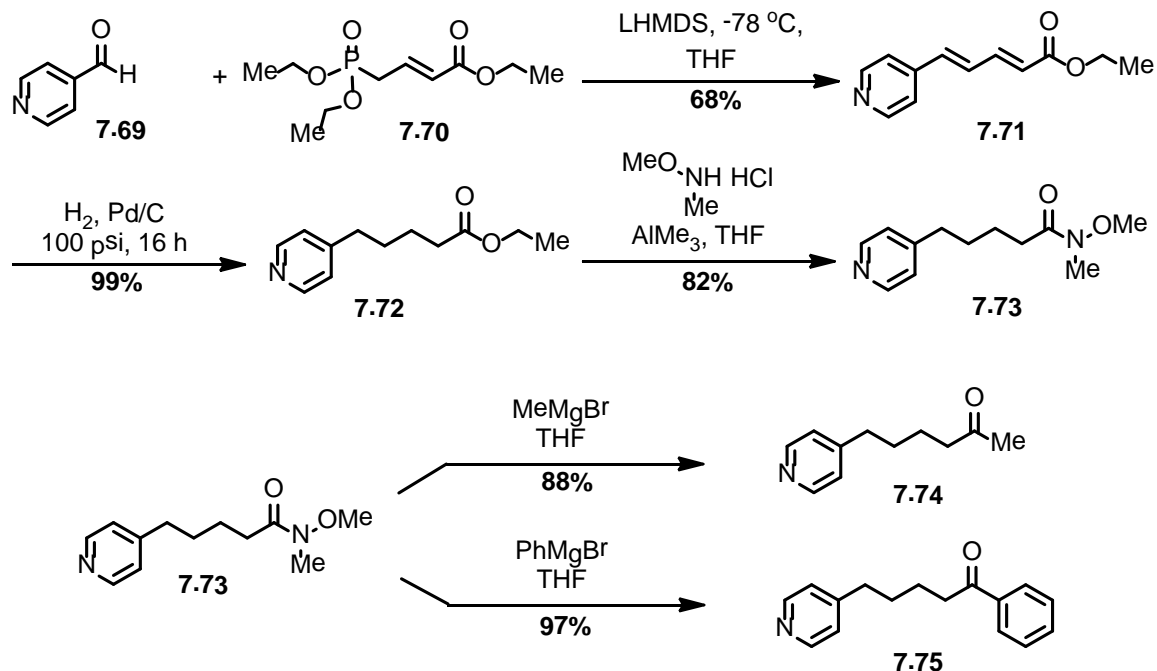


Scheme 7.10. additional substrates subjected to conditions of benzylic cyclization. Reaction conditions: 1)  $\text{EtCO}_2\text{Cl}$  (1.5 equiv), DIPEA (1.5 equiv),  $\text{Ti(O}^i\text{Pr)}_4$  (0.5 equiv), THF, reflux, 20 min. 2) TFA,  $\text{H}_2\text{O}$ .

Several substrates examined in this study behaved differently than shown in Table 7.2. For example, treatment of  $\beta$ -amido ester (7.57 (5.20)) and  $\beta$ -

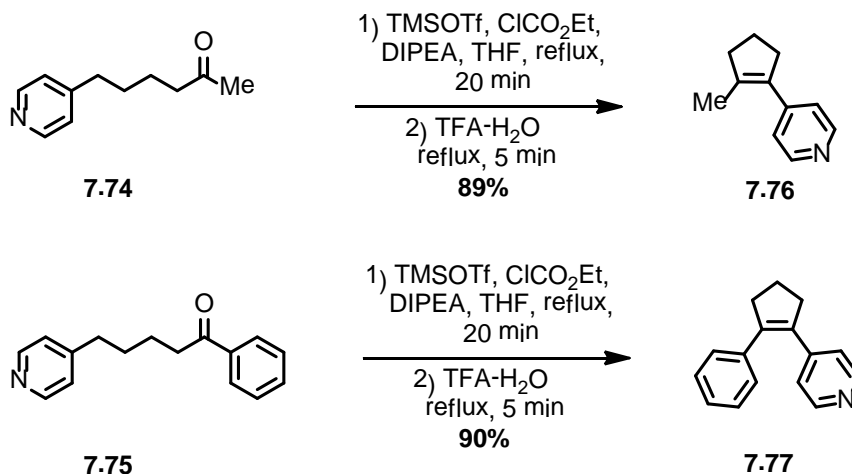


diamide (**7.59** (**5.31**)) substrates according to the procedure outlined in Table 7.2 yielded the corresponding spirocycles **7.58** (**5.48**) and **7.60** (**5.50**) rather than the products of benzylic condensation (Scheme 7.10). 4-alkylpyridines with  $\beta$ -keto ester side chains also behaved differently under these conditions. Acyclic  $\beta$ -keto ester **7.61** (**6.36**) formed a remarkably stable and highly conjugated anhydrobase product (**7.62**) which resisted hydrolysis under acidic conditions. This product was obtained in 77% crude yield, but purification by silica chromatography lowered the isolated yield to 41%. The X-ray crystal structure of **7.62** was also obtained which clearly shows the planar geometry of the highly conjugated product in single crystal (see appendix B). The  $\beta$ -keto ester **7.63** (**6.37**), however, with a cyclopentanone ring in the side chain gave the corresponding spirocycle **7.64** under these same conditions. Interestingly, **7.65** (**5.38**) and related pyridyl esters did not undergo spirocyclization in the absence of base (see Chapter Six). Thus, there appears to be distinct difference in reactivity between pyridyl esters such as **7.63** and pyridyl amides such as **7.25**.  $\beta$ -Keto ester substrate **7.65** also failed to undergo anhydrobase formation/benzylic cyclization and this was attributed to the inappropriate positioning of the electrophilic keto carbonyl center. The  $\beta$ -amido nitrile substrate (**7.67** (**6.39**)) failed to give the corresponding pyrrolidinone product as well but the formation of the presumed anhydrobase intermediate was observed by TLC. So, the reaction mixture after anhydrobase formation was subjected to hydrogenation using Pd/C at 100 psi H<sub>2</sub> for 20 h at room temperature in THF. The completely reduced piperidine moiety **7.68** was obtained and this gave additional proof for the formation of anhydrobase intermediate of these 4-alkylpyridyl substrates. The absence of the cyclization in this instance was attributed to the reduced electrophilicity of the nitrile group.



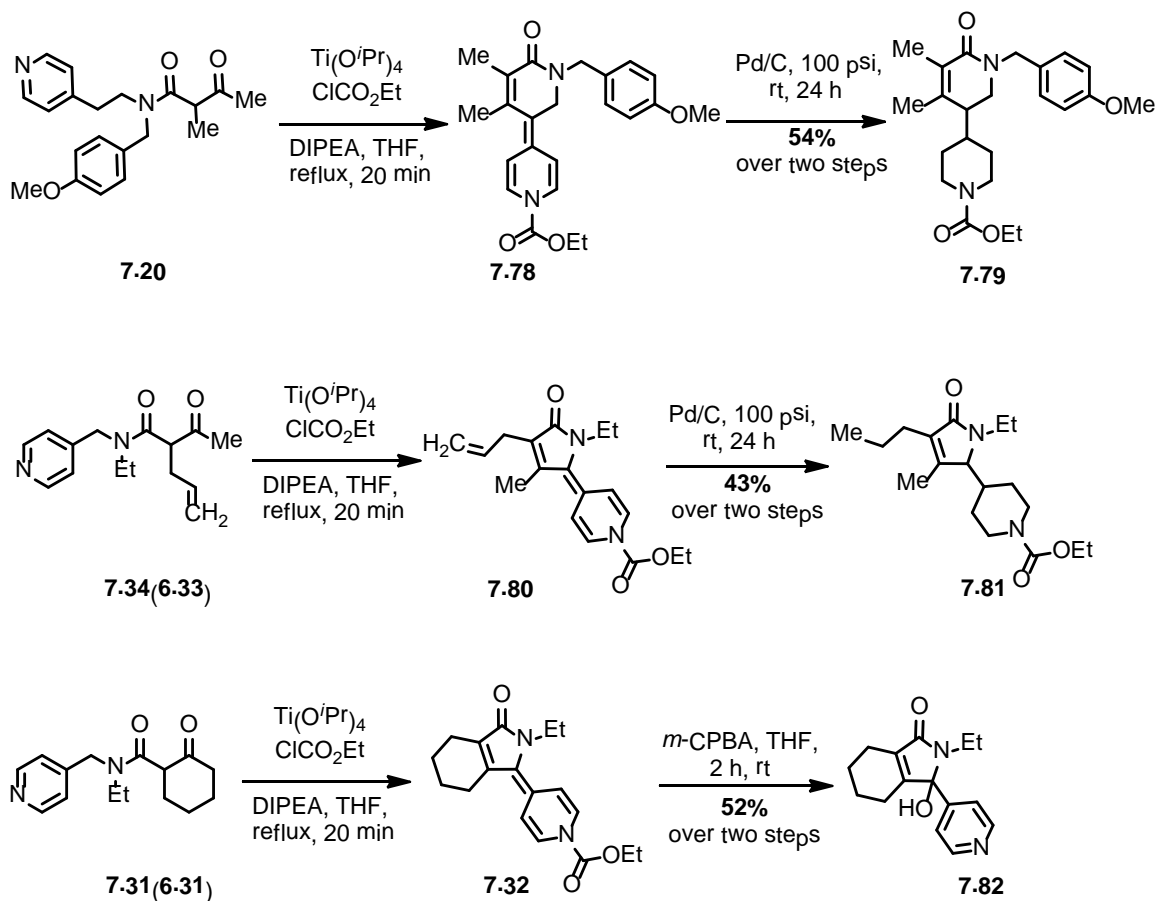
Scheme 7.11. Synthesis of carbon analogues of 4-alkylpyridines

To further investigate the generality of this condensation, carbon analogues possessing keto carbonyl center at appropriate locations relative to pyridine benzylic positions were synthesized as shown in Scheme 7.11. Horner-Wadsworth-Emmons olefination of 4-pyridine carboxaldehyde (**7.69**) with phosphonate **7.70** in the presence of LHMDS in THF yielded the olefin **7.71** which, after hydrogenation, afforded the 4-pyridyl substrate **7.72** in excellent yield. Weinreb amide **7.73** was formed on treatment of **7.72** with N,O-dimethyl hydroxylamine hydrochloride and  $\text{AlMe}_3$ . Methyl ketone **7.74** was synthesized in excellent yield on treatment of the Weinreb amide with methyl magnesium bromide and phenyl ketone **7.75** was obtained by treatment with phenyl magnesium bromide.



Scheme 7.12. Substituted pyridines from carbon analogue condensation

Initially, exposure of **7.74** to anhydrobase condensation reaction conditions developed for cyclization of heteroatom containing side chains (ethyl chloroformate, Ti(O<sup>*i*</sup>Pr)<sub>4</sub> and DIPEA in refluxing THF) gave disappointing results as only a trace amount of desired product was observed by TLC. Fortunately, substituting TMSOTf for Ti(O<sup>*i*</sup>Pr)<sub>4</sub> resulted in formation of the desired product **7.76** in excellent yield (Scheme 7.12). Likewise, substrate **7.75** was converted to cyclopentene **7.77** in similar isolated yield in the presence of TMSOTf. No product formation was observed when **7.74** was treated with TMSOTf or TMSOTf and DIPEA alone in the absence of ClCO<sub>2</sub>Et, indicating that pyridine activation was by N-acylation and not from the Lewis acid.<sup>191</sup> These results demonstrate that anhydrobase condensations of 4-alkyl pyridines possessing appropriately positioned carbonyl groups can be used to access carbocyclic as well as heterocyclic (lactam) pyridine derivatives.



Scheme 7.13. Functionalization of conjugated anhydrobases

The discussion above concerns manipulating anhydrobase intermediates via protonation to allow isolation of stable pyridyl-substituted lactams and cyclopentenones after pyridinium carbamate hydrolysis. The versatility of this general synthetic procedure would be greatly enhanced if alternative means of processing anhydrobase intermediates were available. In particular, hydrogenation of highly unsaturated anhydrobases could provide a remarkably direct route to bis(piperidine) and piperidine-pyrrolidine ring systems. This is significant, especially in the case of bis(piperidine)s, because this structural motif is encountered in numerous bio-active marine natural products (see Figure 7.2).

Thus, elaboration of anhydrobase intermediates via reductive pathways may offer a viable synthetic approach to these interesting alkaloids. With this consideration in mind, pyridine **7.20** was treated with  $\text{EtO}_2\text{CCl}$ ,  $\text{Ti}(\text{O}^i\text{Pr})_4$ , DIPEA to generate a new non-polar compound formulated to be anhydrobase intermediate **7.78**. This crude reaction mixture was then rapidly filtered and the presumed anhydrobase was subjected to catalytic hydrogenation (100 psi  $\text{H}_2$ , Pd/C) for 24 h. Gratifyingly, the partially reduced bis(piperidine) **7.79** was isolated from this reaction mixture in an overall yield of 54% from **7.20**. Evidently, the deactivated lactam olefin is resistant to hydrogenation under these conditions. Nonetheless, the conversion of **7.20** to **7.79** demonstrates the validity of using anhydrobase intermediates to construct bis(piperidine) frameworks, and future work will examine applications of this methodology in target oriented synthesis.

In addition to (aminoethyl)pyridine **7.20**, (aminomethyl)pyridine analogue **7.34 (6.33)** was also subjected to in situ hydrogenation of the corresponding anhydrobase **7.80**. As expected, piperidine **7.81** was obtained in an overall yield comparable to that of **7.79**. Finally, the anhydrobase generated from pyridine **7.31 (6.31)** was processed in the presence of an oxidant in the hopes of also generating tractable reaction products. In the event, treatment of intermediate anhydrobase **7.32** with *m*-CPBA resulted in formation of hydroxylated pyridyl lactam **7.82** in reasonable yield. Alternatively, attempted reactions of **7.32** with hydride reagents (Hantzsch ester,  $\text{Et}_3\text{SiH}$  and  $\text{NaBH}_4$ ) or alkyl electrophile ( $\text{Me}_3\text{O}.\text{BF}_4$ ) were unsuccessful.

### 7.3 Conclusion

An intramolecular aldol-like condensation reaction involving the benzylic position of 4-alkyl pyridines and appropriately positioned ketone electrophiles was developed. The reaction proceeds through activated pyridinium and

anhydrobase intermediates. The 4-alkylpyridine substrates were converted into anhydrobases on treatment with ethyl chloroformate and DIPEA. These intermediates were highly conjugated, colored and unstable. These intermediates were then engaged in intramolecular benzylic cyclization with the assistance of Lewis acid additives. Subsequent addition of TFA resulted in formation of pyridyl-substituted lactams and cyclopentenones. Alternatively, hydrogenation of anhydrobase intermediates afforded bis(piperidine) or linked piperidine-pyrrolidine ring systems.

## 7.4 Experimental section

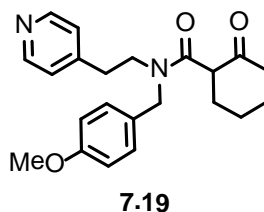
### **General experimental**

All commercially available starting materials and reagents were used as received unless otherwise noted. All the reactions were performed under argon atmosphere. Solvents were dried and purified by passage through activated alumina columns. Proton nuclear magnetic resonance ( $^1\text{H-NMR}$ ) spectra and carbon nuclear magnetic resonance ( $^{13}\text{C-NMR}$ ) spectra were recorded at 300 MHz and 75 MHz respectively. Chemical shifts are reported as  $\delta$  values in parts per million (ppm) relative to tetramethylsilane for  $^1\text{H-NMR}$  in  $\text{CDCl}_3$  and residual undeuterated solvent for all other spectra. The NMR spectra for many of the compounds used in this study reveal the presence of amide rotamers. Resonances corresponding to major and minor isomers are identified when appropriate. IR spectra were recorded on a FT-IR spectrometer as thin films on sodium chloride discs. High resolution mass spectra were obtained using electron spray ionization (ESI). Melting points were recorded using capillary melting point apparatus and are uncorrected.

## Procedures and characterization of 4-alkyl pyridine starting materials

General procedure: Preparation of 4-alkylpyridine with amide side chain. The preparation of **7.19** is representative. A reaction mixture containing 4-[2-(aminoethyl)-N-(*p*-methoxy benzyl)]pyridine (1.00 g, 0.42 mmol, 1 equiv) and ethyl-2-cyclohexanone-carboxylate (0.85 g, 5.00 mmol, 1.2 equiv) in toluene (50 mL) was refluxed for 36 h. The reaction mixture was cooled to room temperature and concentrated in vacuum. The crude product was purified by silica gel column chromatography using 50-80% ethyl acetate in hexanes to afford a brown gummy liquid **7.20** (0.63 g, 42%). The above general procedure was used to synthesize precursors **7.19-7.24** using 1.00-2.00 g of corresponding secondary amines and ester starting materials.

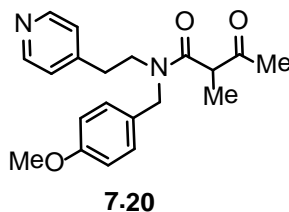
### $\beta$ -keto amide **7.19**



Brown liquid, 42%,  $^1\text{H}$  NMR (300 MHz,  $\text{CDCl}_3$ ),  $\delta$  (ppm), mixture of rotamers: 8.54-8.48 (m, 2H), 7.28-7.24 (m, 2H), 7.04-7.01 (m, 2H), 6.89-6.86 (m, 2H), 4.96-4.91 (m, 0.3H), 4.37-4.29 (m, 1H), 4.11-4.05 (m, 0.7H), 3.94-3.87 (m, 0.7H), 3.80-3.79 (m, 3H), 3.56-3.47 (m, 0.7H), 3.38-3.18 (m, 1.6H), 2.91-2.73 (m, 2H), 2.57-2.52 (m, 1H), 2.35-1.98 (m, 5H), 1.83-1.76 (m, 1H), 1.65-1.46 (m, 1H).  $^{13}\text{C}$  NMR (75 MHz,  $\text{CDCl}_3$ , mixture of rotamers),  $\delta$  (ppm): 207.6, 170.3, 169.9, 159.4, 159.2, 150.3, 150.0, 148.5, 147.5, 129.3, 128.3, 127.8, 124.5, 124.3,

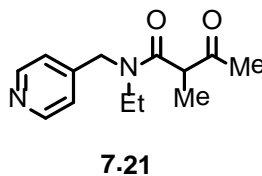
114.6, 114.2, 55.5, 54.7, 54.5, 51.5, 47.8, 47.6, 47.4, 42.1, 42.0, 34.4, 33.4, 30.5, 27.1, 23.8. IR (film): 1704, 1642  $\text{cm}^{-1}$ . HRMS (ESI): calculated for  $\text{C}_{22}\text{H}_{27}\text{N}_2\text{O}_3$  [ $\text{M} + \text{H}$ ] $^+$ , 367.2022; found 367.2040.

### $\beta$ -keto amide 7.20



Brown liquid, 87%,  $^1\text{H}$  NMR (300 MHz,  $\text{CDCl}_3$ ),  $\delta$  (ppm), mixture of rotamers: 8.55-8.48 (m, 2H), 7.19-7.04 (m, 4H), 6.91-6.85 (m, 2H), 4.73-4.68 (m, 0.3H), 4.52-4.44 (m, 1H), 4.31-4.26 (m, 0.7H), 3.80-3.78 (m, 3H), 3.76-3.71 (m, 0.6H), 3.63 (q,  $J = 6.9$  Hz, 0.7H), 3.57-3.44 (m, 1.7H), 2.87-2.77 (m, 2H), 2.12-2.11 (m, 3H), 1.37 (d,  $J = 7.0$  Hz, 2H), 1.32 (d,  $J = 6.9$  Hz, 1H).  $^{13}\text{C}$  NMR (75 MHz,  $\text{CDCl}_3$ , mixture of rotamers),  $\delta$  (ppm): 205.1, 171.0, 170.4, 159.6, 150.4, 150.1, 148.0, 146.9, 129.6, 129.3, 128.2, 127.8, 124.4, 124.2, 114.7, 114.4, 55.5, 52.1, 51.9, 51.6, 48.2, 47.5, 34.5, 33.4, 27.4, 27.0, 14.2. IR (film): 1726, 1633  $\text{cm}^{-1}$ . HRMS (ESI): calculated for  $\text{C}_{20}\text{H}_{25}\text{N}_2\text{O}_3$  [ $\text{M} + \text{H}$ ] $^+$ , 341.1865; found 341.1858.

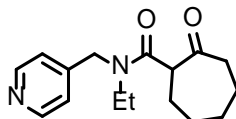
### $\beta$ -keto amide 7.21





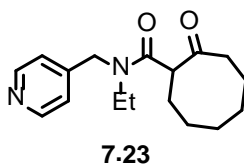
Brown liquid, 64%,  $^1\text{H}$  NMR (300 MHz,  $\text{CDCl}_3$ ),  $\delta$  (ppm), mixture of rotamers: 8.63-8.54 (m, 2H), 7.17-7.12 (m, 2H), 4.78-4.70 (m, 1H), 4.49-4.42 (m, 1H), 3.77-3.70 (q,  $J = 7.0$  Hz, 0.7H), 3.67-3.60 (m, 0.3H), 3.50-3.38 (m, 1H), 3.34-3.22 (m, 1H), 2.24-2.13 (m, 3H), 1.47 (d,  $J = 7.0$  Hz, 2.1H), 1.37 (d,  $J = 7.0$  Hz, 0.9H), 1.21 (t,  $J = 7.1$  Hz, 2.1H), 1.15 (t,  $J = 7.1$  Hz, 0.9H).  $^{13}\text{C}$  NMR (75 MHz,  $\text{CDCl}_3$ , mixture of rotamers),  $\delta$  (ppm): 205.4, 170.7, 170.4, 150.6, 150.2, 146.7, 146.3, 122.5, 121.3, 52.2, 51.5, 50.0, 47.7, 42.8, 42.0, 27.5, 27.1, 14.3, 12.6. IR (film): 1722, 1637  $\text{cm}^{-1}$ . HRMS (ESI): calculated for  $\text{C}_{13}\text{H}_{19}\text{N}_2\text{O}_2$   $[\text{M} + \text{H}]^+$ , 235.1447; found 235.1471.

### **$\beta$ -keto amide 7.22**

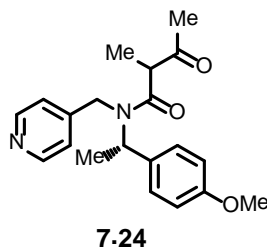


**7.22**

Brown liquid, 69%,  $^1\text{H}$  NMR (300 MHz,  $\text{CDCl}_3$ ),  $\delta$  (ppm), mixture of rotamers: 8.62-8.53 (m, 2H), 7.18-7.14 (m, 2H), 4.92-4.80 (m, 1H), 4.46-4.32 (m, 1H), 3.78-3.73 (m, 0.7H), 3.59-3.44 (m, 1.3H), 3.27-3.17 (m, 1H), 2.89-2.80 (m, 1H), 2.61-2.42 (m, 1H), 2.24-1.90 (m, 6H), 1.57-1.37 (m, 3H), 1.22-1.09 (m, 3H).  $^{13}\text{C}$  NMR (75 MHz,  $\text{CDCl}_3$ , mixture of rotamers),  $\delta$  (ppm): 211.1, 170.8, 170.2, 150.4, 150.1, 146.9, 146.6, 122.3, 121.5, 57.2, 56.5, 50.0, 47.7, 43.3, 42.9, 41.9, 30.4, 28.5, 28.4, 27.8, 25.8, 25.5, 14.4, 12.7. IR (film): 1699, 1642  $\text{cm}^{-1}$ . HRMS (ESI): calculated for  $\text{C}_{16}\text{H}_{23}\text{N}_2\text{O}_2$   $[\text{M} + \text{H}]^+$ , 275.1760; found 275.1776.

**$\beta$ -keto amide 7.23**

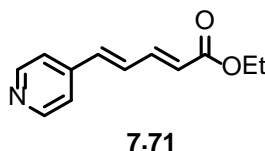
Brown liquid, 70%,  $^1\text{H}$  NMR (300 MHz,  $\text{CDCl}_3$ ),  $\delta$  (ppm), mixture of rotamers: 8.62-8.52 (m, 2H), 7.13-7.06 (m, 2H), 5.03-4.97 (m, 0.3H), 4.70-4.65 (m, 0.7H), 4.45-4.39 (m, 1H), 3.69-3.53 (m, 1.7H), 3.41-3.12 (m, 1.3H), 3.11-3.02 (m, 1H), 2.68-2.53 (m, 1H), 2.33-2.17 (m, 1.4H), 1.96-1.39 (m, 8H), 1.22-1.06 (m, 3.6H).  $^{13}\text{C}$  NMR (75 MHz,  $\text{CDCl}_3$ , mixture of rotamers),  $\delta$  (ppm): 214.3, 169.9, 169.2, 150.4, 150.1, 146.9, 146.5, 122.3, 121.4, 58.1, 57.3, 49.8, 47.8, 42.8, 41.8, 39.1, 38.6, 29.4, 29.1, 27.6, 27.1, 25.9, 25.6, 24.7, 24.6, 14.3, 12.7. IR (film): 1690, 1637  $\text{cm}^{-1}$ . HRMS (ESI): calculated for  $\text{C}_{17}\text{H}_{25}\text{N}_2\text{O}_2$   $[\text{M} + \text{H}]^+$ , 289.1916; found 289.1938.

 **$\beta$ -keto amide 7.24**

Brown liquid, 66%,  $^1\text{H}$  NMR (300 MHz,  $\text{CDCl}_3$ ),  $\delta$  (ppm): 8.56-8.39 (m, 2H), 7.25-7.02 (m, 3H), 6.96-6.78 (m, 3H), 6.21- 6.08 (m, 0.4H), 5.30-5.19 (m, 0.6H), 4.79- 3.90 (m, 2.6H), 3.81-3.76 (m, 3H), 3.33-3.22 (m, 0.4H), 2.25 (d,  $J =$

9.4 Hz, 1.7H), 2.15 (d,  $J = 6.0$  Hz, 1.3H), 1.54-1.48 (m, 4H), 1.42-1.32 (m, 2H).  
 $^{13}\text{C}$  NMR (75 MHz,  $\text{CDCl}_3$ ),  $\delta$  (ppm): 205.7, 204.9, 171.3, 171.0, 159.5, 150.4, 150.2, 149.9, 149.8, 148.1, 148.0, 132.4, 131.9, 131.1, 129.2, 128.8, 128.6, 127.9, 122.2, 122.13, 121.1, 121.0, 114.5, 114.3, 114.2, 114.1, 55.7, 55.6, 55.5, 52.8, 52.4, 52.1, 51.8, 51.6, 46.1, 45.7, 45.4, 27.7, 27.6, 27.2, 19.2, 17.2, 17.1, 14.5, 14.1. IR (film): 1722, 1637  $\text{cm}^{-1}$ . HRMS (ESI): calculated for  $\text{C}_{20}\text{H}_{25}\text{N}_2\text{O}_3$  [ $\text{M} + \text{H}$ ] $^+$ , 341.1865; found 341.1883.

#### 4-alkylpyridine-olefin 7.71

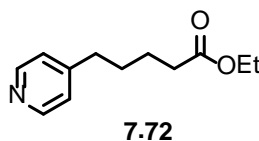


LHMDS (1.0 M solution, 26.4 mL, 1.1 equiv) was added to a reaction mixture containing commercially available 4-triethyl phosphono crotonate **7.70** (6.00 g, 24.0 mmol, 1 equiv) in THF at 0 °C and stirred for 45 min. Then 4-pyridine carboxaldehyde (2.57 g, 24.0 mmol, 1 equiv) was added and the reaction mixture was warmed to room temperature and maintained overnight. Saturated aq. ammonium chloride was added to the reaction mixture, which was then extracted with ethyl acetate (3 X 5 mL) and the combined organic layer was washed with water (10 mL) and brine (5 mL). The organic layer was dried over sodium sulfate, filtered and evaporated in vacuo. The crude product was purified by silica gel column chromatography using 50-70% ethyl acetate in hexanes to yield **7.70**, brown liquid, (4.3 g, 88%).

$^1\text{H}$  NMR (300 MHz,  $\text{CDCl}_3$ ),  $\delta$  (ppm): 8.60 (d,  $J = 4.6$  Hz, 2H), 7.43 (dd,  $J = 15.3, 11.0$  Hz, 1H), 7.31 (d,  $J = 4.5$  Hz, 2H), 7.03 (dd,  $J = 15.6, 10.9$  Hz, 1H),

6.81 (d,  $J = 15.6$  Hz, 1H), 6.09 (d,  $J = 15.2$  Hz, 1H), 4.25 (q,  $J = 7.2$  Hz, 2H), 1.32 (t,  $J = 7.1$  Hz, 3H).  $^{13}\text{C}$  NMR (75 MHz,  $\text{CDCl}_3$ ),  $\delta$  (ppm): 166.7, 150.6, 143.3, 143.2, 137.3, 130.6, 124.3, 121.3, 60.8, 14.5. IR (film):  $1694\text{ cm}^{-1}$ . HRMS (ESI): calculated for  $\text{C}_{12}\text{H}_{14}\text{NO}_2$   $[\text{M} + \text{H}]^+$ , 204.1025; found 204.1050.

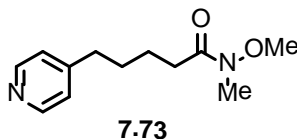
#### 4-Alkylpyridine ester 7.72



Substrate **7.71** (4.0 g) was taken in ethanol (5 mL) and 10% Pd/C was added (10 mg). The resulting mixture was hydrogenated at 100 psi for 14 h and then filtered through Celite bed. The filtrate was evaporated in vacuo and dried to afford **7.72** as brown liquid (4.0 g, 99%).

$^1\text{H}$  NMR (300 MHz,  $\text{CDCl}_3$ ),  $\delta$  (ppm): 8.49 (d,  $J = 6.1$  Hz, 2H), 7.10 (d,  $J = 5.9$  Hz, 2H), 4.13 (q,  $J = 7.1$  Hz, 2H), 2.65-2.61 (m, 2H), 2.35-2.31 (m, 2H), 1.70-1.65 (m, 4H), 1.25 (t,  $J = 7.2$  Hz, 3H).  $^{13}\text{C}$  NMR (75 MHz,  $\text{CDCl}_3$ ),  $\delta$  (ppm): 173.6, 151.2, 149.9, 124.0, 60.5, 35.1, 34.2, 29.8, 24.6, 14.4. IR (film):  $1654\text{ cm}^{-1}$ . HRMS (ESI): calculated for  $\text{C}_{12}\text{H}_{18}\text{NO}_2$   $[\text{M} + \text{H}]^+$ , 208.1338; found 208.1366.

#### 4-Alkylpyridine-weinreb amide 7.73



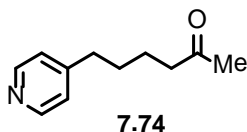
$\text{AlMe}_3$  (2.80 mL, 56 mmol, 4 equiv) was added dropwise to a reaction mixture containing N,O-dimethyl hydroxylamine hydrochloride (5.46 g, 56 mmol, 4 equiv) in THF at  $-78\text{ }^\circ\text{C}$  and the resulting mixture was stirred for 45 min. Substrate **7.72** (2.90 g, 14 mmol, 1 equiv) was added to the reaction mixture and stirred for 16 h more. Saturated aq. ammonium chloride was added to the reaction mixture and then extracted with ethyl acetate (3 X 5 mL) and the combined organic layer was washed with water (10 mL) and brine (5 mL). The organic layer was dried over sodium sulfate, filtered and evaporated in vacuo. The crude product was purified by silica gel column chromatography using 50-70% ethyl acetate in hexanes to yield brown colored Weinreb amide **7.73** (2.6 g, 82%).

$^1\text{H}$  NMR (300 MHz,  $\text{CDCl}_3$ ),  $\delta$  (ppm): 8.48 (d,  $J = 6.0$  Hz, 2H), 7.12 (d,  $J = 6.0$  Hz, 2H), 7.31 (d,  $J = 4.5$  Hz, 2H), 3.67 (s, 3H), 3.18 (s, 3H), 2.66-2.62 (m, 2H), 2.47-2.44 (m, 2H), 1.69 (quintet,  $J = 3.6$  Hz, 4H).  $^{13}\text{C}$  NMR (75 MHz,  $\text{CDCl}_3$ ),  $\delta$  (ppm): 174.3, 151.3, 149.8, 124.0, 61.3, 35.2, 32.3, 31.7, 30.1, 24.3. IR (film):  $1654\text{ cm}^{-1}$ . HRMS (ESI): calculated for  $\text{C}_{12}\text{H}_{19}\text{N}_2\text{O}_2$   $[\text{M} + \text{H}]^+$ , 223.1447; found 223.1470.

#### 4-Alkylpyridine-methyl ketone **7.74**

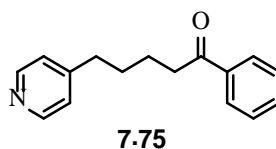
Methyl magnesium bromide (3.0 M solution in THF, 1.1 mL, 3.3 mmol, 1.5 equiv) was added dropwise to a reaction mixture containing Weinreb amide **7.73** (0.50 g, 2.2 mmol, 1 equiv) in THF (25 mL) at  $0\text{ }^\circ\text{C}$ . The reaction mixture was warmed to room temperature and stirred for 16 h. Saturated aq. ammonium chloride was added to the reaction mixture and then extracted with ethyl acetate (3 X 5 mL) and the combined organic layer was washed with water (10 mL) and brine (5 mL). The organic layer was dried over sodium sulfate, filtered and

evaporated in vacuo. The crude product was purified by silica gel column chromatography using 50-70% ethyl acetate in hexanes to get brown liquid **7.74** (0.34 g, 88%).



$^1\text{H}$  NMR (300 MHz,  $\text{CDCl}_3$ ),  $\delta$  (ppm): 8.48 (d,  $J = 5.8$  Hz, 2H), 7.10 (d,  $J = 5.8$  Hz, 2H), 2.62 (t,  $J = 7.0$  Hz, 2H), 2.46 (t,  $J = 6.6$  Hz, 2H), 2.13 (s, 3H), 1.63 (quintet,  $J = 3.6$  Hz, 4H).  $^{13}\text{C}$  NMR (75 MHz,  $\text{CDCl}_3$ ),  $\delta$  (ppm): 208.7, 151.2, 149.9, 124.0, 43.5, 35.2, 30.1, 29.9, 23.4. IR (film):  $1708\text{ cm}^{-1}$ . HRMS (ESI): calculated for  $\text{C}_{11}\text{H}_{16}\text{NO}$   $[\text{M} + \text{H}]^+$ , 178.1232; found 178.1262.

#### 4-Alkylpyridine-phenyl ketone **7.75**

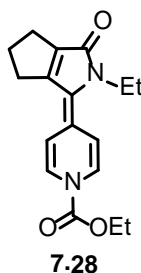


Using the above procedure with  $\text{PhMgBr}$  in the place of  $\text{MeMgBr}$ , **7.73** (0.60 g) was converted into brown liquid **7.75**, in 97%,  $^1\text{H}$  NMR (300MHz,  $\text{CDCl}_3$ ),  $\delta$  (ppm): 8.48 (d,  $J = 6.3$  Hz, 2H), 7.97-7.94 (m, 2H), 7.59-7.54 (m, 1H), 7.49-7.44 (m, 2H), 7.12 (d,  $J = 6.1$  Hz, 2H), 3.01 (t,  $J = 6.7$  Hz, 2H), 2.67 (t,  $J = 7.6$  Hz, 2H), 21.83-1.69 (m, 4H).  $^{13}\text{C}$  NMR (75MHz,  $\text{CDCl}_3$ ),  $\delta$  (ppm): 200.1, 151.2, 149.9, 137.0, 133.2, 128.8, 128.2, 124.0, 38.3, 35.3, 30.1, 23.9. IR (film):  $1681\text{ cm}^{-1}$ . HRMS (ESI): calculated for  $\text{C}_{16}\text{H}_{18}\text{NO}$   $[\text{M} + \text{H}]^+$ , 240.1388; found 240.1415.

## Synthesis of anhydrobases

General procedure: Preparation of **7.32** is representative. Titanium isopropoxide ((58  $\mu\text{L}$ , 0.2 mmol, 0.5 equiv) and diisopropylethylamine (95  $\mu\text{L}$ , 0.58 mmol, 1.5 equiv) were added to a reaction mixture of **7.31** (0.10 g, 0.38 mmol, 1 equiv) in THF (3 mL) and refluxed with a preheated oil bath at 80  $^{\circ}\text{C}$  for 2 min. Ethyl chloroformate (55  $\mu\text{L}$ , 0.58 mmol, 1.5 equiv) was added to the refluxing reaction mixture which immediately turned to dark brown color. The resulting mixture was refluxed for 20-30 min more and cooled to room temperature and basified with sat. aq.  $\text{Na}_2\text{CO}_3$ . Reaction mixture was then extracted with ethyl acetate (3 X 5 mL) and the combined organic layer was washed with water (10 mL) and brine solution (5 mL). The organic layer was dried over sodium sulfate, filtered and concentrated in vacuo to yield the crude anhydrobase product **7.32** (0.10 g, 83%, crude yield).

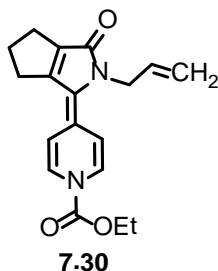
### Anhydrobase 7.28



Brown liquid, 15%,  $^1\text{H}$  NMR (300 MHz,  $\text{CDCl}_3$ ),  $\delta$  (ppm): 7.22 (d,  $J = 8.3$  Hz, 1H), 7.10 (d,  $J = 8.04$  Hz, 1H), 6.32 (d,  $J = 9.0$  Hz, 1H), 6.29 (d,  $J = 8.9$  Hz, 1H), 4.37 (q,  $J = 7.2$  Hz, 2H), 3.88 (q,  $J = 7.1$  Hz, 2H), 2.86-2.81 (m, 2H), 2.59-2.54 (m, 2H), 2.41-2.34 (m, 2H), 1.38 (t,  $J = 7.1$  Hz, 3H), 1.22 (t,  $J = 7.1$  Hz, 3H).

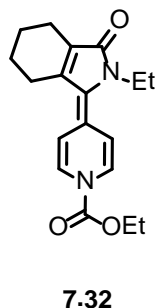
$^{13}\text{C}$  NMR (75 MHz,  $\text{CDCl}_3$ ),  $\delta$  (ppm): 166.9, 152.4, 150.4, 137.4, 127.5, 125.0, 112.7, 109.6, 64.3, 37.2, 31.8, 28.3, 25.4, 15.9, 14.5. HRMS (ESI): calculated for  $\text{C}_{17}\text{H}_{21}\text{N}_2\text{O}_3$   $[\text{M} + \text{H}]^+$ , 301.1552; found 301.1569.

### Anhydrobase 7.30



Using the procedure given above 0.10 g of **7.29** was converted to **7.30**, brown liquid in 80% (crude yield),  $^1\text{H}$  NMR (300 MHz,  $\text{CDCl}_3$ ),  $\delta$  (ppm): 7.16-7.12 (m, 2H), 6.35-6.27 (m, 2H), 6.01-5.89 (m, 1H), 5.23-5.11 (m, 2H), 4.44-4.42 (m, 2H), 4.36 (q,  $J = 7.1$  Hz, 2H), 2.89-2.84 (m, 2H), 2.62-2.58 (m, 2H), 2.43-2.36 (m, 4H), 1.37 (t,  $J = 7.1$  Hz, 3H).  $^{13}\text{C}$  NMR (75 MHz,  $\text{CDCl}_3$ ),  $\delta$  (ppm): 166.8, 152.6, 150.3, 136.8, 135.0, 127.2, 125.3, 124.1, 117.6, 116.1, 112.5, 109.6, 64.2, 44.7, 31.7, 28.3, 25.5, 14.5. HRMS (ESI): calculated for  $\text{C}_{18}\text{H}_{21}\text{N}_2\text{O}_3$   $[\text{M} + \text{H}]^+$ , 313.1552; found 313.1566.

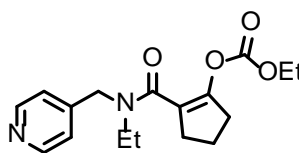
### Anhydrobase 7.32





Brown liquid, 83% (crude yield),  $^1\text{H}$  NMR (300 MHz,  $\text{CDCl}_3$ ),  $\delta$  (ppm): 7.20 (d,  $J = 8.1$  Hz, 1H), 7.12 (d,  $J = 7.9$  Hz, 1H), 6.36 (d,  $J = 8.6$  Hz, 1H), 6.30 (d,  $J = 8.3$  Hz, 1H), 4.37 (q,  $J = 7.1$  Hz, 2H), 3.84 (q,  $J = 7.1$  Hz, 2H), 2.56-2.54 (m, 2H), 2.36-2.34 (m, 2H), 1.77-1.65 (m, 4H), 1.38 (t,  $J = 7.2$  Hz, 3H), 1.22 (t,  $J = 7.1$  Hz, 3H).  $^{13}\text{C}$  NMR (75 MHz,  $\text{CDCl}_3$ ),  $\delta$  (ppm): 171.1, 150.4, 141.9, 128.2, 127.6, 126.4, 125.0, 116.8, 112.4, 110.7, 64.1, 37.7, 27.0, 23.6, 21.8, 21.3, 15.2, 14.5. IR (film): 1731, 1642  $\text{cm}^{-1}$ . HRMS (ESI): calculated for  $\text{C}_{18}\text{H}_{23}\text{N}_2\text{O}_3$   $[\text{M} + \text{H}]^+$ , 315.1709; found 315.1731.

#### 4-Substituted pyridine-ene carbonate 7.33



7.33

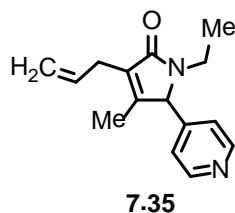
Ethyl chloroformate (66  $\mu\text{L}$ , 0.61 mmol, 1.5 equiv) and titanium isopropoxide (61  $\mu\text{L}$ , 0.20 mmol, 0.5 equiv) were added to a reaction mixture containing **7.25** (0.10 g, 0.41 mmol, 1 equiv) and  $\text{KO}^t\text{Bu}$  (68 mg, 0.61 mmol, 1.5 equiv) in THF (3 mL). The resulting mixture was refluxed for 20-30 min and TFA (10 equiv) was added. Reaction mixture was refluxed for 10 min more and cooled to room temperature and basified with saturated aq.  $\text{Na}_2\text{CO}_3$ . Reaction mixture was extracted with ethyl acetate (3 X 5 mL) and the combined organic layer was washed with water (10 mL) and brine (5 mL). The organic layer was dried over sodium sulfate, filtered and evaporated in vacuo. Crude product was purified using silica gel column chromatography using 70-90% ethyl acetate in hexanes to yield pale brown gummy liquid **7.33** (78 mg, 60%).

$^1\text{H}$  NMR (500 MHz,  $\text{CDCl}_3$ ),  $\delta$  (ppm), mixture of rotamers: 8.57- 8.54 (m, 2H), 7.19-7.15 (m, 2H), 4.66-4.57 (m, 2H), 4.24-4.10 (m, 2H), 3.40-3.35 (m, 2H), 2.75-2.56 (m, 4H), 2.08-1.95 (m, 2H), 1.33-1.30 (m, 3H), 1.13-1.11 (m, 3H).  $^{13}\text{C}$  NMR (125 MHz,  $\text{CDCl}_3$ , mixture of rotamers),  $\delta$  (ppm): 167.5, 151.9, 150.3, 150.1, 148.5, 146.8, 122.6, 122.1, 120.8, 65.2, 61.8, 50.4, 46.1, 42.9, 39.7, 31.6, 31.4, 31.3, 31.2, 29.9, 20.7, 20.4, 14.4, 14.3, 12.3. IR (film): 1690, 1637  $\text{cm}^{-1}$ . HRMS (ESI): calculated for  $\text{C}_{17}\text{H}_{23}\text{N}_2\text{O}_4$   $[\text{M} + \text{H}]^+$ , 319.1658; found 319.1680.

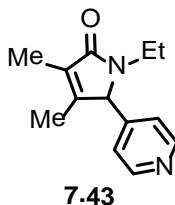
### Synthesis of substituted pyridines

General procedure: Preparation of **7.35** is representative. Titanium isopropoxide (57  $\mu\text{L}$ , 0.19 mmol, 0.5 equiv) and diisopropylethylamine (0.10 mL, 0.58 mmol, 1.5 equiv) were added to a reaction mixture of **7.34** (0.10 g, 0.38 mmol, 1 equiv) in THF (2 mL) and refluxed with a preheated oil bath for 2 min. Ethyl chloroformate (55  $\mu\text{L}$ , 0.58 mmol, 1.5 equiv) was added to the refluxing reaction mixture which immediately turned to dark brown color and the resulting mixture was refluxed for 20-30 min. TFA (10 equiv) was added to the reaction mixture and refluxed for 5 min followed by addition of water (2 mL). The resulting mixture was then refluxed for 10-15 min more before cooled to room temperature and basified with saturated aq.  $\text{Na}_2\text{CO}_3$ . Reaction mixture was then extracted with ethyl acetate (3 X 5 mL) and the combined organic layer was washed with water (10 mL) and brine (5 mL). The organic layer was dried over sodium sulfate, filtered and concentrated in vacuo. Crude product was purified using silica gel column chromatography using 70-90% ethyl acetate in hexanes to afford brown liquid **7.35** (87 mg, 94%).

The above procedure was used to prepare all other substituted pyridines using 0.05-0.10 g of the corresponding starting materials.

**4-Substituted pyridine-pyrrolidinone 7.35**

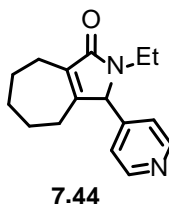
Brown liquid, 94%,  $^1\text{H}$  NMR (300 MHz,  $\text{CDCl}_3$ ),  $\delta$  (ppm): 8.62 (d,  $J = 5.9$  Hz, 2H), 7.1 (d,  $J = 6$  Hz, 2H), 5.96-5.82 (m, 1H), 5.09-5.02 (m, 2H), 4.78 (s, 1H), 3.87-3.75 (m, 1H), 3.09 (d,  $J = 6.2$  Hz, 2H), 2.88-2.76 (m, 1H), 1.74 (s, 3H), 1.05 (t,  $J = 7.1$  Hz, 3H).  $^{13}\text{C}$  NMR (75 MHz,  $\text{CDCl}_3$ ),  $\delta$  (ppm): 171.7, 150.5, 150.1, 145.9, 134.3, 131.0, 122.5, 115.8, 66.6, 35.3, 27.9, 13.8, 12.1. IR (film): 1681  $\text{cm}^{-1}$ . HRMS (ESI): calculated for  $\text{C}_{15}\text{H}_{19}\text{N}_2\text{O}$   $[\text{M} + \text{H}]^+$ , 243.1497; found 243.1520.

**4-Substituted pyridine-pyrrolidinone 7.43**

Brown liquid, 59%,  $^1\text{H}$  NMR (300 MHz,  $\text{CDCl}_3$ ),  $\delta$  (ppm): 8.62 (d,  $J = 5.5$  Hz, 2H), 7.08 (d,  $J = 5.9$  Hz, 2H), 4.73 (s, 1H), 3.88-3.76 (m, 1H), 2.86-2.74 (m, 1H), 1.87 (s, 3H), 1.72 (s, 3H), 1.05 (t,  $J = 7.2$  Hz, 3H).  $^{13}\text{C}$  NMR (75 MHz,  $\text{CDCl}_3$ ),  $\delta$  (ppm): 172.5, 150.6, 148.5, 146.0, 129.3, 122.6, 66.5, 35.3, 13.9, 12.1,

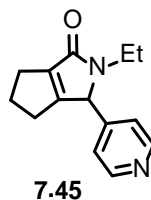
8.9. IR (film): 1685  $\text{cm}^{-1}$ . HRMS (ESI): calculated for  $\text{C}_{13}\text{H}_{17}\text{N}_2\text{O}$   $[\text{M} + \text{H}]^+$ , 217.1341; found 217.1371.

#### 4-Substituted pyrrolidinone 7.44



Brown liquid, 42%,  $^1\text{H}$  NMR (300 MHz,  $\text{CDCl}_3$ ),  $\delta$  (ppm): 8.61 (d,  $J = 5.1$  Hz, 2H), 7.09 (d,  $J = 5.9$  Hz, 2H), 4.73 (s, 1H), 3.83-3.72 (m, 1H), 2.83-2.72 (m, 1H), 2.57-2.50 (m, 2H), 2.28 (m, 2.20 9m, 1H), 2.05-1.94 (m, 1H), 1.76-1.71 (m, 2H), 1.64-1.61 (m, 3H), 1.43-1.35 (m, 1H), 1.04 (t,  $J = 7.3$  Hz, 3H).  $^{13}\text{C}$  NMR (75 MHz,  $\text{CDCl}_3$ ),  $\delta$  (ppm): 172.2, 154.8, 150.5, 145.7, 135.2, 122.8, 66.1, 35.3, 30.9, 28.7, 27.2, 27.1, 25.0, 13.9. IR (film): 1681  $\text{cm}^{-1}$ . HRMS (ESI): calculated for  $\text{C}_{16}\text{H}_{21}\text{N}_2\text{O}$   $[\text{M} + \text{H}]^+$ , 257.1654; found 257.1661.

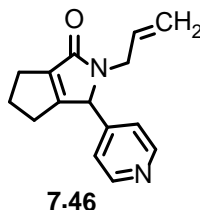
#### 4-Substituted pyrrolidinone 7.45



Brown liquid, 63%,  $^1\text{H}$  NMR (300 MHz,  $\text{CDCl}_3$ ),  $\delta$  (ppm): 8.62 (d,  $J = 5.9$  Hz, 2H), 7.11 (d,  $J = 6.0$  Hz, 2H), 4.97 (s, 1H), 3.88-3.76 (m, 1H), 2.90-2.79 (m, 1H), 2.61-2.12 (m, 6H), 1.08 (t,  $J = 7.2$  Hz, 3H).  $^{13}\text{C}$  NMR (75 MHz,  $\text{CDCl}_3$ ),  $\delta$

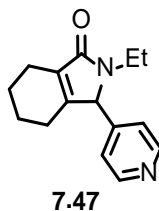
(ppm): 168.6, 164.3, 150.6, 145.1, 142.3, 122.0, 62.2, 35.6, 28.2, 27.5, 26.0, 14.0. IR (film): 1685  $\text{cm}^{-1}$ . HRMS (ESI): calculated for  $\text{C}_{14}\text{H}_{17}\text{N}_2\text{O}$   $[\text{M} + \text{H}]^+$ , 229.1341; found 229.1368.

#### 4-Substituted pyrrolidinone 7.46



Brown liquid, 44%,  $^1\text{H}$  NMR (300 MHz,  $\text{CDCl}_3$ ),  $\delta$  (ppm): 8.61 (d,  $J = 6.1$  Hz, 2H), 7.07 (d,  $J = 6.0$  Hz, 2H), 5.80-5.67 (m, 1H), 5.14-4.93 (m, 3H), 4.56-4.49 (m, 1H), 3.22 (dd,  $J = 15.6, 7.7$  Hz, 1H), 2.62-2.14 (m, 6H).  $^{13}\text{C}$  NMR (75 MHz,  $\text{CDCl}_3$ ),  $\delta$  (ppm): 168.7, 164.9, 150.7, 145.1, 142.3, 133.6, 122.3, 118.1, 62.3, 43.5, 28.4, 27.6, 26.2. IR (film): 1685  $\text{cm}^{-1}$ . HRMS (ESI): calculated for  $\text{C}_{15}\text{H}_{17}\text{N}_2\text{O}$   $[\text{M} + \text{H}]^+$ , 241.1341; found 241.1362.

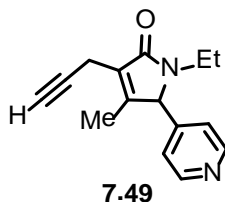
#### 4-Substituted pyrrolidinone 7.47



Brown liquid, 64%,  $^1\text{H}$  NMR (300 MHz,  $\text{CDCl}_3$ ),  $\delta$  (ppm): 8.61 (d,  $J = 5.9$  Hz, 2H), 7.08 (d,  $J = 6.0$  Hz, 2H), 4.80 (s, 1H), 3.89-3.77 (m, 1H), 2.89-2.78 (m, 1H), 2.30-2.11 (m, 3H), 1.82- 1.59 (m, 5H), 1.06 (t,  $J = 7.2$  Hz, 3H).  $^{13}\text{C}$  NMR (75

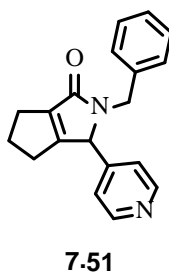
MHz,  $\text{CDCl}_3$ ),  $\delta$  (ppm): 171.8, 152.9, 150.7, 145.9, 132.2, 122.3, 65.7, 35.1, 23.0, 22.2, 21.8, 20.4, 14.0. IR (film):  $1681\text{ cm}^{-1}$ . HRMS (ESI): calculated for  $\text{C}_{15}\text{H}_{19}\text{N}_2\text{O}$   $[\text{M} + \text{H}]^+$ , 243.1497; found 243.1515.

#### 4-Substituted pyridine-pyrrolidinone 7.49



Brown liquid, 86%,  $^1\text{H}$  NMR (300 MHz,  $\text{CDCl}_3$ ),  $\delta$  (ppm): 8.64 (d,  $J = 5.9$  Hz, 2H), 7.1 (d,  $J = 6.1$  Hz, 2H), 4.78 (s, 1H), 3.87-3.75 (m, 1H), 3.29-3.28 (m, 2H), 2.88-2.76 (m, 1H), 2.04 (t,  $J = 2.8$  Hz, 1H), 1.88 (s, 3H), 1.06 (t,  $J = 7.2$  Hz, 3H).  $^{13}\text{C}$  NMR (75 MHz,  $\text{CDCl}_3$ ),  $\delta$  (ppm): 170.6, 151.1, 150.7, 145.2, 127.9, 122.5, 79.9, 69.2, 66.6, 35.3, 13.8, 13.5, 12.2. IR (film):  $1681\text{ cm}^{-1}$ . HRMS (ESI): calculated for  $\text{C}_{15}\text{H}_{17}\text{N}_2\text{O}$   $[\text{M} + \text{H}]^+$ , 241.1341; found 241.1361.

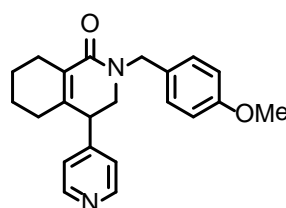
#### 4-Substituted pyridine-pyrrolidinone 7.51



Brown liquid, 48%,  $^1\text{H}$  NMR (300 MHz,  $\text{CDCl}_3$ ),  $\delta$  (ppm): 8.61 (d,  $J = 5.9$  Hz, 2H), 7.29-7.25 (m, 3H), 7.12-7.09 (m, 2H), 7.01 (d,  $J = 6.1$  Hz, 2H), 5.20 (d,  $J$

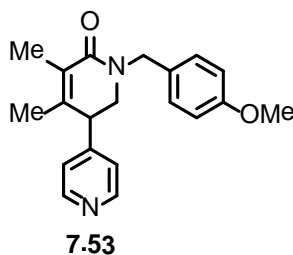
= 15 Hz, 1H), 4.70 (s, 1H), 3.65 (d,  $J = 15.1$  Hz, 1H), 2.65-2.58 (m, 2H), 2.46-2.26 (m, 3H), 2.19-2.11 (m, 1H).  $^{13}\text{C}$  NMR (75 MHz,  $\text{CDCl}_3$ ),  $\delta$  (ppm): 168.8, 165.0, 150.8, 144.8, 142.1, 137.5, 128.9, 128.4, 127.7, 122.3, 61.9, 44.5, 28.4, 27.6, 26.2. IR (film):  $1690\text{ cm}^{-1}$ . HRMS (ESI): calculated for  $\text{C}_{19}\text{H}_{19}\text{N}_2\text{O}$   $[\text{M} + \text{H}]^+$ , 291.1497; found 291.1494.

#### 4-Substituted pyridine-piperidone derivative 7.52

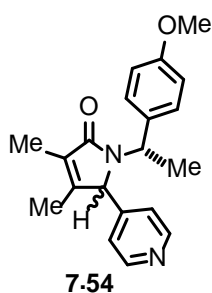


7.52

Brown liquid, 68%,  $^1\text{H}$  NMR (300 MHz,  $\text{CDCl}_3$ ),  $\delta$  (ppm): 8.44 (d,  $J = 5.9$  Hz, 2H), 6.98 (d,  $J = 6.0$  Hz, 2H), 6.91 (d,  $J = 8.6$  Hz, 2H), 6.65 (d,  $J = 8.6$  Hz, 2H), 4.62 (d,  $J = 14.5$  Hz, 1H), 4.23 (d,  $J = 14.5$  Hz, 1H), 3.78-3.72 (m, 4H), 3.23-3.22 (m, 1H), 3.16 (dd,  $J = 12.3, 2.9$  Hz, 1H), 2.66-2.58 (m, 1H), 2.44-2.31 (m, 1H), 2.11-2.05 (m, 1H), 1.95-1.88 (m, 1H), 1.76-1.53 (m, 4H).  $^{13}\text{C}$  NMR (75 MHz,  $\text{CDCl}_3$ ),  $\delta$  (ppm): 165.3, 158.9, 150.1, 149.2, 143.8, 129.9, 129.5, 128.8, 123.2, 113.8, 55.4, 50.5, 49.3, 44.1, 29.4, 23.8, 22.4, 22. IR (film):  $1659\text{ cm}^{-1}$ . HRMS (ESI): calculated for  $\text{C}_{22}\text{H}_{25}\text{N}_2\text{O}_2$   $[\text{M} + \text{H}]^+$ , 349.1916; found 349.1923.

**4-Substituted pyridine-piperidone derivative 7.53**

Brown liquid, 48%,  $^1\text{H}$  NMR (300 MHz,  $\text{CDCl}_3$ ),  $\delta$  (ppm): 8.44 (d,  $J = 5.9$  Hz, 2H), 6.96 (d,  $J = 6.1$  Hz, 2H), 6.91 (d,  $J = 8.6$  Hz, 2H), 6.65 (d,  $J = 8.6$  Hz, 2H), 4.61 (d,  $J = 14.5$  Hz, 1H), 4.22 (d,  $J = 14.5$  Hz, 1H), 3.81-3.68 (m, 4H), 3.28 (s, br, 1H), 3.14 (dd,  $J = 12.4, 2.8$  Hz, 1H), 2.04 (s, 3H), 1.78 (s, 3H).  $^{13}\text{C}$  NMR (75 MHz,  $\text{CDCl}_3$ ),  $\delta$  (ppm): 165.5, 159.1, 150.2, 149.0, 141.5, 129.6, 128.9, 128.4, 123.3, 113.9, 55.4, 50.4, 49.6, 45.4, 19.5, 12.9. IR (film): 1659  $\text{cm}^{-1}$ . HRMS (ESI): calculated for  $\text{C}_{20}\text{H}_{23}\text{N}_2\text{O}_2$   $[\text{M} + \text{H}]^+$ , 323.1760; found 323.1760.

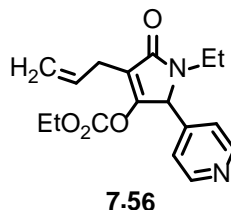
**4-Substituted pyridine-pyrrolidinone 7.54**

Brown liquid, 36%,  $^1\text{H}$  NMR (300 MHz,  $\text{CDCl}_3$ ),  $\delta$  (ppm), mixture of diastereomers (2.7:1), Major isomer: 8.56 (d,  $J = 5.7$  Hz, 2H), 7.08-7.00 (m, 2H), 6.95 (d,  $J = 6.0$  Hz, 2H), 6.85 (d,  $J = 8.8$  Hz, 2H), 5.54 (q,  $J = 7.3$  Hz, 1H), 4.26

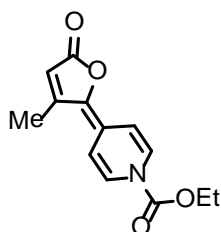


(s, 1H), 3.82 (s, 3H), 1.88-1.86 (m, 3H), 1.52 (s, 3H), 1.17 (d,  $J = 7.3$  Hz, 3H).  
 Minor isomer: 8.35 (d,  $J = 5.7$  Hz, 2H), 7.08-7.00 (m, 2H), 6.78 (d,  $J = 5.8$  Hz, 2H), 6.60 (d,  $J = 8.7$  Hz, 2H), 5.08 (q,  $J = 7.2$  Hz, 1H), 4.64 (s, 1H), 3.71 (s, 3H), 1.88-1.86 (m, 3H), 1.66 (d,  $J = 7.2$  Hz, 3H), 1.59 (s, 3H),  $^{13}\text{C}$  NMR (75 MHz,  $\text{CDCl}_3$ ),  $\delta$  (ppm), mixture of diastereomers: 173.4, 173.2, 159.2, 159.0, 150.4, 150.0, 149.6, 149.1, 147.8, 146.5, 133.4, 132.8, 129.4, 128.9, 128.8, 122.9, 122.7, 114.0, 113.6, 66.3, 65.5, 55.5, 51.4, 50.6, 18.8, 18.3, 12.1, 12.0, 9.0, 8.96. IR (film):  $1668\text{ cm}^{-1}$ . HRMS (ESI): calculated for  $\text{C}_{20}\text{H}_{23}\text{N}_2\text{O}_2$   $[\text{M} + \text{H}]^+$ , 323.1760; found 323.1780.

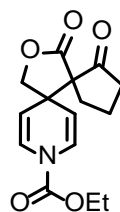
#### 4-Substituted pyridine-pyrrolidinone 7.56



Brown liquid, 62%,  $^1\text{H}$  NMR (300 MHz,  $\text{CDCl}_3$ ),  $\delta$  (ppm): 8.63 (d,  $J = 6.0$  Hz, 2H), 7.14 (d,  $J = 6.1$  Hz, 2H), 5.95-5.82 (m, 1H), 5.36 (m, 1H), 5.17-5.06 (m, 2H), 4.2 (q,  $J = 7.2$  Hz, 2H), 3.85-3.73 (m, 1H), 3.10-3.07 (m, 2H), 2.91-2.79 (m, 1H), 1.27 (t,  $J = 7.1$  Hz, 3H), 1.07 (t,  $J = 7.2$  Hz, 3H).  $^{13}\text{C}$  NMR (75 MHz,  $\text{CDCl}_3$ ),  $\delta$  (ppm): 169.6, 158.5, 151.1, 150.8, 143.5, 133.1, 122.9, 120.4, 116.9, 66.0, 61.9, 35.3, 27.0, 14.1, 13.8. IR (film):  $1766, 1690\text{ cm}^{-1}$ . HRMS (ESI): calculated for  $\text{C}_{17}\text{H}_{21}\text{N}_2\text{O}_4$   $[\text{M} + \text{H}]^+$ , 317.1501; found 317.1501.

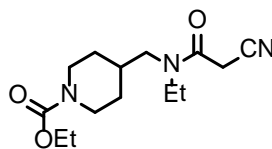
**Anhydrobase 7.62****7.62**

Using the general procedure for the substituted pyridines given above, **7.62** was obtained from 0.10 g of **7.61** as orange-brownish colored crystalline solid, 41% (77%, crude yield),  $^1\text{H}$  NMR (300 MHz,  $\text{CDCl}_3$ ),  $\delta$  (ppm): 7.37 (d,  $J = 6.5$  Hz, 1H), 7.35 (d,  $J = 6.4$  Hz, 1H), 6.54 (dd,  $J = 8.4, 2.2$  Hz, 1H), 6.34 (dd,  $J = 8.5, 2.2$  Hz, 1H), 5.70 (d,  $J = 1.08$  Hz, 1H), 4.40 (q,  $J = 7.1$  Hz, 2H), 2.3 (s, 3H), 1.40 (t,  $J = 7.1$  Hz, 3H).  $^{13}\text{C}$  NMR (75 MHz,  $\text{CDCl}_3$ ),  $\delta$  (ppm): 169.7, 151.4, 150.2, 137.4, 128.2, 127.8, 119.8, 113.0, 110.4, 108.2, 64.7, 15.9, 14.4. IR (film): 1717, 1650  $\text{cm}^{-1}$ . HRMS (ESI): calculated for  $\text{C}_{13}\text{H}_{14}\text{NO}_4$   $[\text{M} + \text{H}]^+$ , 248.0923; found 248.0931.

**Spirocycle 7.64****7.64**

Using the general procedure for the substituted pyridines given above, **7.64** was obtained from 0.10 g of **7.63** as pale yellowish liquid, 61%,  $^1\text{H}$  NMR (300 MHz,  $\text{CDCl}_3$ ),  $\delta$  (ppm), mixture of rotamers: 7.05 (br s, 2H), 4.80-4.72 (m, 2H), 4.52 (d,  $J = 8.7$  Hz, 1H), 4.30 (q,  $J = 7.1$  Hz, 2H), 4.07 (d,  $J = 8.7$  Hz, 1H), 2.45-2.33 (m, 2H), 2.26-2.06 (m, 3H), 1.97-1.88 (m, 1H), 1.35 (t,  $J = 7.1$  Hz, 3H).  $^{13}\text{C}$  NMR (75 MHz,  $\text{CDCl}_3$ , mixture of rotamers),  $\delta$  (ppm): 212.8, 173.8, 151.0, 127.2, 124.2, 106.3, 102.4, 67.4, 63.6, 47.4, 39.8, 29.3, 19.9, 14.5. IR (film): 1775, 1734, 1685  $\text{cm}^{-1}$ . HRMS (ESI): calculated for  $\text{C}_{15}\text{H}_{17}\text{N}_2\text{O}_5 \text{Na}$   $[\text{M} + \text{Na}]^+$ , 314.1004; found 314.1022.

#### 4-Substituted piperidine derivative 7.68



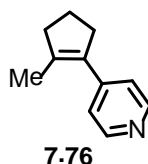
**7.68**

Titanium isopropoxide (74  $\mu\text{L}$ , 0.25 mmol, 0.5 equiv) and diisopropylethylamine (0.12 mL, 0.74 mmol, 1.5 equiv) were added to a reaction mixture of **7.67** (0.10 g, 0.49 mmol, 1 equiv) in THF (5 mL) and refluxed with a preheated oil bath for 2 min. Ethyl chloroformate (71  $\mu\text{L}$ , 0.74 mmol, 1.5 equiv) was added to the refluxing reaction mixture which immediately turned to dark brown color. Resulting mixture was refluxed for 20-30 min before cooled to room temperature and then passed through a plug of basic alumina. The filtrate was then subjected to hydrogenation at 100 psi pressure for 24 h using 10% Pd/C (10 mg) as the catalyst. The resulting mixture was then filtered through Celite bed and concentrated in vacuo. The crude product was purified by silica gel column

chromatography using 70% ethyl acetate in hexanes to afford brown liquid **7.68** (126 mg, 91%).

$^1\text{H}$  NMR (300MHz,  $\text{CDCl}_3$ ),  $\delta$  (ppm): 4.25-4.07 (m, 4H), 3.56 (s, 1.3H), 3.53 (s, 0.7H), 3.50-3.12 (m, 4H), 2.72 (t,  $J = 12.3$  Hz, 2H), 1.94-1.86 (m, 1H), 1.71-1.61 (m, 2H), 1.29-1.12 (m, 8H).  $^{13}\text{C}$  NMR (75MHz,  $\text{CDCl}_3$ ),  $\delta$  (ppm): 161.8, 161.5, 155.5, 155.4, 114.3, 61.4, 61.2, 53.6, 51.3, 44.1, 43.6, 42.1, 35.9, 34.7, 29.8, 25.3, 25.1, 14.7, 13.9, 12.4. IR (film): 2256, 1690, 1655  $\text{cm}^{-1}$ . HRMS (ESI): calculated for  $\text{C}_{14}\text{H}_{23}\text{N}_2\text{O}_3$   $\text{Na}[\text{M} + \text{Na}]^+$ , 304.1637; found 304.1651.

#### 4-Substituted pyridine-pyrrolidinone 7.76

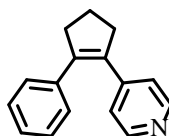


TMSOTf (52  $\mu\text{L}$ , 0.28 mmol, 0.5 equiv) and diisopropylethylamine (0.14 mL, 0.85 mmol, 1.5 equiv) were added to a reaction mixture of **7.74** (0.10 g, 0.56 mmol, 1 equiv) in THF (2 mL) and refluxed with a preheated oil bath at 80  $^{\circ}\text{C}$  for 2 min. Ethyl chloroformate (81  $\mu\text{L}$ , 0.85 mmol, 1.5 equiv) was added to the refluxing reaction mixture which immediately turned to dark brown color. The resulting mixture was refluxed for 20-30 min and TFA (10 equiv) was added to it. Reaction mixture was refluxed for 10 min more before cooled to room temperature and basified with saturated aq.  $\text{Na}_2\text{CO}_3$ . Reaction mixture was extracted with ethyl acetate (3 X 5 mL) and the combined organic layer was washed with water (10 mL) and brine (5 mL). The organic layer was dried over sodium sulfate, filtered and concentrated in vacuo. Crude product was purified

using silica gel column chromatography using 70-90% ethyl acetate in hexanes to yield brown liquid **7.76** (80 mg, 89%).

$^1\text{H}$  NMR (300 MHz,  $\text{CDCl}_3$ ),  $\delta$  (ppm): 8.54 (d,  $J = 4.9$  Hz, 2H), 7.18 (d,  $J = 6.0$  Hz, 2H), 2.78-2.69 (m, 2H), 2.55-2.50 (m, 2H), 1.96-1.86 (m, 4H).  $^{13}\text{C}$  NMR (75 MHz,  $\text{CDCl}_3$ ),  $\delta$  (ppm): 149.7, 146.2, 140.3, 132.7, 122.4, 40.6, 36.5, 21.9, 15.8. HRMS (ESI): calculated for  $\text{C}_{11}\text{H}_{14}\text{N}$   $[\text{M} + \text{H}]^+$ , 160.1126; found 160.1148.

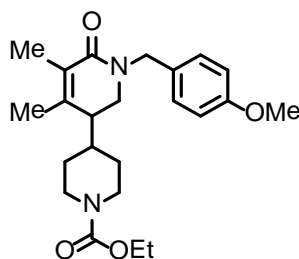
#### 4-Substituted pyridine-pyrrolidinone **7.77**



**7.77**

The procedure given above was used to convert 0.10 g of **7.75** to brown colored liquid **7.77** in 90%,  $^1\text{H}$  NMR (300 MHz,  $\text{CDCl}_3$ ),  $\delta$  (ppm): 8.39 (d,  $J = 5.9$  Hz, 2H), 7.27-7.19 (m, 3H), 7.17-7.13 (m, 3H), 7.02 (d,  $J = 6.2$  Hz, 2H), 2.93-2.88 (m, 4H), 2.07 (p,  $J = 6.6$  Hz, 2H).  $^{13}\text{C}$  NMR (75 MHz,  $\text{CDCl}_3$ ),  $\delta$  (ppm): 150.1, 149.7, 146.0, 142.6, 137.8, 134.7, 128.6, 128.1, 127.5, 122.9, 40.0, 38.1, 22.2. HRMS (ESI): calculated for  $\text{C}_{16}\text{H}_{16}\text{N}$   $[\text{M} + \text{H}]^+$ , 222.1283; found 222.1291.

#### 4-Substituted bis(piperidine) derivative **7.79**

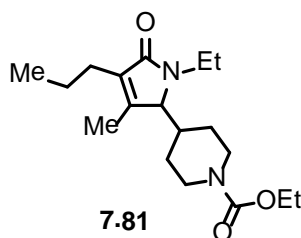


**7.79**

Titanium isopropoxide (44  $\mu$ L, 0.15 mmol, 0.5 equiv) and diisopropylethylamine (73  $\mu$ L, 0.44 mmol, 1.5 equiv) were added to a reaction mixture of **7.20** (0.10 g, 0.29 mmol, 1 equiv) in THF (5 mL) and refluxed with a preheated oil bath at 80  $^{\circ}$ C for 2 min. Ethyl chloroformate (42  $\mu$ L, 0.44 mmol, 1.5 equiv) was added to the refluxing reaction mixture which immediately turned to dark brown color. The resulting mixture was refluxed for 20-30 min before cooled to room temperature and then passed through a plug of basic alumina. The filtrate was then subjected to hydrogenation at 100 psi pressure for 24 h using 10% Pd/C (10 mg) as the catalyst. The resulting mixture was then filtered through Celite bed and concentrated in vacuo. The crude product was purified by silica gel column chromatography using 70% ethyl acetate in hexanes to afford brown liquid **7.79** (64 mg, 54%).

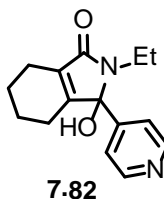
Brown liquid, 54%,  $^1\text{H}$  NMR (300 MHz,  $\text{CDCl}_3$ ),  $\delta$  (ppm): 7.25-7.12 (m, 2H), 6.88-6.78 (m, 2H), 4.94-4.88 (m, 1H), 4.21-4.01 (m, 4H), 3.94-3.92 (m, 1.4H), 3.81-3.72 (m, 3.6H), 3.40 (dd,  $J = 12.9, 4.7$  Hz, 1H), 3.12 (dd,  $J = 12.8, 1.4$  Hz, 1H), 2.54- 2.45 (m, 1H), 2.28-2.20 (m, 1H), 2.00 (s, 0.4H), 1.90 (s, 2.6H), 1.86 (s, 3H), 1.72-1.69 (m, 1H), 1.46-1.39 (m, 2H), 1.29-1.10 (m, 4H), 0.91-0.78 (m, 1H).  $^{13}\text{C}$  NMR (75 MHz,  $\text{CDCl}_3$ ),  $\delta$  (ppm): 165.5, 159.3, 155.5, 144.3, 130.4, 129.8, 126.5, 114.1, 61.3, 55.5, 49.5, 45.3, 45.1, 44.3, 44.1, 37.6, 30.7, 29.7, 21.6, 14.9, 13.0. IR (film): 1690, 1655  $\text{cm}^{-1}$ . HRMS (ESI): calculated for  $\text{C}_{23}\text{H}_{33}\text{N}_2\text{O}_4$   $[\text{M} + \text{H}]^+$ , 401.2440; found 401.2438.

#### 4-Substituted piperidine-pyrrolidinone 7.81



Using the procedure given above **7.34** was converted to brown liquid **7.81** in 43%,  $^1\text{H}$  NMR (300 MHz,  $\text{CDCl}_3$ ),  $\delta$  (ppm): 4.25-4.17 (m, 2H), 4.13 (q,  $J = 7.1$  Hz, 2H), 3.91-3.84 (m, 1H), 3.82 (s, 1H), 3.15-3.03 (m, 1H), 2.70-2.62 (m, 2H), 2.29-2.12 (m, 2H), 2.02-1.91 (m, 4H), 1.52-1.45 (m, 6H), 1.26 (t,  $J = 7.1$  Hz, 3H), 1.13 (t,  $J = 7.2$  Hz, 3H), 0.89 (t,  $J = 7.3$  Hz, 3H).  $^{13}\text{C}$  NMR (75 MHz,  $\text{CDCl}_3$ ),  $\delta$  (ppm): 172.2, 155.6, 148.1, 134.6, 66.1, 61.5, 44.7, 44.5, 37.9, 35.5, 27.4, 25.7, 22.0, 14.8, 14.1, 13.9. HRMS (ESI): calculated for  $\text{C}_{18}\text{H}_{31}\text{N}_2\text{O}_3$   $[\text{M} + \text{H}]^+$ , 323.2335; found 323.2350.

#### 4-Substituted pyridine-pyrrolidinone 7.82



Titanium isopropoxide (58  $\mu\text{L}$ , 0.2 mmol, 0.5 equiv) and diisopropylethylamine (95  $\mu\text{L}$ , 0.58 mmol, 1.5 equiv) were added to a reaction mixture of 4-alkylpyridine **7.31** (0.10 g, 0.38 mmol, 1 equiv) in THF (3 mL) and

refluxed with a preheated oil bath at 80 °C for 2 min. Ethyl chloroformate (55  $\mu$ L, 0.58 mmol, 1.5 equiv) was added to the refluxing reaction mixture which immediately turned to dark brown color. The resulting mixture was refluxed for 20-30 min before cooled to room temperature and then passed through a plug of basic alumina. *m*-CPBA (0.21 g, 1.22 mmol, 3.2 equiv) was added to the filtrate containing anhydrobase **7.32** in THF (5 mL) at 0 °C. The resulting mixture was stirred at room temperature for 9 h and then washed with sat. aq. NaHCO<sub>3</sub> (2 X 5 mL), water (10 mL) and brine (5 mL). The organic layer was dried over sodium sulfate, filtered and concentrated *in vacuo*. The crude product was purified using silica gel column chromatography using 50-70% ethyl acetate in hexanes to afford brown liquid **7.82** (52 mg, 52%).

<sup>1</sup>H NMR (300 MHz, CDCl<sub>3</sub>),  $\delta$  (ppm): 8.51 (d, *J* = 5.8 Hz, 2H), 7.36 (d, *J* = 6.2 Hz, 2H), 3.50-3.38 (m, 1H), 3.09- 2.97 (m, 1H), 2.33-2.12 (m, 3H), 1.66- 1.56 (m, 5H), 1.03 (t, *J* = 7.1 Hz, 3H). <sup>13</sup>C NMR (75 MHz, CDCl<sub>3</sub>),  $\delta$  (ppm): 170.9, 156.0, 149.6, 148.6, 132.2, 121.5, 91.3, 34.3, 22.1, 21.9, 20.6, 20.1, 14.8. IR (film): 3333, 1686 cm<sup>-1</sup>. HRMS (ESI): calculated for C<sub>15</sub>H<sub>19</sub>N<sub>2</sub>O<sub>2</sub> [M + H]<sup>+</sup>, 259.1447; found 259.1472.



## CHAPTER EIGHT

SYNTHESIS OF AZASPIROCYCLES VIA OXIDATIVE  
DEAROMATIZATION USING HYPERVALENT IODINE  
REAGENTS8.1 Introduction

Natural products have always intrigued chemists because of their structural complexity and biological activities. Many of these naturally occurring polycyclic compounds contain spirocycles and fused ring system (Figure 8.1).<sup>192-195</sup> The scope and diversity of these spirocycles as building blocks for natural product synthesis inspired us to embark on synthetic strategies towards their synthesis.

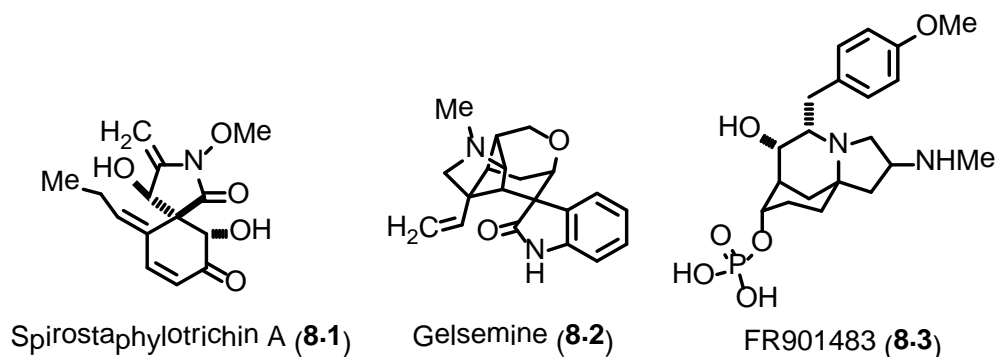
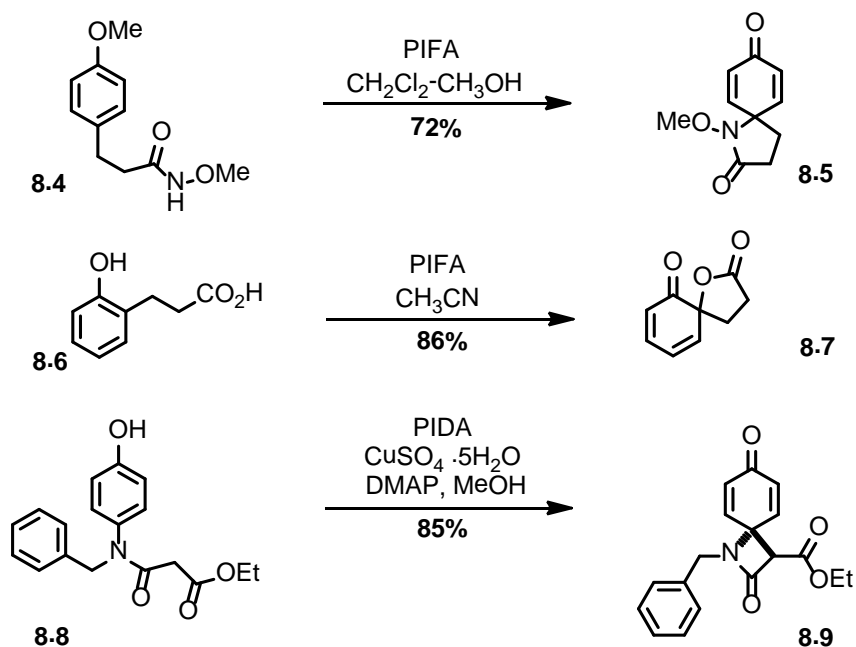


Figure 8.1. Azaspirocycles and fused ring systems in medicinal chemistry

8.2 Background

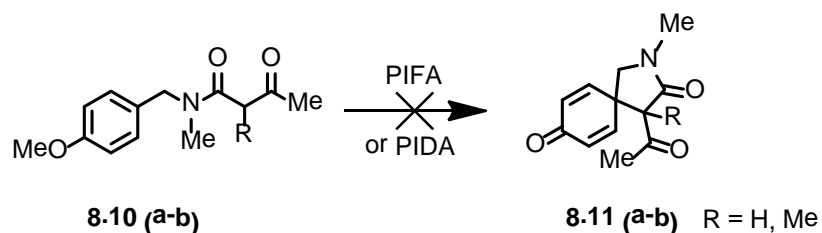
As mentioned in Chapter Five, The Pigge group has extensively studied Ru metal-mediated strategies towards the synthesis of spirocycles via intramolecular addition of stabilized carbon nucleophiles to activated (arene)Ru complexes.<sup>165-170</sup> The ruthenium reagents used in these transformations,

however, are expensive, employed in stoichiometric amounts, and are hard to recover in a form that makes them easy to reuse. These features detract from the attractiveness of (arene)Ru-based spirocyclization strategies. In contrast, dearomatization of pyridine derivatives can be achieved using more practical reaction conditions as described in earlier chapters. As synthetic strategies based on dearomatization reaction sequences have great potential in preparative chemistry, developing more practical and general routes for dearomatization of benzene derivatives is an important goal. Ideally, such transformations would employ environmentally benign, inexpensive, and commercially available reagents. In this context, relatively inexpensive hypervalent iodine reagents have emerged as important and useful tools in organic chemistry due to their versatility, mild reactivity, availability, and safety in handling.<sup>123,196-200</sup> Notably, these reagents, especially  $\text{PhI}(\text{O}_2\text{CCH}_3)_2$  (PIDA) and  $\text{PhI}(\text{O}_2\text{CCF}_3)_2$  (PIFA) are widely used in spiroannulation reactions that proceed via dearomatization as shown in Scheme 8.1. Most reported spiroannulation reactions mediated by hypervalent iodine reagents result in formation of C-heteroatom bonds (compounds **8.5** and **8.7**, Scheme 8.1).<sup>200-202</sup> Only a limited range of carbon nucleophiles have been shown to undergo the reaction (**8.8** to **8.9**, Scheme 8.1).



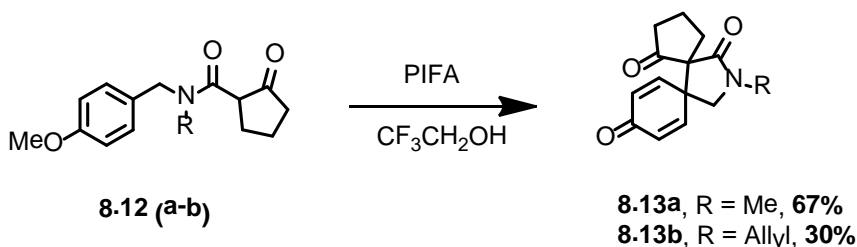
Scheme 8.1. Spiroannulation via hypervalent iodine oxidation

In an effort to overcome the limitations associated with Ru-mediated dearomatization, we initiated a study aimed at developing routes to azaspirocyclic building blocks via oxidative dearomatization. Initial attempts to synthesize azaspirocycles began by treating 4-methoxy benzyl amide derivatives **8.10a-b** with hypervalent iodine reagents as represented in Scheme 8.2. Hypervalent iodine reagents PIDA and PIFA were used in the presence of the non-nucleophilic solvent 2,2,2-trifluoroethanol (TFE) as well as in DCM to oxidize the electron-rich aryl substrates. The stabilized carbon nucleophilic site in these molecules could then be trapped by the oxidized arene ring to form the desired spirocycles. Unfortunately, arene substrates **8.10a-b** did not give the expected product (**8.11a-b**), which was in agreement with similar observations reported by Kita and his group.<sup>203</sup>



Scheme 8.2. Initial attempts to perform oxidative dearomatization (R. Dalvi, unpublished results)

However, certain  $\beta$ -keto amides (**8.12a-b**) were found to undergo oxidative dearomatization to yield the corresponding azaspirocycles in TFE (**8.13a-b**) when treated with PIFA in moderate to good yields (Scheme 8.3). With these preliminary results in hand, we envisioned extending these studies to include dearomatization of additional arene substrates in order to obtain azaspiro[4.5]decane and azaspiro[5.5]undecane scaffolds.

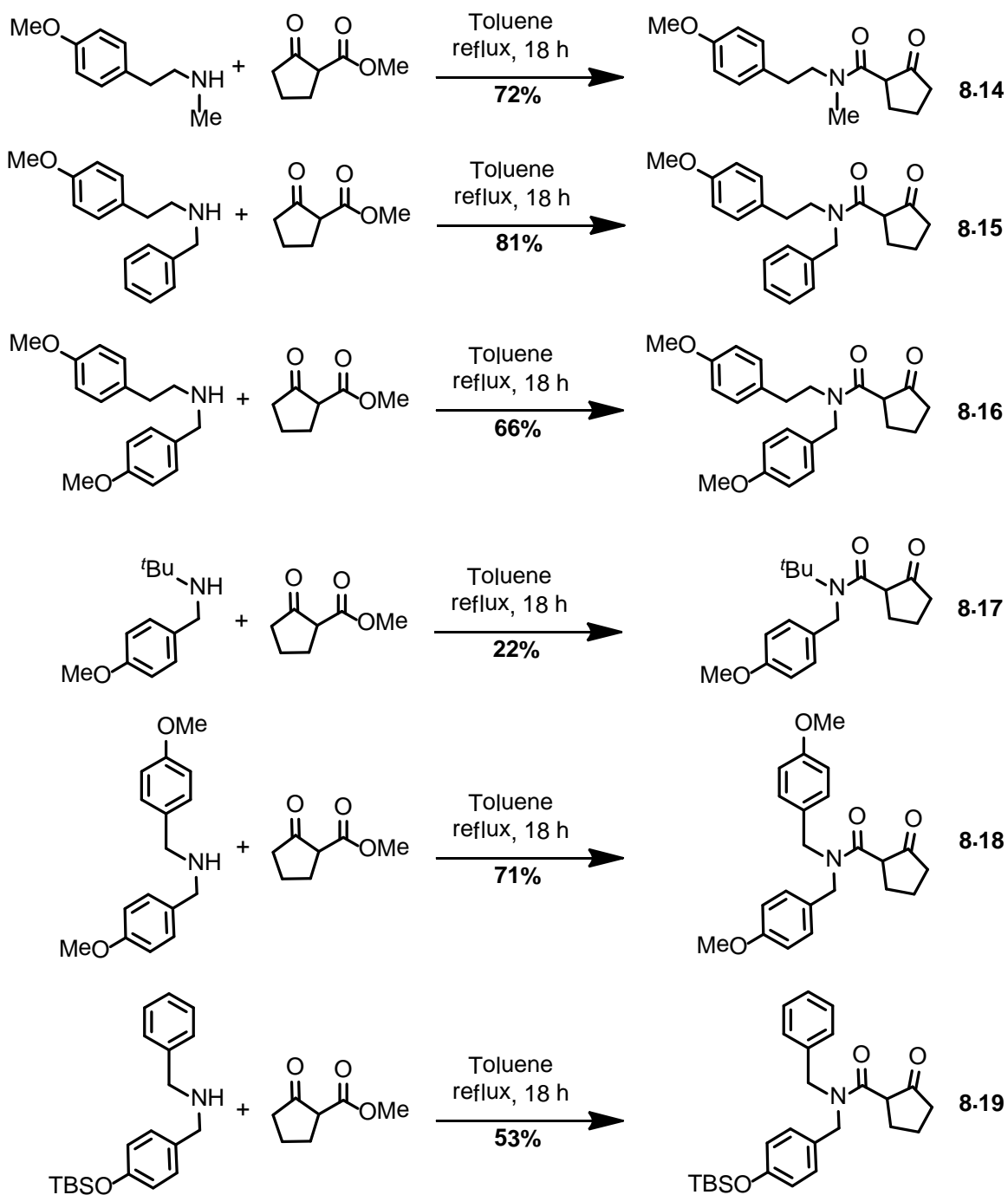


Scheme 8.3. Azaspirocyclic synthesis via oxidative dearomatization

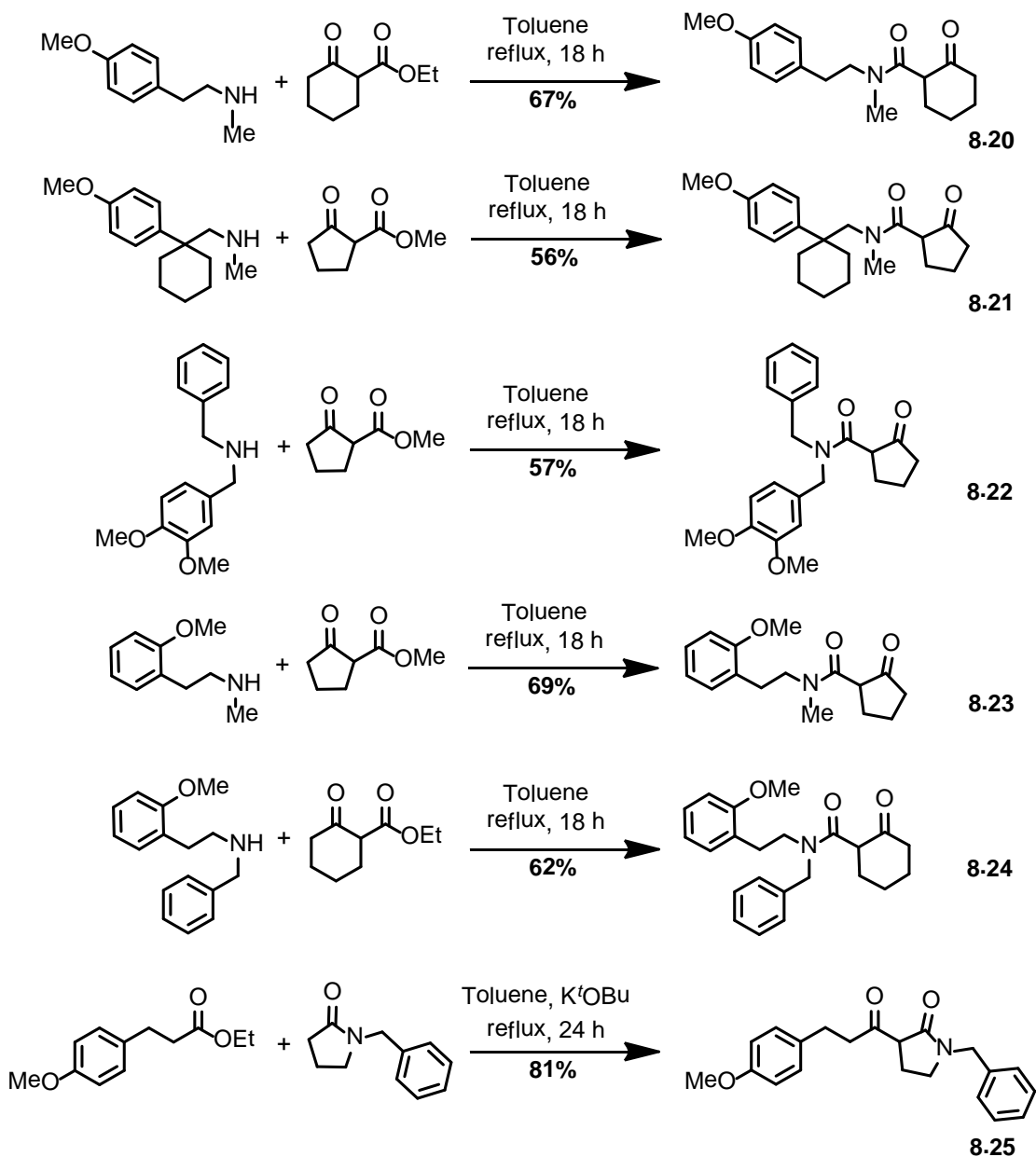
### 8.3 Results and discussion

Studies of oxidatively-induced azaspirocyclization began with the synthesis of  $\beta$ -keto amides as shown in Scheme 8.4. Secondary amines containing at least one 4-methoxy benzyl or 4-methoxy phenethyl substituent were treated with esters in refluxing toluene to yield corresponding  $\beta$ -keto amides

via transamidation. Precursors with different substitution patterns were synthesized to investigate structural parameters affecting the reaction. 4-Methoxy phenethylamine derivatives with N-methyl (**8.14**), N-benzyl (**8.15**) and N-*p*-methoxy benzyl (PMB) (**8.16**) were synthesized. Particularly, **8.16**, possessing both *p*-methoxy phenethyl and *p*-methoxy benzyl substituents, is interesting because it could give rise to two different spirocycles ([4.5] and [5.5] spirocycles with the [4.5] system expected to be kinetically favored. 4-Methoxy benzylamine derivatives substituted with N-*t*-butyl (**8.17**), N-PMB (**8.18**), along with a silyloxy ether derivative (**8.19**) were also considered. A substrate with a cyclohexanone side chain substituent (**8.20**) was synthesized to understand the effect of the ring size on spirocyclization. Electron-rich 3,4-dimethoxyphenyl substrate **8.22** was synthesized and expected to undergo arene oxidation more easily than monomethoxy analogues. Substrate **8.21**, having substitution in the side chain, and 2-methoxy derivatives (**8.23** and **8.24**) were also considered in these studies. Finally, **8.25** was prepared to probe the effect of changing the orientation of  $\beta$ -keto amide group with respect to the methoxy phenyl moiety.



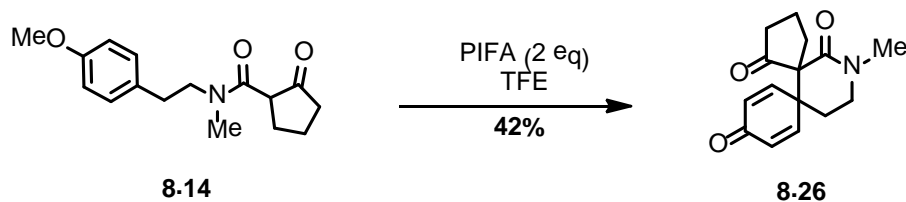
Scheme 8.4. Synthesis of precursors for oxidative dearomatization



Scheme 8.4. (Continued)

With substrates in hand, reaction conditions suitable for oxidative cyclization were examined. First, aryl  $\beta$ -keto amide **8.14** was treated with PIFA in TFE at  $-10\text{ }^{\circ}\text{C}$  (Scheme 8.5). Due to the rapid nature of oxidation and intramolecular cyclization, the reaction was completed within 20 min (according

to TLC). On purification azaspirocycle **8.26** was isolated in moderate yield. Since a moderate yield of **8.26** was obtained from cyclization of phenethylamine  $\beta$ -keto amide **8.14**, further optimization studies were carried out to synthesize spirocycle **8.26** and the results are summarized in the table 8.1. Various readily available hypervalent iodine reagents such as PIFA, PIDA, and PhI(OTs)(OH) (Koser's reagent) were used in the presence of different solvents and temperatures. It was found that PIFA favored the spirocyclization compared to other hypervalent iodine reagents in TFE. Addition of Lewis acid,  $\text{BF}_3 \cdot \text{Et}_2\text{O}$  failed to produce any desired compound. Use of basic conditions resulted in lower product yield. A catalytic approach to carry out spiroannulation using *in situ* generated hypervalent iodine reagent by treating excess of *m*-CPBA and catalytic amount of *p*-iodobenzene in TFE at ambient temperature resulted in moderate yield of the compound **8.26**.<sup>204</sup> PIFA in combination with mild oxidizing and chelating agents such as  $\text{CuCl}_2$  and  $\text{H}_4[\text{SiW}_{12}\text{O}_{40}]$  were also attempted.<sup>205</sup> Thus far, the best set of conditions to synthesize **8.26** is represented in Table 8.1, entry 1.



Scheme 8.5. Azaspirocyclization of **8.14**



Table 8.1. Reaction conditions screened for cyclization of **8.14**

Entry	Reaction Conditions	% Yield
<b>1</b>	<b>PIFA (2 eq), TFE, -10 °C to 0 °C, 15-20 min</b>	<b>42</b>
2	PIDA (2 eq), DCM / nitromethane (1/2), -40 °C to 10 °C, 25 min	0
3	Ph(OTs)(OH) (2 eq), TFE, -10 °C, 20 min	16
4	PIFA (2 eq), BF <sub>3</sub> ·Et <sub>2</sub> O (1 eq), DCM, -40 °C, 15 min	0
5	PIFA (1 eq), K <sub>2</sub> CO <sub>3</sub> (2.1 eq), TFE / CH <sub>3</sub> CN, -10 °C, 15-20 min	20
6	<i>m</i> -CPBA (1.5 eq), <i>p</i> -iodobenzene (0.25 eq), TFE, rt, 16 h	32
7	PIFA (1.2 eq), H <sub>4</sub> [SiW <sub>12</sub> O <sub>40</sub> ] (0.044 eq), CH <sub>3</sub> CN (2.5% H <sub>2</sub> O), 0 °C to rt, 30 min	16
8	PIFA (1.2 eq), CuCl <sub>2</sub> (1 eq), TFE, 0 °C, 15 min	16
9	PIFA (2 eq), neutral Al <sub>2</sub> O <sub>3</sub> (1 eq), TFE, 0 °C, 15 min	38

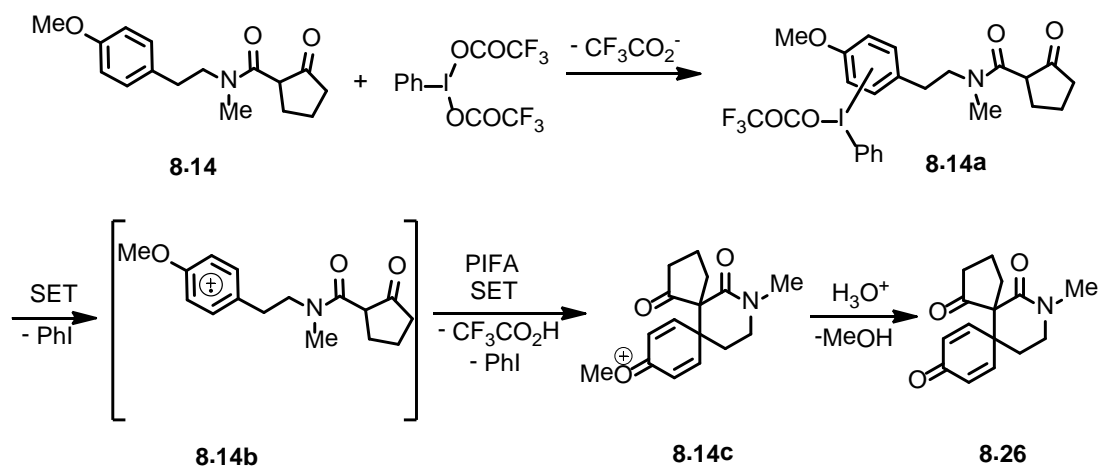
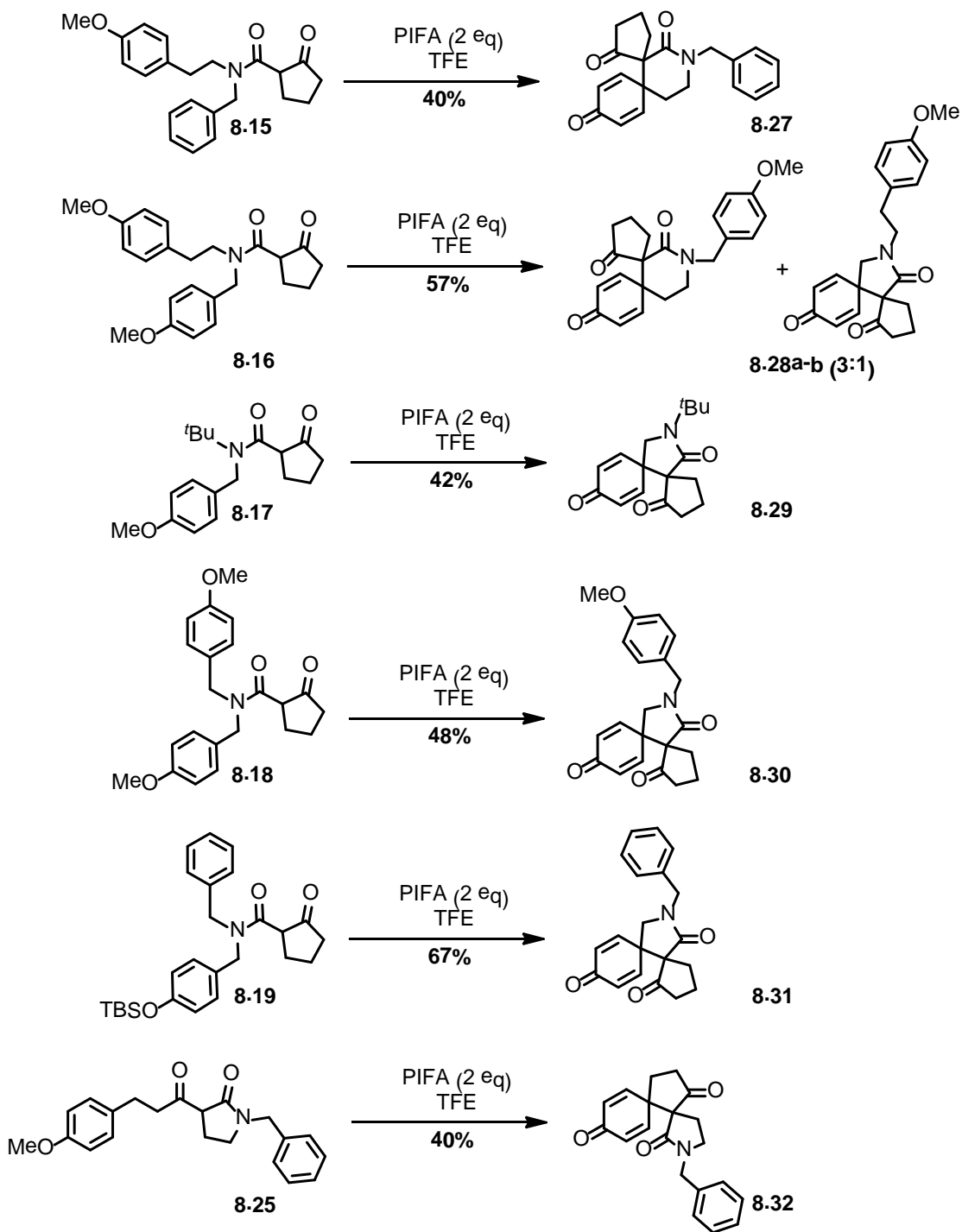


Figure 8.2. Mechanism of hypervalent iodine reagent-mediated oxidative dearomatization

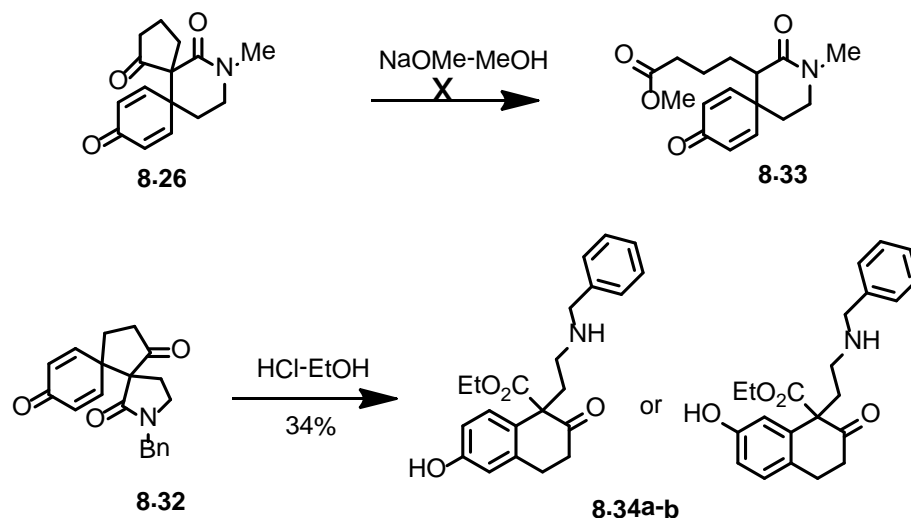
The possible mechanism of hypervalent iodine reagent mediated oxidative dearomatization is shown in Figure 8.2. First, the iodine reagent coordinates to the electronically rich aromatic ring of the aryl substrate which eventually undergoes a single electron transfer (SET) to give radical cation (**8.14b**).<sup>206,207</sup> This, after a second SET, forms a cation which gets attacked by the carbon

nucleophile in the side chain at the *ipso* position. Loss of methanol in the presence of water yields the spirocyclic product.

Using the optimized conditions (Table 8.1, entry 1), azaspiro[4.5]decane and azaspiro[5.5]undecane scaffolds (**8.27-8.32**) were synthesized starting from the corresponding benzylamine and phenethylamine precursors in moderate to good yield as shown in Scheme 8.6. Isolated yields for the azaspirocyclic products ranged between 40-67%. Interestingly, substrate **8.16** gave an inseparable 3:1 mixture of **8.28a** (azaspiro[5.5]undecane) and **8.28b** (azaspiro[4.5]decane). Since one would expect 5-membered ring formation to be kinetically favored, this may indicate that cyclization is not rate determining. Alternatively, this may reflect ring strain in five membered spirocycle transition state compared to the six membered ring system. Phenethyl amide derivatives with cyclohexanone in the side chain, **8.20** and **8.24**, did not give any product, indicating that an increase in the side chain ring size has a negative impact on spirocyclization. Dimethoxy substrate **8.21**, substrate **8.22** with a substitution in the side chain and 2-methoxy analogue (**8.23**) also failed to produce any product under optimized conditions.



Scheme 8.6. Generality of spiroannulation via oxidative dearomatization



Scheme 8.7. Functionalization studies of azaspirocycles

Finally, we briefly explored further elaboration of spirocyclic products (Scheme 8.7). Azaspirocycle **8.26**, obtained as described above was treated with NaOMe-MeOH under *retro*-Dieckmann reaction conditions but none of the expected product was observed (**8.33**). However, spirocycle **8.32**, on acid hydrolysis gave the rearranged ring opened product **8.34**. However, it is not possible to distinguish between the two structures (**8.34a** and **8.34b**) based on 1D NMR spectra in hand.

#### 8.4 Conclusion

Hypervalent iodine mediated spirocyclization does provide a synthetic entry to structurally intriguing azaspirocycles. Many aryl substrates substituted with  $\beta$ -keto amides were synthesized and subjected to oxidative dearomatization using hypervalent iodine reagents to obtain azaspirocyclic derivatives. However, the reaction is moderately yielding and substrate specific, and thus appears to be limited in scope.

## 8.5 Experimental section

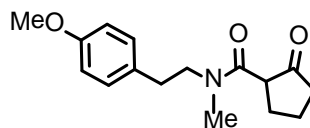
### **General experimental**

All commercially available starting materials and reagents were used as received unless otherwise noted. All the reactions were performed under argon atmosphere. Solvents were dried and purified by passage through activated alumina columns. Proton nuclear magnetic resonance ( $^1\text{H-NMR}$ ) spectra and carbon nuclear magnetic resonance ( $^{13}\text{C-NMR}$ ) spectra were recorded at 300 MHz and 75 MHz respectively. Chemical shifts are reported as  $\delta$  values in parts per million (ppm) relative to tetramethylsilane for  $^1\text{H-NMR}$  in  $\text{CDCl}_3$  and residual undeuterated solvent for all other spectra. The NMR spectra for many of the compounds used in this study reveal the presence of amide rotamers. Resonances corresponding to major and minor isomers are identified when appropriate. IR spectra were recorded on a FT-IR spectrometer as thin films on sodium chloride discs. High resolution mass spectra were obtained using electron spray ionization (ESI). Melting points were recorded using capillary melting point apparatus and are uncorrected.

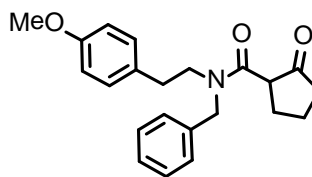
### **Experimental procedures and characterization $\beta$ -keto amide precursors**

General procedure: A reaction mixture containing 4-methoxy phenethylamine derived secondary amine (1.00 g, 0.06 mmol, 1 equiv) and methyl -2-cyclopentanone carboxylate (1.03 g, 7.27 mmol, 1.2 equiv) in toluene (10 mL) was refluxed for 18 h. The reaction mixture was cooled to room temperature and concentrated in vacuo. The crude product was purified by silica gel column chromatography using 50-70% ethyl acetate in hexanes to obtain brown colored liquid **8.14** (1.20 g, 72%).

The above general procedure was used to synthesize the spirocyclization precursors **8-14-8.24** using 1.00-2.00 g of secondary amine and ester starting materials as indicated in scheme 8.4.

**$\beta$ -keto amide 8.14****8.14**

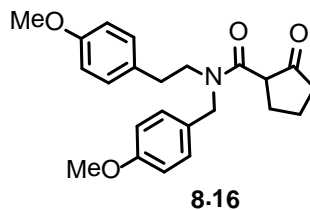
Brown liquid, 72%,  $^1\text{H}$  NMR (300 MHz,  $\text{CDCl}_3$ ),  $\delta$  (ppm), Mixture of rotamers: 7.16-7.06 (m, 2H), 6.86-6.82 (m, 2H), 3.89-3.76 (m, 3.5H), 3.64-3.42 (m, 2H), 3.07-2.98 (m, 3.5H), 2.84-2.76 (m, 2H), 2.51-1.65 (6H).  $^{13}\text{C}$  NMR (75 MHz,  $\text{CDCl}_3$ , mixture of rotamers),  $\delta$  (ppm): 215.0, 214.9, 168.9, 168.7, 158.6, 158.3, 131.3, 130.5, 130.0, 114.3, 114.0, 55.5, 55.4, 52.3, 52.1, 51.9, 50.9, 38.7, 36.7, 34.2, 34.1, 32.9, 27.6, 27.4, 21.2, 21.15. HRMS (ESI): calculated for  $\text{C}_{16}\text{H}_{22}\text{NO}_3$   $[\text{M} + \text{H}]^+$ , 276.1600; found 276.1588.

 **$\beta$ -keto amide 8.15****8.15**

Pale brown liquid, 81%,  $^1\text{H}$  NMR (300 MHz,  $\text{CDCl}_3$ ),  $\delta$  (ppm), mixture of rotamers: 7.34-7.24 (m, 4H), 7.10-7.02 (m, 3H), 6.85-6.82 (m, 2H), 5.00-4.83 (m, 1H), 4.31-4.26 (m, 1H), 3.88-3.75 (m, 4H), 3.44-3.33 (m, 1H), 3.24-3.15 (m, 1H), 2.82-2.76 (m, 2H), 2.55-2.04 (m, 5H), 1.81-1.73 (m, 1H).  $^{13}\text{C}$  NMR (75 MHz,  $\text{CDCl}_3$ , mixture of rotamers),  $\delta$  (ppm): 215.7, 170.4, 170.38, 159.5, 159.2, 138.3,

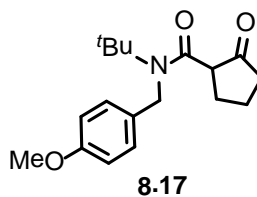
138.0, 131.0, 129.7, 127.3, 115.3, 115.0, 56.4, 52.9, 50.3, 49.9, 49.6, 39.7, 39.6, 34.2, 28.6, 22.2, 22.1. HRMS (ESI): calculated for  $C_{22}H_{26}NO_3$   $[M + H]^+$ , 352.1913; found 352.1899.

### $\beta$ -keto amide 8.16



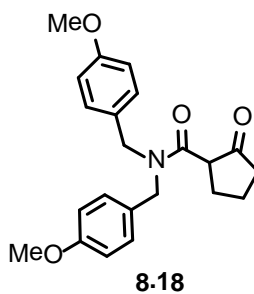
Yellow liquid, 66%,  $^1H$  NMR (300 MHz,  $CDCl_3$ ),  $\delta$  (ppm), mixture of rotamers: 7.20-7.00 (m, 4H), 6.89-6.80 (m, 4H), 4.92-4.71 (m, 1H), 4.26-4.21 (m, 1H), 3.84-3.69 (m, 7H), 3.43-3.34 (m, 1H), 3.26-3.12 (m, 1H), 2.81-2.74 (m, 2H), 2.54-2.11 (m, 4H), 1.88-1.74 (m, 2H).  $^{13}C$  NMR (75 MHz,  $CDCl_3$ , mixture of rotamers),  $\delta$  (ppm): 214.9, 169.5, 169.4, 159.3, 159.0, 158.6, 158.3, 131.4, 130.6, 130.1, 130.0, 129.5, 129.2, 128.9, 127.7, 114.4, 114.3, 114.2, 114.0, 55.5, 55.43, 55.4, 52.3, 52.1, 51.5, 49.2, 48.8, 48.1, 38.8, 38.77, 34.2, 33.3, 27.8, 27.7, 21.3, 21.2. HRMS (ESI): calculated for  $C_{23}H_{28}NO_4$   $[M + H]^+$ , 382.2018; found 382.2024.

### $\beta$ -keto amide 8.17



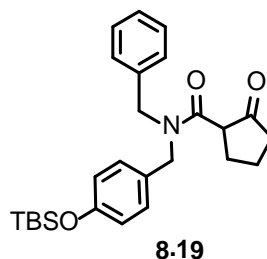
Yellow gummy liquid, 22%,  $^1\text{H}$  NMR (300 MHz,  $\text{CDCl}_3$ , mixture of rotamers),  $\delta$  (ppm): 7.13 (d,  $J = 6.0$  Hz, 2H), 6.89 (d,  $J = 6.0$  Hz, 2H), 4.86 (d,  $J = 15.0$  Hz, 1H), 4.53 (d,  $J = 12.0$  Hz, 1H), 3.80-3.65 (m, 3H), 3.26 (t,  $J = 6.0$  Hz, 1H), 2.47-1.70 (m, 6H).  $^{13}\text{C}$  NMR (75 MHz,  $\text{CDCl}_3$ , mixture of rotamers),  $\delta$  (ppm): 216.6, 159.8, 132.2, 127.6, 115.3, 59.2, 56.4, 55.5, 48.8, 39.8, 29.7, 29.3. HRMS (ESI): calculated for  $\text{C}_{18}\text{H}_{25}\text{NO}_3\text{Na}$   $[\text{M} + \text{Na}]^+$ , 326.1732; found 326.1726.

### $\beta$ -keto amide 8.18

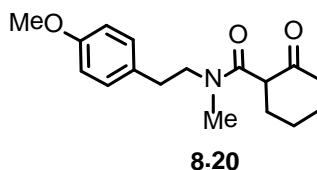


Yellow liquid, 71%,  $^1\text{H}$  NMR (300 MHz,  $\text{CDCl}_3$ , mixture of rotamers),  $\delta$  (ppm): 7.15 (d,  $J = 8.7$  Hz, 2H), 7.08 (d,  $J = 8.7$  Hz, 2H), 6.89 (d,  $J = 8.8$  Hz, 2H), 6.86 (d,  $J = 8.7$  Hz, 2H), 5.02 (d,  $J = 14.8$  Hz, 1H), 4.78 (d,  $J = 17.3$  Hz, 1H), 4.32 (d,  $J = 17.3$  Hz, 1H), 4.09 (d,  $J = 14.8$  Hz, 1H), 3.81-3.79 (m, 3H), 3.48 (t,  $J = 8.8$  Hz, 1H), 2.62-2.51 (m, 1H), 2.38-2.32 (m, 2H), 2.23-2.15 (m, 2H), 1.90-1.78 (m, 1H).  $^{13}\text{C}$  NMR (75 MHz,  $\text{CDCl}_3$ , mixture of rotamers),  $\delta$  (ppm): 215.0, 169.8, 159.3, 159.1, 129.4, 129.2, 128.5, 127.7, 114.5, 114.2, 55.5, 55.46, 52.4, 49.5, 48.0, 38.8, 27.9, 21.3. HRMS (ESI): calculated for  $\text{C}_{22}\text{H}_{25}\text{NO}_4\text{Na}$   $[\text{M} + \text{Na}]^+$ , 390.1681; found 390.1673.



**$\beta$ -keto amide 8.19**

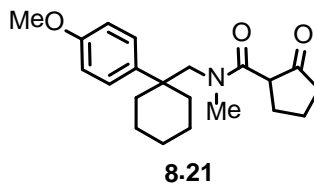
Yellow liquid, 53%,  $^1\text{H}$  NMR (300 MHz,  $\text{CDCl}_3$ , mixture of rotamers),  $\delta$  (ppm): 7.35-7.00 (m, 7H), 6.83-6.77 (m, 2H), 5.12-5.04 (m, 1H), 4.92-4.80 (m, 1H), 4.34-4.07 (m, 2H), 3.50-3.42 (m, 1H), 2.38-1.61 (m, 6H), 0.98 (s, 9H), 0.20-0.18 (m, 6H).  $^{13}\text{C}$  NMR (75 MHz,  $\text{CDCl}_3$ , mixture of rotamers),  $\delta$  (ppm): 215.8, 215.7, 170.8, 170.8, 156.3, 156.0, 138.0, 137.7, 129.7, 127.3, 121.5, 121.2, 53.23, 53.2, 51.0, 50.8, 49.6, 49.3, 39.7, 28.7, 26.7, 26.7, 22.12, 22.1, 19.3, 1.1. HRMS (ESI): calculated for  $\text{C}_{26}\text{H}_{35}\text{NO}_3\text{Si}$   $[\text{M}]^+$ , 437.2386; found 437.2379.

 **$\beta$ -keto amide 8.20**

Brown liquid, 67%,  $^1\text{H}$  NMR (300 MHz,  $\text{CDCl}_3$ ),  $\delta$  (ppm), Mixture of rotamers: 7.16 (d,  $J = 8.7$  Hz, 1H), 7.04 (d,  $J = 8.7$  Hz, 1H), 6.86 (d,  $J = 7.4$  Hz, 1H), 6.83 (d,  $J = 7.4$  Hz, 1H), 3.79-3.78 (m, 3H), 3.61-3.33 (m, 2.5H), 3.03-2.96 (m, 2H), 2.84-2.73 (m, 3.5H), 2.60-1.36 (m, 8H).  $^{13}\text{C}$  NMR (75 MHz,  $\text{CDCl}_3$ , mixture of rotamers),  $\delta$  (ppm): 207.8, 207.7, 169.8, 169.5, 158.7, 158.3, 131.5,

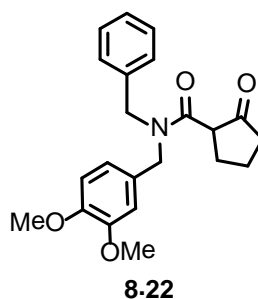
130.6, 130.0, 114.4, 114.1, 55.5, 55.4, 54.8, 54.4, 52.0, 50.8, 42.2, 42.0, 36.3, 34.0, 33.8, 33.0, 30.5, 30.4, 27.3, 27.1, 23.8, 23.7. HRMS (ESI): calculated for  $C_{17}H_{24}NO_3$   $[M + H]^+$ , 290.1756; found 290.1757.

### $\beta$ -keto amide 8.21



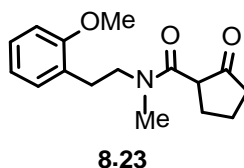
Brown liquid, 56%,  $^1H$  NMR (300 MHz,  $CDCl_3$ ),  $\delta$  (ppm), Mixture of rotamers: 7.32 (d,  $J = 6$  Hz, 1H), 7.18 (d,  $J = 6$  Hz, 1H), 6.90-6.87 (m, 2H), 3.80-3.65 (m, 4H), 3.35-3.09 (m, 1.6H), 2.91 (s, 1.1H), 2.49-1.80 (m, 10H), 1.55-1.21 (m, 8.4H).  $^{13}C$  NMR (75 MHz,  $CDCl_3$ , mixture of rotamers),  $\delta$  (ppm): 215.8, 171.0, 170.9, 150.6, 150.4, 149.6, 149.3, 138.1, 137.7, 129.7, 127.2, 119.4, 112.4, 112.1, 111.7, 110.6, 57.0, 56.98, 56.9, 53.2, 51.0, 49.5, 39.7, 39.6, 28.8, 28.6, 22.2, 22.1. HRMS (ESI): calculated for  $C_{21}H_{30}NO_3$   $[M + H]^+$ , 344.2226; found 344.2214.

### $\beta$ -keto amide 8.22



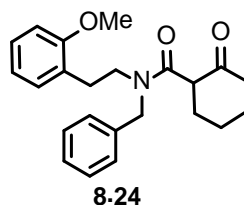
Brown liquid, 57%,  $^1\text{H}$  NMR (300 MHz,  $\text{CDCl}_3$ , mixture of rotamers),  $\delta$  (ppm): 7.38-7.14 (m, 5H), 6.83-6.68 (m, 3H), 5.25-4.75 (m, 2H), 4.37-4.30 (m, 1.5H), 3.87-3.83 (m, 6.5H), 3.50-3.44 (m, 1H), 2.59-1.78 (m, 6H).  $^{13}\text{C}$  NMR (75 MHz,  $\text{CDCl}_3$ , mixture of rotamers),  $\delta$  (ppm): 215.8, 171.0, 170.9, 150.6, 150.4, 149.6, 149.3, 138.1, 137.7, 129.7, 137.7, 119.4, 112.4, 112.1, 11.7, 110.6, 57.0, 57.0, 56.9, 53.2, 51.0, 49.5, 39.7, 39.6, 28.8, 28.6, 22.2, 22.1. HRMS (ESI): calculated for  $\text{C}_{22}\text{H}_{25}\text{NO}_4\text{Na}$   $[\text{M} + \text{Na}]^+$ , 390.1681; found 390.1682.

**$\beta$ -keto amide 8.23**



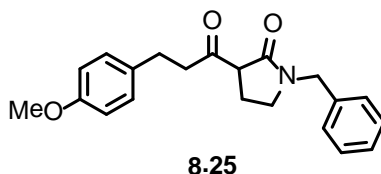
Brown liquid, 69%,  $^1\text{H}$  NMR (300 MHz,  $\text{CDCl}_3$ ),  $\delta$  (ppm), Mixture of rotamers: 7.25-7.08 (m, 2H), 6.92-6.83 (m, 2H), 3.92-3.80 (m, 3.6H), 3.62-3.28 (m, 2.4H), 3.03-2.83 (m, 5H), 2.33-2.12 (m, 4H), 1.91-1.71 (2H).  $^{13}\text{C}$  NMR (75 MHz,  $\text{CDCl}_3$ , mixture of rotamers),  $\delta$  (ppm): 215.1, 214.9, 169.1, 168.6, 157.8, 157.6, 130.9, 127.8, 127.6, 126.6, 120.7, 110.3, 52.3, 51.8, 50.3, 48.9, 38.8, 38.7, 36.6, 34.2, 30.3, 28.6, 27.7, 27.5, 21.4, 21.2. HRMS (ESI): calculated for  $\text{C}_{16}\text{H}_{21}\text{NO}_3\text{Na}$   $[\text{M} + \text{Na}]^+$ , 298.1419; found 298.1403.

**$\beta$ -keto amide 8.24**



Brown gummy liquid, 62%,  $^1\text{H}$  NMR (300 MHz,  $\text{CDCl}_3$ ),  $\delta$  (ppm), Mixture of rotamers: 7.37-6.99 (m, 7H), 6.91-6.79 (m, 2H), 5.29-5.15 (m, 0.8H), 4.41-4.17 (m, 1.2H), 3.86-3.75 (m, 3.5H), 3.44-3.13 (m, 3H), 2.96-2.49 (m, 3H), 2.28-1.43 (m, 7.5H).  $^{13}\text{C}$  NMR (75 MHz,  $\text{CDCl}_3$ , mixture of rotamers),  $\delta$  (ppm): 207.1, 169.7, 157.0, 137.1, 130.4, 128.4, 128.1, 127.9, 127.4, 126.7, 126.0, 125.95, 120.5, 109.9, 54.9, 54.1, 53.7, 47.7, 46.2, 41.6, 29.9, 29.6, 26.6, 23.6. HRMS (ESI): calculated for  $\text{C}_{23}\text{H}_{28}\text{NO}_3$   $[\text{M} + \text{H}]^+$ , 366.2069; found 366.2054.

### $\beta$ -keto amide **8.25**



A reaction mixture containing N-benzyl pyrrolidinone (0.84 g, 4.80 mmol, 1 equiv) and  $\text{K}^t\text{OBu}$  (0.54 g, 4.80 mmol, 1 equiv) in toluene (15 mL) was stirred for 10 min at room temperature. Ethyl 3-(4-methoxyphenyl)propionate (1.00 g, 4.80 mmol, 1 equiv) in toluene (10 mL) was added to it and resulting mixture was then refluxed for 24 h. after cooling to room temperature, the reaction mixture was quenched with water (20 mL) and extracted with ethyl acetate (3 X 5 mL). The combined organic layer was then dried over sodium sulfate, filtered and evaporated in vacuo. The crude product was purified by silica gel column chromatography using 50-70% ethyl acetate in hexanes to obtain yellow liquid **8.25** (1.30 g, 81%).

$^1\text{H}$  NMR (300 MHz,  $\text{CDCl}_3$ ),  $\delta$  (ppm), mixture of rotamers: 7.35-7.24 (m, 3H), 7.19-7.11 (m, 4H), 6.84-6.79 (m, 2H), 4.48-4.36 (m, 2H), 3.77 (s, 3H), 3.63-3.58 (m, 1H), 3.45-3.26 (m, 2H), 3.22-3.14 (m, 1H), 2.94-2.82 (m, 3H), 2.64-2.42

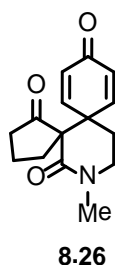
(m, 1H), 2.04-1.91 (m, 1H).  $^{13}\text{C}$  NMR (75 MHz,  $\text{CDCl}_3$ , mixture of rotamers),  $\delta$  (ppm): 205.4, 170.1, 158.1, 136.1, 133.1, 129.5, 129.4, 128.9, 128.2, 127.9, 114.1, 114.0, 55.4, 55.3, 47.2, 45.3, 44.6, 36.0, 30.1, 28.7, 19.8. HRMS (ESI): calculated for  $\text{C}_{21}\text{H}_{24}\text{NO}_3$   $[\text{M} + \text{H}]^+$ , 338.1756; found 338.1740.

### Experimental procedures and characterization for spirocyclization products

General procedure: **8.14** (0.25 g, 0.91 mmol, 1 equiv) in TFE (5 mL) was cooled to 0 °C. PIFA (0.78 g, 1.82 mmol, 2 equiv) was added to the reaction mixture in one portion and stirring was maintained at 0 °C for 20 min. Resulting mixture was then directly loaded on to the silica gel column and purified using 50-70% ethyl acetate in hexanes to get off white solid **8.26** (0.10 g, 42%).

The above procedure has been used to synthesize all the spirocycles (**8.26-8.32**) from 0.10 g-0.25 g of the corresponding precursors.

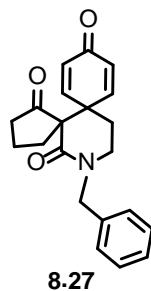
#### Spirocycle 8.26



M.p.: 112-114 °C.  $^1\text{H}$  NMR (300 MHz,  $\text{CDCl}_3$ ),  $\delta$  (ppm): 6.85 (dd,  $J = 10.5$ , 3.2 Hz, 1H), 6.60 (dd,  $J = 10.4$ , 3.0 Hz, 1H), 6.44-6.37 (m, 2H), 3.57-3.52 (m, 2H), 3.29-3.12 (m, 1H), 3.04 (s, 3H), 2.51-2.43 (m, 2H), 2.30-2.18 (m, 2H), 1.91-1.79 (m, 1H), 1.60-1.48 (m, 2H).  $^{13}\text{C}$  NMR (75 MHz,  $\text{CDCl}_3$ ),  $\delta$  (ppm): 216.1, 185.0, 167.4, 149.3, 148.5, 131.6, 131.3, 58.4, 47.0, 46.5, 39.7, 35.8, 32.1, 27.6,

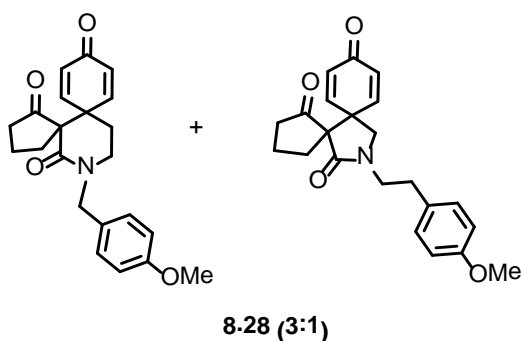
20.7. HRMS (ESI): calculated for  $C_{15}H_{18}N_2O_3$   $[M + H]^+$ , 260.1287; found 260.1274.

### Spirocycle 8.27



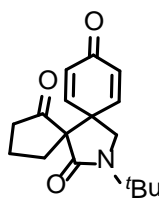
Yellow solid, 40%, MP: 132-134 °C.  $^1H$  NMR (300 MHz,  $CDCl_3$ ),  $\delta$  (ppm): 7.40-7.25 (m, 5H), 6.79 (dd,  $J = 10.4, 3.1$  Hz, 1H), 6.61 (dd,  $J = 10.3, 3.2$  Hz, 1H), 6.42-6.37 (m, 2H), 4.84 (d,  $J = 14.7$ , 1H), 4.50 (d,  $J = 14.8$ , 1H), 3.52-3.35 (m, 2H), 3.23-3.12 (m, 1H), 2.56-2.48 (m, 2H), 2.33-2.21 (m, 2H), 1.94-1.85 (m, 1H), 1.64-1.44 (m, 2H).  $^{13}C$  NMR (75 MHz,  $CDCl_3$ ),  $\delta$  (ppm): 216.1, 184.9, 167.6, 149.3, 148.3, 136.5, 131.6, 131.4, 129.1, 127.9, 58.5, 50.9, 46.4, 39.8, 32.3, 27.5, 20.8. HRMS (ESI): calculated for  $C_{21}H_{22}NO_3$   $[M + H]^+$ , 336.1600; found 336.1583.

### Spirocycle 8.28 (3:1)



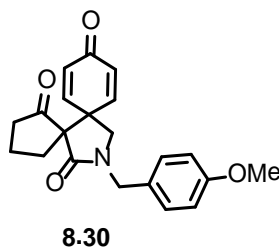
Colorless liquid, 57%,  $^1\text{H}$  NMR (300 MHz,  $\text{CDCl}_3$ ),  $\delta$  (ppm), mixture of products(a:b) (~3.1:1): 7.22-7.14 (m, 2.6H), 6.92-6.84 (m, 3H), 6.76 (dd,  $J = 10.4$ , 3.1 Hz, 1H), 6.60 (dd,  $J = 10.3$ , 3.1 Hz, 1H), 6.41-6.36 (m, 2.6H), 6.28-6.24 (m, 0.3H), 4.71 (d,  $J = 14.5$  Hz, 1H), 4.48 (d,  $J = 14.6$  Hz, 1H), 4.00 (d,  $J = 9.6$  Hz, 0.3H), 3.81-3.79 (m, 4H), 3.71-3.56 (m, 0.7H), 3.50-3.33 (m, 2H), 3.20-3.09 (m, 1H), 2.89-2.82 (m, 0.9H), 2.56-2.48 (m, 2H), 2.33-2.12 (m, 3.4H), 1.93-1.81 (m, 1H), 1.63-1.43 (m, 2.4H).  $^{13}\text{C}$  NMR (75 MHz,  $\text{CDCl}_3$ ),  $\delta$  (ppm): 216.1, 215.2, 184.9, 167.4, 159.3, 158.6, 149.3, 148.3, 148.2, 145.8, 133.3, 131.6, 131.3, 130.1, 129.9, 129.7, 129.4, 128.6, 114.4, 114.2, 64.7, 58.4, 55.4, 52.4, 50.3, 48.3, 46.4, 44.6, 44.0, 39.8, 38.8, 32.9, 32.2, 28.7, 27.5, 20.8, 19.9. HRMS (ESI): calculated for  $\text{C}_{22}\text{H}_{24}\text{NO}_4$   $[\text{M} + \text{H}]^+$ , 366.1705; found 366.1688.

### Spirocycle 8.29

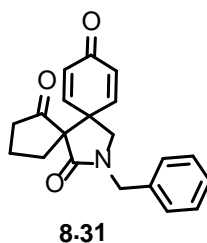


8.29

Off white gummy liquid, 42%,  $^1\text{H}$  NMR (300 MHz,  $\text{CDCl}_3$ ),  $\delta$  (ppm): 6.90 (dd,  $J = 10.3$ , 3.2 Hz, 1H), 6.80 (dd,  $J = 11.7$ , 3.0 Hz, 1H), 6.44-6.38 (m, 2H), 4.12 (d,  $J = 9.7$  Hz, 1H), 3.22 (d,  $J = 9.7$  Hz, 1H), 2.40-2.09 (m, 4H), 1.84-1.77 (m, 1H), 1.60-1.50 (m, 1H), 1.44 (s, 9H).  $^{13}\text{C}$  NMR (75 MHz,  $\text{CDCl}_3$ ),  $\delta$  (ppm): 215.5, 185.0, 171.1, 148.3, 146.1, 133.2, 130.0, 65.4, 55.1, 50.5, 47.5, 38.9, 28.7, 27.7, 19.9. HRMS (ESI): calculated for  $\text{C}_{17}\text{H}_{22}\text{NO}_3$   $[\text{M} + \text{H}]^+$ , 288.1600; found 288.1586.

**Spirocycle 8.30**

Colorless liquid, 48%,  $^1\text{H}$  NMR (300 MHz,  $\text{CDCl}_3$ ),  $\delta$  (ppm): 7.22-7.19 (m, 2H) 6.91-6.86 (m, 3H), 6.63 (dd,  $J = 10.1, 3.0$  Hz, 1H), 6.38 (dd,  $J = 10.2, 2.0$  Hz, 1H), 6.32 (dd,  $J = 10.1, 1.9$  Hz, 1H), 4.51 (s, 2H), 3.96 (d,  $J = 9.6$  Hz, 1H), 3.81 (s, 3H), 2.94 (d,  $J = 9.8$  Hz, 1H), 2.44-2.30 (m, 2H), 2.24-2.12 (m, 2H), 1.90-1.81 (m, 1H), 1.66-1.56 (m, 1H).  $^{13}\text{C}$  NMR (75 MHz,  $\text{CDCl}_3$ ),  $\delta$  (ppm): 215.3, 184.8, 170.9, 159.5, 147.8, 145.9, 133.2, 130.0, 129.7, 127.3, 114.4, 64.7, 55.4, 51.3, 48.0, 46.8, 38.9, 28.7, 19.9. HRMS (ESI): calculated for  $\text{C}_{21}\text{H}_{22}\text{NO}_4$   $[\text{M} + \text{H}]^+$ , 352.1549; found 352.1528.

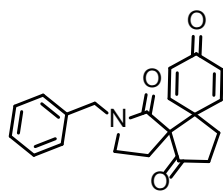
**Spirocycle 8.31**

Yellow liquid, 67%,  $^1\text{H}$  NMR (300 MHz,  $\text{CDCl}_3$ ),  $\delta$  (ppm): 7.41-7.27 (m, 5H), 6.88 (dd,  $J = 10.2, 3.0$  Hz, 1H), 6.65 (dd,  $J = 10.1, 3.0$  Hz, 1H), 6.41-6.31 (m, 2H), 4.58-4.57 (m, 2H), 3.99 (d,  $J = 9.8$  Hz, 1H), 2.95 (d,  $J = 9.8$  Hz, 1H),



2.45-2.32 (m, 2H), 2.25-2.12 (m, 2H), 1.89-1.82 (m, 1H), 1.67-1.57 (m, 1H).  $^{13}\text{C}$  NMR (75 MHz,  $\text{CDCl}_3$ ),  $\delta$  (ppm): 215.3, 184.8, 171.1, 147.8, 145.8, 135.4, 133.3, 130.1, 129.1, 128.4, 128.3, 64.7, 51.5, 48.1, 47.4, 38.9, 28.8, 20.0. HRMS (ESI): calculated for  $\text{C}_{20}\text{H}_{20}\text{NO}_3$   $[\text{M} + \text{H}]^+$ , 322.1443; found 322.1444.

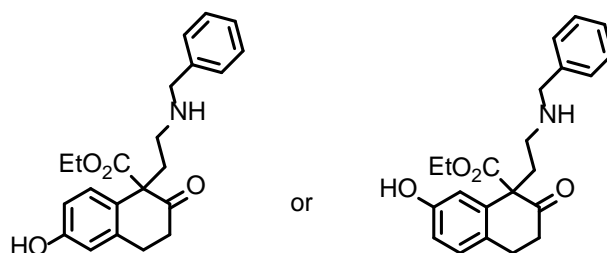
### Spirocycle 8.32



8.32

Pale yellow liquid, 40%,  $^1\text{H}$  NMR (300 MHz,  $\text{CDCl}_3$ ),  $\delta$  (ppm): 7.33-7.14 (m, 7H), 6.59 (dd,  $J = 10.1, 3.0$  Hz, 1H), 6.41-6.32 (m, 2H), 4.47 (d,  $J = 14.7$  Hz, 1H), 4.37 (d,  $J = 14.7$  Hz, 1H), 3.36-2.86 (m, 5H), 2.62-2.49 (m, 1H), 2.25-2.17 (m, 1H), 2.00-1.92 (m, 1H), 1.55-1.45 (m, 1H).  $^{13}\text{C}$  NMR (75 MHz,  $\text{CDCl}_3$ ),  $\delta$  (ppm): 213.3, 185.4, 169.0, 150.0, 148.2, 135.4, 131.9, 129.8, 129.0, 128.1, 128.0, 114.0, 66.1, 55.4, 51.3, 47.2, 44.3, 34.6, 29.1, 23.2. HRMS (ESI): calculated for  $\text{C}_{20}\text{H}_{20}\text{NO}_3$   $[\text{M} + \text{H}]^+$ , 322.1443; found 322.1442.

### Ring opened product 8.34



8.34a-b

Spirocycle **8.32** (1 equiv) was taken in anhydrous ethanol (2 mL) and cooled to 0 °C. 5 mL ethanolic HCl solution was added to the reaction mixture and stirred at room temperature for 16 h. Reaction mixture was then evaporated in vacuo and the residue was then neutralized with aq. NaHCO<sub>3</sub> solution and extracted with ethyl acetate (3 X 5 mL). The combined organic layer was then dried over sodium sulfate, filtered and evaporated in vacuo. Crude product was purified by silica gel column chromatography using 50-70% ethyl acetate in hexanes to afford **8.34**.

Colorless liquid, 34%, <sup>1</sup>H NMR (300 MHz, CDCl<sub>3</sub>), δ (ppm): 7.38-7.24 (m, 6H), 7.00-6.98 (m, 1H), 6.81-6.73 (m, 2H), 4.59 (d, *J* = 14.8 Hz, 1H), 4.43 (d, *J* = 14.7 Hz, 1H), 4.03 (q, *J* = 7.0 Hz, 2H), 3.53-3.45 (m, 1H), 3.39-3.24 (m, 2H), 3.13-2.99 (m, 2H), 2.91-2.83 (m, 1H), 2.72-2.66 (m, 1H), 2.18-2.09 (m, 1H), 1.41 (t, *J* = 7.0 Hz, 3H). <sup>13</sup>C NMR (75 MHz, CDCl<sub>3</sub>), δ (ppm): 209.2, 172.5, 158.2, 138.1, 136.3, 130.8, 129.0, 128.3, 127.9, 114.2, 113.9, 63.7, 62.4, 47.5, 44.8, 38.5, 31.5, 29.1, 15.0. HRMS (ESI): calculated for C<sub>22</sub>H<sub>24</sub>NO<sub>3</sub> [M + H – H<sub>2</sub>O]<sup>+</sup>, 350.1756; found 350.1761.

## CHAPTER NINE

## PART B: SUMMARY AND FUTURE DIRECTIONS

9.1 Summary

The objective of the research described in Part B was to explore dearomatization methods for the synthesis of heterocyclic frameworks. Specifically, our efforts were directed toward intramolecular dearomatization of pyridine derivatives to obtain an array of structurally unique synthetic building blocks to access biologically important natural products. 4-Alkylpyridine derivatives substituted with different carbon nucleophiles were synthesized and subjected to intramolecular spirocyclization under various conditions to afford diazaspiro[4.5]decanes as well as diazaspiro[5.5]undecanes in good yields. We have found that 4-alkyl pyridines substituted with  $\beta$ -amido esters in the side chain participated in this titanium isopropoxide mediated spirocyclization effectively compared to all other stabilized carbon nucleophiles. Under our mild optimized conditions, it was found that spirocyclization was rapid and efficient, whereas competing anhydrobase formation was not observed. 4-Alkylpyridyl substrate tethered with  $\beta$ -dicarbonyl nucleophiles such as  $\beta$ -keto amides and  $\beta$ -diesters were less effective in producing the spirocycles under optimized conditions. 4-Alkylpyridine derivatives with  $\beta$ -dicarbonyls substituted at the active methylene positions,  $\beta$ -keto esters, 2-alkylpyridyl analogues and carbon nucleophiles other than  $\beta$ -dicarbonyls failed to generate spirocycles. We successfully demonstrated the functionalization of these synthesized diazaspirocycles into synthetically useful heterocycles by subjecting them to various conditions such as hydrogenation, oxidation using *m*-CPBA, and alkylation of the lactam carbon. Particularly, gold(III)-catalyzed cycloisomerization was utilized to synthesize tricyclic ring systems from diazaspiro-1,6-enynes.

We have utilized the same 4-alkyl substrates used in spirocyclization to synthesize anhydrobases under basic conditions. These anhydrobases were found to be unstable. So, reaction conditions were developed to engage anhydrobase intermediates in aldol-like condensation in the presence of Lewis acid. Under the optimized conditions, 4-alkyl pyridines underwent benzylic cyclization to yield highly conjugated dihydropyridines which on acid hydrolysis produced substituted pyridines tethered with functionalized butyro- and valero lactams. Alternatively, hydrogenation of substituted anhydrobase intermediates resulted in the formation of piperidine-pyrrolidine or bis(piperidine) heterocyclic frameworks structurally similar to the core structure of biologically important natural products.

We have also investigated oxidative dearomatization via intramolecular spirocyclization of 4-methoxy substituted benzyl and phenethyl substrates having  $\beta$ -keto amide nucleophiles in the side chain using hypervalent iodine reagents. Even though we synthesized a few azaspirocycles using this methodology, this approach was found to be very much substrate specific and low yielding.

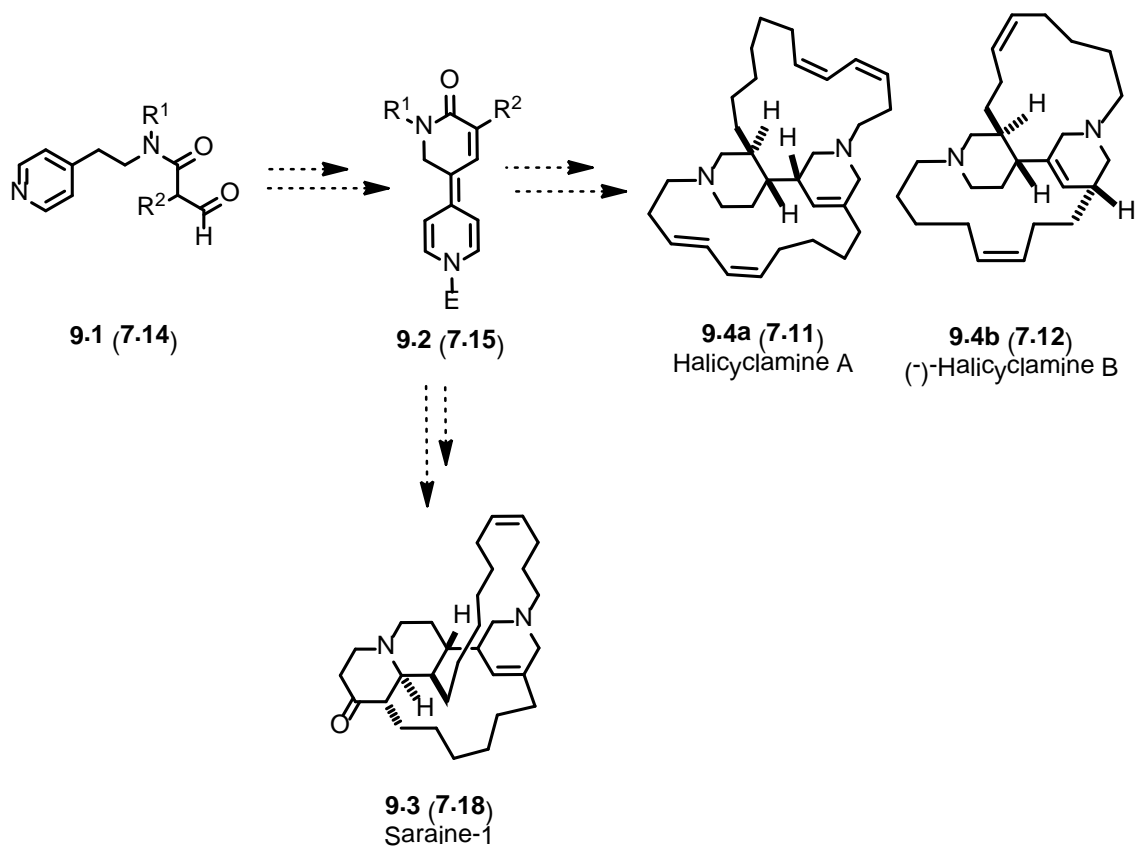
In conclusion, heterocycle synthesis via dearomatization of 4-alkylpyridines is rapid, mild and utilizes readily available aryl substrates. This methodology provides a novel route to valuable medicinal chemistry scaffolds.

## 9.2 Future directions

### **Benzylic cyclization of 4-alkylpyridyl substrates in natural product synthesis**

We have demonstrated that benzylic cyclization of 4-alkylpyridine substrates with appropriately positioned electrophilic carbon centers can proceed through anhydrobase intermediates. The methodology provides potential synthetic building blocks in an efficient way. Indeed, approaches to natural

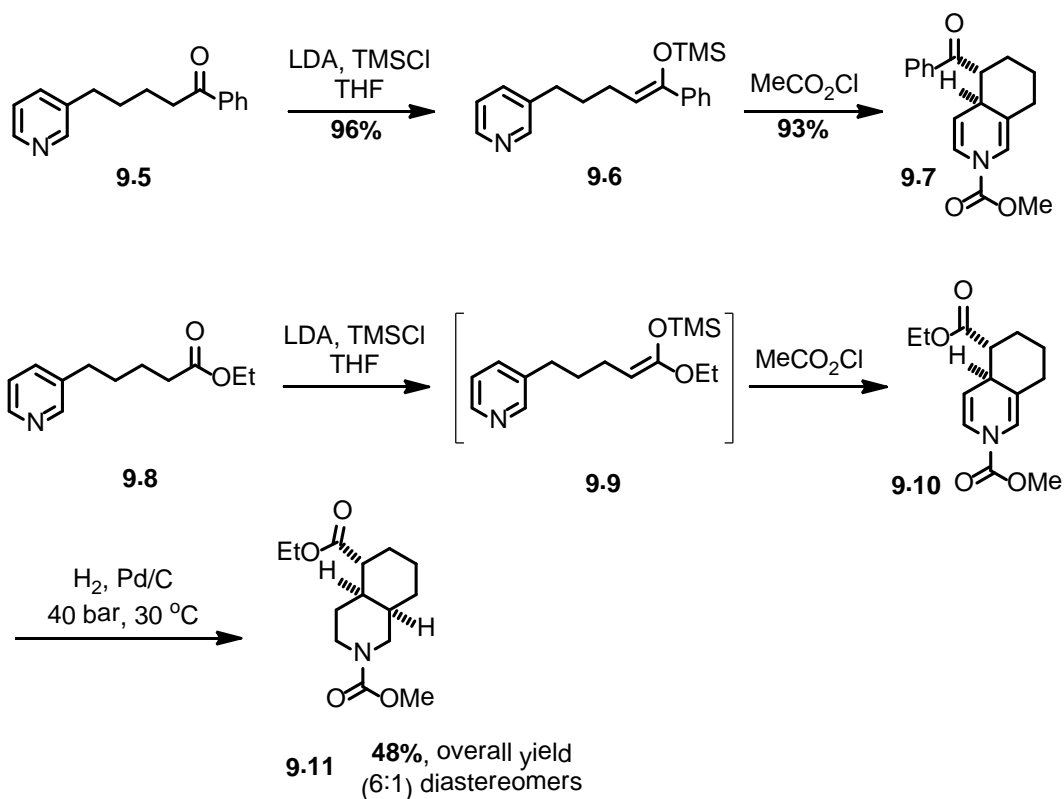
products such as the halicyclamines and sarains can be formulated from this approach as shown in Scheme 9.1.<sup>185,186,188</sup> These biologically active polycyclic alkaloids have two piperidine rings linked to each other. Pyridine derivatives (**9.1**) can be transformed into their corresponding anhydrobases (**9.2**) by subjecting them to benzylic condensation conditions as discussed in Chapter Seven. These anhydrobases then could be converted into basic bis(piperidine) scaffolds on reduction. Obviously, further extensive synthetic sequences would be required to yield the natural products.



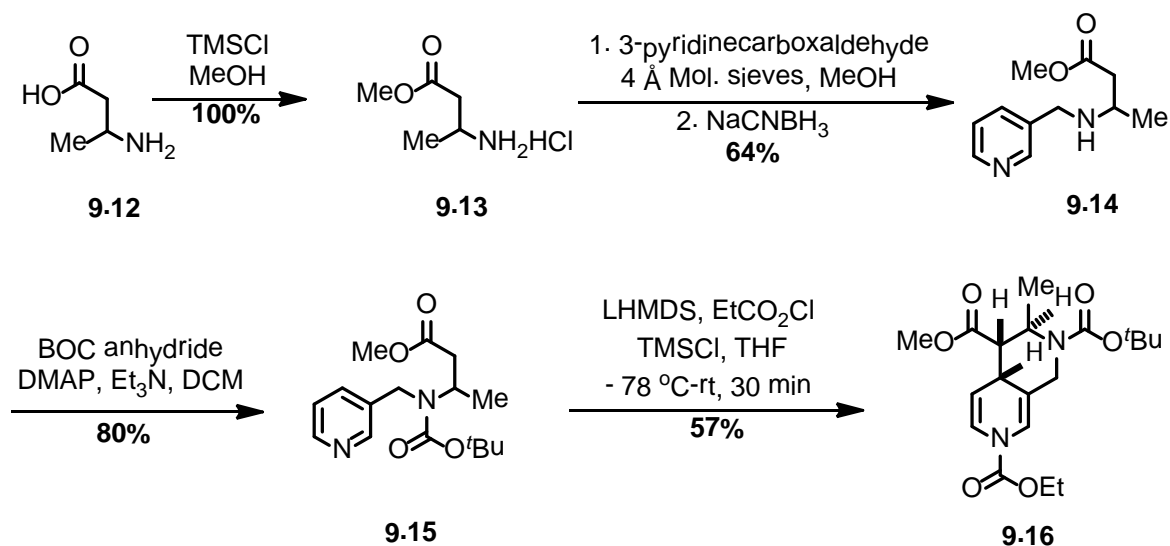
Scheme 9.1. Benzylic cyclization of 4-alkylpyridines in potential natural product synthesis

### 3-Alkyl pyridyl substrates in natural product synthesis

Fused ring systems are abundant in natural products and particularly alkaloids containing 3,4-fused ring piperidines are very common. There are only a few reports available related to synthesis of these frameworks using pyridine substrates. Earlier, Clayden and coworkers reported that addition of silyl ether (**9.6**) and silyl ketene acetal (**9.9**) to the corresponding 3-pyridinium salt gave fused ring system **9.7** and **9.10** respectively (Scheme 9.2).<sup>208</sup> The intermediate **9.10** was found to be unstable and hydrogenation yielded completely reduced bicyclic ring system.



Scheme 9.2. Bicyclic ring systems from 3-pyridyl dearomatization



Scheme 9.3. Fused ring systems from 3-alkylpyridine dearomatization

Many alkaloids such as the madangamines (**9.20a-b**) contain polycyclic rings along with azacycles in their core structures.<sup>209,210</sup> A possible synthetic route to these diazadecaline scaffolds entails cyclization of 3-substituted pyridines to afford fused ring dihydropyridines. Moreover, stereoselective cyclizations might be realized if side chain substituents could exert diastereocontrol over the cyclization event. For initial studies along these lines, we focused on investigating the effect of a methyl group on an intramolecular cyclization. Our synthesis started with esterification of commercially available 3-aminobutanoic acid (**9.12**) in the presence of TMSCl and methanol to obtain **9.13** as a hydrochloride salt.<sup>211</sup> This, on reductive amination with 3-pyridine carboxaldehyde, yielded the corresponding secondary amine **9.14**. Protection of **9.14** using standard conditions afforded **9.15** in good yield. The strategic reaction was then performed by treating precursor **9.15** with LHMDS and TMSCl at  $-78^\circ\text{C}$  to generate silyl ketene acetal, which was then treated with ethyl chloroformate to

form the product **9.16**. This 1,4-dihydropyridine was then isolated and purified using neutral alumina column chromatography.

The bicyclic compound (**9.16**) was stable, but room temperature NMR spectra were complicated because of the presence of amide rotamers. So, variable temperature NMR studies were performed and it was found that at 333 K better resolved NMR spectra could be obtained in deuterated DMSO. Further 1D and 2D NMR studies ( $^1\text{H}$  NMR,  $^{13}\text{C}$ , HSQC, COSY, HMBC and NOESY) revealed that **9.16** was obtained as a single diastereomer. The relative stereochemistry was assigned based on the NOESY correlations observed (Figure 9.1). It was found that of the possible products the observed diastereomer corresponds to the lowest energy stereoisomer (**9.16b**) as indicated in molecular modeling (Figure 9.2). Thus, it appears that the methyl group in the side chain has considerable influence over the cyclization outcome.

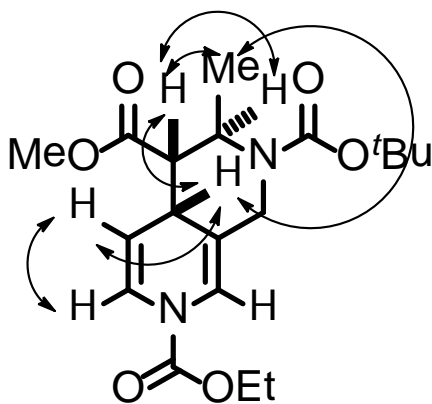


Figure 9.1. NOESY correlations of 1,4-dihydropyridine **9.16**



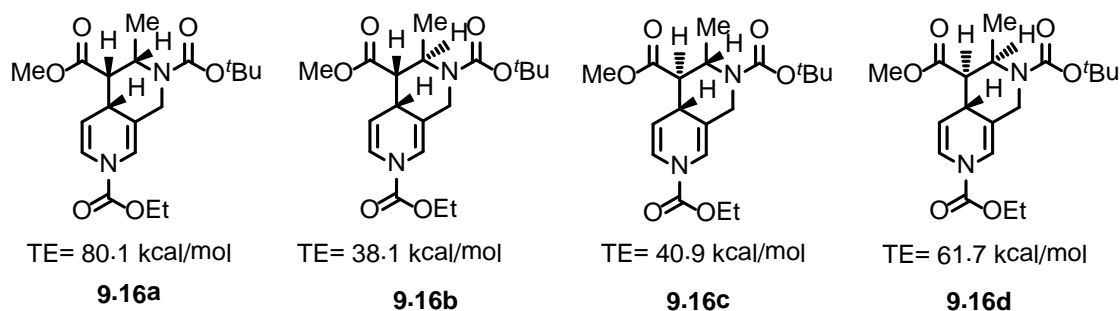
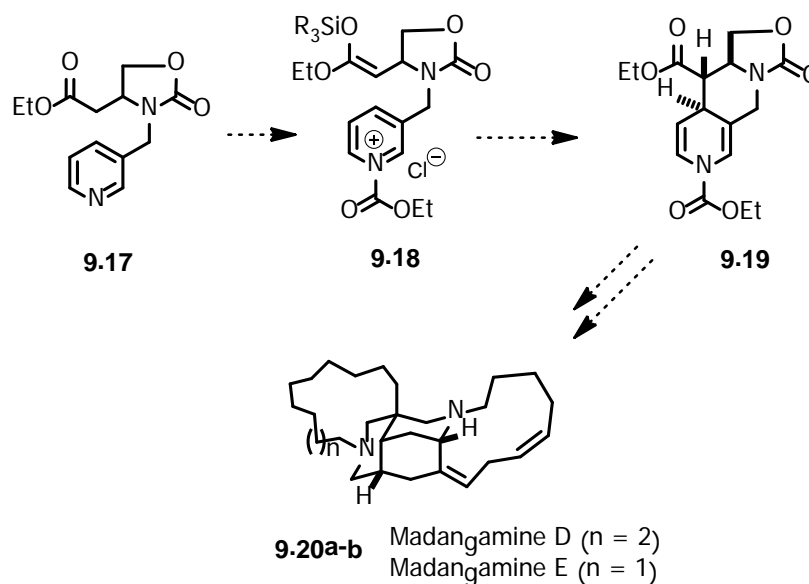


Figure 9.2. Molecular modeling of **9.16**

So, in preliminary studies we have established successfully that fused ring systems can be synthesized by the intramolecular addition of a silyl ketene acetal to the C4 position of a pyridinium salt formed *in situ* from 3-alkylpyridine substrates. Furthermore, molecular modeling may be capable of predicting the diastereochemical outcome of cyclizations involving substituted side chains. In the future, stereoselective synthetic approaches to diazadecaline derivatives, such as **9.19** may be considered. Molecular modeling has indicated that **9.19** is the lowest-energy diastereomer arising from cyclization of **9.18**. In turn, **9.19** may be suited for elaboration to more complex heterocycles, including natural products such as madangamines D and E (**9.20a-b**).



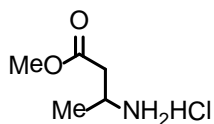
Scheme 9.4. 3-Alkylpyridyl substrates in natural product synthesis

### 9.3 Experimental Section

#### **General experimental**

All commercially available starting materials and reagents were used as received unless otherwise noted. All the reactions were performed under argon atmosphere. Solvents were dried and purified by passage through activated alumina columns. Proton nuclear magnetic resonance ( $^1\text{H-NMR}$ ) spectra and carbon nuclear magnetic resonance ( $^{13}\text{C-NMR}$ ) spectra were recorded at 300, 500 MHz and 75 and 125 MHz respectively. 2D NMR spectra were recorded at 500 MHz. Chemical shifts are reported as  $\delta$  values in parts per million (ppm) relative to tetramethylsilane for  $^1\text{H-NMR}$  in  $\text{CDCl}_3$  and residual undeuterated solvent for all other spectra. The NMR spectra for many of the compounds used in this study reveal the presence of amide rotamers. Resonances corresponding to major and minor isomers are identified when appropriate. High resolution mass spectra were obtained using electron spray ionization (ESI).

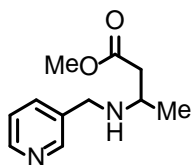
### Experimental procedures and characterization substrates (9.13-9.16)



**9.13**

A suspension of 3-aminobutanoic acid (**9.12**) (0.50 g, 4.85 mmol, 1 equiv) and TMSCl (1.24 mL, 9.69 mmol, 2 equiv) in MeOH (50 mL) was stirred at room temperature for 18 h. The light green colored reaction mixture was then evaporated under vacuum to yield brownish-green colored gummy liquid (**9.13**) (0.74 g, 100%)

$^1\text{H}$  NMR (300 MHz,  $\text{D}_2\text{O}$ ),  $\delta$  (ppm), 3.83-3.70 (m, 4H), 3.36 (s, 0.4H), 2.79 (d,  $J = 6.2$  Hz, 2H), 1.38 (d,  $J = 6.6$  Hz, 3H).  $^{13}\text{C}$  NMR (75 MHz,  $\text{D}_2\text{O}$ ),  $\delta$  (ppm): 173.0, 52.8, 44.6, 38.0, 17.9. HRMS (ESI): calculated for  $\text{C}_{12}\text{H}_{11}\text{NO}_2$  [M], 117.0795; found 117.0790.

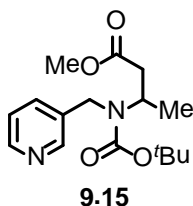


**9.14**

3-Pyridine carboxaldehyde (0.59 g, 5.49 mmol, 1.2 equiv) and amine hydrochloride **9.13** (0.70 g, 4.58 mmol, 1 equiv) were combined in anhydrous methanol (30 mL) containing dried 4 Å molecular sieves (2.00 g) at room temperature. The resulting mixture was then stirred for 24 h before cooling to 0

°C, followed by the addition of NaCNBH<sub>3</sub> and continued stirring for 6 h at room temperature. The reaction mixture was then quenched with water (25 mL), stirred for an additional 30 min, and filtered through a bed of Celite. The filtrate was then evaporated under vacuum. The residue was then dissolved in DCM (30 mL) and washed with water (3 X 20 mL), brine (15 mL), and dried over anhydrous sodium sulfate. Filtration and concentration in vacuum gave a pale brown colored liquid (**9.14**) (0.60 g, 64%). This product was used in the next step without further purification.

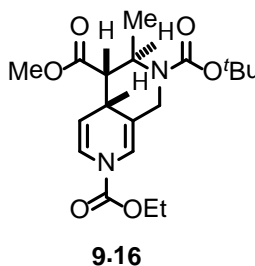
<sup>1</sup>H NMR (300 MHz, CDCl<sub>3</sub>), δ (ppm): 8.55 (d, *J* = 2.1 Hz, 1H), 8.49 (dd, *J* = 4.8, 2.1 Hz, 1H), 7.69 (dt, *J* = 7.7, 2.0 Hz, 1H), 7.26 (dd, *J* = 7.7, 4.9 Hz, 1H), 3.87-3.74 (m, 2H), 3.67 (s, 3H), 3.18-3.11 (m, 1H), 2.53-2.38 (m, 2H), 1.17 (d, *J* = 6.4 Hz, 3H). <sup>13</sup>C NMR (75 MHz, CDCl<sub>3</sub>), δ (ppm): 172.8, 149.7, 148.6, 136.0, 123.6, 51.7, 49.9, 48.6, 41.5, 20.5. HRMS (ESI): calculated for C<sub>11</sub>H<sub>17</sub>N<sub>2</sub>O<sub>2</sub> [M + H]<sup>+</sup>, 209.1290; found 209.1272.



A reaction mixture containing **9.14** (0.55 g, 2.67 mmol, 1 equiv) and catalytic DMAP (10 mg) and Et<sub>3</sub>N (0.56 mL, 4.00 mmol, 1.5 equiv) in DCM (20 mL) was cooled to 0 °C. BOC-anhydride (0.87 g, 4.00 mmol, 1.5 equiv) was added to it and the resulting mixture was stirred at room temperature for 18 h. The reaction mixture was concentrated under vacuum to minimum volume and

then purified by silica gel column chromatography using 50% ethyl acetate in hexanes to afford yellow colored oil (**9.15**) (0.65 g, 80%)

$^1\text{H}$  NMR (300 MHz,  $\text{CDCl}_3$ ),  $\delta$  (ppm), mixture of rotamers: 8.58-8.49 (m, 2H), 7.74-7.59, (m, 1H), 7.32-7.23 (m, 1H), 4.66-4.12 (m, 3H), 3.66-3.62 (m, 3H), 2.98-2.41 (m, 2H), 1.56-1.39 (m, 9H), 1.27-1.17 (m, 3H).  $^{13}\text{C}$  NMR (75 MHz,  $\text{CDCl}_3$ , mixture of rotamers),  $\delta$  (ppm): 171.9, 149.5, 149.3, 148.7, 147.5, 135.8, 135.3, 123.8, 123.5, 85.4, 80.7, 52.6, 51.9, 51.5, 49.3, 47.0, 40.0, 38.6, 28.6, 27.6, 19.8, 18.4. HRMS (ESI): calculated for  $\text{C}_{16}\text{H}_{25}\text{N}_2\text{O}_4$   $[\text{M} + \text{H}]^+$ , 309.1814; found 309.1796.



LHMDS (1.0 M solution in THF, 0.49 mL, 0.49 mmol, 1.5 equiv) was added to a solution of **9.15** (0.10 g, 0.33 mmol, 1 equiv) in THF (3 mL) at  $-78\text{ }^\circ\text{C}$  and stirred for 5 min. TMSCl (62.7  $\mu\text{L}$ , 0.49 mmol, 1.5 equiv) was added and the resulting mixture was stirred for 20 min before the addition of ethyl chloroformate (0.16 mL, 1.63 mmol, 5 equiv). The reaction mixture was stirred at  $-78\text{ }^\circ\text{C}$  for 30 min, at room temperature for 15 min, and then quenched with saturated aq.  $\text{NaHCO}_3$  (10 mL), and extracted with EtOAc (3 X 5 mL). The combined organic layer was then washed with brine (5 mL), dried over sodium sulfate, filtered and concentrated in vacuum. The residue was purified by neutral alumina column

chromatography using 25-40% EtOAc in hexanes to obtain pale yellow liquid

**9.16** (70 mg, 57%).

$^1\text{H}$  NMR (500 MHz, DMSO),  $\delta$  (ppm), mixture of rotamers at 298 K: 6.70 (br s, 2H), 4.75-4.69 (m, 1H), 4.60-4.53 (m, 1H), 4.31-4.28 (m, 1H), 4.19-4.15 (m, 3H), 3.63 (br s, 1H), 3.55-3.41 (m, 4H), 2.60 (d,  $J = 4.6$  Hz, 1H), 1.42-1.36 (m, 9H), 1.29-1.24 (m, 6H).  $^1\text{H}$  NMR (500 MHz, DMSO),  $\delta$  (ppm), at 333 K: 6.72-6.70 (m, 2H), 4.73 (d,  $J = 8.0$  Hz, 1H), 4.59 (br s, 1H), 4.27-4.23 (m, 1H), 4.19 (q,  $J = 7.1$  Hz, 2H), 3.63 (br s, 1H), 3.52-3.45 (m, 4H), 2.60 (d,  $J = 5.0$  Hz, 1H), 1.44-1.39 (m, 9H), 1.28-1.24 (m, 6H).  $^{13}\text{C}$  NMR (125 MHz, DMSO, mixture of rotamers at 333 K),  $\delta$  (ppm): 171.0, 153.2, 150.4, 123.0, 117.5, 106.1, 78.4, 62.0, 50.4, 48.7, 48.1, 29.8, 27.8, 16.0, 13.9. HRMS (ESI): calculated for  $\text{C}_{19}\text{H}_{28}\text{N}_2\text{O}_6 \text{Na} [\text{M} + \text{H}]^+$ , 403.1845; found 403.1844. Stereochemical assignments were made on the basis of extensive 2D NMR spectroscopic analysis (see Appendix C for details).

## APPENDIX A

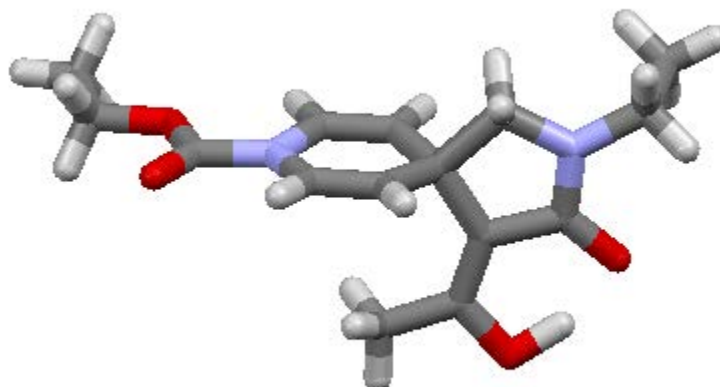
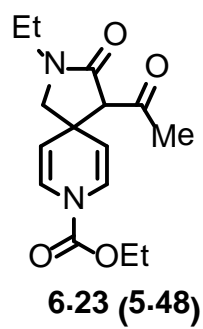
X-RAY CRYSTALLOGRAPHIC DATA FOR SPIROCYCLE **6.23****(5.48)**Figure A.1. Crystal structure of spirocycle **6.23 (5.48)**

Table A.1. Crystal structure data for **6.23 (5.48)**

Emperical formula	$C_{15}H_{20}N_2O_4$
Formula weight	292.33
crystal system	monoclinic
space group	$P2_1/n$
$a/\text{\AA}$	7.3882(2)
$b/\text{\AA}$	22.8275(7)
$c/\text{\AA}$	9.3124(3)
$\alpha/^\circ$	90
$\beta/^\circ$	107.7749(16)
$\gamma/^\circ$	90
$V/\text{\AA}^3$	1495.60(8)
Z	4
$D_{\text{calc}}$	1.298



Table A.1. (Continued)

$\mu$ (mm <sup>-1</sup> )	0.095
T/K	150
no. of reflns	12435
no. of unique reflns	3570
no. of reflns with $I > 2\sigma(I)$	2558
no. of params	194
R1 [ $I > 2\sigma(I)$ ]	0.0574
wR2	0.1776

## APPENDIX B

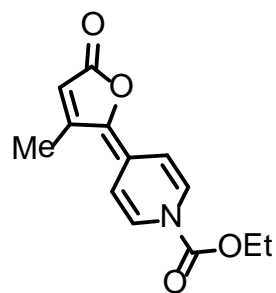
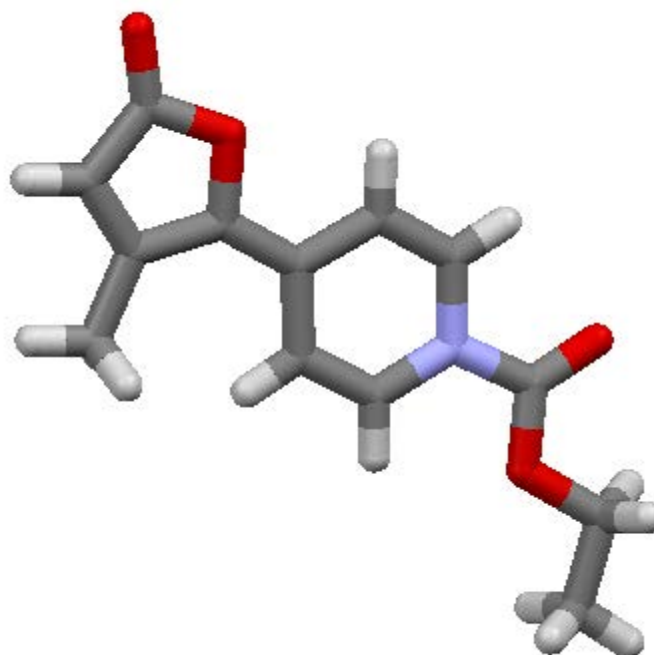
X-RAY CRYSTALLOGRAPHIC DATA FOR CONJUGATED  
PRODUCT **7.62****7.62**Figure B.1. Crystal structure of conjugated product **7.62**

Table B.1. Crystal structure data for **7.62**

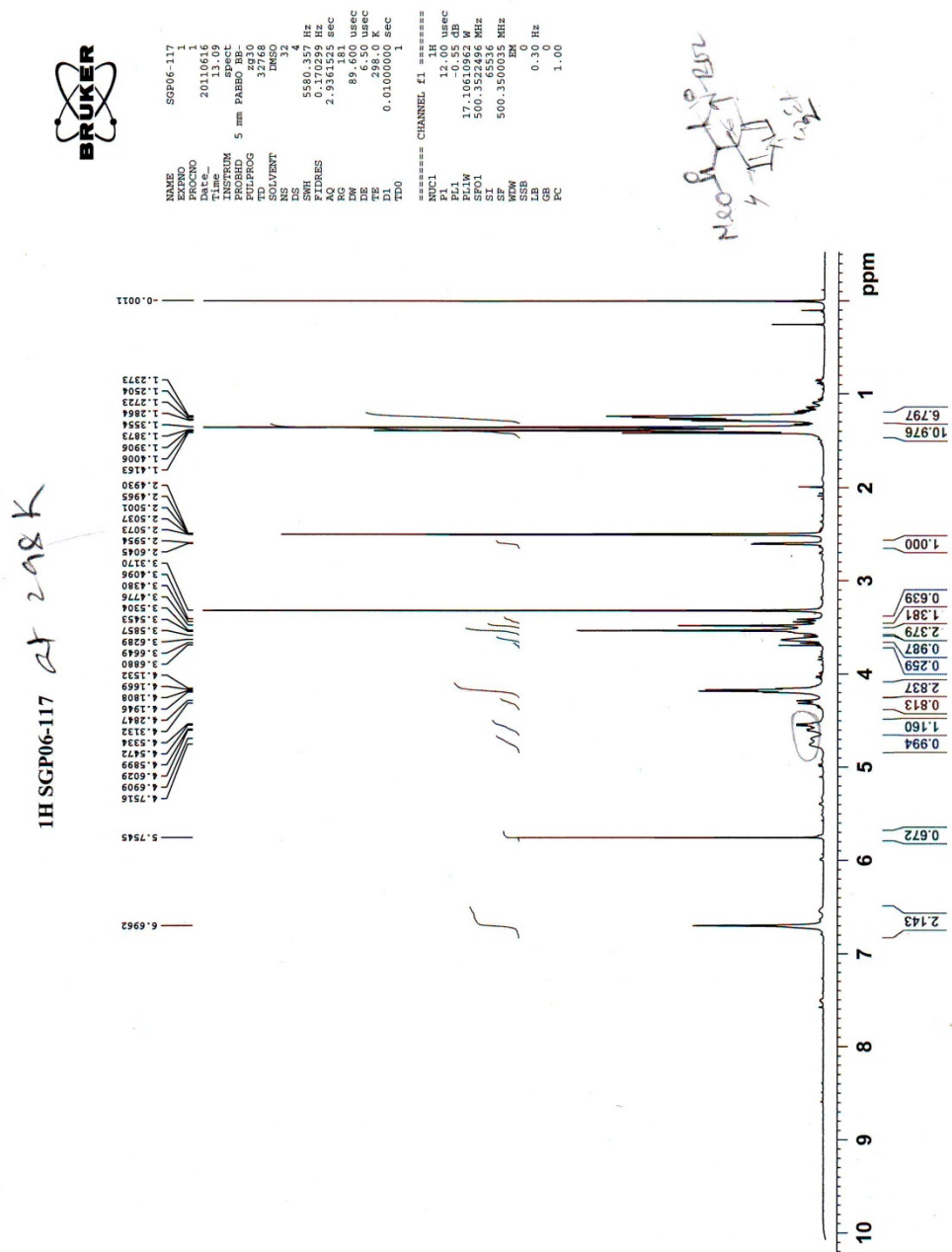
Empirical formula	$C_{13}H_{13}NO_4$
Formula weight	247.25
crystal system	triclinic
space group	P-1
$a/\text{\AA}$	7.3151(4)
$b/\text{\AA}$	7.7610(4)
$c/\text{\AA}$	11.2261(7)
$\alpha/^\circ$	110.235(3)
$\beta/^\circ$	93.780(4)
$\gamma/^\circ$	93.453(4)
$V/\text{\AA}^3$	594.35(6)
$Z$	2
$D_{\text{calc}}$	1.382
$\mu$ ( $\text{mm}^{-1}$ )	0.103

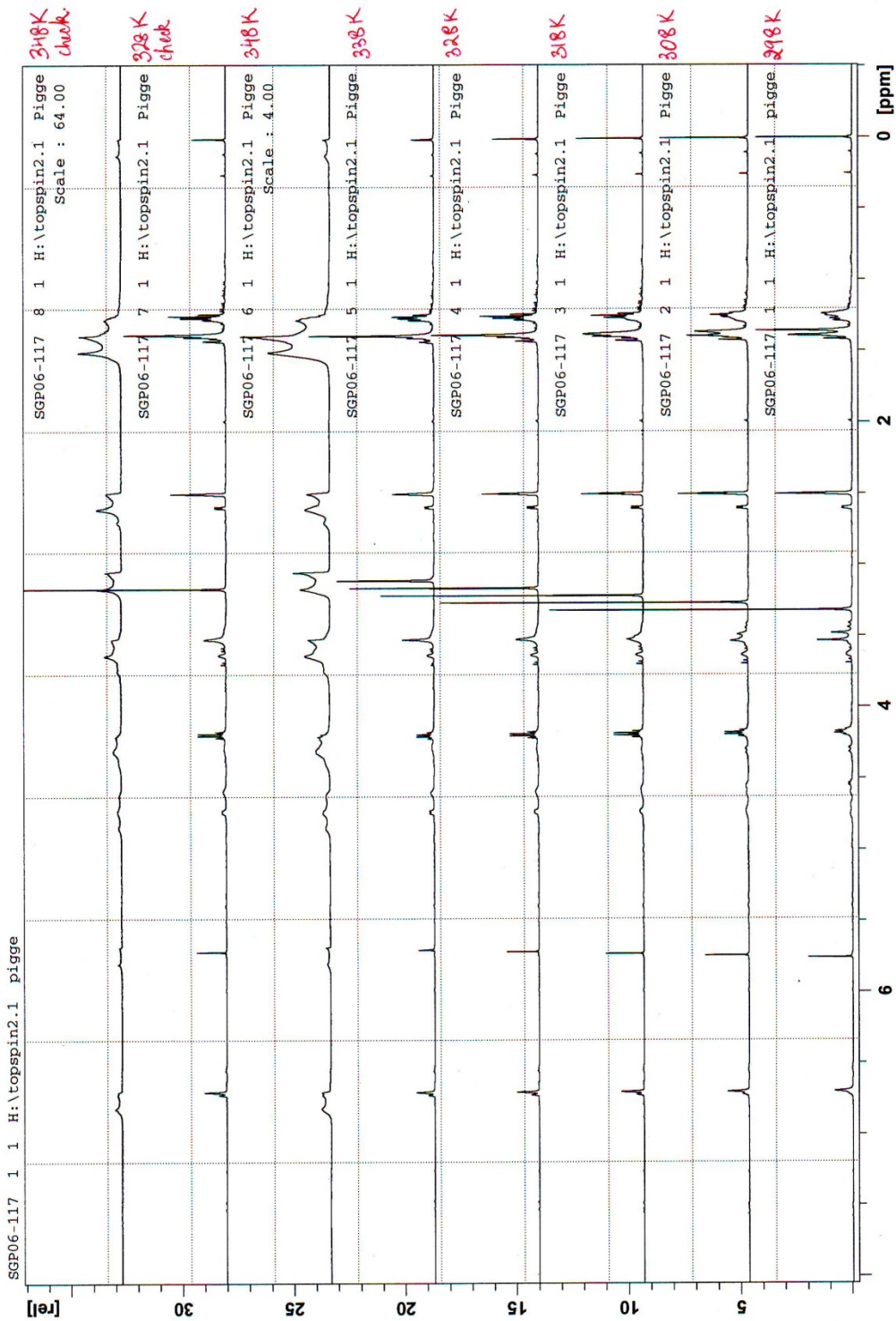
Table B.1. (Continued)

T/K	200
no. of reflns	3967
no. of unique reflns	2163
no. of reflns with $I > 2\sigma(I)$	2163
no. of params	154
R1 [ $I > 2\sigma(I)$ ]	0.0688
wR2	0.1695

APPENDIX C

NMR SPECTROSCOPIC DATA FOR 9.16



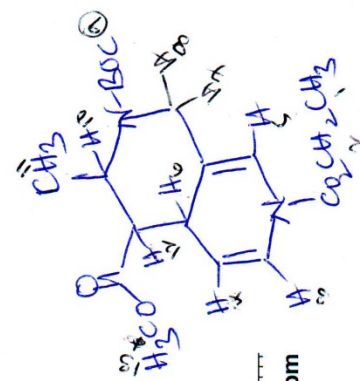
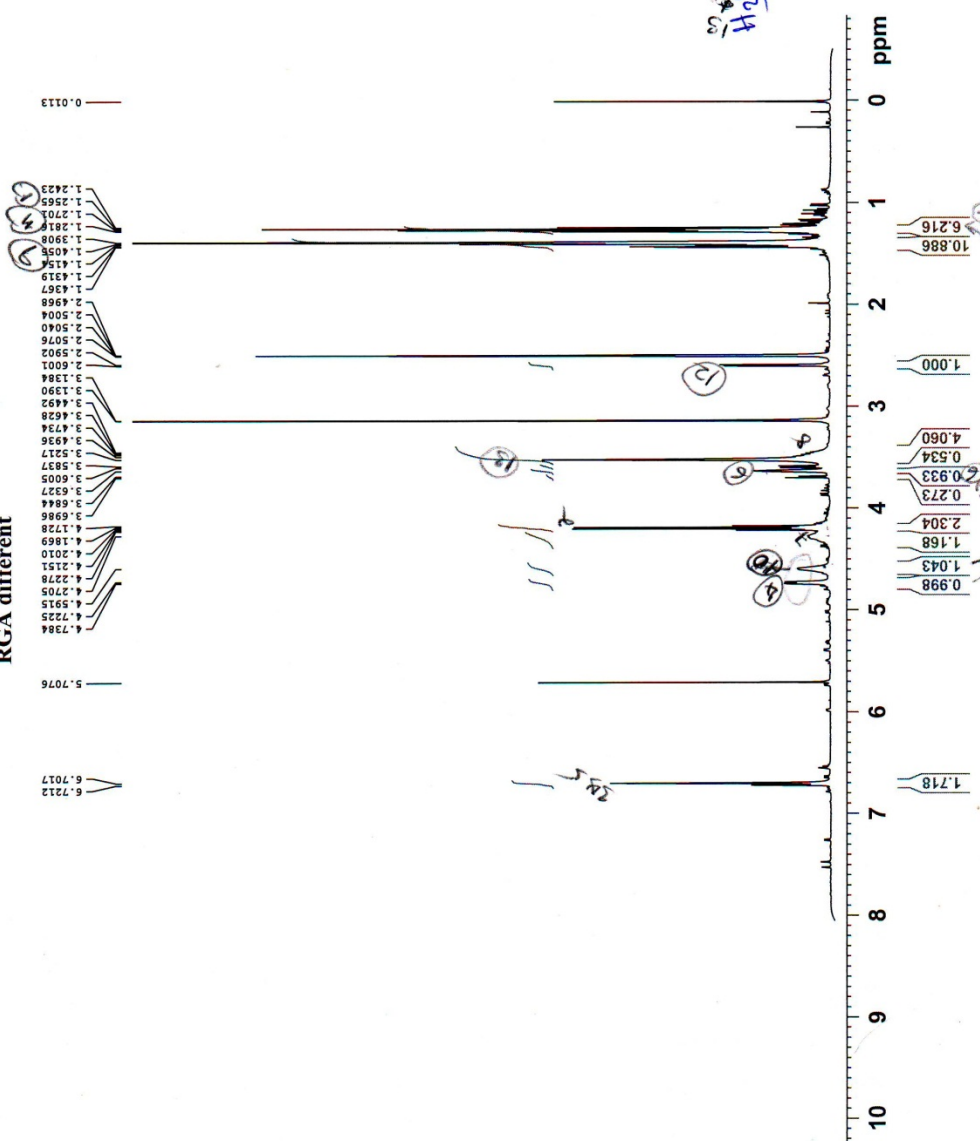


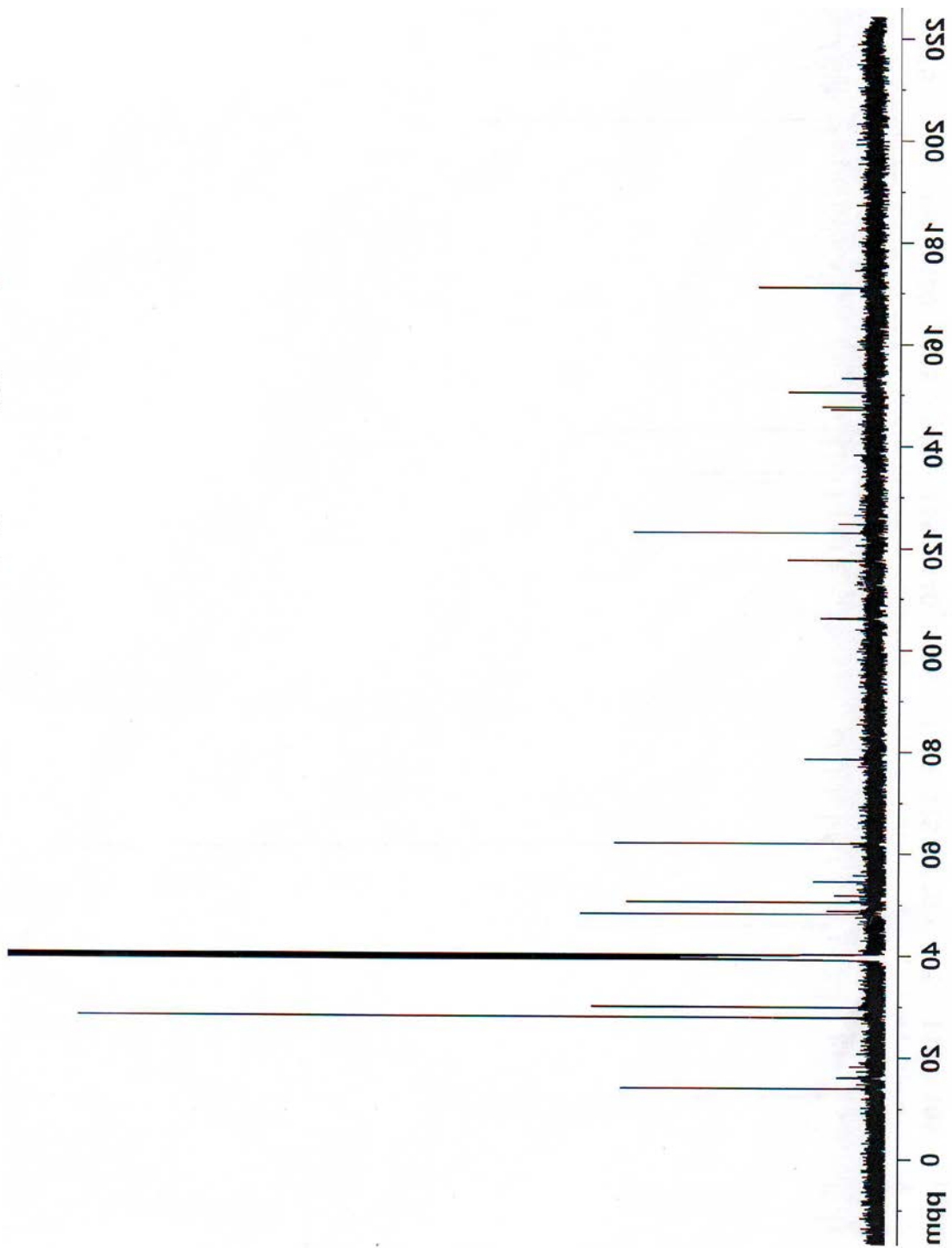


1H SGP06-117-  
temp=333 K-2  
RGA different

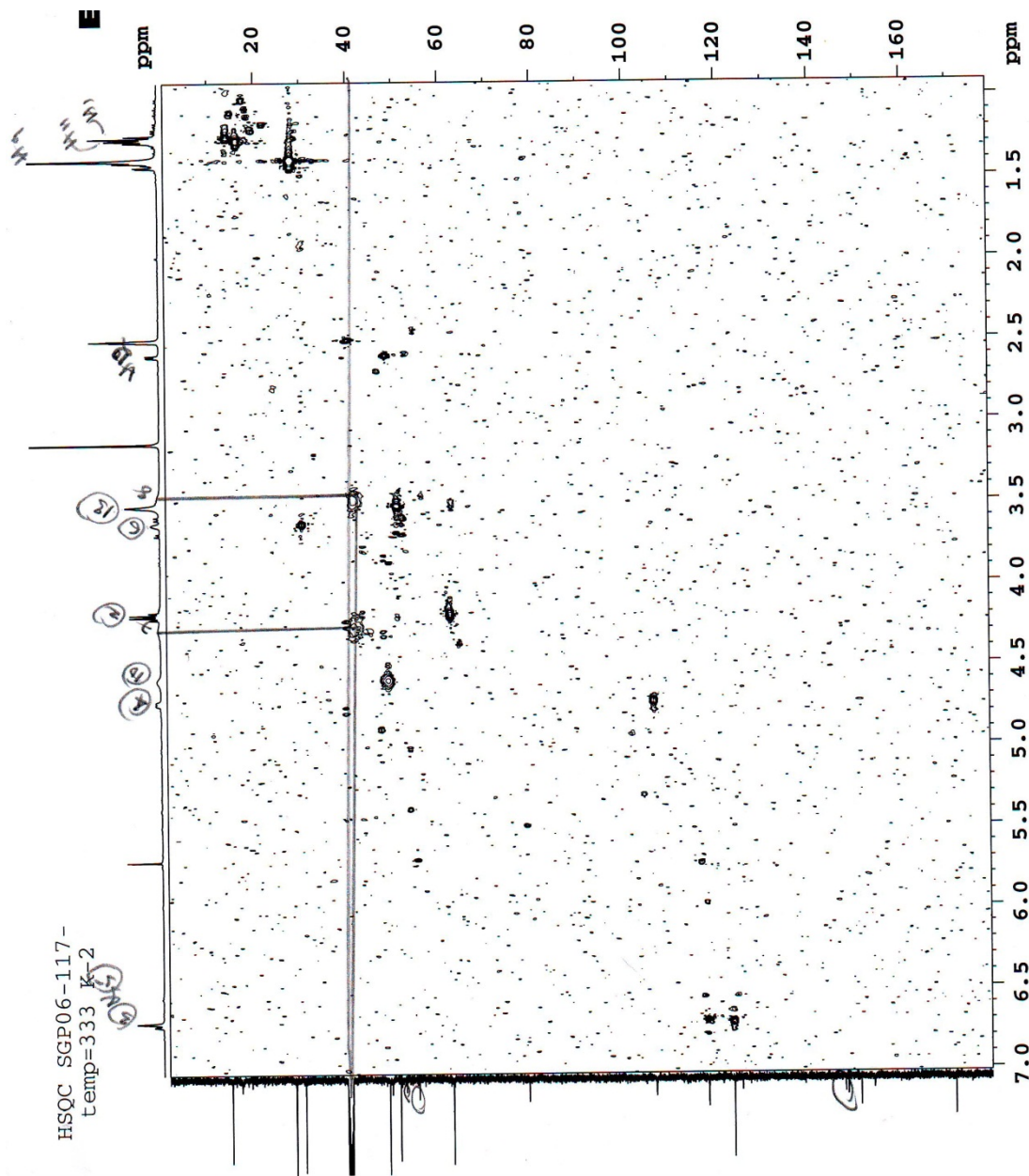
NAME SGP06-117  
PROCNO 11  
Date\_ 20110616  
Time 17.45  
INSTRUM spect  
PROBHD 5 mm PABBO  
PULPROG zgpg30  
TD 32768  
SOLVENT DMSO  
NS 32  
DS 4280.822 Hz  
SFR 0.130640 Hz  
FIDRES 3.8274691 sec  
AQ 116.650 usec  
RG 181  
DE 6.50 usec  
TE 333.0 K  
D1 0.01000000 sec  
TD0 1

===== CHANNEL f1 =====  
NUC1 1H  
P1 12.00 usec  
PL1 -0.55 dB  
RF 17.10000000 MHz  
SFO1 500.351884 MHz  
SI 65536  
SF 500.3500035 MHz  
WDW EM  
SSB 0  
LB 0.30 Hz  
GB 0  
PC 1.00



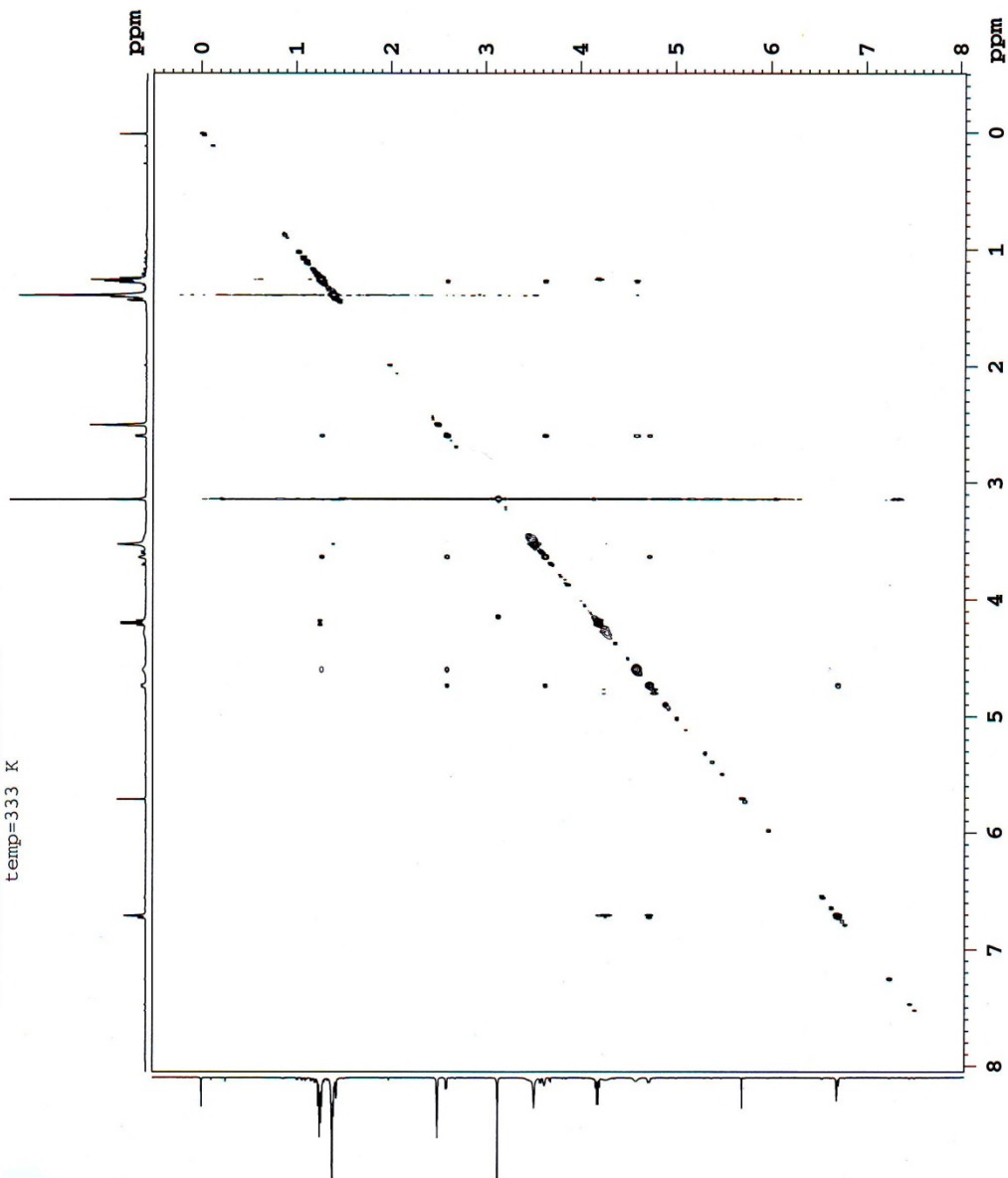








1H-1H NOESY d8=2.14 SGP06-117-  
temp=333 K



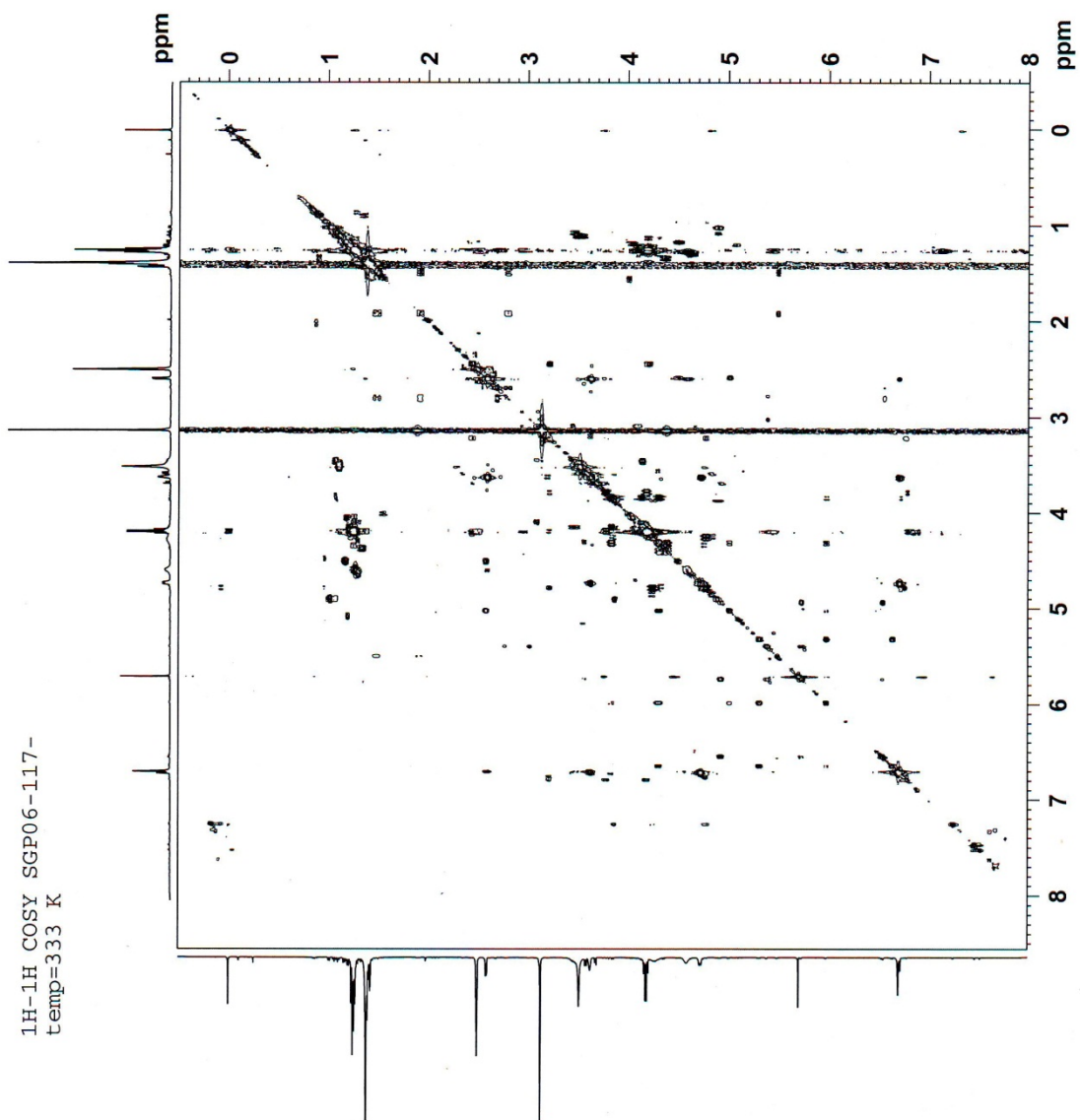
```

NAME SGP06-117
EXPNO 21
PROCNO 1
Date_ 20110618
Time 0.41
INSTRUM spect
PROBHD 5 mm PABBO BB-
PULPROG noesygpcph
TD 4096
SOLVENT DMSO
NS 16
DS 32
SMH 4280.822 Hz
FIDRES 1.045123 Hz
AQ 0.4785796 sec
RG 90.5
DW 116.800 usec
DE 6.50 usec
TE 333.0 K
D0 0.00010038 sec
D1 2.00000000 sec
D8 2.14280009 sec
D16 0.00020000 sec
IN0 0.00023360 sec

===== CHANNEL f1 =====
NUC1 1H
P1 12.90 usec
P2 25.80 usec
PL1 -0.60 dB
PL1W 17.30418968 W
SFO1 500.3518893 MHz

===== GRADIENT CHANNEL =====
GFNAM1 SINE.100
GFZ1 10.00 %
P16 1000.00 usec
ND0 1
TD 256
SFO1 500.3519 MHz
FIDRES 16.721916 Hz
SW 8.556 ppm
FMODE States-TPPI
SI 4096
SF 500.3500032 MHz
WDW QSINE
SSB 2
LB 0.00 Hz
GB 0
PC 1.40
SI 1024
MC2 States-TPPI
SF 500.3500014 MHz
WDW QSINE
SSB 2
LB 0.00 Hz
GB 0

```



## BIBLIOGRAPHY

- (1) <http://www.who.int/mediacentre/factsheets/fs297/en/> (accessed Sept 8, 2011).
- (2) Phelps, M. E. *Proc. Natl. Acad. Sci. U S A* **2000**, *97*, 9226.
- (3) Wangler, C.; Schirrmacher, R.; Bartenstein, P.; Wangler, B. *Curr. Med. Chem.* **2010**, *17*, 1092.
- (4) [http://www.csulb.edu/~cwallis/482/petscan/pet\\_lab.html](http://www.csulb.edu/~cwallis/482/petscan/pet_lab.html) (accessed Sept 2, 2011).
- (5) Liu, S. *Chem. Soc. Rev.* **2004**, *33*, 445.
- (6) Lattuada, L.; Barge, A.; Cravotto, G.; Giovenzana, G. B.; Tei, L. *Chem. Soc. Rev.* **2011**, *40*, 3019.
- (7) Morcos, S. K. *Eur. J. Radiol.* **2008**, *66*, 175.
- (8) Volkert, W. A.; Hoffman, T. J. *Chem. Rev.* **1999**, *99*, 2269.
- (9) Kruper, W. J.; Rudolf, P. R.; Langhoff, C. A. *J. Org. Chem.* **1993**, *58*, 3869.
- (10) McMurry, T. J.; Brechbiel, M.; Wu, C.; Gansow, O. A. *Bioconjugate Chem.* **1993**, *4*, 236.
- (11) Tanaka, K.; Fukase, K. *Org. Biomol. Chem.* **2008**, *6*, 815.
- (12) Anelli, P. L.; Lattuada, L.; Gabellini, M.; Recanati, P. *Bioconjugate Chem.* **2001**, *12*, 1081.
- (13) Li, C.; Winnard, P. T.; Takagi, T.; Artemov, D.; Bhujwala, Z. M. *J. Am. Chem. Soc.* **2006**, *128*, 15072.
- (14) Weisman, G. R.; Rogers, M. E.; Wong, E. H.; Jasinski, J. P.; Paight, E. S. *J. Am. Chem. Soc.* **1990**, *112*, 8604.
- (15) Weisman, G. R.; Wong, E. H.; Hill, D. C.; Rogers, M. E.; Reed, D. P.; Calabrese, J. C. *Chem. Commun.* **1996**, 947.
- (16) Wong, E. H.; Weisman, G. R.; Hill, D. C.; Reed, D. P.; Rogers, M. E.; Condon, J. S.; Fagan, M. A.; Calabrese, J. C.; Lam, K.-C.; Guzei, I. A.; Rheingold, A. L. *J. Am. Chem. Soc.* **2000**, *122*, 10561.
- (17) Lebedev, A. Y.; Holland, J. P.; Lewis, J. S. *Chem. Commun.* **2010**, *46*, 1706.
- (18) Shokeen, M.; Anderson, C. J. *Acc. Chem. Res.* **2009**, *42*, 832.
- (19) Boswell, C. A.; Regino, C. A. S.; Baidoo, K. E.; Wong, K. J.; Bumb, A.; Xu, H.; Milenic, D. E.; Kelley, J. A.; Lai, C. C.; Brechbiel, M. W. *Bioconjugate Chem.* **2008**, *19*, 1476.

- (20) Eisenwiener, K.-P.; Prata, M. I. M.; Buschmann, I.; Zhang, H.-W.; Santos, A. C.; Wenger, S.; Reubi, J. C.; Mäcke, H. R. *Bioconjugate Chem.* **2002**, *13*, 530.
- (21) De León-Rodríguez, L. M.; Kovacs, Z. *Bioconjugate Chem.* **2008**, *19*, 391.
- (22) Kolb, H. C.; Finn, M. G.; Sharpless, K. B. *Angew. Chem., Int. Ed.* **2001**, *40*, 2004.
- (23) Kolb, H. C.; Sharpless, K. B. *Drug Discovery Today* **2003**, *8*, 1128.
- (24) Huisgen, R. *Angew. Chem., Int. Ed.* **1963**, *2*, 565.
- (25) Huisgen, R. *1,3-Dipolar Cycloaddition Chemistry*, Wiley, 1984.
- (26) Tron, G. C.; Pirali, T.; Billington, R. A.; Canonico, P. L.; Sorba, G.; Genazzani, A. A. *Med. Res. Rev.* **2007**, *28*, 278.
- (27) Tornøe, C. W.; Christensen, C.; Meldal, M. *J. Org. Chem.* **2002**, *67*, 3057.
- (28) Rostovtsev, V. V.; Green, L. G.; Fokin, V. V.; Sharpless, K. B. *Angew. Chem., Int. Ed.* **2002**, *41*, 2596.
- (29) Hein, J. E.; Fokin, V. V. *Chem. Soc. Rev.* **2010**, *39*, 1302.
- (30) Moses, J. E.; Moorhouse, A. D. *Chem. Soc. Rev.* **2007**, *36*, 1249.
- (31) El-Sagheer, A. H.; Brown, T. *Chem. Soc. Rev.* **2010**, *39*, 1388.
- (32) Gierlich, J.; Burley, G. A.; Gramlich, P. M. E.; Hammond, D. M.; Carell, T. *Org. Lett.* **2006**, *8*, 3639.
- (33) Ami, T.; Fujimoto, K. *Chembiochem* **2008**, *9*, 2071.
- (34) Dijkgraaf, I.; Rijnders, A. Y.; Soede, A.; Dechesne, A. C.; van Esse, G. W.; Brouwer, A. J.; Corstens, F. H. M.; Boerman, O. C.; Rijkers, D. T. S.; Liskamp, R. M. J. *Org. Biomol. Chem.* **2007**, *5*, 935.
- (35) Link, A. J.; Tirrell, D. A. *J. Am. Chem. Soc.* **2003**, *125*, 11164.
- (36) Agard, N. J.; Prescher, J. A.; Bertozzi, C. R. *J. Am. Chem. Soc.* **2004**, *126*, 15046.
- (37) van Berkel, S. S.; Dirks, A. J.; Debets, M. F.; van Delft, F. L.; Cornelissen, J. J. L. M.; Nolte, R. J. M.; Rutjes, F. P. J. T. *Chembiochem* **2007**, *8*, 1504.
- (38) van Berkel, S. S.; Dirks, A. J.; Meeuwissen, S. A.; Pingen, D. L. L.; Boerman, O. C.; Laverman, P.; van Delft, F. L.; Cornelissen, J. J. L. M.; Rutjes, F. P. J. T. *Chembiochem* **2008**, *9*, 1805.
- (39) Wittig, G. K., A. *Chem. Ber.* **1961**, *94*.
- (40) Jewett, J. C.; Bertozzi, C. R. *Chem. Soc. Rev.* **2010**, *39*, 1272.

- (41) Chenoweth, K.; Chenoweth, D.; Goddard Iii, W. A. *Org. Biomol. Chem.* **2009**, *7*, 5255.
- (42) Bach, R. D. *J. Am. Chem. Soc.* **2009**, *131*, 5233.
- (43) Codelli, J. A.; Baskin, J. M.; Agard, N. J.; Bertozzi, C. R. *J. Am. Chem. Soc.* **2008**, *130*, 11486.
- (44) Chang, P. V.; Prescher, J. A.; Sletten, E. M.; Baskin, J. M.; Miller, I. A.; Agard, N. J.; Lo, A.; Bertozzi, C. R. *Proc. Natl. Acad. Sci. U S A* **2010**, *107*, 1821.
- (45) Agard, N. J.; Baskin, J. M.; Prescher, J. A.; Lo, A.; Bertozzi, C. R. *ACS Chem. Biol.* **2006**, *1*, 644.
- (46) Sletten, E. M.; Bertozzi, C. R. *Org. Lett.* **2008**, *10*, 3097.
- (47) Ning, X.; Guo, J.; Wolfert, M. A.; Boons, G. J. *Angew. Chem., Int. Ed.* **2008**, *47*, 2253.
- (48) Debets, M. F.; van Berkel, S. S.; Schoffelen, S.; Rutjes, F. P.; van Hest, J. C.; van Delft, F. L. *Chem Commun (Camb)* **2010**, *46*, 97.
- (49) Jewett, J. C.; Sletten, E. M.; Bertozzi, C. R. *J. Am. Chem. Soc.* **2010**, *132*, 3688.
- (50) Sletten, E. M.; Nakamura, H.; Jewett, J. C.; Bertozzi, C. R. *J. Am. Chem. Soc.* **2010**, *132*, 11799.
- (51) Johnson, J. A.; Baskin, J. M.; Bertozzi, C. R.; Koberstein, J. T.; Turro, N. *J. Chem. Commun.* **2008**, 3064.
- (52) Reubi, J. C. *Endocrine Rev.* **2003**, *24*, 389.
- (53) Sharma, S. D.; Granberry, M. E.; Jiang, J.; Leong, S. P. L.; Hadley, M. E.; Hruby, V. J. *Bioconjugate Chem.* **1994**, *5*, 591.
- (54) Sharma, S. D.; Jiang, J.; Hadley, M. E.; Bentley, D. L.; Hruby, V. J. *Proc. Natl. Acad. Sci.* **1996**, *93*, 13715.
- (55) Yarden, Y.; Sliwkowski, M. X. *Nat. Rev. Mol. Cell Biol.* **2001**, *2*, 127.
- (56) Handl, H. L.; Sankaranarayanan, R.; Josan, J. S.; Vagner, J.; Mash, E. A.; Gillies, R. J.; Hruby, V. J. *Bioconjugate Chem.* **2007**, *18*, 1101.
- (57) Xu, L.; Vagner, J.; Josan, J.; Lynch, R. M.; Morse, D. L.; Baggett, B.; Han, H.; Mash, E. A.; Hruby, V. J.; Gillies, R. J. *Mol. Cancer Ther.* **2009**, *8*, 2356.
- (58) Vagner, J.; Xu, L.; Handl, H. L.; Josan, J. S.; Morse, D. L.; Mash, E. A.; Gillies, R. J.; Hruby, V. J. *Angew. Chem., Int. Ed.* **2008**, *47*, 1685.
- (59) Monguchi, Y.; Vagner, J.; Handl, H. L.; Jana, U.; Begay, L. J.; Hruby, V. J.; Gillies, R. J.; Mash, E. A. *Tetrahedron Lett.* **2005**, *46*, 7589.

- (60) Shewmake, T. A.; Solis, F. J.; Gillies, R. J.; Caplan, M. R. *Biomacromolecules* **2008**, *9*, 3057.
- (61) Cantorias, M. V.; Figueroa, S. D.; Quinn, T. P.; Lever, J. R.; Hoffman, T. J.; Watkinson, L. D.; Carmack, T. L.; Cutler, C. S. *Nucl. Med. Biol.* **2009**, *36*, 505.
- (62) Froidevaux, S.; Calame-Christe, M.; Schuhmacher, J.; Tanner, H.; Saffrich, R.; Henze, M.; Eberle, A. N. *J. Nucl. Med.* **2004**, *45*, 116.
- (63) Lee, Y. S.; Fernandes, S.; Kulkarani, V.; Mayorov, A.; Davis, P.; Ma, S.-w.; Brown, K.; Gillies, R. J.; Lai, J.; Porreca, F.; Hruby, V. J. *Bioorg. Med. Chem. Lett.* **2010**, *20*, 4080.
- (64) Josan, J.; Vagner, J.; Handl, H.; Sankaranarayanan, R.; Gillies, R.; Hruby, V. *Int. J. Pept. Res. Ther.* **2008**, *14*, 293.
- (65) Cheng, Z.; Xiong, Z.; Subbarayan, M.; Chen, X.; Gambhir, S. S. *Bioconjugate Chem.* **2007**, *18*, 765.
- (66) Miao, Y.; Gallazzi, F.; Guo, H.; Quinn, T. P. *Bioconjugate Chem.* **2008**, *19*, 539.
- (67) Bapst, J.-P.; Calame, M.; Tanner, H.; Eberle, A. N. *Bioconjugate Chem.* **2009**, *20*, 984.
- (68) Pirrung, M. C.; Webster, N. J. G. *J. Org. Chem.* **1987**, *52*, 3603.
- (69) Schultz, M. K.; Parameswarappa, S. G.; Pigge, F. C. *Org. Lett.* **2010**, *12*, 2398.
- (70) Frew, A. J.; Proctor, G. R. *J. Chem. Soc., Perkin Trans. 1* **1980**, 1245.
- (71) Banks, R. E.; Lawrence, N. J.; Popplewell, A. L. *J. Chem. Soc., Chem. Commun.* **1994**, 343.
- (72) Wilbur, D. S.; Hamlin, D. K.; Vessella, R. L.; Stray, J. E.; Buhler, K. R.; Stayton, P. S.; Klumb, L. A.; Pathare, P. M.; Weerawarna, S. A. *Bioconjugate Chem.* **1996**, *7*, 689.
- (73) Kessler, D.; Roth, P. J.; Theato, P. *Langmuir* **2009**, *25*, 10068.
- (74) Martin, M. E.; Parameswarappa, S. G.; O'Dorisio, M. S.; Pigge, F. C.; Schultz, M. K. *Bioorg. Med. Chem. Lett.* **2010**, *20*, 4805.
- (75) Zwanziger, D.; Khan, I. U.; Neundorf, I.; Sieger, S.; Lehmann, L.; Friebe, M.; Dinkelborg, L.; Beck-Sickinger, A. G. *Bioconjugate Chem.* **2008**, *19*, 1430.
- (76) Olsen, C. A.; Witt, M.; Jaroszewski, J. W.; Franzyk, H. *J. Org. Chem.* **2004**, *69*, 6149.
- (77) Müller, P.; Imogal, H. *Tetrahedron: Asymmetry* **1998**, *9*, 4419.

- (78) Igarashi, J.; Kobayashi, Y. *Tetrahedron Lett.* **2005**, *46*, 6381.
- (79) Baumhover, N. J.; Martin, M. E.; Parameswarappa, S. G.; Kloeping, K. C.; O'Doriso, M. S.; Pigge, F. C.; Schultz, M. K. *Bioorg. Med. Chem. Lett.* **2011**, *21*, 5757.
- (80) Kálai, T.; Fleissner, M. R.; Jeko, J.; Hubbell, W. L.; Hideg, K. *Tetrahedron Lett.* **2011**, *52*, 2747.
- (81) Jølck, R. I.; Sun, H.; Berg, R. H.; Andresen, T. L. *Chem.–Eur. J.* **2011**, *17*, 3326.
- (82) <http://www.berryassoc.com/default.asp> (accessed Sept 8, 2011).
- (83) Eberle, A. N.; Verin, V. J.; Solca, F.; Siegrist, W.; Kuenlin, C.; Bagutti, C.; Stutz, S.; Girard, J. *J. Recept. Res.* **1991**, *11*, 311.
- (84) Charest, M. G.; Lerner, C. D.; Brubaker, J. D.; Siegel, D. R.; Myers, A. G. *Science* **2005**, *308*, 395.
- (85) Thiele, B. r.; Rieder, O.; Golding, B. T.; Müller, M.; Boll, M. *J. Am. Chem. Soc.* **2008**, *130*, 14050.
- (86) Kung, J. W.; Baumann, S.; von Bergen, M.; Müller, M.; Hagedoorn, P.-L.; Hagen, W. R.; Boll, M. *J. Am. Chem. Soc.* **2010**, *132*, 9850.
- (87) Hoffmann, N. *Tetrahedron* **2002**, *58*, 7933.
- (88) Boyd, J. D.; Foote, C. S.; Imagawa, D. K. *J. Am. Chem. Soc.* **1980**, *102*, 3641.
- (89) Liu, R. S. H. *J. Am. Chem. Soc.* **1968**, *90*, 215.
- (90) Bryce-Smith, D.; Gilbert, A.; McColl, I. S.; Drew, M. G. B.; Yianni, P. *J. Chem. Soc., Perkin Trans. 1* **1987**, 1147.
- (91) López Ortiz, F.; Iglesias, M. J.; Fernández, I.; Andújar Sánchez, C. M.; Ruiz Gómez, G. *Chem. Rev.* **2007**, *107*, 1580.
- (92) Ohno, H.; Iwasaki, H.; Eguchi, T.; Tanaka, T. *Chem. Commun.* **2004**, 2228.
- (93) Ohno, H.; Maeda, S.-i.; Okumura, M.; Wakayama, R.; Tanaka, T. *Chem. Commun.* **2002**, 316.
- (94) Lu, S.; Xu, Z.; Bao, M.; Yamamoto, Y. *Angew. Chem., Int. Ed.* **2008**, *47*, 4366.
- (95) Roell, B. C.; McDaniel, K. F.; Vaughan, W. S.; Macy, T. S. *Organometallics* **1993**, *12*, 224.
- (96) Li, F.; Tartakoff, S. S.; Castle, S. L. *J. Am. Chem. Soc.* **2009**, *131*, 6674.



- (97) Mejorado, L. H.; Pettus, T. R. R. *J. Am. Chem. Soc.* **2006**, *128*, 15625.
- (98) Schultz, A. G.; Wang, A. *J. Am. Chem. Soc.* **1998**, *120*, 8259.
- (99) Crich, D.; Hwang, J.-T. *J. Org. Chem.* **1998**, *63*, 2765.
- (100) Crich, D.; Patel, M. *Org. Lett.* **2005**, *7*, 3625.
- (101) Crich, D.; Krishnamurthy, V. *Tetrahedron* **2006**, *62*, 6830.
- (102) Aulenta, F.; Berndt, M.; Brüdgam, I.; Hartl, H.; Sörgel, S.; Reißig, H.-U. *Chem.–Eur. J.* **2007**, *13*, 6047.
- (103) Gaich, T.; Mulzer, J. *J. Am. Chem. Soc.* **2008**, *131*, 452.
- (104) Campbell, E. L.; Zuhl, A. M.; Liu, C. M.; Boger, D. L. *J. Am. Chem. Soc.* **2010**, *132*, 3009.
- (105) Andrews, R. C.; Teague, S. J.; Meyers, A. I. *J. Am. Chem. Soc.* **1988**, *110*, 7854.
- (106) Beak, P.; Meyers, A. I. *Acc. Chem. Res.* **1986**, *19*, 356.
- (107) Clayden, J.; Tchabanenko, K. *Chem. Commun.* **2000**, 317.
- (108) Clayden, J.; Knowles, F. E.; Baldwin, I. R. *J. Am. Chem. Soc.* **2005**, *127*, 2412.
- (109) Abd-El-Aziz, A. S.; Bernardin, S. *Coord. Chem. Rev.* **2000**, *203*, 219.
- (110) Pape, A. R.; Kaliappan, K. P.; Kundig, E. P. *Chem. Rev.* **2000**, *100*, 2917.
- (111) Chordia, M. D.; Harman, W. D. *J. Am. Chem. Soc.* **1998**, *120*, 5637.
- (112) Keane, J. M.; Harman, W. D. *Organometallics* **2005**, *24*, 1786.
- (113) Kündig, E. P.; Cannas, R.; Laxmisha, M.; Ronggang, L.; Tchertchian, S. *J. Am. Chem. Soc.* **2003**, *125*, 5642.
- (114) Kolis, S. P.; Kopach, M. E.; Liu, R.; Harman, W. D. *J. Am. Chem. Soc.* **1998**, *120*, 6205.
- (115) Chordia, M. D.; Harman, W. D. *J. Am. Chem. Soc.* **2000**, *122*, 2725.
- (116) Surendranath, Y.; Welch, K. D.; Nash, B. W.; Harman, W. H.; Myers, W. H.; Harman, W. D. *Organometallics* **2006**, *25*, 5852.
- (117) Lis, E. C.; Salomon, R. J.; Sabat, M.; Myers, W. H.; Harman, W. D. *J. Am. Chem. Soc.* **2008**, *130*, 12472.
- (118) Braun, N. A.; Ousmer, M.; Bray, J. D.; Bouchu, D.; Peters, K.; Peters, E. M.; Ciufolini, M. A. *J. Org. Chem.* **2000**, *65*, 4397.
- (119) Quideau, S.; Pouységu, L. *Org. Prep. Proced. Int.* **1999**, *31*, 617.

- (120) Quideau, S.; Pouységu, L.; Deffieux, D. *Synlett* **2008**, 2008, 467.
- (121) Barradas, S.; Carreño, M. C.; González-López, M.; Latorre, A.; Urbano, A. *Org. Lett.* **2007**, 9, 5019.
- (122) Nicolaou, K. C.; Baran, P. S.; Zhong, Y. L.; Barluenga, S.; Hunt, K. W.; Kranich, R.; Vega, J. A. *J. Am. Chem. Soc.* **2002**, 124, 2233.
- (123) Wirth, T.; Wirth, T., Ed.; Springer Berlin / Heidelberg: 2003; Vol. 224, p 185.
- (124) Frie, J. L.; Jeffrey, C. S.; Sorensen, E. J. *Org. Lett.* **2009**, 11, 5394.
- (125) Nicolaou, K. C.; Edmonds, D. J.; Li, A.; Tria, G. S. *Angew. Chem., Int. Ed.* **2007**, 46, 3942.
- (126) Chia, W.-L.; Shiao, M.-J. *Tetrahedron Lett.* **1991**, 32, 2033.
- (127) Comins, D. L.; Stolze, D. A.; Thakker, F.; McArdle, C. L. *Tetrahedron Lett.* **1998**, 39, 5693.
- (128) Comins, D. L. *Tetrahedron Lett.* **1983**, 24, 2807.
- (129) Akiba, K.; Nakatani, M.; Wada, M.; Yamamoto, Y. *J. Org. Chem.* **1985**, 50, 63.
- (130) Comins, D. L.; Weglarz, M. A.; O'Connor, S. *Tetrahedron Lett.* **1988**, 29, 1751.
- (131) Yamaguchi, R.; Hata, E.-i.; Utimoto, K. *Tetrahedron Lett.* **1988**, 29, 1785.
- (132) Akiba, K.-y.; Iseki, Y.; Wada, M. *Tetrahedron Lett.* **1982**, 23, 429.
- (133) Comins, D. L.; Hong, H. *J. Org. Chem.* **1993**, 58, 5035.
- (134) Akiba, K.-y.; Nishihara, Y.; Wada, M. *Tetrahedron Lett.* **1983**, 24, 5269.
- (135) Comins, D. L.; Brown, J. D. *Tetrahedron Lett.* **1984**, 25, 3297.
- (136) Andersson, H.; Gustafsson, M.; Boström, D.; Olsson, R.; Almqvist, F. *Angew. Chem., Int. Ed.* **2009**, 48, 3288.
- (137) Fernández-Ibáñez, M. A.; Maciá, B.; Pizzuti, M. G.; Minnaard, A. J.; Feringa, B. L. *Angew. Chem., Int. Ed.* **2009**, 48, 9339.
- (138) Christian, N.; Aly, S.; Belyk, K. *J. Am. Chem. Soc.* **2011**, 133, 2878.
- (139) Sun, Z.; Yu, S.; Ding, Z.; Ma, D. *J. Am. Chem. Soc.* **2007**, 129, 9300.
- (140) Black, D. A.; Beveridge, R. E.; Arndtsen, B. A. *J. Org. Chem.* **2008**, 73, 1906.

- (141) Taylor, M. S.; Tokunaga, N.; Jacobsen, E. N. *Angew. Chem., Int. Ed.* **2005**, *44*, 6700.
- (142) Février, F. C.; Smith, E. D.; Comins, D. L. *Org. Lett.* **2005**, *7*, 5457.
- (143) Kuethe, J. T.; Comins, D. L. *Org. Lett.* **1999**, *1*, 1031.
- (144) Kuethe, J. T.; Comins, D. L. *Org. Lett.* **2000**, *2*, 855.
- (145) Comins, D. L.; Sahn, J. J. *Org. Lett.* **2005**, *7*, 5227.
- (146) Lemire, A.; Charette, A. B. *Org. Lett.* **2005**, *7*, 2747.
- (147) Larivée, A.; Charette, A. B. *Org. Lett.* **2006**, *8*, 3955.
- (148) Focken, T.; Charette, A. B. *Org. Lett.* **2006**, *8*, 2985.
- (149) Weller, D. D.; Luellen, G. R.; Weller, D. L. *J. Org. Chem.* **1983**, *48*, 3061.
- (150) Goldmann, S.; Born, L.; Kazda, S.; Pittel, B.; Schramm, M. *J. Med. Chem.* **1990**, *33*, 1413.
- (151) Sandham, D. A.; Meyers, A. I. *J. Chem. Soc., Chem. Commun.* **1995**, 2511.
- (152) Barbe, G.; Pelletier, G.; Charette, A. B. *Org. Lett.* **2009**, *11*, 3398.
- (153) Clayden, J.; Hamilton, S. D.; Mohammed, R. T. *Org. Lett.* **2005**, *7*, 3673.
- (154) Brice, H.; Clayden, J. *Chem. Commun.* **2009**, 1964.
- (155) Arnott, G.; Clayden, J.; Hamilton, S. D. *Org. Lett.* **2006**, *8*, 5325.
- (156) Wanner, M. J.; Koomen, G. J.; Pandit, U. K. *Tetrahedron* **1982**, *38*, 2741.
- (157) Kucherenko, T. T.; Gutsul, R.; Kisel, V. M.; Kovtunencko, V. A. *Tetrahedron* **2004**, *60*, 211.
- (158) Weller, D. D.; Ford, D. W. *Tetrahedron Lett.* **1984**, *25*, 2105.
- (159) Badger, A. M.; Newman-Tarr, T. M.; Satterfield, J. L. *Immunopharmacology* **1997**, *37*, 53.
- (160) Selig, P.; Bach, T. *Angew. Chem., Int. Ed.* **2008**, *47*, 5082.
- (161) Rabinovitch, A.; Suarez, W. L.; Qin, H.-Y.; Power, R. F.; Badger, A. M. *J. Autoimmun.* **1993**, *6*, 39.
- (162) Liu, P.; Seo, J. H.; Weinreb, S. M. *Angewandte Chemie., Int. Ed.* **2010**, *49*, 2000.
- (163) Fischer, D. F.; Sarpong, R. *J. Am. Chem. Soc.* **2010**, *132*, 5926.

- (164) Nicolaou, K. C.; Dalby, S. M.; Majumder, U. *J. Am. Chem. Soc.* **2008**, *130*, 14942.
- (165) Pigge, F. C.; Coniglio, J. J.; Dalvi, R. *J. Am. Chem. Soc.* **2006**, *128*, 3498.
- (166) Pigge, F. C.; Dhanya, R.; Hoefgen, E. R. *Angew. Chem., Int. Ed. Engl* **2007**, *46*, 2887.
- (167) Pigge, F. C.; Dhanya, R.; Swenson, D. C. *Organometallics* **2009**, *28*, 3869.
- (168) Pigge, F. C.; Coniglio, J. J.; Rath, N. P. *J. Org. Chem.* **2004**, *69*, 1161.
- (169) Pigge, F. C.; Coniglio, J. J.; Rath, N. P. *Org. Lett.* **2003**, *5*, 2011.
- (170) Pigge, F. C.; Dalvi, R. *Tetrahedron* **2008**, *64*, 10123.
- (171) Arnott, G.; Brice, H.; Clayden, J.; Blaney, E. *Org. Lett.* **2008**, *10*, 3089.
- (172) Parameswarappa, S. G.; Pigge, F. C. *Org Lett* **2010**, *12*, 3434.
- (173) Pigge, F. C. Dalvi., R. unpublished results.
- (174) Arcadi, A. *Chem. Rev.* **2008**, *108*, 3266.
- (175) Harrison, T. J.; Patrick, B. O.; Dake, G. R. *Org. Lett.* **2006**, *9*, 367.
- (176) Kiselyov, A. S.; Piatnitski, E.; Semenova, M.; Semenov, V. V. *Bioorg. & Med. Chem. Lett.* **2006**, *16*, 602.
- (177) Shamovsky, I.; de Graaf, C.; Alderin, L.; Bengtsson, M.; Bladh, H. k.; Börjesson, L.; Connolly, S.; Dyke, H. J.; van den Heuvel, M.; Johansson, H.; Josefsson, B.-G. r.; Kristoffersson, A.; Linnanen, T.; Lisius, A.; Männikkö, R.; Nordén, B.; Price, S.; Ripa, L.; Rognan, D.; Rosendahl, A.; Skrinjar, M.; Urbahns, K. *J. Med. Chem.* **2009**, *52*, 7706.
- (178) Yang, H.; Lin, X.-F.; Padilla, F.; Gabriel, S. D.; Heilek, G.; Ji, C.; Sankuratri, S.; deRosier, A.; Berry, P.; Rotstein, D. M. *Bioorg. Med. Chem. Lett.* **2009**, *19*, 209.
- (179) Mehrotra, M. M.; Heath, J. A.; Rose, J. W.; Smyth, M. S.; Seroogy, J.; Volkots, D. L.; Ruhter, G.; Schotten, T.; Alaimo, L.; Park, G.; Pandey, A.; Scarborough, R. M. *Bioorg. Med. Chem. Lett.* **2002**, *12*, 1103.
- (180) Burgey, C. S.; Potteiger, C. M.; Deng, J. Z.; Mosser, S. D.; Salvatore, C. A.; Yu, S.; Roller, S.; Kane, S. A.; Vacca, J. P.; Williams, T. M. *Bioorg. Med. Chem. Lett.* **2009**, *19*, 6368.
- (181) Parameswarappa, S. G.; Pigge, F. C. *Tetrahedron Lett.* **2011**, *52*, 4357.
- (182) Katritzky, A. R.; Urogdi, L.; Patel, R. C. *J. Chem. Soc., Perkin Trans. 1* **1982**, 1349.

- (183) Martin-Cantalejo, Y. S., B.; Soto, J.; Villa, M. J.; Brana, M. F. *Synthesis* **2003**, 2211.
- (184) Bosch, J.; Bennasar, M. L.; Zulaica, E. *J. Org. Chem.* **1986**, 51, 2289.
- (185) Arai, M.; Sobou, M.; Vilchéze, C.; Baughn, A.; Hashizume, H.; Pruksakorn, P.; Ishida, S.; Matsumoto, M.; Jacobs Jr, W. R.; Kobayashi, M. *Bioorg. Med. Chem.* **2008**, 16, 6732.
- (186) Harrison, B.; Talapatra, S.; Lobkovsky, E.; Clardy, J.; Crews, P. *Tetrahedron Lett.* **1996**, 37, 9151.
- (187) Torres, Y. R.; Berlinck, R. G. S.; Magalhães, A.; Schefer, A. B.; Ferreira, A. G.; Hajdu, E.; Muricy, G. *J. Nat. Prod.* **2000**, 63, 1098.
- (188) Cimino, G.; Scognamiglio, G.; Spinella, A.; Trivellone, E. *J. Nat. Prod.* **1990**, 53, 1519.
- (189) Wei, X.; Nieves, K.; Rodriguez, A. D. *Bioorg. Med. Chem. Lett.* **2010**, 20, 5905.
- (190) Smith, B. J.; Sulikowski, G. A. *Angew. Chem.* **2010**, 122, 1643.
- (191) Deng, G.; Li, C.-J. *Org. Lett.* **2009**, 11, 1171.
- (192) Sandmeier, P.; Tamm, C. *Helv. Chim. Acta* **1989**, 72, 774.
- (193) Ng, F. W.; Lin, H.; Danishefsky, S. J. *J. Am. Chem. Soc.* **2002**, 124, 9812.
- (194) Yokoshima, S.; Tokuyama, H.; Fukuyama, T. *Angew. Chem., Int. Ed.* **2000**, 39, 4073.
- (195) Scheffler, G.; Seike, H.; Sorensen, E. J. *Angew. Chem., Int. Ed.* **2000**, 39, 4593.
- (196) Koser, G.; Wirth, T., Ed.; Springer Berlin / Heidelberg: 2003; Vol. 224, p 173.
- (197) Koser, G.; Wirth, T., Ed.; Springer Berlin / Heidelberg: 2003; Vol. 224, p 137.
- (198) Varvoglis, A.; Wirth, T., Ed.; Springer Berlin / Heidelberg: 2003; Vol. 224, p 69.
- (199) Zhdankin, V.; Wirth, T., Ed.; Springer Berlin / Heidelberg: 2003; Vol. 224, p 99.
- (200) Tohma, H.; Kita, Y.; Wirth, T., Ed.; Springer Berlin / Heidelberg: 2003; Vol. 224, p 209.
- (201) Miyazawa, E.; Sakamoto, T.; Kikugawa, Y. *J. Org. Chem.* **2003**, 68, 5429.
- (202) Liang, J.; Chen, J.; Du, F.; Zeng, X.; Li, L.; Zhang, H. *Org. Lett.* **2009**, 11, 2820.

- (203) Arisawa, M.; Ramesh, N. G.; Nakajima, M.; Tohma, H.; Kita, Y. *J. Org. Chem.* **2001**, *66*, 59.
- (204) Dohi, T.; Maruyama, A.; Minamitsuji, Y.; Takenaga, N.; Kita, Y. *Chem. Commun.* **2007**, 1224.
- (205) Hamamoto, H.; Shiozaki, Y.; Nambu, H.; Hata, K.; Tohma, H.; Kita, Y. *Chem.–Eur. J.* **2004**, *10*, 4977.
- (206) Kita, Y.; Arisawa, M.; Gyoten, M.; Nakajima, M.; Hamada, R.; Tohma, H.; Takada, T. *J. Org. Chem.* **1998**, *63*, 6625.
- (207) Kita, Y.; Gyoten, M.; Ohtsubo, M.; Tohma, H.; Takada, T. *Chem. Commun.* **1996**, 1481.
- (208) Brice, H.; Clayden, J.; Hamilton, S. D. *Beilstein J. Org. Chem.* **2010**, *6*, 22.
- (209) Quirante, J.; Paloma, L.; Diaba, F.; Vila, X.; Bonjoch, J. *J. Org. Chem.* **2008**, *73*, 768.
- (210) Yamazaki, N.; Kusanagi, T.; Kibayashi, C. *Tetrahedron Lett.* **2004**, *45*, 6509.
- (211) Li, J.; Sha, Y. *Molecules* **2008**, *13*, 1111.